

AD666727

FOREIGN TECHNOLOGY DIVISION



LENINGRAD. UNIVERSITY. HERALD. PHYSICS AND
CHEMISTRY SERIES (COLLECTION OF ARTICLES)



GOLDEN ANNIVERSARY
FOREIGN TECHNOLOGY DIVISION



Distribution of this document is unlimited. It may be released to the Clearinghouse, Department of Commerce, for sale to the general public.



Reproduced by the
CLEARINGHOUSE
for Federal Scientific & Technical
Information Springfield Va. 22151

EDITED MACHINE TRANSLATION

LENINGRAD. UNIVERSITY. HERALD. PHYSICS AND
CHEMISTRY SERIES (COLLECTION OF ARTICLES)

English Pages: 217

UR/0054-064-000-001

TP7500499-524

THIS TRANSLATION IS A RENDITION OF THE ORIGINAL FOREIGN TEXT WITHOUT ANY ANALYTICAL OR EDITORIAL COMMENT. STATEMENTS OR THEORIES ADVOCATED OR IMPLIED ARE THOSE OF THE SOURCE AND DO NOT NECESSARILY REFLECT THE POSITION OR OPINION OF THE FOREIGN TECHNOLOGY DIVISION.

PREPARED BY:
TRANSLATION DIVISION
FOREIGN TECHNOLOGY DIVISION
WP-AFB, OHIO.

FTD-MT- 64-358

Date 9 May 1967

This Document Contains
Missing Page/s That Are
Unavailable In The
Original Document

pg 62

Best Available Copy

This document is a machine translation of Russian text which has been processed by the AN/GSQ-16(XW-2) Machine Translator, owned and operated by the United States Air Force. The machine output has been post-edited to correct for major ambiguities of meaning, words missing from the machine's dictionary, and words out of the context of meaning. The sentence word order has been partially rearranged for readability. The content of this translation does not indicate editorial accuracy, nor does it indicate USAF approval or disapproval of the material translated.

| | |
|------------------------------------|---------------|
| TO: (NAME) | WRITE MESSAGE |
| FROM: | NOV 20 1954 |
| CLASSIFIED | |
| JUSTIFICATION | |
| BY: DISTRIBUTION/AVAILABILITY CODE | |
| DOC. | AVAIL. CODE |

VESTNIK LENINGRADSKOGO UNIVERSITETA

God Izdaniya Devyatnadsatyy

No. 4

Seriya
Fiziki i Khimii

Vypusk 1

v 19 22 24

Redaktsionnaya kollegiya serii:

P. P. Pavinskiy (otv. redaktor),
A. V. Storonkin (zam. otv. redaktora),
S. S. Tolkachev (sekretar'),
O. N. Grigorov, I. A. D'yakonov,
K. Ya. Kondrat'yev, I. G. Mikhaylov,
N. P. Penkin, S. E. Frish

Izdatel'stvo
Leningradskogo Universiteta

1964

Page 1-167

ITIS INDEX CONTROL FORM

| | | | | | | | |
|------------------------|----------------|--------------------------------|---------------|--------------------------|-------------------|------------------------------------|-----------------|
| 01 Acc Nr TP7500499 | | 68 Translation Nr MT6400358 | | 65 X Ref Acc Nr | | 75 Serial/Frame Nr 245 | |
| 97 Header Clas UNCL | | 63 Clas UNCL, 0 | | 64 Control Markings 0 | | 94 Expansion 40 Ctry Info UR | |
| 02 Ctry UR | 03 Ref 0054 | 04 Yr 64 | 05 Vol 000 | 06 Iss 001 | 07 B. Pg. 0005 | 08 B. Pg. 0013 | 10 Date NONE |

Transliterated Title

URAVNENIYA DLYA VERSHINNYKH CHASTEY I SVYAZANNYYE SOSTOYANIYA

09 English Title

EQUATIONS FOR VERTEX PARTS AND BOUND STATES

43 Source Leningrad. Universitet. Vestnik. Seriya Fiziki i Khimii (Russian)

42 Author

BRAUN, M. A.

98 Document Location

16 Co-Author

NONE

47 Subject Codes 20

16 Co-Author

NONE

39 Topic Tags: nucleon, nucleon interaction, deuteron, deuteron interaction, particle physics

16 Co-Author

NONE

16 Co-Author

NONE

ABSTRACT The system of dispersion theoretic equations for the vertex parts π NN and NND with a nucleon off the mass shell is studied in the low energy region in the spinless particle model. The anomalous threshold is calculated by analytic continuation in the mass variable. Under the assumption that the deuteron is a bound state of the nucleons, an equation is obtained for the determination of its mass. English Translation: 13 pages.

ITIS INDEX CONTROL FORM

| | | | |
|-------------------------|--------------------------------|------------------------------|------------------------------------|
| 61 Acc Nr BT7500500 | 62 Translation Nr MT6400358 | 63 X Ref Acc Nr AP4024455 | 76 Reel/Frame Nr 1651 1446 |
| 67 Number Class UNCL | 68 Class UNCL, 0 | 64 Control Markings 0 | 94 Expansion 40 Ctry Info UR |
| 69 City UR | 03 Ref 0054 | 04 Yr 64 | 05 Vol 000 |
| | 06 Iss 001 | 07 B. Pg. 0014 | 08 B. Pg. 0020 |
| | | | 10 Date NONE |

Unabbreviated Title

ASSOTSIROVANIYE NUKLONOV V YADRAKH

09 English Title

ASSOCIATING OF NUCLEONS IN NUCLEI

43 Source

LENINGRAD. UNIVERSITET. VESTNIK. SERIYA FIZIKI I KHIMII (RUSSIAN)

44 Author

BUNAKOV, V. YE.

98 Document Location

15 Co-Author

NONE

47 Subject Codes 20, 18

16 Co-Author

NONE

39 Topic Tags: quantum number, wave function, nuclear binding energy, light nucleus, nuclear spin

16 Co-Author

NONE

16 Co-Author

NONE

ABSTRACT The connection between the probable existence of nuclear clustering and quantum numbers, characterized irreducible group representations of commutation and orthogonal groups (forming shell-model wave functions of a nucleus) has been investigated. The relation between the S-state of the two-nucleon relative motion and the seniority quantum number ν of its shell-model wave function has been studied. For $\nu = 0$ the state of the two-nucleon can be represented by the J-state. Using the seniority operator definition

$$Q = \sum_{i < j} q_{ij} \tau_{ij}$$

$$\langle J, M | Q | J, M \rangle = (2J+1) \delta_{J,0}$$

A similar analysis is made for the case of n nucleons. It is shown that classification by the quantum number $[f]$ and w can appear at the same time as an S-state nucleon weight classification in relative motion. An experimental regularity is found to be present in the values of binding energies of light nuclei, which assumes the existence of two-, three-, and four-nucleon clusters. The method under consideration makes it possible to treat double, triple, and quadruple nucleon correlations on the basis of the same effective two-body interactions of nucleons. A physical interpretation is given for the experimental facts concerning energy advantage of states with the lowest seniority and isotopic spin. "The author is grateful to A. I. Baz', Doctor of physical and mathematical sciences, and to Professors G. F. Drukarev, V. G. Ippolitov, and V. Feyfrlik and to G. A. Chilashvili, Candidate of physical and mathematical sciences, for their valuable help." Orig. art. has: 8 formulas, 1 figure, and 1 table. English Translation: 15 pages.

ITIS INDEX CONTROL FORM

| | | | | | | | |
|------------------------|--------------------------------|------------------------------|-------------------------------------|---------------|-------------------|-------------------|-----------------|
| 01 Acc Nr TP7500501 | 68 Translation Nr MT6400353 | 65 X Ref Acc Nr AP4024456 | 76 Reel/Frame Nr 1654 1447 | | | | |
| 97 Header Clas UNCL | 63 Clas UNCL, 0 | 64 Control Markings 0 | 94 Expansion 40 Ctry Info IIR | | | | |
| 02 Ctry UR | 03 Ref 0054 | 04 Yr 54 | 05 Vol 000 | 06 Iss 001 | 07 B. Pg. 0021 | 08 B. Pg. 0025 | 10 Date NONE |

Transliterated title

OKOLOPOROGOVOYE POVEDENIYE SECHENIYA NEUPRUGOGO RASSEYANIYA

09 English Title NEAR-THRESHOLD BEHAVIOR OF THE INELASTIC-SCATTERING CROSS SECTION

43 Source LENINGRAD. UNIVERSITET. VESTNIK. SERIYA FIZIKI I KHIMII (RUSSIAN)

42 Author ZHIKHAREVA, T. V. 98 Document Location

16 Co-Author NONE 47 Subject Codes 18, 20

16 Co-Author NONE 39 Topic Tags: inelastic scattering, nuclear resonance, orbit momentum, nuclear cross section

16 Co-Author NONE

16 Co-Author NONE

ABSTRACT The partial cross-section transition from the l-channel to the i-th channel for complete orbital momentum L is given by

$$\sigma_{ij} = \frac{4\pi}{k^2} \frac{2L+1}{2L+3} |T_{ij}|^2$$

where T - scattering matrix. A three-channel case is considered, and the resonance effect in the inelastic cross section σ_{12} is also considered.

The nature of the inelastic cross section σ_{12} anomaly near the threshold $K_3 = 0$ is studied, and it is shown that the greater the probability of inelastic processes σ_{13} and σ_{23} the greater will be the anomaly in the threshold $K_3 = 0$ of inelastic cross section σ_{12} . The behavior of p-wave inelastic cross section σ_{12} near the threshold of secondary inelastic reaction is investigated. Above the threshold this is given by

$$\sigma_{12}(\epsilon_0) \sigma_{12}(0)^{-1} = 1 - \frac{2M_1^2(M_2^2 + \epsilon_0^2) \epsilon_0^2 + 2M_2^2(M_1^2 + \epsilon_0^2) \epsilon_0^2}{M_1^2 M_2^2}$$

and below the threshold, by

$$\sigma_{12}(\epsilon_0) \sigma_{12}(0)^{-1} = 1 + \frac{2M_1^2(M_2^2 + \epsilon_0^2) M_1^2 + 2M_2^2(M_1^2 + \epsilon_0^2) M_2^2}{M_1^2 M_2^2}$$

TP7500501

MT6400358

"The author is grateful to G. F. Drukarev for evaluating the work."
Orig. art. has: 18 equations and 1 figure. English Translation:
5 pages.

ITIS INDEX CONTROL FORM

| | | | | | | | |
|------------------------|--------------------|--------------------------------|---------------|------------------------------|-------------------|-------------------------------|-----------------|
| 01 Acc Nr TP7500502 | | 68 Translation Nr MT6400358 | | 65 X Ref Acc Nr AP4024463 | | 76 Reel/Frame Nr 1654 1449 | |
| 97 Header Clas UNCL | 63 Clas UNCL, 0 | 64 Control Markings 0 | | | 94 Expansion | 40 Ctry Info UR | |
| 02 Ctry UR | 03 Ref 0054 | 04 Yr 64 | 05 Vol 000 | 06 Iss 001 | 07 B. Pg. 0026 | 45 B. Pg. 0052 | 10 Date NONE |

Transliterated Title YADERNO-REZONANSNYY GENERATOR S TEKUSHCHEY ZHIDKOST'YU

09 English Title NUCLEAR-RESONANCE GENERATOR WITH FLOWING LIQUID

43 Source LENINGRAD. UNIVERSITET. VESTNIK. SERIYA FIZIKI I KHMII (RUSSIAN)

42 Author JKRIPOV, F. I.

98 Document Location

16 Co-Author
NONE

47 Subject Codes 20, 18

16 Co-Author
NONE

39 Topic Tags: nuclear resonance, magnetic field, polarization filter, magnetization

16 Co-Author
NONE

16 Co-Author
NONE

ABSTRACT A theory of the operation of the nuclear resonance generator in the earth's magnetic field is given. The Packard-Varian theory (Bull. Amer. Phys. Soc 28, No. 7, 1953) is reviewed and found to be inefficient for continuous measurement of fields. A new method developed by the author in 1957 is discussed which is based on a nuclear resonance generator with continuous polarization of a flowing liquid (water in this case). The water flows through a magnetizing (polarization) coil of strength H which induces a nuclear magnetization M in the fluid proportional to field strength $H + H_0(H_0 - \text{terrestrial field})$. The liquid then flows through a tube into a sensing (observing) coil which creates an alternating field at resonance frequencies. A mock-up test is described with a flow rate of 100 cm³ per sec and $H = 400$ gauss. A similar instrument utilizing the Overhauser nuclear polarization method, devised by A. Abragam, J. Combricou and I. Solomon (Compt. rend., 247, 1957, 1957), is also discussed. Theoretical expressions are obtained for the magnetizing and sensing coils. A simplified form for nuclear magnetization in a time interval $0 < t < \tau$ is given by

$$M(t) = M_0 \left(1 - e^{-t/T_1} \right)$$

where τ = time of flow through a polarized coil. At large frequency differences the alternating phasing coil field H_1 exerts only a high-speed modulation on M with small angular amplitudes. For $H_1 \ll H_0$ it is so small that M cannot be observed. The characteristics of the generator in the narrow band filter regime are studied in detail and given as two mathematical expressions. The discussion is extended to include non-homogeneity effects. (See also related art. has: 4 equations and 11 figures. English Translation: 27 pages)

ITIS INDEX CONTROL FORM

| | | | |
|------------------------|--------------------------------|------------------------------|-------------------------------|
| 01 Acc Nr TF7500503 | 68 Translation Nr MT6400358 | 65 X Ref Acc Nr AP4024458 | 76 Reel/Frame Nr 165A 1450 |
| 07 Reader Clas UNCL | 83 Clas UNCL, 0 | 84 Control Markings 0 | 94 Expansion UR |
| 08 Ctry UR | 09 Ser 0054 | 04 Nr 64 | 05 Vol 000 |
| | | 06 Iss 001 | 07 B. Pg. 0053 |
| | | 45 E. Pg. 0059 | 10 Date NONE |

Transliterated Title

IZLUKLENIYE Sb¹²⁵

09 English Title RADIATION OF Sb¹²⁵

43 Source LENINGRAD. UNIVERSITET. VESTNIK. SERIYA FIZIKI I KHIMII (RUSSIAN)

48 Author ANTON'YEVA, N. M.

98 Document Location

16 Co-Author
KATYKHIN, G. S.

47 Subject Codes 20

16 Co-Author
NONE

39 Topic Tags: conversion electron spectrum, spectrometer, spectrograph, neutron irradiation, beta spectrum

16 Co-Author
NONE

16 Co-Author
NONE

ABSTRACT The β -spectrum and the spectrum of conversion electrons of Sb¹²⁵ have been studied with the help of a magnetic spectrometer type "Ketron" (B. S. Dzhelapov and A. A. Bashilov. Izv. AN SSSR, ser, fiz. 14, 263, 1950) with 0.5% resolving power and a magnetic spectrograph with 0.15% resolution. Investigation was conducted on a single source specimen, chemically separated and neutron irradiated. Among the various Sb¹²⁵ measurements conducted were: the β -spectrum, K and L conversion spectra, γ -radiation energy, multipole order transitions, and the Sb¹²⁵-Te¹²⁵ decay process where more precise data were obtained than hitherto possible for the energy of 145, 321.3 and 463.1 KeV levels. The authors are grateful to V. I. Perrimond, A. A. Zhdanov, N. Stegalkina, L. Kolmy*kova and Yu. Golubev for their assistance." Orig. art. has: 5 figures, 4 tables, and 1 formula. English Translation: 7 pages

ITIS INDEX CONTROL FORM

| | | | |
|------------------------|--------------------------------|------------------------------|-------------------------------|
| 01 Acc Nr TP7500504 | 68 Translation Nr MT6400358 | 65 X Ref Acc Nr AP4024459 | 76 Eecl/Frame Nr 1654 1451 |
| 97 Header Clas UNCL | 63 Clas UNCL, 0 | 64 Control Markings 0 | 64 Expansion UR |
| 02 Ctry UR | 03 Ref 0054 | 04 Yr 64 | 05 Vol 000 |
| 06 Iss 001 | 07 B. Pg. 0060 | 08 B. Pg. 0068 | 10 Date NONE |

Transliterated title ZAVISIMOST' UGLOV ORYENTATSII V DINAMICHESKOM DVOYNOM
LUCHEPRELOMLENII OT GRADIENTA SKOROSTI. UCHET ANIZOTROPII GIDRODINAMICHESKOGO
VZAIMODEYSTVIYA

09 English Title DEPENDENCE OF ANGLES OF ORIENTATION IN DYNAMIC DOUBLE
REFRACTION ON THE VELOCITY GRADIENT

43 Source LENINGRAD. UNIVERSITET. VESTNIK. SERIYA FIZIKI I KHIMII (RUSSIAN)

42 Author RUDTOV, V. P. 98 Document Location

16 Co-Author NONE 47 Subject Codes 07

16 Co-Author NONE 39 Topic Tags: flow angle, double refraction
molecule, macromolecule, polymerization
flow velocity

16 Co-Author NONE

16 Co-Author NONE

ABSTRACT The orientation angle of polymethylmetacryl (PMMA) solutions in tetrabromethane for six fractionated and unfractionated specimens has been studied in a velocity gradient range (shear rate) 4 to 2000 sec⁻¹. The velocity of the solvent η_0 varied from 6 to 15.6 cp. In the region of small velocity gradients it is shown that $\tan 2\phi/g$ is a function of g^2 , where $\phi = \pi/4 - \chi$ (χ - angle between macromolecule orientation direction and flow velocity) and g - shear rate. A general parameter gr (r - initial slope of extinction angle) is found to correlate the experimental data successfully. For $gr \ll 1$ this relationship is given by $\frac{\tan 2\phi}{g} = 1 - \frac{A}{gr} + \dots$

It is seen that $\tan 2\phi$ is proportional to gr for $gr \ll 1$, and for $gr > 15$ the coefficient of proportionality changes from 1 to 0.2. For $\eta_0 > 5 \times 10^{-2}$ poise, $A = 0.23 \pm 0.07$ for all 6 fractions studied. The influence of the hydrodynamic anisotropy interaction is taken into account, leading to

$$[\alpha]_{gr} = gr \left[1 - \frac{3}{8} (gr)^2 + \dots \right]$$
 with the corresponding viscosity

$$[\eta]_{gr} = [\eta]_{gr=0} \left(1 - \frac{7}{8} (gr)^2 + \dots \right)$$
. The magnitude of double refraction then becomes

$$\left(\frac{\Delta n}{c} \right)_{gr=0} = k \beta' \left[1 + \frac{1}{2} \beta'^2 \left(1 - \frac{7}{4} \zeta \right) + \dots \right]$$
; where $\beta' = \beta \left(1 + \frac{\zeta}{2} \right)$ and k is a constant.

A good agreement is observed between the theory (taking into account the hydrodynamic anisotropy) and the experimental data. Orig. art. has: 15 formulas and 7 figures. English Translation: 9 pages.

ITIS INDEX CONTROL FORM

| | | | | | | | |
|--|----------------|--------------------------------|---------------|---|-------------------|------------------------------------|-----------------|
| 61 Acc Nr TP7500505 | | 68 Translation Nr MT6400358 | | 65 X Ref Acc Nr AP4024460 | | 76 Reel/Frame Nr 1654 1452 | |
| 62 Number Clas UNCL | | 63 Clas UNCL, 0 | | 64 Control Markings 0 | | 94 Expansion 40 Ctry Info UR | |
| 69 Ctry UR | 85 Ref 0054 | 84 Yr 64 | 83 Vol 000 | 86 Iss 001 | 87 B. Pg. 0069 | 88 B. Pg. 0074 | 89 Date NONE |
| 66 Transliterated Title OPREDELENIYE VODORODA V ALYUMINYEVIKH SPLAVAKH METODOM IZOTOPICHESKOGO URAVNOVESHIVANIYA | | | | | | | |
| 67 English Title DETERMINATION OF HYDROGEN IN ALUMINUM ALLOYS BY THE METHOD OF ISOTOPIC BALANCING | | | | | | | |
| 43 Source LENINGRAD. UNIVERSITET. VESTNIK. SERIYA FIZIKI I KHIMII (RUSSIAN) | | | | | | | |
| 48 Author ORLOVA, N. M. | | | | 98 Document Location | | | |
| 14 Co-Author PETROV, A. A. | | | | 47 Subject Codes 07 | | | |
| 16 Co-Author NONE | | | | 39 Topic Tags: alloy, hydrogen, aluminum, chemical equilibrium, exchange reaction, sorption, desorption | | | |
| 18 Co-Author NONE | | | | | | | |
| 19 Co-Author NONE | | | | | | | |

ABSTRACT A spectral isotopic method for the determination of hydrogen in aluminum and in some of its alloys has been developed. Both cast aluminum alloys and pressure-worked specimens were studied. The isotopic equilibrium was carried out on cylindrical specimens 5-6 mm in diameter, weighing 10-20 grams at 500 C temperatures (much lower than melting point of aluminium), with experimental errors in hydrogen volume determination of the order of $0.05 \pm 0.01 \text{ cm}^3$. The isotopic equilibrium duration in Mg, Mn, and Cu alloys was 25-30 min. The type of treatment previously used on the specimen showed no observable effect on the isotopic exchange. The residual hydrogen content measured for the various aluminium alloys was 0.1-0.2 $\text{cm}^3/100 \text{ gm}$. This method enables one to determine separately the gas content in the surface layer as well as in the bulk of the aluminum specimen. Because of hygroscopic films observed on the aluminum and the absorption of water vapor, some of the aspects of the sorption and desorption of hydrogen in the surface oxide layer were also studied. "The authors wish to thank Professor A. N. Zaydel' for the advice given." Orig. Art. has: 4 tables and 1 figure. English Translation: 6 pages.

ITIS INDEX CONTROL FORM

| | | | | | | | |
|------------------------|--------------------------------|------------------------------|------------------------------------|---------------|-------------------|-------------------|-----------------|
| 01 Acc Nr TP7500506 | 68 Translation Nr MT6400353 | 65 X Ref Acc Nr AP4024461 | 76 Reel/Frame Nr 1654 1453 | | | | |
| 97 Header Clas UNCL | 63 Clas UNCL, 0 | 64 Control Markings 0 | 94 Expansion 40 Ctry Info UR | | | | |
| 02 Ctry UR | 03 Ref 0054 | 04 Yr 64 | 05 Vol 000 | 06 Iss 001 | 07 B. Pg. 0075 | 08 E. Pg. 0078 | 10 Date NONE |

Transliterated Title

O "SREDNEM VREMENI SVOBODNOGO PROBEGA" MOLEKUL O₂

09 English Title ON THE "MEAN TIME OF THE FREE PATH" OF O₂ MOLECULES

43 Source Leningrad. Universitet. Vestnik. Seriya Fiziki i Khimii (Russian)

42 Author
SUSLOV, A. K.

98 Document Location

16 Co-Author
NONE

47 Subject Codes 20

16 Co-Author
NONE

39 Topic Tags: telluric current, absorption line, atmosphere, kinetic theory, Doppler effect

16 Co-Author
NONE

16 Co-Author
NONE

ABSTRACT Assuming that the broadening of the O₂ telluric lines is due to collision attenuation, the line contour can be described by the expression

$$I = I_0 \exp\left(-\frac{2\pi \nu \Delta \nu}{c} T_0\right)$$

for lines whose intensity at the line center is zero. Several lines in the spectrum of the center of the solar disk, which satisfy this condition, were scanned photometrically to determine the mean free flight time T_0 . Investigation of the P₁₈ line in the A band (wavelength 7659.37 Å) gave $T_0 = 8.4 \times 10^{-12}$ sec. Measurements at 3060 m above sea level of the P₈ line (wavelength 7632.17 Å) resulted in the value $T_0 = 8.21 \times 10^{-12}$ sec. A theoretical calculation based on the kinetic theory of gases leads to a mean collision frequency of 2×10^9 sec⁻¹ for O₂. The discrepancy is due somewhat to Doppler broadening but primarily to the nonuniform distribution of oxygen in the atmosphere and to the differences of pressure and temperature in the various layers of the atmosphere. It is concluded that from the observed values of T_0 a more precise model of the standard atmosphere can be made. Orig. art. has: 8 equations and 2 figures. English Translation. 4 pages.

ITIS INDEX CONTROL FORM

| | | | | | | | |
|---|--------------------------------|------------------------------|-------------------------------|--|-------------------|-------------------|-----------------|
| 01 Acc Nr TP7500507 | 68 Translation Nr MT6400358 | 65 X Ref Acc Nr AP4024462 | 76 Reel/Frame Nr 1654 1654 | | | | |
| 02 Number Clas UNCL | 63 Clas UNCL, 0 | 64 Control Markings 0 | 94 Expansion UR | | | | |
| 03 Ctry UR | 08 Ser 0054 | 04 Yr 64 | 05 Vol 000 | 06 Iss 001 | 07 E. Pg. 0079 | 43 E. Pg. 0081 | 10 Date NONE |
| Transliterated Title PRIBLIZHENIYE IZOLIROVANNOY LINII PRI PERENOSE LUCHISTOY ENERGII V VERKHNEY ATMOSFERE | | | | | | | |
| 09 English Title APPROXIMATION OF ISOLATED LINE DURING TRANSFER OF RADIATIVE ENERGY IN THE UPPER ATMOSPHERE | | | | | | | |
| 43 Source LENINGRAD. UNIVERSITET. VESTNIK. SERIYA FIZIKI I KHIMII (RUSSIAN) | | | | | | | |
| 44 Author SHVED, G. M. | | | | 98 Document Location | | | |
| 17 Co-Author NONE | | | | 47 Subject Codes 20, 04 | | | |
| 16 Co-Author NONE | | | | 39 Topic Tags: line spectrum, upper atmospheric radiation, stratosphere, absorption spectrum, optical path | | | |
| 16 Co-Author NONE | | | | | | | |
| 16 Co-Author NONE | | | | | | | |

ABSTRACT The use of the approximation of an insulated line for simulation of infrared spectra of absorption in the mesosphere and upper stratosphere is possible, thanks to the decrease in the width of the line with the drop in pressure. The author discusses the limits of validity of this approximation for computing flows and influxes of radiant energy. The first requires the giving of

$$\frac{\partial A_p(z, z')}{\partial z}, \text{ the second, of } \frac{\partial^2 A_p(z, z')}{\partial z \partial z'}, \text{ where } A_p(z, z') \text{ is the absorption}$$

function for radiation flow between levels of the atmosphere z and z' . Orig. art. has: 2 figures and 2 formulas. English Translation: 3 pages.

ITIS INDEX CONTROL FORM

| | | | | | | | |
|------------------------|--------------------|--------------------------------|---------------|-----------------|-------------------|-------------------------------|--------------------|
| 01 Acc Nr TP7500508 | | 68 Translation Nr MT6400358 | | 65 X Ref Acc Nr | | 76 Reel/Frame Nr 1654 1455 | |
| 97 Header Clas UNCL | 63 Clas UNCL, 0 | 64 Control Markings 0 | | | 94 Espanski | | 40 Ctry Info UR |
| 02 Ctry UR | 03 Ref 0054 | 04 Yr 64 | 05 Vol 000 | 06 Iss 001 | 07 E. Pg. 0082 | 45 E. Pg. 0094 | 10 Date NONE |

Transliterated title O POLIANIONAKH V RASTVORAKH

09 English Title ON POLYANIONS IN SOLUTIONS

43 Source LENINGRAD. UNIVERSITET. VESTNIK. SERIYA FIZIKI I KHMII (RUSSIAN)

42 Author
SILLEN, L. G.

98 Document Location

16 Co-Author
NONE

47 Subject Codes 07

16 Co-Author
NONE

39 Topic Tags: boron compound, equilibrium constant, vanadate, molybdate, chromate, polymer structure

16 Co-Author
NONE

16 Co-Author
NONE

ABSTRACT In this paper is given a critical survey on the polymerization of anion-complexes in aqueous solutions. The author draws his attention to the systems of polyborates, wolframates, vanadates, molybdates and chromates. A new theoretical method using computer technique has been proposed. This method has given good results based on experimental measurements. The question on the structure of polymers is studied as well. English Translation: 5 pages.

ITIS INDEX CONTROL FORM

| | | | | | | | |
|------------------------|--------------------------------|--------------------------|------------------------------------|---------------|-------------------|-------------------|-----------------|
| 61 Acc Nr TF7500509 | 68 Translation Nr MI6400358 | 65 X Ref Acc Nr | 76 Reel/Frame Nr 1654 1456 | | | | |
| 67 Header Clas UNCL | 63 Clas UNCL, 0 | 64 Control Markings 0 | 94 Expansion 40 Ctry Info UR | | | | |
| 08 Ctry UR | 09 Noz 0054 | 04 Yr 64 | 05 Vol 000 | 06 Iss 001 | 07 B. Pg. 0095 | 08 B. Pg. 0098 | 10 Date NONE |

Transliterated Title

K VOPROSU O FAZOVYKH PEREKHODAKH V TVERDYKH TELAKH

09 English Title QUESTION ABOUT PHASE TRANSITIONS IN SOLID BODIES

43 Source Leningrad. Universitet. Vestnik. Seriya Fiziki i Khimii (Russian)

| | |
|-------------------------------------|--|
| 45 Author DOBROTIN, R. B. | 98 Document Location |
| 16 Co-Author SUVOROV, A. V. | 47 Subject Codes 07, 20 |
| 16 Co-Author KONDRAT'YEV, YU. V. | 39 Topic Tags: phase transition, heat absorption, heat transfer, calorimetry, heat of fusion, thermal effect |
| 16 Co-Author NONE | |
| 16 Co-Author NONE | |

ABSTRACT The heat absorption in the temperature region of phase transformation of WCl_6 and $TaCl_5$ has been measured. Some considerations concerning the influence of the character of heat transfer in the calorimetric cell on the temperature interval of specific heat anomaly have been expressed. English Translation: 5 pages.

ITIS INDEX CONTROL FORM

| | | | |
|------------------------|--------------------------------|--------------------------|-------------------------------|
| 01 Acc Nr TP7500510 | 68 Translation Nr MT6400358 | 65 X Ref Acc Nr | 76 Reel/Frame Nr 1654 1457 |
| 97 Header Clas UNCL | 63 Clas UNCL, 0 | 64 Control Markings 0 | 94 Expansion UR |
| 02 Ctry UR | 03 Ref 0054 | 04 Yr 64 | 05 Vol 000 |
| 06 Iss 001 | 07 B. Pg. 0099 | 08 B. Pg. 0104 | 10 Date NONE |

Transliterated Title ELEKTROKINETICHESKIYE SVOYSTVA OSADKOV FERROTSIANIDA
MEDL. POLUCHENNYKH V RAZLICHNYKH USLOBIYAKH

09 English Title ELECTROKINETIC PROPERTIES OF DEPOSITS OF COPPER FERROCYANIDE
OBTAINED IN DIFFERENT CONDITIONS

43 Source LENINGRAD. UNIVERSITET. VESTNIK. SERIYA FIZIKI I KHIMII (RUSSIAN)

42 Author KARPOVA, I. F.

98 Document Location

16 Co-Author SMIRNOVA, V. N.

47 Subject Codes 20, 07

16 Co-Author FIRDRIKHSBERG, D. A.

39 Topic Tags: copper, chloride, potassium
chloride, cyanide, ion concentration

16 Co-Author NONE

16 Co-Author NONE

ABSTRACT The charge of precipitates measured in KCl and HCl solutions depends on the anionic nature of copper salt employed for precipitation. The precipitates formed under the conditions of the excess of copper ions are positively charged in the cases of copper sulphate and copper chloride. In other investigated cases the charge is negative. In CuCl₂ solutions all precipitates acquire positive charge. Surface conductance has a minimum and in some cases reaches zero at the isoelectric point. English Translation: 7 pages.

ITIS INDEX CONTROL FORM

| | | | | | | | |
|---|----------------|--------------------------------|---------------|---|-------------------|------------------------------------|-----------------|
| 61 Acc Nr TF7500511 | | 68 Translation Nr MT6400358 | | 65 X Ref Acc Nr | | 76 Reel/Frame Nr 1654 1458 | |
| 67 Header Clas UNCL | | 63 Clas UNCL, 0 | | 64 Control Markings 0 | | 94 Expansion 40 Ctry Info UR | |
| 62 Ctry UR | 68 Ind 0054 | 64 Yr 64 | 65 Vol 000 | 66 Iss 001 | 67 E. Pg. 0105 | 68 E. Pg. 0110 | 69 Date NONE |
| Transliterated Title RAZDELENIYE I IDENTIFIKATSIYA PRODUKTOV REAKTSII GLUBOKOGO RASSHCHESPLENIYA GERMANIYA BYSTRYMI PROTONAMI | | | | | | | |
| 69 English Title SEPARATING AND IDENTIFYING REACTION PRODUCTS OF DEEP SPLITTING OF GERMANIUM BY FAST PROTONS | | | | | | | |
| 43 Source LENINGRAD. UNIVERSITET. VESTNIK. SERIYA FIZIKI I KHIMII (RUSSIAN) | | | | | | | |
| 48 Author MURIN, A. N. | | | | 98 Document Location | | | |
| 15 Co-Author TOMILOV, S. B. | | | | 47 Subject Codes 07 | | | |
| 16 Co-Author YUTLANDOV, I. A. | | | | 39 Topic Tags: ion exchange chromatography, germanium, isotope | | | |
| 16 Co-Author NONE | | | | | | | |
| 16 Co-Author NONE | | | | | | | |

ABSTRACT A germanium target was irradiated with 660 Mev protons. The spallation products were separated by ion-exchange chromatographic methods. Identification of isotopes and check of radiochemical purity of separated fractions was carried out by means of a gamma-spectrometer. A 145 kev γ -line found out in the zinc fraction was ascribed to Zn^{72} . English Translation: 7 pages.

ITIS INDEX CONTROL FORM

| | | | | | | | |
|--|--------------------------------|--------------------------|------------------------------------|--|-------------------|-------------------|-----------------|
| 01 Acc Nr TP7500512 | 68 Translation Nr MT6400358 | 85 X Ref Acc Nr | 76 Reel/Frame Nr 1654, 1459 | | | | |
| 97 Header Clas UNCL | 63 Clas UNCL, 0 | 64 Control Markings 0 | 94 Expansion 40 Ctry Info UR | | | | |
| 02 Ctry UR | 03 Ref 0054 | 04 Yr 64 | 05 Vol 000 | 06 Iss 001 | 07 B. Pg. 0111 | 08 E. Pg. 0121 | 10 Date NONE |
| Transliterated Title TERMODINAMICHESKOYE ISSLEDOVANIYE TVERDYKH RASTVOROV V SISTEME NaCl - KCl - CdCl ₂ PRI TEMPERATURAKH 540, 580, 623° C | | | | | | | |
| 09 English Title THERMODYNAMIC INVESTIGATION OF SOLID SOLUTIONS IN A NaCl - KCl - CdCl ₂ SYSTEM AT TEMPERATURES OF 540, 580, 623° C. | | | | | | | |
| 43 Source LENINGRAD. UNIVERSITET. VESTNIK. SERIYA FIZIKI I KHIMII (RUSSIAN) | | | | | | | |
| 42 Author SHUL'TS, M. M. | | | | 98 Document Location | | | |
| 16 Co-Author RUSHUEVA, I. M. | | | | 47 Subject Codes 07, 20 | | | |
| 16 Co-Author NONE | | | | 99 Topic Tags: thermodynamic characteristic, thermodynamic equilibrium, solid solution, sodium chloride, potassium chloride, cadmium compound | | | |
| 16 Co-Author NONE | | | | | | | |
| 16 Co-Author NONE | | | | | | | |

ABSTRACT The activities of the components of the solid solutions NaCl - KCl - CdCl at 540, 580, 623° C have been determined by the method of the third component. $\Delta\phi$, ΔH , ΔS of the formation of these solid solutions have been calculated. English Translation: 12 pages.

ITIS INDEX CONTROL FORM

| | | | | | | | |
|--|----------------|--------------------------------|---------------|---|-------------------|---------------------------------|-----------------|
| 01 Acc Nr TP7500513 | | 68 Translation Nr MT6400358 | | 65 X Ref Acc Nr | | 76 Reel/Frame Nr 1654 1460 | |
| 97 Header Class, C: Class UNCL | | 64 Control Markings UNCL, 0 | | 0 | | 94 Expansion 40 Ctry Info UR | |
| 02 Ctry UR | 03 Ind 0054 | 04 Pr 64 | 05 Vol 000 | 06 Iss 001 | 07 E. Pg. 0122 | 08 E. Pg. 0125 | 10 Date NONE |
| Transliterated Title AMPEROMETRICHESKOYE TITROVANIYE TRILONOM B NEKOTORYKH KATIONOV S VRASHCHAYUSHCHIMSYA MIKROPLATINOVYM ELEKTRODOM | | | | | | | |
| 09 English Title AMPEROMETRIC TITRATING CERTAIN CATIONS BY TRILON B WITH REVOLVING MICROPLATINUM | | | | | | | |
| 43 Source Leningrad. Universitet. Vestnik. Seriya Fiziki i Khimii (Russian) | | | | | | | |
| 42 Author REYSHAKHRIT, L. S. | | | | 98 Document Location | | | |
| 45 Co-Author PUSTOSHKINA, M. P. | | | | 47 Subject Codes 07, 20 | | | |
| 16 Co-Author TIKHONOVA, Z. I. | | | | 39 Topic Tags: oxidation, anodic oxidation, amperometric titration, polarographic analysis, electrode potential | | | |
| 16 Co-Author NONE | | | | | | | |
| 16 Co-Author NONE | | | | | | | |

ABSTRACT An investigation of the oxidation process of trylone B has been carried out on rotating platinum anodes in solutions of 0.1 n $\text{NH}_4\text{NO}_3 + \text{NH}_4\text{OH}$ (PH = 8.2 - 10.0) and 1 n KNO_2 (PH = 5.7) at 20° C. The oxidation rate is determined by diffusion at potentials more positive, than +0.7 v and +0.85 v respectively. Demonstrated is the possibility of amperometric titration with a microplatinum rotating electrode of $\text{Sr}(\text{NO}_3)_2$ solutions against 0.1 n $\text{NH}_4\text{NO}_3 + \text{NH}_4\text{OH}$ and those of CuSO_4 , NiSO_4 , $\text{H}_7 [\text{P} (\text{Mo}_2\text{O}_7)_6]$ - against 0.2 n KNO_2 with the contents of Sr, Cu, Ni and Mo from .25 to 70 mg using trylone B? English Translation: 5 pages.

ITIS INDEX CONTROL FORM

| | | | | | | | |
|--|----------------|--------------------------------|---------------|---|-------------------|-------------------------------|-----------------|
| 01 Acc Nr TP7500514 | | 68 Translation Nr MT6400358 | | 65 X Ref Acc Nr | | 76 Reel/Frame Nr 1654 1461 | |
| 97 Header Clas UNCL | | 63 Clas UNCL, 0 | | 64 Control Markings C | | 94 Expansion UR | |
| 02 Ctry UR | 03 Ref 0054 | 04 Yr 64 | 05 Vol 000 | 06 Iss 001 | 07 B. Pg. 0126 | 08 B. Pg. 0131 | 10 Date NONE |
| Transliterated Title SKOROST' OKISLENIYA MEDI PRI KRATKOVREMENNYKH NAGREVAKH DO VYSOKOY TEMPERATURY | | | | | | | |
| 09 English Title OXIDATION RATE OF COPPER DURING BRIEF HEATING TO HIGH TEMPERATURES | | | | | | | |
| 43 Source LENINGRAD. UNIVERSITET. VESTNIK. SERIYA FIZIKI I KHIMII (RUSSIAN) | | | | | | | |
| 42 Author TIKHOMIROV, V. I. | | | | 98 Document Location | | | |
| 16 Co-Author KORYTKOVA, E. I. | | | | 47 Subject Codes 07, 20 | | | |
| 16 Co-Author NONE | | | | 39 Topic Tags: oxidation rate, high temp- erature oxidation, copper, anodic oxidation | | | |
| 16 Co-Author NONE | | | | | | | |
| 16 Co-Author NONE | | | | | | | |

ABSTRACT The methods of investigation of the oxidation rate of metals and alloys during heatings of short duration (about some seconds) up to the high temperature have been developed. It has been shown that copper oxidation during heatings of short duration (10-20 seconds) up to 1020-1070° C follows the parabolic law. When the temperature decreases as low as 900-1000° C, the linear law begins to predominate. English Translation: 8 pages.

ITIS INDEX CONTROL FORM

| | | | | | | | |
|---|--|--------------------------------|-------------|--|---------------|-------------------------------|-------------------|
| 01 Acc Nr TP7500515 | | 68 Translation Nr MT6400358 | | 63 X Ref Acc Nr | | 76 Reel/Frame Nr 1654 1462 | |
| 97 Header Clas UNCL | | 63 Clas UNCL, 0 | | 64 Control Markings 0 | | 94 Expansion UR | |
| 02 Ctry UR | | 03 Ref 0054 | 04 Yr 54 | 05 Vol 000 | 06 Iss 001 | 07 B. Pg. 0132 | 08 B. Pg. 0141 |
| 10 Date NONE | | | | | | | |
| Transliterated title SPEKTROFOTOMETRICHESKOYE ISSLEDOVANIYE ASKORBINATNYKH KOMPLEKSOV | | | | | | | |
| 09 English Title SPECTROPHOTOMETRIC INVESTIGATION OF ASCORBINATE COMPLEXES | | | | | | | |
| 43 Source LENINGRAD. UNIVERSITET. VESTNIK. SERIYA FIZIKI I KHIMII (RUSSIAN) | | | | | | | |
| 42 Author STOLYAROV, K. P. | | | | 98 Document Location | | | |
| 16 Co-Author AMANTOVA, I. A. | | | | 47 Subject Codes 07, 20 | | | |
| 16 Co-Author NONE | | | | 39 Topic Tags: spectrophotometric analysis, absorption spectrum, absorption band, ascorbic acid, optic density, barium, zinc | | | |
| 16 Co-Author NONE | | | | | | | |
| 16 Co-Author NONE | | | | | | | |

ABSTRACT The formation of ascorbic complexes of the elements of the second and third groups of the periodic system (excluding strontium and mercury) causes variations in the absorption spectra of simple salt solutions: the maxima of light absorption increase and sometimes shift into long wave region (Pr, Nd, Ho, Er.); there increases absorption in the 320-340 μ k region associated with the displacement of the absorption band of ascorbic acid into long wave region (Zn, Cd and elements of the third group, excluding B); obtained for some elements are negative values of optical density in the $\lambda = 320-370$ μ k region, i.e. light absorption decreases (Be, Zn, Cd, B, Al, Sc, Y, La, Is, Dy, Ho, Er, Ln); there appear new maxima (Mg 320-340 μ k; Ca and Ba 345 μ k; Zn and Cd 390 μ k). English Translation: 11 pages.

ITIS INDEX CONTROL FORM

| | | | | | | | |
|------------------------|----------------|--------------------------------|---------------|--------------------------|-------------------|------------------------------------|-----------------|
| 01 Acc Nr TP7500516 | | 68 Translation Nr MT6400358 | | 65 X Ref Acc Nr | | 76 Reel/Frame Nr 1654 1463 | |
| 97 Header Clas UNCL | | 63 Clas UNCL, 0 | | 64 Control Markings 0 | | 94 Expansion 40 Ctry Info UR | |
| 02 Ctry UR | 03 Ref 0054 | 04 Yr 64 | 05 Vol 000 | 06 Iss 001 | 07 B. Pg. 0142 | 08 E. Pg. 0146 | 10 Date NONE |

Transliterated Title
VOSSTANOVITEL'NYYE SVOYSTVA IONITOV

09 English Title
REDUCING PROPERTIES OF IONITES

43 Source
LENINGRAD. UNIVERSITET. VESTNIK. SERIYA FIZIKI I KHIMII (RUSSIAN)

| | | | |
|----------------------------------|--|--|--|
| 42 Author NECHAY, N. A. | | 98 Document Location | |
| 16 Co-Author ZVEREVA, M. N. | | 47 Subject Codes 07 | |
| 16 Co-Author GREKOVICH, T. M. | | 39 Topic Tags: ion, ion exchange resins, ion concentration, ion temperature, cation exchange resin, potassium, hydrogen ion concentration | |
| 16 Co-Author NONE | | | |
| 16 Co-Author NONE | | | |

ABSTRACT

It has been demonstrated by the present investigation that ion-exchange resins KV-2, KB-4П-2, СБСР, ЭДЭ-10-П, АН-1, АВ-17 are not oxidized by 0,06 n solutions $Fe_2(SO_4)_3$ at $[H^+] = 10^{-10} - 5 \frac{g-ion}{l}$; the resins АВ-17 and KB-4П-2 are not oxidized by 0,02 n solutions NH_4VO_3 at $[H^+] = 10^{-7} - 5 \frac{g-ion}{l}$ and KV-2 - at $[H^+] = 10^{-7} - 2,6 \frac{g-ion}{l}$; KB-4П-2 is not oxidized by 0,02 n solutions $K_2Cr_2O_7$ at $[H^+] = 10^{-10} - 2,6 \frac{g-ion}{l}$, and АВ-17 - at $[H^+] = 10^{-10} - 10^{-3} \frac{g-ion}{l}$; all investigated ion-exchange resins are oxidized by 0,02 n solutions $KMnO_4$ at $[H^+] = 10^{-10} - 5 \frac{g-ion}{l}$.

According to their stability towards oxidants ion-exchange resins can be arranged in a row as follows: KB-4 П-2 > АВ-17 > KV-2 > АН-1 > СБСР > ЭДЭ-10-П > АВ-16.

The partial oxidation of the ion-exchange resins by 0,02 n solution $K_2Cr_2O_7$ has been stated to have practically no effect on the exchange capacity value. English Translation: 6 pages.

ITIS INDEX CONTROL FORM

| | | | | | | | |
|------------------------|----------------|--------------------------------|---------------|--------------------------|-------------------|-------------------------------|-----------------|
| 61 Acc Nr TF7500517 | | 68 Translation Nr MT6400358 | | 65 X Ref Acc Nr | | 76 Reel/Frams Nr 1654 1464 | |
| 97 Reader Clas UNCL | | 63 Clas UNCL 0 | | 64 Control Markings 0 | | 94 Expansion UR | |
| 62 Ctry UR | 63 Res 0054 | 64 Yr 64 | 65 Vol 000 | 66 Iss 001 | 67 B. Pg. 0147 | 68 E. Pg. 0151 | 10 Date NONE |

Transliterated Title **INFRAKRASNYE SPEKTRY POGLOSHCHENIYA BEZVODNYKH SERNOY I ORTOFOSFORNOY KISLOT**

09 English Title **INFRARED ABSORPTION SPECTRA OF ANHYDROUS SULFURIC AND ORTHOPHOSPHORIC ACIDS**

43 Source **LENINGRAD. UNIVERSITET. VESTNIK. SERIYA FIZIKI I KHIMII (RUSSIAN)**

| | |
|---|--|
| 42 Author SHCHUKAREV, S. A. | 98 Document Location |
| 16 Co-Author BALICHEVA, T. G. | 47 Subject Codes 07 |
| 16 Co-Author BORCHA, K. YA. | 99 Topic Tags: sulfuric acid, sulfuric oxide, phosphoric acid, phosphorus, hydrogen compound, orthophosphoric acid, hydrogen bonding |
| 16 Co-Author KUKHAREVA, M. A. | |
| NONE | |

ABSTRACT The infra-red absorption spectra from 3700 to 2350 cm^{-1} of concentrated anhydrous sulphuric and orthophosphoric acids at 20° C and in the region of valent O-H vibrations at -40° C have been studied. The roughly estimated values of the force constant and those of the interatomic C-H bond length in these acids point to the considerable increase of the strength of hydrogen bonds among molecules in the series $\text{HClO}_4 < \text{H}_2\text{SO}_4$ as the length of the O-H bond increases. Molar absorption coefficients of sulphuric and orthophosphoric acids have been determined. English Translation: 6 pages.

ITIS INDEX CONTROL FORM

| | | | | | | | |
|--|--------------------------------|------------------------------|------------------------------------|---|-------------------|-------------------|-----------------|
| 01 Acc Nr TP7500518 | 68 Translation Nr MT6400358 | 65 X Ref Acc Nr AP4024463 | 76 Reel/Frame Nr 1654 1655 | | | | |
| 97 Header Clas UNCL | 63 Clas UNCL, 0 | 64 Control Markings 0 | 94 Expansion 40 Ctry Info UR | | | | |
| 02 Ctry UR | 03 Ref 0054 | 04 Yr 64 | 05 Vol 000 | 06 Iss 001 | 07 B. Pg. 0152 | 08 E. Pg. 0155 | 10 Date NONE |
| Transliterated title ZAVISIMOST' UGLA ORIENTATSII DVOYNOGO LUCHEPRELOMLENIYA V POTOKE OT KONTSENTRATSII RASTVORA | | | | | | | |
| 09 English Title DEPENDENCE OF ORIENTATION ANGLE OF DOUBLE REFRACTION IN FLOW ON CONCENTRATION OF SOLUTION | | | | | | | |
| 43 Source LENINGRAD. UNIVERSITET. VESTNIK. SERIYA FIZIKI I KHIMII (RUSSIAN) | | | | | | | |
| 42 Author BUDTOV, V. P. | | | | 98 Document Location | | | |
| 16 Co-Author NONE | | | | 47 Subject Codes 20, 18 | | | |
| 16 Co-Author NONE | | | | 39 Topic Tags: acetone, flow angle, solution concentration, macromolecule | | | |
| 16 Co-Author NONE | | | | | | | |
| 16 Co-Author NONE | | | | | | | |

ABSTRACT An analytic study has been made of concentration dependence of the extinction angle in polymer solutions for 6 fractions of PMMA in solvents of high ($3 \leq \eta_0 \leq 15.6$ sp, tetrabromoethane) and low ($\eta_0 < 1$ sp, acetone, butylacetate, ethylacetate, methyl-ethyl ketone) viscosities. Some methods of extrapolation of

$$\left[\frac{1}{\epsilon} \right]_{c \rightarrow 0} = \nu = A \Delta \left(\frac{\nu}{c} \right)_{c \rightarrow 0} = [\eta] (1 + k_1 [\eta] + \dots)$$

(ν -velocity gradient, M -molecular weight, η_0 - viscosity, and $[\eta]$ characteristic relaxation time) have been offered for C , polymer concentration in solution (tending towards zero) in the high viscosity solvents. It is shown that the study of the dependence

$$\left[\frac{1}{\epsilon} \right]_{c \rightarrow 0} \text{ vs } \left(\frac{\nu}{c} \right)$$

with γ as a function of η_{sp}/c makes it possible to draw conclusions concerning the nature of dynamo-optical effects and internal kinematic viscosity of macromolecules. "The author is grateful to Professor V. N. Tsvetkov for his advice and help in the work." Orig. art. has: 3 figures, 2 formulas, and 1 table. English Translation: 4 pages

ITIS INDEX CONTROL FORM

| | | | | | | | |
|------------------------|--------------------------------|--------------------------|------------------------------------|---------------|-------------------|-------------------|-----------------|
| 01 Acc Nr TP7500519 | 68 Translation Nr MT6400358 | 65 X Ref Acc Nr | 76 Reel/Frame Nr 1654 1465 | | | | |
| 97 Header Clas UNCL | 63 Clas UNCL, 0 | 64 Control Markings 0 | 94 Expansion 40 Ctry Info UR | | | | |
| 02 Ctry UR | 03 Ref 0054 | 04 Yr 64 | 05 Vol 000 | 06 Iss 001 | 07 B. Pg. 0155 | 08 B. Pg. 0157 | 10 Date NONE |

Transliterated Title

OB INFRAKRASNOM SPEKTRE SUMERECHNOGO NEBA

09 English Title ABOUT INFRARED SPECTRUM OF TWILIGHT SKY

43 Source Leningrad, Universitet. Vestnik. Seriya Fiziki i Khimii (Russian)

45 Author
GNILOVSKIY, YE. V.

98 Document Location

15 Co-Author
NONE

47 Subject Codes 04

16 Co-Author
NONE

39 Topic Tags: spectrum, electrophotography, spectrophotometry, light reflection, twilight, atmospheric diffusion optic phenomena

16 Co-Author
NONE

16 Co-Author
NONE

Abstract The data on the observation of the twilight sky in the infra-red part of the spectrum of about 1.1 micron are given. Apparatus are described, typical spectrum of the twilight sky with different setting angle of the sun behind the horizon is regarded. English Translation: 3 pages.

ITIS INDEX CONTROL FORM

| | | | | | | | |
|---|--|--------------------------------|-------------|--|---------------|-------------------------------|-----------------|
| 01 Acc Nr TP7500520 | | 68 Translation Nr MT6400358 | | 65 X Ref Acc Nr AP4024464 | | 76 Reel/Frame Nr 165A 1466 | |
| 97 Header Clas UNCL | | 63 Clas UNCL, 0 | | 64 Control Markings 0 | | 94 Expansh UR | |
| 02 Ctry UR | | 03 Ref 0054 | 04 Yr 64 | 05 Vol 000 | 06 Iss 001 | 07 B. Pg. 0157 | 10 Date NONE |
| Transliterated Title FAZOVYY METOD IZMERENIYA MAGNITNOGO POLYA ZEMLI PRI POMOSHCHI YADERNO-REZONANSNOGO FIL'TRA | | | | | | | |
| 09 English Title PHASE METHOD OF MEASURING MAGNETIC FIELD OF EARTH WITH A NUCLEAR-RESONANCE FILTER | | | | | | | |
| 43 Source Leningrad. Universitet. Vestnik. Seriya Fiziki i Khimii (Russian) | | | | | | | |
| 42 Author BORODIN, P. M. | | | | 98 Document Location | | | |
| 16 Co-Author NONE | | | | 47 Subject Codes 20, 08 | | | |
| 16 Co-Author NONE | | | | 39 Topic Tags: nuclear resonance, earth magnetic field, magnetic field measurement, filter, Lissajous figure | | | |
| 16 Co-Author NONE | | | | | | | |
| 16 Co-Author NONE | | | | | | | |

ABSTRACT The F. I. Skripov (DAN AN SSSR, 121,998, 1958) generator has been used as a nuclear resonance filter for terrestrial magnetic field measurements with a broken reverse couplin, the input of which consists of a phasing coil and the output-- a receiver coil. The phase shift obtained from measuring the terrestrial field H_0 is displayed as Lissajous figures on an oscilloscope. The sensitivity γ of this device is shown to be 0.1 to 0.3 gamma, and an undistorted signal registered from magnetic perturbations of $\gamma \geq 2$ second [equation missing] is ensured. This is shown to allow simultaneous measurement of short-period field variations as well as slow changes. "The author is grateful to A. V. Mel'nikov and A. A. Morozov." orig. art. has: 3 figures and 1 equation. English Translation: 3 pages

ITIS INDEX CONTROL FORM

| | | | |
|------------------------|--------------------------------|------------------------------|--------------------------------|
| 01 Acc Nr TF7500521 | 68 Translation Nr MT6400358 | 65 X Ref Acc Nr AP4024465 | 76 Reel/Frame Nr 165A, 1667 |
| 97 Header Clas UNCL | 63 Clas UNCL, 0 | 64 Control Markings 0 | 94 Expansion UR |
| 02 Ctry UR | 03 Rez 0054 | 04 Yr 64 | 05 Vol 000 |
| 06 Iss 001 | 07 B. Pg. 0159 | 08 B. Pg. 0162 | 10 Date NONE |

Transliterated Title: POVERKHOZHNAYA STRUKTURA, ELEKTRICHESKIYE I FOTOLEKTRICHESKIYE SVOYSTVA TONKIKH SLOYEV SERNISTOGO SVINTSA, POLUCHENNYKH KATODNOY RASPLYENIYEM

09 English Title: SURFACE STRUCTURE, ELECTRICAL AND PHOTOELECTRIC PROPERTIES OF THIN LAYERS OF SULFUROUS LEAD OBTAINED BY CATHODE SPUTTERING

45 Source: Leningrad. Universitet. Vestnik. Seriya Fiziki i Khimii (Russian)

| | |
|--------------------------------|--|
| 48 Author BERLAGA, R. YA. | 98 Document Location |
| 15 Co-Author RUDENOK, M. I. | 47 Subject Codes 20 |
| 16 Co-Author NONE | 39 Topic Tags: activation energy, absorption spectrum, electron diffraction analysis, evaporation, single crystal film, polycrystalline film |
| 16 Co-Author NONE | |
| 16 Co-Author NONE | |

ABSTRACT Thin PbS layers were produced by the cathode-sputtering method under a bell jar at 10^{-1} to 10^{-2} mm Hg pressures and at temperatures of 250-270 C. Average evaporation rate was 0.2μ per hour; the substrate was at a 3.5-4 cm distance from the cathode. The activation energy was calculated from temperature dependence of conductivity using both the cathode sputtering technique and evaporation in vacuum with noticeable differences in the measured conductivity between the two methods. The adsorption spectrum was measured in thin polycrystalline layers of PbS obtained by the cathode sputtering method. Electron microscopic and electron diffraction studies were carried out. The PbS layers obtained exhibit the same properties as the layers produced by the vacuum evaporation method. The ability to produce polycrystalline and single crystal PbS films is shown to be possible by the cathode-sputtering method. "L. I. Meshcherskaya took part in the experiments." Orig. art. has: 5 figures. English Translation: 4 pages.

ITIS INDEX CONTROL FORM

| | | | | | | | |
|---|----------------|--------------------------------|---------------|--|-------------------|-------------------------------|-----------------|
| 01 Acc Nr TP7500522 | | 68 Translation Nr MI6400358 | | 65 X Ref Acc Nr | | 76 Reel/Frame Nr 1654 1468 | |
| 97 Header Clas UNCL | | 63 Clas UNCL, 0 | | 64 Control Markings 0 | | 94 Expansion UR | |
| 02 Ctry UR | 03 Ref 0054 | 04 Yr 64 | 05 Vol 000 | 06 Iss 001 | 07 B. Pg. 0162 | 08 B. Pg. 0164 | 10 Date NONE |
| Transliterated Title SREDNYAYA TEPLYEMKOST' TVERDYKH RASTVOROV Fe ₂ O ₃ - Al ₂ O ₃ PRI PROVYSHENNYKH TEMPERATURAKH | | | | | | | |
| 09 English Title AVERAGE HEAT CAPACITY OF SOLID Fe ₂ O ₃ - Al ₂ O ₃ SOLUTIONS AT HEIGHTENED TEMPERATURES | | | | | | | |
| 43 Source Leningrad. Universitet. Vestnik. Seriya Fiziki i Khimii (Russian) | | | | | | | |
| 42 Author POPOV, Yu. G. | | | | 98 Document Location | | | |
| 16 Co-Author NONE | | | | 47 Subject Codes 07 | | | |
| 16 Co-Author NONE | | | | 39 Topic Tags: heat capacity, heat measurement, heat of solution, enthalpy, iron oxide, aluminum oxide | | | |
| 16 Co-Author NONE | | | | | | | |
| 16 Co-Author NONE | | | | | | | |

ABSTRACT The mean heat capacities of solid solutions of the Fe₂O₃-Al₂O₃ system have been found to be a linear function of the composition. This in good agreement with the assumption of the segregation of aluminum and iron atoms. English Translation: 4 pages.

ITIS INDEX CONTROL FORM

| | | | | | | | |
|---|----------------|--------------------------------|---------------|--|-------------------|-------------------------------|--------------------|
| 01 Acc Nr TP7500524 | | 68 Translation Nr MT6400358 | | 65 X Ref Acc Nr | | 76 Reel/Frame Nr 1654 1470 | |
| 97 Header Clas UNCL | | 63 Clas UNCL, 0 | | 64 Control Markings 0 | | 94 Expansion | 40 Ctry Info UR |
| 02 Ctry UR | 03 Ref 0054 | 04 Yr 64 | 05 Vol 000 | 06 Iss 001 | 07 B. Pg. 0165 | 43 B. Pg. 0167 | 10 Date NONE |
| Transliterated Title PRIMENENIYE UL'TRAZVUKA DLYA USKORENIYA KOLICHESTVENNOGO OSAZHDENIYA KAL'TSIYA, MAGNIYA I BARIYA | | | | | | | |
| 09 English Title APPLICATION OF ULTRASONICS TO ACCELERATE QUANTITATIVE DEPOSITION OF CALCIUM, MAGNESIUM AND BARIUM | | | | | | | |
| 43 Source LENTINGRAD. NIVERSITET. VESTNIK. SERIYA FIZIKI I KHIMII (RUSSIAN) | | | | | | | |
| 42 Author VASIL'YEV, V. V. | | | | 98 Document Location | | | |
| 16 Co-Author SIT'KO, I. L. | | | | 47 Subject Codes 20, 07 | | | |
| 16 Co-Author NONE | | | | 39 Topic Tags: ultrasonic effect, barium, magnesium, oxide, ammonium compound, calcium compound, heat effect | | | |
| 16 Co-Author NONE | | | | | | | |
| 16 Co-Author NONE | | | | | | | |

ABSTRACT The data on the new application of ultrasonic in analytical chemistry are given in this paper. In using ultrasonic quantitative precipitation of barium sulphate, magnesium and ammonium diphosphate and calcium oxalate may be achieved for five minutes instead of lengthy exposure of the precipitate with mother liquor to heating or leaving them overnight before filtering.
English Translation: 5 pages.

TABLE OF CONTENTS

U. S. Board on Geographic Names Transliteration System..... 111
 Designation of the Trigonometric Functions..... 1v

PHYSICS

M. A. Braun. Equations for Vertex Parts and Bound States;..... 5
 V. Ye. Bunakov. Associating of Nucleons in Nuclei;..... 15
 T. V. Zhikhareva. Near-Threshold Behavior of the Inelastic-Scattering
 Cross Section;..... 21
F. I. Skripov. Nuclear-Resonance Generator with Flowing Liquid..... 31
 N. M. Anton'yeva and G. S. Katykhin. Radiation of Sb^{125} 47
 V. P. Rudtov. Dependence of Angles of Orientation in Dynamic Double-
 Refraction on the Velocity Gradient;..... 71
 N. M. Orlova and A. A. Petrov. Determination of Hydrogen in Aluminum
 Alloys by the Method of Isotopic Balancing;..... 71
 A. K. Suslov. On the "Mean Time of the Free Path" of O_2 Molecules;..... 79
 I. M. Shved. Approximation of Isolated Line During Transfer of Radiative
 Energy in the Upper Atmosphere;..... 103

CHEMISTRY

L. G. Sillen. On Polyanions in Solutions..... 111
 M. B. Debratin, A. V. Suvorov, and Yu. V. Kondrat'yev. Question About
 Phase Transitions in Solid Bodies;..... 117
 I. F. Karpova, V. N. Smirnova, and D. A. Fridrikhsberg. Electrokinetic
 Properties of Deposits of Copper Ferricyanide Obtained in Different
 Conditions;..... 127
 A. N. Murin, G. B. Tomilov, and I. A. Yutlandov. Separating and
 Identifying Reaction Products of Deep Splitting of Germanium by
 Fast Protons..... 137
 M. M. Shalits and I. M. Sushneva. Thermodynamic Investigation of a HCl
 Solution in a NaCl - KCl - $CaCl_2$ System at Temperatures of 240, 280,
 and 320°C..... 147
 I. N. Semyachkin, M. F. Iust'ukina, and E. I. Tikhonova. Amperometric
 Titrating Certain Cations by Triion B with Revolving Microplatin
 Electrode..... 157
 V. I. Tikhonov and G. I. Kopylova. Oxidation Rate of Copper in
 Aqueous Solution at High Temperatures..... 167

| | |
|---|-----|
| Y. P. Stolyarov and I. A. Amantova. Spectrophotometric Investigation of Ascorbate Complexes;..... | 165 |
| N. A. Nechay, M. N. Zvereva, and T. M. Grekovich. Reducing Properties of Ionites;..... | 175 |
| S. A. Shchukarev, T. G. Balicheva, K. Ye. Borchka, and M. A. Kukhareva. Infrared Absorption Spectra of Anhydrous Sulfuric and Orthophosphoric Acids;..... | 181 |

SHORT SCIENTIFIC REPORTS

| | |
|--|-----|
| V. P. Budtov. Dependence of Orientation Angle of Double Refraction in Flow on Concentration of Solution;..... | 189 |
| Ye. V. Gnilovskiy. About Infrared Spectrum of Twilight Sky | 195 |
| P. M. Borodin. Phase Method of Measuring Magnetic Field of Earth with a Nuclear-Resonance Filter;..... | 199 |
| R. Ya. Berlaga and M. I. Rudenok. Surface Structure, Electrical and Photoelectric Properties of Thin Layers of Sulfurous Lead Obtained by Cathode Sputtering;..... | 205 |
| Yu. G. Popov. Average Heat Capacity of Solid $Fe_2O_3 - Al_2O_3$ Solutions at Heightened Temperatures;..... | 207 |
| Ye. K. Smirnova and I. V. Vasil'kova. On Chloroniobates of Alkali with Composition of $Me_2^I NbOCl_5$;..... | 211 |
| V. V. Vasil'yev and I. L. Sit'ko. Application of Ultrasonics to Accelerate Quantitative Deposition of Calcium, Magnesium and Barium;..... | 215 |

U. S. BOARD ON GEOGRAPHIC NAMES TRANSLITERATION SYSTEM

| Block | Italic | Transliteration | Block | Italic | Transliteration |
|-------|----------|-----------------|-------|----------|-----------------|
| А | <i>А</i> | A, а | Р | <i>Р</i> | R, r |
| Б | <i>Б</i> | B, b | С | <i>С</i> | S, s |
| В | <i>В</i> | V, v | Т | <i>Т</i> | T, t |
| Г | <i>Г</i> | G, g | У | <i>У</i> | U, u |
| Д | <i>Д</i> | D, d | Ф | <i>Ф</i> | F, f |
| Е | <i>Е</i> | Ye, ye; E, e* | Х | <i>Х</i> | Kh, kh |
| Ж | <i>Ж</i> | Zh, zh | Ц | <i>Ц</i> | Ts, ts |
| З | <i>З</i> | Z, z | Ч | <i>Ч</i> | Ch, ch |
| И | <i>И</i> | I, i | Ш | <i>Ш</i> | Sh, sh |
| Й | <i>Й</i> | Y, y | Щ | <i>Щ</i> | Shch, shch |
| К | <i>К</i> | K, k | Ъ | <i>Ъ</i> | " |
| Л | <i>Л</i> | L, l | Ы | <i>Ы</i> | Y, y |
| М | <i>М</i> | M, m | Ь | <i>Ь</i> | ' |
| Н | <i>Н</i> | N, n | Э | <i>Э</i> | E, e |
| О | <i>О</i> | O, o | Ю | <i>Ю</i> | Yu, yu |
| П | <i>П</i> | P, p | Я | <i>Я</i> | Ya, ya |

* ye initially, after vowels, and after ъ, ѓ; e elsewhere.
 When written as ѐ in Russian, transliterate as yě or ě.
 The use of diacritical marks is preferred, but such marks
 may be omitted when expediency dictates.

FOLLOWING ARE THE CORRESPONDING RUSSIAN AND ENGLISH
 DESIGNATIONS OF THE TRIGONOMETRIC FUNCTIONS

| Russian | English |
|------------|--------------------|
| sin | sin |
| cos | cos |
| tg | tan |
| ctg | cot |
| sec | sec |
| cossec | csc |
| sh | sinh |
| ch | cosh |
| th | tanh |
| cth | coth |
| sch | sech |
| csch | csch |
| arc sin | sin ⁻¹ |
| arc cos | cos ⁻¹ |
| arc tg | tan ⁻¹ |
| arc ctg | cot ⁻¹ |
| arc sec | sec ⁻¹ |
| arc cossec | csc ⁻¹ |
| arc sh | sinh ⁻¹ |
| arc ch | cosh ⁻¹ |
| arc th | tanh ⁻¹ |
| arc cth | coth ⁻¹ |
| arc sch | sech ⁻¹ |
| arc csch | csch ⁻¹ |
| ret | curl |
| lg | log |

PHYSICS

EQUATIONS FOR VERTEX PARTS AND BOUND STATES

M. A. Braun

There exists a point of view, according to which in the usual dispersion approach or in the method of double dispersion relations at least part of the poles of amplitude and residues at them are not arbitrary, but are determined through other poles and residues. Particles associated with such poles are naturally considered to be compound, i.e., bound states of independent particles. No convincing results here, unfortunately, have yet been obtained. If we make certain approximations (finite number of partial waves, consideration only of nearby singularities), then the appearance of poles corresponding to the bound states can be observed. In work [1] such a method was used for finding bound states of a nonrelativistic particle in a potential field, and turned out to be fully satisfactory. However, there are expressed opinions that the limitations on the position of poles and their residues which appear during approximate calculations are essentially connected with the approximations, and may be absent in exact theory. Another weak place such an approach to the problem of bound states is the fact that determination of bound states should occur simultaneously with the finding of all scattering amplitudes - a problem of incredible complexity.

Blankenbecler and Cook [2] recently proposed another method for the study of bound states, based on vertex parts. Authors considered a nucleon-deuteron vertex in the lowest nontrivial order of perturbation theory, and disregarding spins obtained an equation for mass of deuteron. With consideration of spins, the equation was not obtained, but it was possible to estimate the ratio of D-wave to

S-wave in the ground state of the deuteron.

The present work is dedicated to generalization and development of method of Blankenbecler and Cook. We will try to avoid perturbation theory.

We will everywhere consider scattering amplitudes to be uniquely defined by known quantities. We will not be concerned with the question of their construction. As it turns out within the bounds of contemporary theory it is impossible to decide whether it is indeed possible, on the basis of the equations obtained in this method, to consider the deuteron to be a bound state of nucleons. If, however, this is assumed from the very beginning, the equations actually make it possible to determine approximately the mass of the deuteron through the masses π -mesons and nucleons and their constant of interaction. In this work we will consider all particles to be spinless.

We will designate by $F(s, t)$ and $G(s, t)$ the usual invariant amplitudes (divided by 16π) for the reactions $\pi_1 + N_1 \rightarrow \pi_2 + N_2$ and $\pi_1 + N_1 \rightarrow D + N$, respectively. Variable s in both cases is $(p_{\pi_1} + p_{N_1})^2$, and $t = (p_{\pi_1} - p_{\pi_2})^2$ for the first reaction and $t = (p_{\pi_1} - p_N)^2$ for the second. We will introduce two vertex parts:

$$V(s) = 2(p_1 p_2)^{\mu\nu} \langle 0 | j_N(s) | N_1 \rangle_{\mu\nu} \quad s = (p_1 + p_2)^2;$$

$$W(s) = 2(p_1 p_2)^{\mu\nu} \langle 0 | j_N(s) | RD \rangle_{\mu\nu} \quad s = (p_1 + p_2)^2$$

(j_N - nucleon current).

For vertex parts in the interval $(m + \mu)^2 \leq s \leq (m + 2\mu)^2$ the following relationships of unitarity will, obviously, be accurate:¹

$$\text{Im } V(s) = \rho^+(s) V^*(s) F_0(s) \quad (1)$$

$$\text{Im } W(s) = \rho^+(s) V^*(s) G_0(s) \quad (2)$$

F_0 and G_0 represent S-waves of corresponding amplitudes $F(s, t)$ and $G(s, t)$ and function $\rho^+(s)$ is the boundary value on the upper side of the section $s \geq (m + \mu)^2$ of the function

$$\rho(s) = \frac{1}{2} \sqrt{[s - (m + \mu)^2][s - (m - \mu)^2]}.$$

The relation of unitarity for F_0 and G_0 with the same s have the form

¹ m and μ are the mass of the nucleon and π -meson.

$$\text{Im } F_0(s) = \rho^+(s) F_0^*(s) F_0(s), \quad (3)$$

$$\text{Im } G_0(s) = \rho^+(s) F_0^*(s) G_0(s). \quad (4)$$

The main assumption which we take as the basis of our reasoning is, just as in [2], the assumption of the fact that V and W represent the analytical functions in the whole complex plane except the section along the real axis, diminishing as $|s| \rightarrow \infty$. As some justification to the latter we can cite work [3] about the behavior of vertex parts at large values of the argument.

We will consider F_0 and G_0 to be given functions. Besides s , they contain as parameters the constants of the πNN -bond g and NND -bond f , and also the mass of the π -meson μ , of the nucleon m , and of the deuteron m_D . If we consider that equations (1)-(4) are accurate at all $s \geq (m + \mu)^2$, then from (1) we can determine V through F_0 and from (2) we can find W through V and G_0 . After this we must require fulfillment of the evident conditions:

$$V(m^2) = g, \quad (5)$$

$$W(m^2) = f. \quad (6)$$

Condition (5) can always be satisfied, inasmuch as equation (1) determines V with an accuracy up to a constant factor. After that condition (6), as one might think, gives an equation connecting the quantities f , g , m , μ , and m_D . As we will see below, the basic contribution to W is introduced by members proportional to f . Therefore f drops from equation (6) and there remains the bond between g , m , μ , and m_D .

If fact we should, of course, consider that starting with $s = (m + 2\mu)^2$ new members containing nonelastic amplitudes are added to the right sides of equations (1)-(4). At present consideration of these members is impossible. We can only refer to the usual argumentation that nearby peculiarities give the main contribution. Later we will pause in slightly greater detail on the question of how much the highest amplitudes can change the qualitative and quantitative side of the arguments.

Very curious, however, is the fact that even in disregarding the contribution from highest amplitudes conditions (5) and (6) by no means always lead to a connection between masses and constants of interaction. This is explained by the fact that equation (5) can have not one, but several linear-independent solutions. (A discussion of this question will be conducted below.) First of all we must consider that the jump W is different than zero also at $s < (m + \mu)^2$ (anomalous threshold).

Dispersion Relation for W

In order to find jump W in the nonphysical region, we will resort to analytic continuation by mass. The general scheme of calculations is presented in work [4] where, indeed, a considerably simple case is examined. We will consider the mass of the antinucleon, appearing in determination of W , equal to $\sqrt{s} < m$. Then the physical regions will cover beams $s < (m_0 - \sqrt{s})^2$ and $s > (m_0 + \sqrt{s})^2$. At sufficiently small x the region $s \leq (m + 2\mu)^2$ of interest to us will become physical, and we will be able to write the dispersion relationship

$$W(s, x) = \frac{1}{2\pi} \int_{(m_0 - \sqrt{s})^2}^{(m_0 + \sqrt{s})^2} \frac{d\sigma'}{s' - s} \rho^*(\sigma') a(\sigma', x) + \frac{1}{2\pi} \int_{(m + 2\mu)^2}^{\infty} \frac{d\sigma'}{s' - s} \text{Im } W(\sigma' + i0, x), \quad (7)$$

where $a(s, x) = V^*(s) G_0(s, x)$. In (7) our main assumption is used: $W \rightarrow 0$ as $|s| \rightarrow \infty$.

Now it is necessary analytically to continue (7) in terms of the variable x up to $x = m^2$. The possibility of such a continuation is assumed. Let us assume also that in the second integral in (7) the continuation is carried out in trivial form, i.e., $\text{Im } W(s, x)$ is replaced by $\text{Im } W(s, m^2)$.¹ In the first integral the matter is more complicated. $a(s, x)$ as a function of x has a singularity. The amplitude $G_0(s, x)$ has a right section when $s \geq (m + \mu)^2$ and a left section which approaches in the complex plane s . With a growth in x the origin of the left section emerges on the real axis and at $x = x_0$ it reaches to point $s = (m + \mu)^2$. This prevents direct the analytic continuation of expression (7) in terms of x .

Singularities of $G_0(s, x)$ in terms of variables s , when $s \geq (m + \mu)^2$, are determined by conditions $t = t_0$ or $u = u_0$ when $\cos \theta = \pm 1$; t and u are Mandelstam variables for amplitude $G(s, t, x)$ expressed through s and the cosine of the scattering angle in the system of the center of mass (c. m. s.), $\cos \theta$; t_0 and u_0 are singularities $G(s, t, x)$ in terms of the corresponding Mandelstam variables. The nearest singularities are obviously, poles $t_0 = m^2$ and $u_0 = m_D^2$. The following singularities are $t_0 = (m + \mu)^2$ and $u_0 = (2m)^2$.

Let us consider the closest singularity $t = m^2$. When $\cos \theta = \pm 1$

$$t = p^2 + x - \frac{1}{2\mu} (s - m^2 + p^2) (s - m_D^2 + x) \pm 2p \cdot q,$$

where q , and q_D are magnitudes, of 3 momentums of the π -meson and deuteron in the c. m. s.:

$$q^2 = \frac{1}{4} [s - (m + \mu)^2] [s - (m - \mu)^2],$$

$$q_D^2 = \frac{1}{4} [s - (m_0 + \sqrt{s})^2] [s - (m_0 - \sqrt{s})^2].$$

¹We consider only the lowest anomalous threshold.

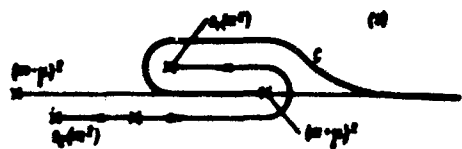


Fig. 1. Singularities s_1 and s_2 of the amplitude G_0 . Arrows indicate the motion of singularities during an increase of x from $(m - \mu)^2$ to m^2 .

Equation $t = m^2$ gives four values of s in which singularities of G_0 occur: $s = -\infty$, $s = 0$ and two more values s_1 and s_2 . When $x < (m - \mu)^2$ s_1 and s_2 are complex. When $x \geq (m - \mu)^2$ singularities s_1 and s_2 emerge on the real axis and diverge into various sides in the interval $(m - \sqrt{x})^2 < s < (m + \sqrt{x})^2$.

If we consider $s_1 \approx s_2$, then when

$x = x_0 = (m + \mu)^2 - \frac{1}{2} m_0^2$, $s_1 = (m + \mu)^2$, and with the subsequent increase in x , s_1 moves to the left. When $x = m^2$ the singularity occupies the position $s_1(m^2)$. We know that $m_0^2 \approx 4m^2$. Designating $m_0^2 = 4m^2 - \gamma^2$, where γ is small, we will find correct to γ^2

$$s_1(m^2) = m^2 + 2\mu^2 + \frac{1}{2} \sqrt{4m^2 - \gamma^2} - \frac{\gamma^2}{2m^2}. \quad (8)$$

During the analytic continuation we should consider x to be complex:

$x = x_1 + ix_2$. We will take $x_2 < 0$ and $x_2 \ll 1$. Then the singularities $s_1(x)$ and $s_2(x)$ of amplitude $G_0(s, x)$, proceeding from singularity $t = m^2$, with an increase of x_1 from $(m - \mu)^2$ to m^2 will circumscribe the lines which are shown in Fig. 1. So that the singularity $s_1(x)$ does not hinder analytic continuation with respect to x , path of integration in (7) should be displaced to contour C , depicted in the same figure. This signifies the addition of a new section of integration $s_1(m^2) < s < (m + \mu)^2$.

If we consider other singularities when $t \geq (m + \mu)^2$ or $u = u_0$, then it turns out that on plane s singularities of $G_0(s, x)$, not reaching up to $(m + \mu)^2$ with an increase of x up to m^2 correspond to them. Therefore these singularities do not hinder the analytic continuation with respect to x .

We separate from $G_0(s, x)$ that term which has the singularity corresponding $t = m^2$, $a_0 = \bar{a}_0 + a_0$. \bar{a}_0 does not contain singularities connected with $t = m^2$, and the contribution of \bar{a}_0 to (7) continues with respect to x trivially. G_{01} represents an S-wave for only one diagram (Fig. 2):

$$G_{01}(s, x) = \frac{1}{2\pi i} \frac{1}{s_0} \ln \frac{s+1}{s-1}. \quad (9)$$

where

$$s = \frac{1}{4m_0^2} [(s - m^2 + \mu^2)(s - m_0^2 + x) - 2x(x + \mu^2 - m^2)].$$

During which the branch of the logarithm which is real when $s < -1$ and $s > 1$ is

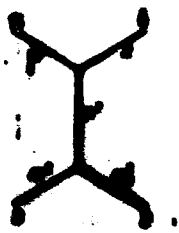


Fig. 2.
Diagram corresponding to G_{01} .

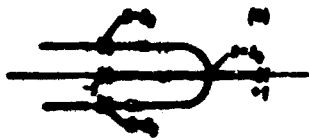


Fig. 3. Behavior of z with a change in s from $(m + \mu)^2 + 10$ to $(m - \mu)^2 + 10$.

selected. When s decreases from $(m + \mu)^2$ to $(m - \mu)^2$ remaining higher than the real axis, z describes the curve depicted in Fig. 3. At the point $s = s_3$ G_{01} undergoes the first discontinuity. This means that through point s_3 on plane s there passes a complex section perpendicular to the real axis. For the

analytic continuation with respect to the mass it is more convenient to consider the function $G_{02}(s, x)$, coinciding with G_{01} when $s \geq s_3$ but not having a complex section. After the section, obviously, $G_{02} = G_{01} + \frac{V(s)}{s - s_3}$. In the interval $s_1 < s < s_3$ $\ln G_{02}(s + i0, x) = \frac{V(s)}{s - s_3}$.

Vertex part $W(s, x)$ when $x < x_0$ can be written in the form $W = \bar{W} + W_1$. By \bar{W} we designate dispersion integrals, continuing with respect to x in a trivial form

$$W_1(s, x) = \frac{1}{\pi} \int_{s_1}^{s_3} \frac{V(s') a_1(s', x)}{s - s'} ds' \quad (10)$$

where

$$a_1(s', x) = V'(s') G_{02}(s', x) = V'(s') G_{01}(s', x).$$

We will take advantage of the fact that according to (1) the function $V'(s)$ can be continued analytically on the upper half-plane s , and we will displace in (10) the integration contour to curve C (see Fig. 1). Then

$$W_1 = \frac{1}{\pi} \int_{s_1}^{s_3} \frac{V'(s') a_1(s', x)}{s - s'} ds' + \frac{1}{\pi} \int_{s_3}^{s_1} \frac{V'(s') [a_1(s', x) - a_1(s', x)]}{s - s'} ds' \quad (11)$$

(signs "+" and "-" pertain to values of a_1 on the upper and lower parts of the loop of integration). When $x < x_0$ the second term is equal to zero.

For the function $a_1(s, x)$ it is possible, in turn, to write the dispersion relationship

$$a_1(s, x) = \frac{1}{\pi} \int_{s_1}^{s_3} \frac{V(s') a_1(s', x)}{s - s'} ds' + \frac{1}{\pi} \int_{s_3}^{s_1} \dots + \frac{1}{\pi} \int \dots \quad (12)$$

Contour C_1 includes the remaining left sections proceeding both from G_{02} , and from V' . All of them do not reach point $s = (m + \mu)^2$. When $x > x_0$ point s_1 rounds $(m + \mu)^2$, and with the analytic continuation a_1 in the first integral we should turn to the second lamina of the function $\ln a_1 = \frac{V(s)}{s - s_3} V'(s)$. We find when $x > x_0$

$$a_1(s, x) = \frac{1}{2} \int_0^{m+\mu} \frac{d\omega}{\omega-s} \ln a_1(\omega, x) + \frac{1}{2} \int_0^{\infty} \dots + \frac{1}{2} \int_0^{\infty} \dots - \frac{1}{2} \int_0^{\infty} \frac{d\omega}{\omega-s} \frac{d\omega}{\omega+s} V(\omega) \quad (13)$$

It follows from this that when $x > x_0$ in the interval $a_1(s) < s < (m+\mu)^2$ the difference $a_1^+ - a_1^-$ is nonvanishing and is equal to

$$a_1^+ - a_1^- = \frac{i\pi}{2\pi(\omega-s)} V(\omega) \quad (14)$$

We will find that when $x = m^2$ for W the accurately dispersion ratio

$$W(s) = \frac{1}{2} \int_0^{m+\mu} \frac{d\omega}{\omega-s} V(\omega) a_1(\omega) + \frac{1}{2} \int_0^{\infty} \frac{d\omega}{\omega-s} \ln W(\omega) + \frac{1}{2} \int_0^{\infty} \frac{d\omega}{\omega-s} \frac{V(\omega)}{\sqrt{(m+\mu)^2 - \omega^2} \sqrt{\omega^2 - (m-\mu)^2}} \quad (15)$$

Let us note that $\text{Im } W$ is continuous at point $s = (m + \mu)^2$.

Equations for the Bound State

If we disregard the contribution of multitail amplitudes and very high energies, then the dispersion relationship (15) together with equation (1) allow the determining of V and W in terms of quantities F_0 and G_0 , considered to be known. The question appears, indeed, whether relationships (5) and (6) lead to the bond between constants g, f, m, μ and m_0 entering into F_0 and G_0 , and is not this bond the result of the approximation made.

Let us assume now that disregard of multitail amplitudes and very high energies is valid with all s 's. We will consider that in the dispersion relationship (15) the last member is negligible, and that equation (1) is accurate when all $s \geq (m + \mu)^2$. In this case we can find $V(s)$ in the general form in terms of S -phase δ_0 πN -scattering. If when $s \rightarrow \infty, \delta_0 \rightarrow \pi(s + \lambda)$ ($s = 0, \pm 1, \pm 2, \dots, 0 < \lambda < 1$), then, as is well-known [5], equation (1) allows for V : independent solutions. When $s < 0, l = 0$; when $s > 0$ and $\lambda > 0, l = s + 1$; when $s > 0$ and $\lambda = 0, l = s$. A general solution of the equation is obtained from the solution diminishing fastest of all by multiplication by the polynomial $P_{l-1}(s)$ with arbitrary coefficients. Substituting the found V in equality (15) we uniquely determine W .

Let us turn to relationships (5) and (6). Only in one case do they immediately lead to a bond between the masses and constants of interaction: if $l = 1$. With this V is determined correct to the constant factor, which is found from (5). Equation (6) gives the unknown bond.

If $l \neq 1$, the picture changes fundamentally. If $l = 0$, then the equations, in general, do not have solutions. If $l \geq 1$, then relationships (5) and (6) are

satisfied with arbitrary masses and coupling constants, i.e., in this case the particles are independent.

It is possible to introduce into the consideration not one state with a nucleon charge 2 (deuteron) but several with masses m_D^1, m_D^2, \dots and coupling constants f^1, f^2, \dots . All the arguments would be applicable to each of the vertex parts $W^{(1)}$ for these particles. The number l of linearly independent solutions of equation (1) can be naturally interpreted as the number of independent particles (including the nucleon). The l relationships on the mass surface $V=g, W^{(1)}=f^{(1)}$ allow uniquely fixing of all l arbitrary constants. The remaining particles prove to be states of independent particles. Their masses and constants of interaction are not arbitrary but satisfy the relationship $W(m)^2=f$, in which W no longer contains arbitrary constants. It is curious that the number of independent particles in this model is simply connected with the asymptotic behavior of b_0 when $s \rightarrow \infty$ and is accessible to experimental observation.

In a real case, when contributions from more distant sections are considered, it is impossible to determine the number of independent solutions for V and W in the contemporary theory. We believe, however, that qualitatively the picture does not change, i.e., a definite number of independent solutions exists, and this number in principle can be obtained experimentally. Some support for this conviction can be found in the fact that if equations (1) and (2) are supplemented by the contribution of two-particle amplitudes, appearing during very high energies (for instance, from intermediate states ND), then the character of the solutions does not change, although the bond between the number of independent solutions and the experimentally observed quantities is essentially complicated.

From what has been said it follows that at present it is impossible to decide whether relationship (5) and (6) can actually serve for determining parameters of the deuteron or whether the deuteron is an independent particle, and relationship (5) and (6) serve for the determination of constants in V and W . The answer to this question requires an investigation of V and W when $s \rightarrow \infty$. We can however, assume from the very beginning that the deuteron is a bound state, i.e., that only one solution exists for V and W . Then equations (5) and (6) become nontrivial. If solutions of equations (5) and (6) in the assumption about the uniqueness of V and W give a reasonable value of the mass of the deuteron, then this is a strong argument in favor of "connectivity," of a nonelementary character of the deuteron.

Otherwise the deuteron is an independent particle.

In the following section we will briefly discuss the question of the approximate calculation of V and W in the assumption about their uniqueness.

Determination of the Mass of the Deuteron

During the calculation of $W(m^2)$ the main role in the dispersion integral is played, by low-energy domains of integration, mainly the anomalous domain. This is explained, on the one hand, by the assumed decrease in $W(s)$ with large s 's and, on the other hand, by the proximity of the anomalous threshold (8) to the point $s = m^2$ and the behavior of $\text{Im } W(s)$ when $s \approx m^2$. Near $s = m^2$, $\text{Im } W$ is great, since it is proportional here to $1/\gamma$ (let us remember that $m_0^2 = 4m^2 - \gamma^2$ and γ is small).

It is necessary for us to know therefore the vertex part $V(s)$ with s lying in the region of m^2 . For the determination of V the condition of unitarity (1) is at our disposal, which can be rewritten in the form

$$V^+(s) = \kappa(s) V^-(s) + r(s), \quad (16)$$

where

$$\kappa(s) = \begin{cases} 1 & s < (m+r)^2 \\ \exp(i\delta_0(s)) & s > (m+r)^2 \end{cases}$$

V^+ and V^- are values of V on the upper and lower boundaries of the section; $r(s)$ is the contribution from the inelastic terms, $r = 0$ when $s < (m+2r)^2$.

If $r(s)$ were a given function, the solution (which we consider to be unique and correct to the coefficient) could have been written in an evident form. We could then directly verify that when $s \sim m^2$ the quantity $V(s)$ is a slowly varying function of values of $\kappa(s)$ and $r(s)$ when $s \gg m^2$ (see, for instance, [5]). More exactly, their influence would be reduced to the multiplication of V by the factor, which is immaterial in view of the condition (5). In fact it is impossible to consider $r(s)$ as a given function, since $r(s)$ itself depends on V . Nevertheless, we will assume that in this case the behavior of $V(s)$ in the region of low energies immaterially depends on values $\delta_0(s)$ and $r(s)$ with large s , under the condition that the solution remains unique. Then the approximate solution of equation (16) can be constructed, for instance, in this way. Let us reject $r(s)$ in general, and $\delta_0(s)$, and starting from some large value $s = N$ we will replace the constant $\delta_0(N)$. If in the interval $(m+r)^2 < s < N$ the phase δ_0 does not pass through resonance, then the solution to the new equation will be unique and equal (see [5])

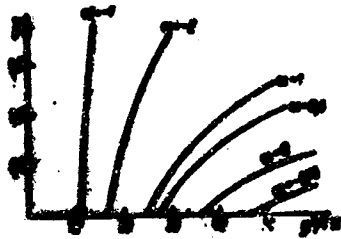


Fig. 4. Dependence of γ on g with different α . In the interval $0 < \alpha < \pi/2$ no solutions exist. $N = (m + \mu)^2$.

to

$$V^*(s) = \frac{A}{(s \pm \mu)^2} \exp \left\{ \frac{i}{\alpha} \int_{-s}^{s} \frac{\lambda(s') \theta(s' - (m + \mu)^2 - m + \lambda \operatorname{arctg} s'}{s' - s} ds' \right\}. \quad (17)$$

In the integral we should consider $\lambda_0(s) = \lambda_0(N)$ when $s > N$; $\lambda = \lambda_0(N)/s$; A is an arbitrary constant, which is determined from (5).

The use of formula (17) requires knowledge of the S-phase of πN -scattering in the interval

$$(m + \mu)^2 < s < N. \quad \text{The phase can be taken, for instance,}$$

from experiment. In our spin-zero model, for the purpose of illustration of the method, it is reasonable to start from the rougher approximation, in which it is necessary to know only the length of the πN -scattering.

In the vicinity of $s = (m + \mu)^2$ the vertex part of V on the basis of (1) is in the form

$$\begin{aligned} V(s) &= v_1(s) + h_1(s) v_2(s), \\ h_1(s) &= \sqrt{s - (m + \mu)^2}. \end{aligned} \quad (18)$$

(cf. [4]). Functions v_1 and v_2 are analytic in the vicinity of $(m + \mu)^2$ and there can be expanded in series in powers of ρ_1^2 : $v_{1,2}(s) = v_{1,2}^0 + \rho_1^2 v_{1,2}^1 + \dots$. Constants of $v_{1,2}^0$ are determined uniquely from (5) and the requirement of realness of the right side of equation (1):

$$\begin{aligned} v_1^0 &= g / (1 - h_1(m^2) \alpha \sqrt{m\rho_1}), \\ v_2^0 &= -\alpha \sqrt{m\rho_1} v_1^0. \end{aligned} \quad (19)$$

α is the length of S-scattering $\pi + N \rightarrow \pi + N$. The remaining terms will be disregarded, since in the main domain of integration ρ_1 is small. By this consideration we replace quantity $\rho_1^*(s) V^*(s) G_0(s)$ in integral (15) by

$f s v_1^0 / \alpha \sqrt{[(m + m_0)^2 - s][s - (m_0 - m)^2]}$ (the difference is proportional to ρ_1^2). We obtain for $W(m^2)$ the expression

$$W(m^2) = \frac{f s v_1^0}{\alpha (1 - h_1(m^2) \alpha \sqrt{m\rho_1})} \left[\int_{s_0}^s ds v_1(s) - \alpha \sqrt{m\rho_1} \int_{s_0}^{m + \mu} ds h_1(s) v_2(s) \right]. \quad (20)$$

where

$$v_1(s) = 1 / (s - m^2) \sqrt{[(m + m_0)^2 - s][s - (m_0 - m)^2]}.$$

Equating (20) to constant f , we find an equation not dependent on f and determining m_0 in terms of g , m , μ and α . Represented in Fig. 4 is the obtained

dependence of quantity γ , connected with m_D by the equality $m_D^2 = 4m^2 - \gamma^2$, on the constant πN -interaction of g with different values of the scattering length a . The system of units $\hbar = c = \mu = 1$ is used. In view of the model character of the problem these curves have, mainly, an illustrative value. We would like, however, to point out the reasonable order of magnitude of the coupling constant g , needed for the appearance of a bound state, and the natural character of the dependence of γ on a .

The author thanks Prof. Yu. V. Novozhilov, L. A. Khal'fin, L. V. Prokhorov and V. A. Franke for their attention given to the work and their interesting discussions.

Summary

The system of dispersion theoretic equations for the vertex parts πNN and NND with a nucleon off the mass shell is studied in the low energy region in the spinless particle model. The anomalous threshold is calculated by analytic continuation in the mass variable. Under the assumption that the deuteron is a bound state of the nucleons, an equation is obtained for the determination of its mass. (English Summary)

Submitted
April 25, 1963

Literature

1. I. D. Bjorken and A. Goldberg. Nuovo Cim, 16, 538, 1960.
2. R. Blankenbecler and L. F. Cook. Phys. rev., 119, 1745, 1960.
3. H. Lehmann, K. Symanzik, and W. Zimmermann. Nuovo Cim, 2, 425, 1955.
4. R. Oehme. Phys. rev., 121, 1840, 1961.
5. F. D. Gakhov. Boundary value problems, Moscow, 1958.

ASSOCIATING OF NUCLEONS IN NUCLEI

B. Ye. Bunakov

At present much attention is paid to the question of the existence in nuclei of nucleon associations. There are numerous of experimental data indicating the presence of such associations in nuclei. However, thus for the use of the shell model of the nucleus has enjoyed the greatest success. With its help it is possible (although roughly) to predict the sequence of levels in nuclei and the characteristics, of the levels, to calculate the probability of different processes, etc. The weakest point of the model of the shells lies in the calculations of binding energies of the nuclei, i.e., the very region in which the model of nucleon associations proved itself very well (see, for instance, [1]).

It is known that the shell model of independent particles reduces all real two-nucleon interactions to a certain averaged self-consistent potential. However, from first the steps of this model it became clear that this potential only very roughly reflects the properties of real interactions between nucleons. For a more exact description of the nuclei a computation of the effective residual paired interactions is necessary.

Taking into account all the above-mentioned, it is of interest to try to design a model, which in the bounds of the model of independent particles (with the preservation of all its valuable properties) will allow the consideration of the associating of nucleons in nuclei. It is natural to examine such associating with the help of different residual interactions between nucleons.

The assumption was earlier declared [2] on the fact that nucleons which are

in an S-state with respect to each other (in a system of their general center of mass) interact most intensely in the nucleus. The given assumption will be fundamental in our article. In accordance with this association we will use the name m nucleons for that group of m nucleons found in an S-state relative to each other.¹ The thus defined associating of nucleons, in distinction from "radial" associating (for instance, the usual α -model), can be called "energy" or "angular."

In this work we will show the bond between the probability of existence of such associations in the nucleus and the quantum numbers characterizing the irreducible representations of a group of transpositions and orthogonal group (symplectic group for the j - j bond), on which the orbital wave function of the given state of the nucleus will be transformed. Further we will consider which residual interactions lead to the associating of nucleons in the nuclei.

1. In the article of A. I. Baz' [2] it was shown that in order that in a group of n nucleons the S-state of the relative motion of m nucleons be realized, it is necessary that among lines of the scheme of Young [f] of the n -nucleon state there be at least one line $f_k \geq m$. If such lines of f_k are several, then in this state there can be several such m nucleon groups.

Let us now turn to the question on the bond of the S-state of the relative motion of two nucleons and the quantum number of seniority v of their orbital wave function. Let us consider the spatial part of the wave function of two nucleons in the state with seniority $v = 0$:

$$|P \rangle |L=0 M=0\rangle = R_l(r_1) R_l(r_2) |\Theta(\theta_1, \varphi_1, \theta_2, \varphi_2)\rangle_{M=0}^{L=0}, \quad (1)$$

where R_l is the radial part of the wave function of the l -nucleon in independent particle model; \vec{r}_1, \vec{r}_2 are radius-vectors of individual nucleons in the system of center of mass of the nucleus; θ_1, φ_1 and θ_2, φ_2 are spherical angles of vectors \vec{r}_1 and \vec{r}_2 .

The angular part of the wave function (1) can be presented in the form (see, for instance, [3]),

$$|\Theta(\theta_1, \varphi_1, \theta_2, \varphi_2)\rangle_0^0 = (-1)^{\frac{l+1}{2}} P^l(\cos \mu_{12}),$$

where μ_{12} is the angle between vectors \vec{r}_1 and \vec{r}_2 .

¹This means that every nucleon of our group is in an S-state with reference to any other nucleon of this same group [2].

Let us now accomplish a transition to new coordinates, $\vec{R} = \frac{\vec{r}_1 + \vec{r}_2}{2}$ is the radius vector of the center of mass of the two nucleons; $\vec{r} = \frac{\vec{r}_1 - \vec{r}_2}{2}$ is the radius vector of the relative motion of nucleons. We designate the spherical angles of vectors \vec{R} and \vec{r} as θ, ϕ and θ, φ respectively.

Elementary trigonometric computations give the ratio

$$\cos \omega = \frac{R^2 - r^2}{r_1 r_2} = \sqrt{\frac{R^2 - r^2}{(R^2 + r^2 - 4r_1 r_2 \cos \omega)}}.$$

where ω is the angle between vectors \vec{r} and \vec{R} . Consequently, in the new coordinates (1) will take the form

$$\begin{aligned} |P[2] 00\rangle &= A(r, R, \omega) = \sum_l B_l(r, R) P_l(\cos \omega) = \\ &= \sum_l C_l(r, R) Y_l^0(\theta, \phi) Y_l^0(\theta, \varphi). \end{aligned} \quad (2)$$

During the derivation of this formula we took advantage of the fact that in the case $v = 0$ the two-nucleon wave function is invariant to rotations, and in the selection of the new system of coordinates let us assume great arbitrariness. This arbitrariness is the result of the fact that we consider the motion of two noninteracting nucleons. The real two-nucleon interactions, obviously, will lead to such changes of wave functions of individual nucleons that the angular dependence of the two-nucleon function of form (2) will become the only possible one.¹ In case of the oscillator potential, wave function (1) is expanded into a sum of wave functions of S-states of the relative motion of two nucleons with different main quantum numbers n . However, for us this is immaterial. The energy advantage of the S-state for the central short-range interaction consists in its angular isotropism near the origin of the coordinates (i.e., where the force of interaction is maximum). The presence of nodes for the wave function far off from the origin of the coordinates is immaterial for the energy of the interactions considered.

Thus, the state of the two nucleons with a seniority $v = 0$ can always be represented as the S-state of the relative motion of the two nucleons. In case $v \neq 0$ during the transition to the new system of coordinates in function $|P[2] LM\rangle$ a term will appear not depending on the angular coordinates of vector \vec{r} , but, together with it, terms will be present containing this dependence; i.e., the weight of the S-state is lowered (see, for instance, the calculations of A. I. Baz' for nucleons

¹The author thanks A. I. Baz' who turned attention to such a possibility of the physical interpretation of formula (2).

of the p-shell [2].

Let us now turn to the case of n nucleons. It is known that every state of n nucleons can be characterized with help of the operator of seniority $Q = \sum_{i,j} a_{ij}^2$ where

$$P L M | q_n \rangle P L M = (2I+1) \delta_{L,0}$$

The mathematical expectation Q shows what number of pairs $(P, 0, 0)$ is contained in the state $|P, I, L, M\rangle$.

From the above it is clear that the greater the values of operator Q , the greater the weight with which they will enter into our configuration of the S-state of the relative motion of the two nucleons. It is known [3] that the mathematical expectation of operator Q

$$\langle Q \rangle = \frac{1}{2} [C(SU_{2n+1}) - 2C(R_{2n+1})] + \frac{n(n-1)-2In}{2(2I+1)},$$

where

$$C(SU_{2n+1}) = [f_1(f_1-1) + f_2(f_2-2) + \dots] - \frac{n^2 - n(2I+1)}{2I+1}$$

is the eigenvalue of the Casimir operator of the group of unitary unimodular transformations SU_{2n+1} ; f_1, f_2, \dots lines of the Young diagram $[I]$;

$$C(R_{2n+1}) = \frac{1}{2} [a_1(a_1+2I-1) + a_2(a_2+2I-3) + \dots + a_r(a_r+1)]$$

is the eigenvalue of the Casimir operator for the group of orthogonal transformations R_{2n+1} (a_1, a_2, \dots, a_r are numbers characterizing the irreducible representations of group R_{2n+1} and connected uniquely with the number of seniority).

2. Thus, we see that the classification by quantum numbers $[I]$ and w is at the same time a classification by weights of nucleon S-states of relative motion contained in a given state. Inasmuch as the interaction of nucleons in the S-state is maximum, then the most favorable from the energy viewpoint will be the configuration of n nucleons containing the maximum number of groups of nucleons in S-states and with a maximum weight, i.e., a configuration with a maximum length of f_1 lines of the Young diagram for the spatial part of the wave function and with minimum numbers w_1 (with minimum seniority).

In the independent particle model there is degeneration by quantum numbers $[I]$ and w . This is natural, since all interactions of the nucleons are reduced to an averaged self-consistent field. It is possible to remove the degeneration only with help of computation of some residual interactions between the nucleons.

These interactions will be responsible for the association of the nucleons.

Taking into account all the considerations about the energy role of S-states and about their weight in the n nucleon wave function, we must select residual interactions so that they are maximum for states with maximum f_1 , and minimum w_1 .

Such interactions in the model of the L-S coupling are a very broad class of central forces. For the p-shell this will be any mixture of Wigner and Majorana forces [4]. For the d-shell any mixture of Wigner and Majorana forces gives us matrix elements of residual interactions depending on Slater integrals [4]. Having used the appraisal of these integrals for the d-shell carried out by Swiatecki [5], we are convinced that if the effective radius of residual interactions does not exceed the radius of the nucleus, then any mixture of Wigner and Majorana forces will also be the class of residual interactions which we need.

3. In case of the diagram of the j-j coupling everything is slightly more complicated. Here there clearly exist states of two nucleons with seniority $v \neq 0$, being, however, in an S-state relative to the motion. Such a state will be the isotopic singlet $T = 0$, the space-spin part of the wave function of which will be $|J=1, M_1\rangle$. But, as before, every pair of nucleons with $v=0$ $|J=0, M_1=0\rangle$ is in an S-state of relative motion. Proof of this is found analogously to the case of the L-S coupling. It is necessary only to remember that the S-state of the two nucleons in case of the isotopic triplet $T = 1$ is realized only when their spins are antiparallel.¹

The above-considered operator $Q = \sum_{ij} d_{ij}$, where

$$\langle J' M_1 | d_{ij} | J M \rangle = (2J+1) \delta_{J'J} \delta_{M_1 M}$$

for the j-j coupling will have the magnitude of mathematical expectation [6]:

$$\langle Q \rangle = \frac{n-2(v+1-t-t)}{2} - T(T+1) + t(t+1)$$

where n is the number of nucleons in the subshell j , v is the seniority of the state J'' , T is the isotopic spin, and t is the reduced isotopic spin of the system.

Hence, it is clear that the smaller are v and T , the greater the nucleon pairs connected in an S-state of the relative motion will be present in the

¹Inasmuch as the wave function of two identical particles (two neutrons or two protons) always belongs to the state $T = 1$, in examining the interactions of identical particles the pure S-state of the two nucleons will appear only in the case $v = 0$. Our results, thus, are of interest for the case of intermediate and heavy nuclei, since here interactions of identical particles are considered.

given configuration of n nucleon pairs i.e., the more suitable the energy state. As in the case of the L-S coupling, for noninteracting particles a degeneration of states with respect to T , v , and t will take place.

Let us again consider the form of residual interactions, removing these degenerations in such a manner that the energy of interactions is maximum for the least values of T and v and the largest values of t . These interactions, obviously, will be responsible for the associating of nucleons in S-states. We again arrive at the conclusion that such properties will be possessed by different central forces: for the subshell $j = \frac{1}{2}$, any mixture of Wigner and Heisenberg forces [3]; for $j = \frac{3}{2}$, definite combinations of all forms of exchange nuclear forces. In the articles of Talmi and Unna [6], [7] there was consideration of such a form of interactions. For the energy of interaction of n nucleons of configuration $(\frac{2n}{j})$, the following expression was obtained:

$$E \sim T(T+1)\beta + \left[\frac{2-2(2n-2-v)}{6} + t(t+1) \right] c. \quad (3)$$

Parameters β and c were determined from experimental data by levels and binding energies of nuclei of the shell $j = \frac{3}{2}$. The best agreement with the experiment is obtained for the following values of β and c : for the subshell $p_{3/2}$, $\beta = -3.22$, $c = 0.25$; for the subshell $d_{3/2}$, $\beta = -1.22$, $c = 0.70$. For subshell $j = \frac{5}{2}$ such a form (3) of energy of interaction can be obtained only for basic states of nuclei under the condition that the seniority is a good quantum number. However, for the case of the interaction of identical particles of the subshell $j = \frac{5}{2}$, the dependence of the energy of interaction on the seniority of form (3) is retained [6].

Thus, we can confirm that the above-mentioned residual interactions, which agree well with the experiment, will lead to the associating of nucleons being in an S-state of motion with respect to one another.

4. Let us now consider the basic states of the nuclei. They should be characterized by the maximum value of the operator Q . Furthermore, as we have seen, in the case of L-S coupling, when the symmetry of the spatial part of the wave function is uniquely characterized by Young's scheme \mathcal{U} , this diagram indicates what groups of n nucleons, being in S-states, can be contained in the given n -nucleon wave function. In case of two nucleons in the basic state (diagram of Young [2]) this can be $s + p_2$ or $2p$. In case of three nucleons (scheme of Young [3]) this is $2s + p$ or $3p + s$, i.e., associations, analogous to the nuclei d^3 and h^3 .

In the case of four nucleons (scheme of Young [4]) this is $2s+2p$, i.e., an analog of the α -particle. In case of five nucleons (scheme of Young [41]) this is He^4+s or He^4+p , etc.

From an energy point of view we should expect that nucleons, being in S-states, are more strongly connected with each other than with the remaining nucleons. Therefore, for instance, a six-nucleon group with the scheme of Young [42] is easier to split into two groups with schemes of Young [4] and [2] than, let us say, into groups with schemes of Young [3] and [3]. From this there immediately follow the rules for selection from schemes of Young in the various reactions, which were discussed in report [8]. Hence also the periodicity in the binding energy of the last nucleon which was discussed in articles [2] and [9]. The periodicity curve of binding energies of the last nucleon indicates the presence of associations from three nucleons. Actually, in the case of only paired and fourfold associating dipoles would be observed on the curve of the binding energy for $A=4n+3$ (see Figure 1). Preliminary appraisals of binding energies with the help of calculation of nucleon associating by the above-mentioned procedure provide a shape of the curve of the binding energy of the last nucleon agreeing well with experimental data. Exact calculation of the binding energy of the last nucleon is outside the scope of this work and will be subsequently undertaken.



The solid line denotes the experimental curve of binding energies [2]. The dotted line is the curve for the case of only paired and fourfold associating.

Inasmuch as the S-state of four nucleons and two protons, we can predict that, for instance, it is easier to extract triton from N^{15} than He^4 (see table). Let us consider that experimental data on binding energies of different nucleon associations in light nuclei (table). In the compilation of the table data of articles [10] and [11] were used.

Data of the table confirm the existence of the connection between nucleon associating and the structure of the orbital wave function of the nucleus. It should be noted that in a number of works of Wildermuth and others (for instance, in [1]), the structure of nucleon associations in each nucleus was determined with a great degree of arbitrariness. The proposed consideration makes it possible to determine uniquely the structure of associations for basic states of nuclei by the known schemes of Young.

| Nucleus | Configuration and diagram of Young | Type of splitting | Young diagram of splitting products | Binding energy, Mev |
|--------------------|------------------------------------|--|---|--|
| ${}^6\text{Li}$ | $s^2 [4] p^2 [2]$ | $\text{He}^4 + d$ $\text{He}^4 + p$ $\text{Li}^3 + n$ | $[4] + [2]$ $[41] + [1]$ $[41] + [1]$ | 1.47 4.75 5.50 |
| ${}^7\text{Li}$ | $s^2 [4] p^3 [4]$ | $\text{He}^4 + \text{He}^4$ $\text{Li}^3 + d$ $\text{Li}^3 + p$ $\text{Be}^4 + n$ | $[4] + [4]$ $[42] + [2]$ $[42] + [1]$ $[43] + [1]$ | -0.89 22.39 17.35 18.99 |
| ${}^8\text{Li}$ | $s^2 [4] p^4 [42]$ | $\text{He}^4 + \text{He}^4$ $\text{Be}^4 + n + n$ $\text{Li}^3 + \text{He}^4$ | $[42] + [4]$ $[44] + [1] + [1]$ $[43] + [3]$ | 7.43 8.66 17.35 |
| ${}^9\text{Li}$ | $s^2 [4] p^5 [42]$ | $\text{Li}^3 + \text{He}^4$ $\text{Be}^4 + d$ $\text{Be}^4 + p$ $\text{B}^5 + n$ $\text{Li}^3 + \text{He}^4$ $\text{B}^5 + n + n$ | $[42] + [4]$ $[44] + [2]$ $[441] + [1]$ $[441] + [1]$ $[43] + [3]$ $[431] + [1] + [1]$ | 4.66 6.42 6.38 8.04 17.78 27.80 |
| ${}^{10}\text{Li}$ | $s^2 [4] p^6 [423]$ | $\text{B}^5 + \text{He}^4$ $\text{C}^6 + \text{He}^4$ $\text{C}^6 + d$ $\text{B}^5 + \text{He}^4$ | $[423] + [4]$ $[444] + [3]$ $[4441] + [2]$ $[431] + [3]$ | 19.89 14.84 16.16 28.20 |
| ${}^{10}\text{B}$ | $s^2 [4] p^7 [444]$ | $\text{C}^6 + \text{He}^4$ $\text{N}^7 + p$ $\text{O}^8 + n$ $\text{N}^7 + \text{He}^4$ | $[444] + [4]$ $[4441] + [1]$ $[4443] + [1]$ $[4441] + [3]$ | 7.15 12.11 15.68 25.02 |
| ${}^{10}\text{Be}$ | $s^2 [4] p^8 [444] s^2 [42]$ | $\text{He}^4 + \text{He}^4$ $\text{Ne}^{10} + d$ $\text{Ne}^{10} + \text{He}^4$ | $[44442] + [4]$ $[44444] + [2]$ $[44443] + [3]$ | 8.49 11.38 21.89 |
| ${}^{10}\text{Al}$ | $s^2 [4] p^9 [444] s^2 [442]$ | $\text{Ne}^{10} + \text{He}^4$ $\text{Ne}^{10} + \text{He}^4$ $\text{Ne}^{10} + \text{He}^4$ | $[444443] + [4]$ $[444444] + [3]$ $[4444431] + [3]$ | 19.99 18.22 23.71 |

The table gives data only for certain randomly selected nuclei. In general, such a regularity is observed for all nuclei in the region of $A < 30$. It should be noted that into the binding energy there enters not only energy of residual interactions, but also the binding energy of nucleons in a self-consistent field. It is clear that two nucleons are bound in the self-consistent field more strongly than one. However, the role of residual interactions is so great that, for instance, to extract a neutron from the nucleus B^{10} is more difficult than to extract a deuteron (see table). With an increase in A the role of the Coulomb interaction increases, which conceals the observed regularity.

The author wishes to thank Doctor of Physic and Mathematic A. I. Baz', Prof. G. F. Drukarev, V. G. Ippolitov, V. Feyfrlik, and Candidate of physics and mathematics G. A. Chilashvili for their valuable discussions.

Summary

A relation between the nucleon clustering and the form of shell-model wave function of a nucleus is considered. A large class of effective two-body interactions is shown to cause clustering. An experimental regularity is found to be present in the values of binding energies of light nuclei, which assumes the existence of two-, three- and four-nucleon clusters. The method under consideration makes it possible to treat pairing, triple and quadrucleon correlations on the basis of the same effective two-body interactions of nucleons. A transparent physical

interpretation is given for the experimental facts of energetical advantage of states with the lowest seniority and isotopic spin.

Submitted
12 September 1963

Literature

- 1. Y. C. Tang, L. D. Pearlstein, and K. Wildermouth. Phys. rev., 123, 548, 1961.
2. A. I. Baz'. ZhETF, 31, 831, 1956.
3. B. F. Beyman. Lectures on the application of the theory of groups in nuclear spectroscopy. Moscow, Fizmatgiz, 1961.
4. G. Racah. L. Farkas memorial volume, p. 294. Jerusalem, 1952.
5. W. J. Swiatecki. Proc. Roy. soc., A 205, 238, 1951.
6. I. Talmi and I. Unna. Annual review of nuclear science, 10, 353, 1960.
7. I. Talmi. Rev. mod. phys., 32, 704, 1962.
8. V. V. Balashov, V. G. Neudachin, Yu. F. Smirnov, and N. P. Yudin. News of the AS USSR, physics series, 25, 170, 1961.
9. D. M. Brink and A. K. Kerman. Nucl. phys, 12, 314, 1959.
10. F. Everling, L. A. König, J. H. E. Mattauch, and A. H. Wapstra. Nucl. phys., 18, 529, 1960.
11. F. Ajzenberg-Selove and T. Lauritsen. Nucl. phys., 11, 1, 1959.

NEAR-THRESHOLD BEHAVIOR OF THE INELASTIC-SCATTERING
CROSS SECTION

T. V. Zhikhareva

As Ross and Shaw [1] indicated, the behavior of sections near the threshold of new channel is conveniently investigated with the help of M-matrix, connected with the matrix of reaction of the K relationship

$$M = \kappa^{l+\frac{1}{2}} K^{-1} \kappa^{l+\frac{1}{2}}, \quad (1)$$

where κ is the momentum, and l is the orbital moment of the channel.

Near the threshold of a new channel, where the sections can undergo considerable changes, elements of the M-matrix are smoothly changing functions of energy. In the approximation of the effective radius the first two members of decomposition of M_{ij} in powers of energy are considered

$$M_{ij}(E) = M_{ij}(E_0) + R_{ij}(E_0)(E - E_0) = M_{ij}(E_0) + \frac{1}{2} R_{ij} R_0 [\kappa_i^2 - \kappa_i^2(E_0)]. \quad (2)$$

The initial expression is the relationship between the M-matrix and scattering matrix T

$$T = \kappa^{l+\frac{1}{2}} (M - i\kappa^{2l+1})^{-1} \kappa^{l+\frac{1}{2}}. \quad (3)$$

The partial cross section of the transition from the l -channel to the i -channel for the full orbital moment L equals

$$\sigma = \frac{4\pi}{k^2} \frac{2L+1}{2L+1} |T_{ij}|^2. \quad (4)$$

nondiagonal interactions with the third channel should be small.

(7) can be rewritten thus:

$$\hat{K}_0 = -M_{20} + c_1 M_{20}.$$

In the author's work [2] it is shown that the position of the prethreshold resonance in the elastic cross section can be presented in the analogous form

$$\hat{K}_1 = -M_{20} + c_1 M_{20}.$$

Therefore, if the elastic channel is not connected with the second inelastic channel namely, $M_{20} = 0$, then the position of both resonances coincides and on the curve of the complete cross section a narrow resonance is observed. The presence of this bond results in the resonance in the complete cross section being eroded.

Let us show that the approximation of the effective radius allows describing only one prethreshold resonance. Let us use (2) below the threshold

$$M_{20}(k_0) = M_{20}(0) - \frac{R_0}{2} k_0^2 \quad (8)$$

and substitute (8) in (16). Then from the condition of resonance from k_0 a quadratic equation having two roots, is obtained; k_0^0 coincides with (7), and $k_0^1 = \frac{2}{R_0}$. But the second resonance is artificial, because the domain of applicability of the approximation of the effective radius is determined by the condition [1]

$$R_0^2 |k_1^2 - k_1^2(E_0)| \leq 1. \quad (9)$$

In particular, in work [3] in the singlet case two narrow resonances in the elastic cross section were obtained, of which the second turned out to be artificial, since in the region of its location the highest members of decomposition of the matrix are very large (of the order of $10 \cdot 10^3$).

2. Threshold Behavior of σ_{12}

Let us consider the character of singularity of the inelastic cross section σ_{12} in the threshold $k_0 = 0$. From (5) we can obtain

$$\begin{aligned} & \frac{\sigma_{12}(k_0) \sigma_{12}(0)^{-1}}{2M_{20}^2 (M_{20}^2 + k_0^2) k_1 + 2M_{20}^2 (M_{11}^2 + k_1^2) k_2} \quad k_0 \text{ above the threshold} \\ & \frac{\sigma_{12}(k_0) \sigma_{12}(0)^{-1}}{2M_{20}^2 (M_{20}^2 + k_0^2) M_{11} + 2M_{20}^2 (M_{11}^2 + k_1^2) M_{20}} \quad k_0 \text{ below the threshold} \end{aligned} \quad (10)$$

$s > 0$ is a constant not depending on κ_1 and $|\kappa_2|$. Calculations are made disregarding M_{12} , $s > 3, i \neq \pi$.

Hence for identical signs of M_{11} and M_{22} the case $M_{11} < 0, M_{22} < 0$ corresponds to the singularity, step, and the case $M_{11} > 0, M_{22} > 0$ to the peak. As we will subsequently see, in the case of different signs the type of singularity is determined by the largest of the sections σ_{13} and σ_{23} .

Let us show that the quantity of the singularity in cross section σ_{12} is proportional to the sum of the cross sections of inelastic processes σ_{13} and σ_{23} .

From relationship (3) it follows

$$\begin{aligned} T_{12} &= (\kappa_1 \kappa_2)^{\frac{1}{2}} [M_{12} M_{22} - M_{22} (M_{11} - i\kappa_1)] D^{-1}, \\ T_{21} &= (\kappa_1 \kappa_2)^{\frac{1}{2}} [M_{12} M_{11} - M_{11} (M_{22} - i\kappa_2)] D^{-1}. \end{aligned} \quad (11)$$

Producing the calculation in the same approximation in which (10) is obtained, we have

$$\begin{aligned} |T_{12}|^2 &= \frac{M_{22}^2 (M_{11} + \kappa_1^2) \kappa_2}{s} \kappa_1, \\ |T_{21}|^2 &= \frac{M_{11}^2 (M_{22} + \kappa_2^2) \kappa_1}{s} \kappa_2. \end{aligned} \quad (12)$$

Thus, the greater the probability of inelastic processes σ_{13} and σ_{23} , the larger the singularity in threshold $\kappa_2 = 0$ in the inelastic cross section σ_{12} .

Let us note that in work [4] on the cross section of the creation of the Λ -hyperon near the threshold of the creation of the Σ -hyperon, the singularity in the partial differential cross section, Λ -hyperon creation was obtained proportional to the product of amplitudes of reactions $(T_{12} \cdot T_{21})$.¹

3. Near-Threshold Behavior of the p-Wave of the Inelastic Cross Section σ_{12}

Let us consider the behavior of the p-section of σ_{12} near the threshold of the second inelastic reaction. In this case, according to the law of preservation of the full orbital moment L , orbital moments 1 and 3 of the channels are equal to 1

$$\begin{aligned} T_{12} &= (A_1 A_2)^{\frac{1}{2}} [M_{12} M_{22} - M_{22} (M_{11} - i\kappa_1)] D^{-1}, \\ D &= |M - M^2| = (M_{11} - i\kappa_1)(M_{22} - i\kappa_2)(M_{33} - i\kappa_3) + 2M_{12} M_{21} M_{33} - \\ &\quad - M_{13}^2 (M_{22} - i\kappa_2) - M_{23}^2 (M_{11} - i\kappa_1) - M_{33}^2 (M_{11} - i\kappa_1). \end{aligned} \quad (13)$$

¹Footnote omitted in original text [Tr. Ed. note].

After algebraic transformations we have

$$\begin{aligned} \sigma_{12}(A_2) \sigma_{12}(0)^{-1} &= \\ &= 1 - \frac{2M_{22}^2(M_{22}^2 + A_2^2) \kappa_1^2 + 2M_{22}^2(M_{11}^2 + A_1^2) \kappa_2^2}{\nu} \kappa_2^2 \text{ above the threshold} \\ \sigma_{12}(A_2) \sigma_{12}(0)^{-1} &= \\ &= 1 + \frac{2M_{22}^2(M_{22}^2 + A_2^2) M_{22} + 2M_{22}^2(M_{11}^2 + A_1^2) M_{22}}{\nu} \kappa_2^2 \text{ below the threshold} \end{aligned} \quad (14)$$

It will be obtained from (14) by the replacement of $\kappa_1 \rightarrow \kappa_1^*$, $\kappa_2 \rightarrow \kappa_2^*$

$$\lim_{\kappa_1 \rightarrow 0} \frac{\kappa_1^2}{2\kappa_1} = 0+, \quad \lim_{\kappa_1 \rightarrow 0} \frac{\kappa_1^2}{2\kappa_1} = 0-$$

The picture of the threshold behavior of p cross section σ_{12} is represented in the figure.

This result can be obtained from the ratio of unitarity for the S-matrix

$$|S_{22}^*|^2 + |S_{21}^*|^2 + |S_{12}^*|^2 = 1. \quad (15)$$

Since $T_{22} = \frac{S_{22}^* - 1}{i} \sim \kappa_2^{\frac{1}{2}}$ in the vicinity of the threshold of creation, then

$$\begin{aligned} |S_{22}^*|^2 &\sim 1 - a_1 \kappa_2^2 \\ \sigma_{12} &= \frac{S_{12}^*}{\kappa_1} (2\kappa_1 + 1) |S_{22}^*|^2 \sim 1 - a_1 \kappa_2^2 \end{aligned} \quad (16)$$

whence it follows that $\frac{\sigma_{12}}{\kappa_2} = 0$ in the threshold.

Now let us turn to question of the prethreshold resonance. Below the threshold

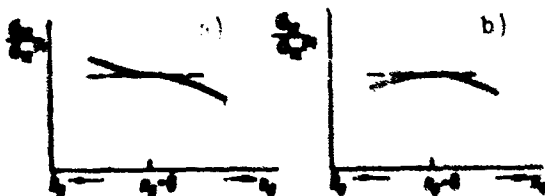
$$\kappa_2 = M_{22} (M_{22} - i\kappa_2^2) = M_{22} - M_{22}^2 \quad (17)$$

Considering the decomposition of M_{33} in powers of energy for $l > 0$ [1]

$$\begin{aligned} M_{33}(E) &= M_{33}(E_0) - \frac{A_2^2}{2M_{22}^2} (\kappa_1^2 - \kappa_1^2(E_0)), \\ \kappa_2 &= (2\kappa_1 + 1) \kappa_1 (2\kappa_1 - 1)^{-1}, \\ M_{22}(A_2) &= M_{22}(0) + \frac{1}{2} A_2^2 M_{22}^2 \end{aligned} \quad (18)$$

we can disregard quantity M_{22}^2 in (17).

The condition of resonance in this case leads to $\hat{\kappa}_2 = \left(\frac{1}{2} A_2 M_{22}\right)^{\frac{1}{2}}$ where $\hat{\kappa}_2$ is obtained from (17) by the replacement of $\kappa_1 \rightarrow \kappa_1^*$, $\kappa_2 \rightarrow \kappa_2^*$



Threshold behavior of p cross section of σ_{12}

$M_{22} > A_2 M_{22} > 0$ (a) $M_{22} < A_2 M_{22} < 0$ (b)

If this resonance appears artificial, i.e., inequality (9) is not achieved, then it is necessary to attract following members of decomposition of the M-matrix.

For instance, in work [3] the resonance in the p-section of elastic scattering was revealed in considering term $\sim \sigma^2$.

In examining the bond of $a_p - a_p - a_p$ of nondegenerate levels for $L = 0$ with a weak bond of $a_p - a_p$ the position of resonance is determined by formula (7) with the replacement of $a_p \rightarrow a_p^2$.

In conclusion I wish to express deep gratitude to G. F. Drukarev for his useful discussions.

Summary

The resonance effect and the behavior of s- and p-sections, the first isotropic section near the threshold of the second one is studied using the limits of the effective range theory.

It is shown that for p-section a_p , the value of threshold anomaly is proportional to the sum of isotropic sections a_s and a_p .

Submitted
1 July 1963

Literature

1. M. H. Ross and G. L. Shaw. Ann. phys., 13, 147, 1961.
2. T. V. Zhikhareva. Transactions of the 15th All-Union Conference on optics and spectroscopy. Moscow, Publishing House of the Academy of Sciences of the USSR, 1964.
3. R. Ya. Damburg and P. K. Peterkop. ZhETF, 44, 244, 1963.
4. A. N. Bar'. ZhETF, 35, 757, 1958.

NUCLEAR-RESONANCE GENERATOR WITH FLOWING LIQUID¹

F. I. Skripov

§ 1. Introduction

The phenomenon of nuclear magnetic resonance, discovered at the end of 1945, soon produced a true revolution in the methods of measurement of strong magnetic fields. The well-known relationship between the frequency of resonance (i.e., the frequency of the Larmor precession of nuclei) ν , and the intensity of the magnetic H_0 superimposed on the sample

$$\nu = \frac{\gamma(1-\sigma)}{2\pi} \cdot H_0 \quad (1)$$

γ - gyromagnetic ratio; σ - a small correction as compared to unity, considering the shielding of nuclei by the electron shell) allows reducing the measurement of the field to a considerably more convenient and accurate measurement of frequency. The extreme narrowness of the resonance peak in liquid samples (sometimes up to fractions of cycles per second) and the exceptional stability of the coefficient $k = \frac{\gamma(1-\sigma)}{2\pi}$ (up to 10^{-8} and above, in a sufficiently wide range of external conditions, if the invariability of the chemical composition of the substance is ensured) cause a sufficiently high sensitivity of the method and, especially, high reproducibility of the obtained results. Moreover, the only unit of equipment requiring

¹Article was prepared by the author in 1961.

experimental calibration is the frequency meter. Comparative measurements, during which the knowledge of the magnitude of the k factor is not required, are fulfilled especially well. During absolute measurements (i.e., when not only are values of intensity expressed in the same units, but these units are also directly connected with standards of mass, length, and time), the accuracy is limited by the error in the experimental measurement of the quantity k. This error is determined by the accuracy of absolute electrical measurements and is at present 0.003-0.005%. For instance, for proton resonance in water the coefficient k is equal to 4257.77 ± 0.15 cps/gs. Of the number of other merits of the nuclear-resonance method in magnetometry we should mention the absence of the need for accurate orientation of the transducer with the sample in space, and also the possibility of direct and undistorted transmission of the result (frequency of the signal!) by wires or radio.

The basic deficiencies are: a) the low intensity of the nuclear-resonance signal, leading to complication of the receiving equipment; b) the presence of certain limitations of the speed of measurement, owing to nonstationary phenomena during nuclear precision measurement of frequency inevitably requires a certain not too small, time interval; c) the high requirements for homogeneity of the measured field.

a) Nuclear-Resonance Measurements of Weak Fields.
Procedure of Packard and Varian

The expansion of the nuclear-resonance method to weaker fields, and especially its application of it to geomagnetic measurements, has encountered very considerable difficulties, which have been overcome only in recent years. During transition from the range of strong fields to the terrestrial field the intensity of the nuclear-resonance signal drops more than one million times. An increase in the dimensions of the sample, fully possible in connection with the high homogeneity of the geomagnetic field, can compensate the indicated decrease of the signal only partially. Therefore, although in separate works, we managed with the help of the usual procedure to observe a signal at $H_0 \sim 0.5$ gs [1], experimental difficulties remained so significant that the problem could not be considered satisfactorily solved. The creation of practically useful measuring equipment as before required radical improvements of the method, considering the specific character of the range of weak fields.

Aside from the work of Schmidt, now of only historical interest [2], it is possible to say that nuclear-resonance measurements of the Earth's magnetic field became practically possible after the fundamental work of Packard and Varian [3, 4]. These authors proposed and carried out in practice new procedure, applicable only in weak fields, of the excitation of free nuclear precession, during which (true, at the price of giving up continuous observation) the intensity of the signal can be increased by hundreds of times.

For the method of Packard and Varian the alternating of periods of magnetization of the sample and observation of the signal is characteristic. The sample with a volume of the order of hundreds of cubic centimeters (water or another slightly viscous liquid possessing a high concentration of protons) is surrounded by a multiturn receiving coil, which is part of an oscillatory circuit. The circuit is turned to the frequency of nuclear precession ν . In order to measure the Earth's magnetic field H_0 an auxiliary (polarizing) field H^* is superimposed on the sample beforehand. Both H^* , and the axis of the receiving coil should be approximately perpendicular to H_0 . However, there is no need for exact orientation, which is an important merit of the method (changes, of orientation affect the intensity of the signal but not its frequency). Regarding, however, the angle between the axes of the polarizing and receiving coils, then it can be arbitrary, often the same coil is used as both polarizing and receiving. Upon the lapse of a certain time after the inclusion of H^* (usually from one to several seconds), nuclear magnetization \vec{M} , is established in the sample proportional in magnitude to the total effective field $\vec{H} = \vec{H}_0 + \vec{H}^*$ and directed along it. Then H^* will be released so fast that during the time Δt of the release the vector \vec{M} does not change not only in magnitude but also in direction ($\Delta t \approx 5 \cdot 10^{-4}$ sec). As a result there appears a unique unsteady state, which we sometimes call coherent or emitting: nuclear magnetization is not in parallel to the remaining field H_0 but precesses around H_0 (with a frequency of ν , see (1)), forming approximately a right angle with it. The gradually attenuating revolving component of vector \vec{M} for several seconds still retains a considerable magnitude, caused by the strong field superimposed earlier. It is precisely this circumstance which leads to the above-mentioned gain in intensity of the signal. The precessing magnetization induces in the receiving coil a variable emf of corresponding frequency; the variable emf after amplification proceeds to some variant of the measuring circuit.

Distinguished by their comparative simplicity (while retaining the majority of the merits of nuclear-resonance methods), the magnetometric devices based on the indicated principle quickly obtained a wide distribution. In the USSR work in the indicated direction was started in 1956 by the Laboratory of Magnetic Microwave Spectroscopy of the Leningrad State University jointly with the All-Union Institute of Methodology and Technology of Exploration [5]; of later foreign works references [6-9] are noteworthy. At present in our country many organizations are engaged in the development of different applications of the method of Packard and Varian.

b) Method of Continuous Observation of the Nuclear-Resonance Signal in the Terrestrial Field

The most important deficiency of the method of Packard and Varian is the necessity to polarize the sample again after every measurement. With a given accuracy this leads to limitations of the speed of taking readings, which do not always satisfy practical requirements (especially in aeromagnetometry). Therefore, the development of continuous methods of observation of the signal in weak magnetic fields is very desirable.

One such method was proposed in January of 1957 by the author and is based on the principle of the nuclear-resonance generator with continuous polarization of the liquid sample flowing through the system [10]. The principal diagram of the transducer of the nuclear-resonance generator [NRG] (RPT) is shown in Fig. 1. During the flow of the sample (water) through the magnetizing (polarizing) coil H nuclear magnetization \vec{M} , is established in the substance proportional to the strong field $\vec{H}_0 + \vec{H}$. Then through a long thin tube BF the water reaches the region in which measurement of the field H_0 should be produced. Moreover, the speed of the flow is selected as great enough so that the quantity \vec{M} does not become greatly decreased. Since the field acting on the element of the volume of the sample at any practically attainable speed of flow changes adiabatically, at point F vector \vec{M} is directed along the weak field \vec{H}_0 . Further the sample flows between the two coils CD deflecting vector \vec{M} (i.e., phasing the nuclear precession), which create an alternating magnetic field of resonance frequency. With a correctly selected amplitude the field of the phasing coils overturns the nuclear magnetization of an angle of the order of 90° , exactly as this takes place in the method of the spin echo (for greater detail see below). The appearing precession, gradually fading, continues during motion through the receiving coil D, which



Fig. 1. Diagram of transducer of the nuclear-resonance generator. Sample (water) flows from left to right. H - magnetizing coil, HK - its compensating windings, $\Phi\Phi$ - phasing coils, Π - receiving coil, ΠK - its compensating windings. The long tube connecting points B and Γ is not shown on the figure. Below the distribution of the constant magnetic field along the axis of the device is shown; the character of the vector movement of nuclear magnetization is shown on the axis of the main figure.

causes the induction in it of a continuous signal. The power supply of the phasing coils can be carried out from an independent external source (operation in narrow-band nuclear-resonance filter mode).

However, continuous observation requires automatic fine tuning of the frequency of the phasing signal with a high degree of accuracy. It is more convenient to use for this purpose the signal appearing in the receiving coil, after its amplification

up to the corresponding magnitude (operation in NRG mode), which ensures automatic tracking of the level of the measured field without any additional devices. In the latter case the narrow-band nuclear-resonance filter is essentially included in the feedback circuit of the amplifier. If we select the position of the phasing coils in such a way that their direct induction on the receiving coil is as small as possible, the feedback closes practically only through the nuclear precession in the flowing water.

In first experimental model of the instrument the flow rate of the water was $100 \text{ cm}^3/\text{sec}$, $H^* \approx 400 \text{ gs}$, the volume inside the magnetizing coil was in 350 cm^3 , and that inside the receiving coil was 400 cm^3 . As operational experience with a model and subsequent calculations showed, the dimensions of the system can be considerably decreased.

Compensation of the field H^* at the location of the receiving coil is carried out by the three windings HK, connected in series with the magnetizing coil. They are calculated in such a way that the field in the center is weakened by not more than 20%, but the dipole and octupole moments of the system as a whole are made equal to zero. Inasmuch as multipoles of even orders are absent in virtue of symmetry, the first uncompensated moment is 32-pole with use of the simple system of such adjustment it proved to be possible to lower the field H^* at a distance of 150 cm from the center of the magnetizing coil to 0.5 γ .

The receiving coil possesses analogous system of compensating coils (ПК).

During tests the generator operated quite stably; the signal-to-noise ratio reached 20. When the feedback circuit was closed there was observed a characteristic process of self-excitation (mild regime). Since, however, the effective of the nuclear-resonance filter is very high (of the order of 10^4) the establishment of the amplitude takes several seconds, i.e., it occurs incomparably slower than in the usual radio-frequency generator. A second cause of the slowness of the establishment of amplitude is the fact that the flowing water creates something like a delay line, included in the feedback circuit. Regarding, however, the frequency of the signal, as qualitative experiments showed, it follows the change of field H_0 practically instantly.



Fig. 2.

Fig. 2. Outer view of model of nuclear-resonance generator.

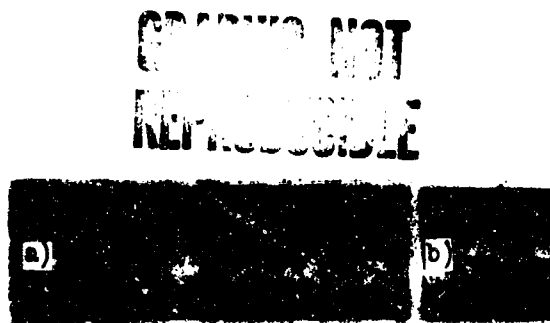


Fig. 3.

Fig. 3. Photograph of an NRG signal obtained on a loop oscillograph in the nuclear-resonance filter mode (speed of film 10 mm/sec), a) attenuated signal (method of Packard and Varian) obtained in the same mode b).

COPIES NOT REPRODUCIBLE

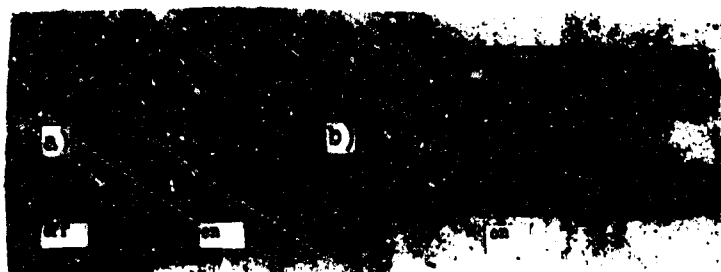


Fig. 4. Turning off and connection of the magnetizing field a); turning off and connection of the phasing signal b). Speed of film 10 mm/sec.

The outer view of the NRG model is shown in Fig. 2. Figures 3 and 4 photographs show of signals obtained with help of a loop oscillograph in the process of experiments with the instrument.

c) Other Continuous Methods of Observations Applicable
in Weak Fields

The above-described method was proposed and its development was begun in the Laboratory of Magnetic Microwave Spectroscopy of the Leningrad State University at a time when in the literature there was a complete absence of any signs of practically applicable methods of the continuous observation of the nuclear-resonance signal in such weak fields as the terrestrial field. Now, however, it is known that several authors worked independently and almost simultaneously on this problem.

K. V. Vladimirskiy [11] theoretically examined conditions of self-excitation of nuclear precession in a sample preliminarily magnetized antiparallel to the terrestrial field and placed in a coil of a sufficiently good quality resonant circuit. The Q and the magnetizing field H^* had to be very high (at room temperature in any case $H^*Q > 10^4$ gs). The author indicates that the generating of a stationary signal is possible, if in a similar system the continuous replacement of the sample is accomplished. Concrete variants of the realization of this system are not considered in [11].

In the system of K. V. Vladimirskiy, if a solenoid, and not a magnet, is used for polarization of the sample (which is extremely desirable for reducing the system's weight and also because of the need for very accurate compensation of H^* in the region in which the measurement of the weak field is taken), fulfilment of the ratio $H^*Q > 10^4$ is very difficult. In any case, it appears necessary to obtain a maximum Q (most likely by means of the use of a regenerated receiving circuit). As a result, the range of values of the field in which generating of the signal is possible without the fine tuning of this circuit is narrowed; furthermore, the measuring error caused by the inaccurate adjustment to the frequency of nuclear precession greatly increases (see point "c," § 2).

In the work, carried out under the leadership of G. D. Latyshev [12], a flowing sample and preliminary polarization by a strong field are also used, but the system does not use the principle of the nuclear-resonance generator (Fig. 5). In the proposed variant of the method polarization is carried out with the help of an electromagnet \mathcal{E} , (the method of observation does not differ from the conventional method in strong magnetic fields). Measurement of the weak magnetic field H_0 is produced at point A, where an additional radio-frequency field, created by an external source, acts on the sample. In its action it is completely analogous to the phasing field mentioned above: upon entering into resonance with the frequency



Fig. 5. Measurement of a weak magnetic field per [12].

of precession of the nuclei, vector \vec{M} deviates from the direction of \vec{H}_0 and starts to precess. If the amplitude of the radio-frequency field is selected appropriately, deflection occurs at an angle of the order of 90° , i.e., the longitudinal component of \vec{M} turns into zero. Regarding, however, the transverse (precessing) component, then it is inevitably disturbed in the region of the nonuniform magnetic field B (field of scattering \mathcal{E}_0), since in the nonuniform field various elements of the volume of the sample precess with unequal speeds and fall out of phase. Thus, the onset of resonance in coil A leads to the destruction of nuclear magnetization, which can be fixed indirectly by the attenuation or disappearance of the signal observed in \mathcal{E}_1 .

The method described is of considerable interest for magnetometry of weak fields of great heterogeneity (measurement can be carried out in a small volume). It is true, moreover, that a certain decrease in accuracy is inevitable, since a decrease in the volume of coil A will reduce the time of the stay of an element of the sample's volume in this coil and, correspondingly, will increase the width of the spectrum of the phasing signal.¹ Another interesting characteristic is the possibility of measuring fields considerably weaker than the terrestrial field. However, for precision geomagnetic measurements the method discussed is not convenient enough. First of all the system is more complicated than that in [10], and the automatic tracking of frequency for the variable field is absent. Secondly, any instrument not based on the NRG principle requires modulation of the measured field for the periodic passage through the line circuit; with slow modulation the speed of the measurement will be considerably lowered, and its acceleration is inevitably connected with appearance of extremely undesirable transient processes in the motion of the vector of nuclear magnetization.

Finally, Abraham, Combrison, and Solomon published an extraordinarily interesting work [13] in which one of the new varieties of the Overhauser method of polarization of nuclei is used. As is known, the Overhauser effect can be observed in samples which are characterized still by uncompensated electron magnetism as well as nuclear (metals, paramagnetic solutions, etc.). The essence

¹The influence of the phasing field will be examined quantitatively below; it will be shown that in the system developed by us the effective width of resonance is determined by the time of the stay of the element of volume in the receiving coil and not in the phasing coil.

of this phenomenon consists of the fact that owing to the internal bond between the electrons and nuclei the influence of an intense high-frequency field on electron magnetism causes a very strong polarization of the nuclei, many times exceeding the equilibrium value in the same constant magnetic field. It is interesting to note that in the case essential for us of paramagnetic solutions of small concentration, the Overhauser effect causes the appearance of nuclear magnetization oriented opposite the field. In the usual ("classical") effect, when $H_0 \sim 0.5$ gs the influence on electrons constitutes a saturation of electron resonance at a frequency of about 1.4 Mc with a power from several watts and larger, depending on how successfully the sample is selected. Moreover, it is possible to obtain nuclear magnetization 200-300 times greater than equilibrium magnetization i.e., that type which is obtained in H_0 fields of the order of 100-150 gs. Inasmuch as in the method of Packard and Varian and also in [10] somewhat stronger polarizing fields are usually used, the classical Overhauser effect in the terrestrial field does not possess any advantages with respect to the intensity of the signal. Its merit, however, is the possibility of continuous polarization in the actual volume in which the signal is observed, i.e., in a motionless sample.

In work [13] another still more effective variant of the method is used in which there is applied some paramagnetic substance, possessing a hyperfine structure of electron resonance permitted at room temperature. In this case even during complete absence of the external magnetic field influence on electrons at a rather high frequency is possible (quantum transitions between sublevels of the hyperfine structure). The superposition of $H_0 \sim 0.5$ gs acts very slightly, so that the frequency of electron transitions can be considered independent of the field.

The sample in work [13] was a weak aqueous solution of the potassium salt of disulfonate of peroxyamine $KNO(SO_3)_2$. As a result of the electrolytic dissociation in the solution ions are present - free radicals of the following structure:



with one unsaturated valence for the nitrogen atom. The high-frequency field saturated the transition between the sublevels at a frequency of 56 Mc (in the zero field, 54.7 ± 0.5 Mc [14]). The exact figures for the magnitude of nuclear magnetization are not cited, but from appraisal of the theoretical formulas the conclusion can be made that values of M , 2000-3000 times greater than the

equilibrium values are accessible.

Report [13] is dedicated, basically, to the observation of the line contour on the screen of the oscillograph with help of the modulation method, widespread in strong fields. In the sample with a volume of 100 cm^3 a very good signal-to-noise ratio is obtained. However, for our purposes the modulation method, as was already indicated, is unsuitable.

The article also contains a very brief indication of the fact that with an increase in Q (regenerated circuit) operation of the system in the NRG mode was observed. Inasmuch as the initial magnetization was antiparallel to the field, this variant is very close to the diagram of Vladimirskiy, but without the necessity of a continuous replacement of the sample. Possessing many essential merits, it also is connected with necessity of very exact fine tuning of the receiving circuit during changes of H_0 . We should also mention deficiencies common for all methods based on the Overhauser effect: a) a certain complication of the radio-frequency circuit, making it necessary to have an additional high-frequency generator of considerable power, and b) the broadening (by at least 2-3 times) of the line of nuclear resonance, owing to the presence of paramagnetic material.

The advantages of Overhauser polarization, nevertheless, are so considerable that, this method will be used in the future (we have in mind not a concrete variant [13] but all the region as a whole). However, disulfonate of peroxyamine in aqueous solutions is chemically unstable, being half decomposed in several minutes [15]. Although the use of buffer solutions delays decomposition [15] and in solutions of sodium carbonate the substance exists for up to several days [16], nevertheless the chemical stability of this substance cannot be considered satisfactory for practical applications. At the same time, until now not one replacing substance which possessed at least approximately the same effectiveness of Overhauser polarization in weak fields has been known. Probably, such objects will be found. However, if we were to consider that they have extremely unique and partially contradictory requirements,¹ it is very difficult to forecast when this

¹We should consider, in particular, the necessity to have a very narrow line of electron resonance, since otherwise its saturation will demand considerable power. Narrow lines and simultaneously a hyperfine structure are possessed only by certain substances of the class of free radicals, which by their very nature are usually chemically active compounds.

problem will be satisfactorily solved.¹

Summing up what has been said, from our point of view, we should come to the conclusion that the development of high-speed magnetometric instruments on the basis of the NRG diagram, proposed in [10], is at present still urgent. Moreover, we should consider that many elements of such development (especially, of course, the measuring circuit of frequency and the recording part) will remain the same even when subsequently Overhauser polarization will be used in a certain concrete variant of the instrument.

§ 2. General Theory of the Nuclear-Resonance Generator with Flowing Water

a) Processes in Magnetizing and Phasing Coils

A quantitative description of the processes of magnetization (polarization) of a flowing sample in a constant magnetic field is not difficult. As it is well known, the establishment of magnetization is described by the following differential equation:

$$\frac{dM_z}{dt} = -\frac{M_z - M_0}{T_1} \quad (2)$$

where M_z is the nuclear magnetization (magnetic moment of a unit volume of the sample caused by the predominant orientation of nuclear magnetic dipoles); index z indicates the fact that vector \vec{M} is directed at each moment of time along the effective field $\vec{H} = \vec{H}_0 + \vec{H}_p$.² $M_0 = \chi H$ is the magnitude of nuclear magnetization which is equilibrium at a given value of the field H . χ is the nuclear magnetic susceptibility, which is expressed by the known Curie formula; for water it is equal to $3.3 \cdot 10^{-10}$, which is almost the maximum value among all substances at room temperature (for greater detail see [5]). T_1 is the time of longitudinal relaxation, which is an important characteristic of the sample; for water without

¹In the present brief survey we do not touch upon investigations carried out in medium or strong fields but which represent a certain indirect interest for methods of magnetometry of the terrestrial field. Certain works on the Overhauser effect in fields stronger than terrestrial are also not mentioned.

²It is simple to show that in real conditions of the operation of the instrument this indeed takes place (at least, in a good approximation). Furthermore, if even within separate small elements of the volume component \vec{M} existed in plane xy , it would not play any role; field \vec{H}_p is too nonuniform for these components to be in the same phase for the whole sample.

dissolved oxygen $T_1 = 3.6$ sec; the presence of paramagnetic molecules noticeably reduces T_1 .

For the considered element of volume the quantity H will be a function of time (owing to its displacement from one point to another). It is convenient to rewrite the differential equation (2) in the following form:

$$\frac{dM_z}{dt} + \frac{1}{T_1} M_z = \frac{1}{T_1} H(t) \quad (3)$$

If we were to consider that the magnetizing field starts to act at moment $t = 0$, where magnetization at this instant is equal to $M_z(0)$, the solution to equation (3) can be written in the following way:

$$M_z(t) = \left[M_z(0) + \frac{1}{T_1} \int_0^t H(t') e^{-\frac{t-t'}{T_1}} dt' \right] e^{-\frac{t}{T_1}} \quad (4)$$

(see, for instance, Bronshteyn and Semendyayev, "Handbook on mathematics," First edition, p. 404). Function $H(t)$, can be calculated in form of a table, if the distribution of the magnetic field along the axis of the polarizing coil and speed of flow of the sample are known (certainly, this operation bears an approximate character, but attempts at further, more precise definition are hardly justified, since they require computations of turbulence). After this formula (4) can be used for numerical calculations.

In most cases, however, we can limit ourselves to a more rough approximation, disregarding quantity $M_z(0)$ and assigning $H(t)$ in the form of $H(t) = \bar{H}$ when $0 < t < \tau$ and $H(t) = 0$ outside this interval (τ is the time of flow through the polarizing coil, \bar{H} is the mean value of the field in this coil). Then magnitude of nuclear magnetization at the moment of exit from the strong field is expressed by the following simple formula:

$$M_z(\tau) = \bar{H} T_1 \left[1 - e^{-\frac{\tau}{T_1}} \right] \quad (5)$$

which is very easily obtained, directly from (2) when $M_z = \text{const}$ in the interval $0 < t < \tau$.

Let us now consider the movement of the sample through the tube connecting the region of magnetization with the region of the phasing field. Although the presence of the system of compensational windings (HK in Fig. 1) leads to a very fast decrease of the field in this part of space, nevertheless the transition

from $\vec{H}_0 + \vec{H}^*$ to \vec{H}_0 during practically realizable speeds of flow will occur after a time interval of 0.1 sec or more. Such a change of \vec{H} is sufficiently slow so that vector \vec{M} remains at each moment of time parallel to the field.¹ The decrease of the magnitude of vector \vec{M} (process of demagnetization) is described as before by differential equation (2) with new, considerably smaller values of $M_0(t)$. In connection with this the dependence of M_z on time is expressed by the general formula, analogous to (4) and formally coinciding with (4) if we were to put $\tau_1 = 0$, i.e., count off the time from the moment of exit from the strong field,

$$M_z(t) = \left[M_z(\tau) + \frac{1}{T_1} \int H(t') e^{-\frac{t-t'}{T_1}} dt' \right] e^{-\frac{t-\tau}{T_1}} \quad (6)$$

The quantity $H(t')$ in this formula is a function quickly decreasing to H_0 .

In a more rough approximation we may assume that when $t > \tau$, the effective field is already much less than that inside the magnetizing coil. With this $M_0(t) \ll M_0(\tau)$ (inasmuch as M_z still retains large values!), so that in (2) quantity M_0 can be disregarded. Then instead of (6) we have

$$M_z(t) = M_z(\tau) e^{-\frac{t-\tau}{T_1}} \quad (7)$$

In the phasing coil, as a result of the influence of the radio-frequency field, vector \vec{M} deviates from the direction of the axis z (i.e., from \vec{H}_0). The longitudinal component, as before, decreases according to the law (2), and for the transverse component we can write

$$\frac{dM_1}{dt} = -\frac{M_1}{T_2} \quad (8)$$

where $M_1 = \sqrt{M_x^2 + M_y^2}$ and T_2 is the time of the transverse relaxation. Inasmuch as, however, M_z and M_1 in reality are functions of time not only as a result of processes of relaxation, but also owing to the continuing influence of the radio-frequency field, the analysis of the motion of the vector of nuclear magnetization in the phasing coil requires, in general, solution of equations of Bloch. We will not examine these solutions, since from practical considerations it turns out to be

¹With certain simplifying assumptions this is easy to show with help of known equations of Bloch. But this is not necessary, since from experiments by the method of Packard and Varian it is well-known that the "breaking away" of vector \vec{M} from the direction of the field occurs only when \vec{H} will be turned off in approximately 10^{-4} sec or faster.

expedient to select the time of flow through the phasing field as $\ll T_1, T_2$. With this the relaxation processes in the first approximation can be disregarded. Then, as this follows from further text of the present section, the influence of the radio-frequency signal changes the orientation of the vector of nuclear magnetization but does not affect its length. In the following approximation we can consider the small relaxation effects in accordance with (2) and (8), disregarding the distinction of T_1 and T_2 , which in a sufficiently uniform field of H_0 is considerably small. If, furthermore, we replace 0 by M_0 , as is done in the derivation of (7) then (2) and (8) becomes identical. Hence, it directly follows that the absolutely analogous differential equation

$$\frac{dM}{dt} = -\frac{M}{T_1} \quad (9)$$

takes place for the change of the length of the vector $M = \sqrt{M_x^2 + M_y^2}$. Inasmuch as the radio-frequency field does not affect the quantity M , equation (9), unlike (2) and (8), remains in force for the phasing coil.

Since the solution to (9) has a form completely analogous to (7), in the considered approximation we arrive at a very simple result: the magnitude of nuclear magnetization continues to change according to the law (7) and at the moment of entry into the receiving coil is equal to

$$M(t_0 + t_1 + t_2 + t_3) = M_0(t_0) e^{-\frac{t_0 + t_1 + t_2 + t_3}{T_1}} \quad (10)$$

where by t_0 , t_1 and t_2 we designate the time of flow through the connecting tube, the region of the phasing field, and the second (short) piece of connecting tube respectively.

Now we can turn to the study of the influence of the phasing radio-frequency field, disregarding, as was already stated, the relaxation processes. In order to write the equation of the motion of the vector of nuclear magnetization, let us remember that besides the magnetic moment \vec{p} , each nucleus possesses spin \vec{P} (spin angular momentum). The quantity $\gamma = \frac{p}{P}$, called gyromagnetic ratio, was already found in (1). The vector of nuclear magnetization is obviously expressed as follows:

$$\vec{M} = \sum \vec{p}_i \quad (11)$$

For $\gamma > 0$ (as in the case of protons) vectors \vec{p}_i and \vec{P}_i are parallel to each other. It follows from this that the macroscopic vector \vec{M} is connected with spin \vec{P}

corresponding to it:

$$\vec{P} = \sum \vec{p}_i = \sum \frac{\vec{h}}{T} = \frac{1}{T} \vec{M} \quad (12)$$

(the summation (11) and (12) extends to all nuclei per unit volume of the sample).

Whereas the motion of a separate nucleus is described by quantum-mechanical formulas, the macroscopic vector \vec{P} satisfies the usual equations of motion of classical mechanics. According to the second law of Newton, we will equate the change of angular momentum to the moment of acting force

$$\frac{d\vec{P}}{dt} = [\vec{M} \times \vec{H}] \quad (13)$$

or, finally,

$$\frac{d\vec{M}}{dt} = \gamma [\vec{M} \times \vec{H}]. \quad (14)$$

In these expressions under \vec{H} is understood the totality of all the constant or alternating magnetic fields acting on sample.¹

In particular, if $H_x = H_0 = \text{const}$, $H_z = H_y = 0$, the absolutely elementary solution to (14) gives

$$\begin{aligned} M_x &= M_1 \cos(\gamma H_0 t + \psi), \\ M_y &= -M_1 \sin(\gamma H_0 t + \psi), \\ M_z &= \text{const}, \end{aligned} \quad (15)$$

where $M_1 = M \sin \theta$ and $M_z = M \cos \theta$ (Fig. 6). Angle θ and phase ψ are determined by the initial conditions of motion. When $M_1 = 0$ (magnetization directed along the field) vector \vec{M} rests, although its component magnetic moments of separate nuclei continue, of course, to precess. This case corresponds completely to the random phases of the motion of separate nuclei, so that components of \vec{p}_i in plane xy destroy one another; this very point was considered in the first half of the section.

When $M_1 \neq 0$ the formulas of (15) describe the simple precession of nuclear magnetization in the presence of only the constant field \vec{H}_0 . In reality the precessing component M_1 gradually decreases (with the characteristic time T_2), as was mentioned in the description of the method of Packard and Varian; however, our consideration is limited by the interval of time $\ll T_2$ and does not consider the

¹From (14) the above-mentioned invariability of the length of vector \vec{M} directly follows (if we disregard relaxation), since in any external fields $dM^2/dt = 0$.

relaxation processes. In this case ($\delta \neq 0$) the phases of motion of separate nuclei are partially ordered, and a decrease in M_1 indicates a gradually occurring dephasing. Therefore T_2 sometimes is called, the time of the spin phase memory. From (15) it follows that the frequency of precession ν_0 is equal to $\frac{1}{2\pi} H_0$. The little difference from the more accurate formula (1) is due to the fact that here we disregarded the insignificant difference between H_0 and the field actually effective on the nuclei.

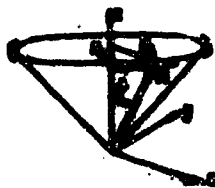


Fig. 6. Precession of \vec{M} in the constant external field. The case of the positive gyromagnetic ratio.

After these preliminary remarks we can turn to the more complicated case of the simultaneous action of the constant and alternating magnetic field. Inasmuch as the consideration is produced most clearly of all in a revolving coordinate system, it is necessary to use the transformation of (14) to revolving coordinates, namely,

$$\left(\frac{d\vec{M}}{dt}\right)_r = \gamma \left[\vec{M} \times \left(\vec{H} + \frac{\vec{\omega}}{\gamma} \right) \right], \quad (16)$$

where $\vec{\omega}$ is the vector of the angular velocity of the considered coordinate system with respect to the motionless (inertial) coordinates, and index r indicates that the derivative is calculated in the revolving system.

The graphic meaning of equality (16) consists in the fact that during the use of the revolving coordinates it is possible to preserve the equation of motion in the form of (14) and, consequently, also all derivations from it, if to the totality of effective fields of \vec{H} we add the fictitious field $\frac{\vec{\omega}}{\gamma}$. For instance, for the above-considered simple case $\vec{H} = \vec{H}_0$, the introduction of the coordinate system $x'y'z'$, rotating around direction z' , leads to the replacement of H_0 by $H_0 - \frac{\omega}{\gamma}$ (see Fig. 7 when $M_1 = 0$). In particular, if we were to select $\omega = \omega_0 = \gamma H_0$, then in the revolving system the magnetic field is absent and $\left(\frac{d\vec{M}}{dt}\right)_r = 0$. It is not difficult to see that this corresponds to the rotation of coordinates in the direction of precession and with the very same angular velocity, so that in the system $x'y'z'$ the vector of nuclear magnetization is indeed at rest.

Let us introduce still motionless coordinates xyz , and we will consider that axis z , like z' , coincides with the direction of the constant field \vec{H}_0 (Fig. 7). Let us assume that the variable phasing field oscillates along the axis, and its semiamplitude is designated by H_1 . Then the totality of the magnetic fields acting on vector \vec{M} in a motionless coordinate system will be written as follows:

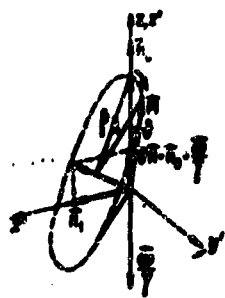


Fig. 7. Vector \vec{M} in a rotating system of coordinates.

$$\begin{aligned} H_x &= 2H_1 \cos \omega t, \\ H_y &= 0, \\ H_z &= H_0. \end{aligned} \quad (17)$$

We separate the fluctuating field into two revolving fields in plane xy in opposite directions:

$$\begin{aligned} H_x &= H_1 \cos \omega t, \\ H_y &= -H_1 \sin \omega t, \\ (H_z &= H_0). \end{aligned} \quad (18a) \qquad \begin{aligned} H_x &= H_1 \cos \omega t, \\ H_y &= H_1 \sin \omega t \end{aligned} \quad (18b)$$

and disregard the influence of the component (18b) revolving in a direction opposite to the precession of vector \vec{M} . The possibility of such disregard will be validated below. Now it is possible to convert the totality of the fields (18a) to the revolving system of coordinates, axis x' of which is directed along vector \vec{H}_1 (Fig. 7). Thus, we select coordinates rotating with a frequency of the phasing signal. The effective field along axis z' is now equal to

$$H = H_0 - \frac{\omega}{\gamma} \quad (19)$$

and is a measure of the detuning of the phasing signal with respect to the resonance of the frequency.

It is interesting to note that in coordinates $x'y'z'$ only the constant field $\vec{H}_1 + \vec{H}_0$, acts on vector \vec{M} , so that the motion of \vec{M} bears a character of simple precession. If, as usually, $H_1 \ll H_0$ and the detuning is small, the angular velocity of this precession $|\vec{H}_1 + \omega|$ is much smaller than the speed of rotation of the whole picture of Fig. 7 together with the primed coordinate system. This means that in fixed coordinates the motion of \vec{M} as before constitutes precession, but with a gradually variable apex angle of the cone (nutation).

Especially simple is the case of exact coincidence of the frequency of the phasing signal with the resonance frequency ($\omega = 0$). Vector \vec{M} revolves uniformly in plane $z'y'$ with an angular velocity of H_1 . Passing to the fixed coordinates, we find that the radio-frequency field in resonance excites precession of nuclear magnetization with a frequency $\omega = \omega_0 = \frac{1}{2} H_0$. During the first half-period of nutation angle θ between \vec{M} and z changes according to the law

$$\theta = \gamma H_1 (t - t_0 - \tau_0) \quad (20)$$

and in phase the vector \vec{M} will lag 90° behind the rotating component H_1 . In the second half-period $\theta = 2\pi - \gamma H_1 (t - t_0 - \tau_0)$, during which precession leads H_1 90° , etc.

However only the first half-period is of practical value. From the point of view of obtaining the largest amplitude of the signal in the receiving coil, it is desirable to have $\theta \sim 90^\circ$, i.e., to select the time of flow through the phasing field equal to a quarter of the period of nutation:

$$\omega_0 \tau = \frac{\pi}{2}; \quad \nu = \frac{\pi}{4H_1}. \quad (21)$$

Let us now turn to the case of inaccurate tuning to resonance. As can be seen from Fig. 7, the character of nutation changes in such a way that the value $\theta = 180^\circ$ is not attained. $\theta = 90^\circ$ can be obtained during not too large detunings ($\Delta H \ll H_1$). Vector \vec{M} emerges from plane $z'y'$, so that as compared to the case of exact resonance additional phase shift φ_0 is accumulated the sign of which depends on the sign of detuning.¹ The obtaining of quantitative expressions for M_x (or θ) and φ_0 as functions of time is now reduced to elementary trigonometric computations, which need not be reproduced here. Since the expressions in general turn out to be somewhat bulky, we limit ourselves to only small detunings of ($\Delta H \ll H_1$):

$$\begin{aligned} \theta &= \arcsin \left\{ \sin \theta_0 - \cos \theta_0 \left(1 - \cos \pi \left(\frac{\Delta H}{H_1} \right)^2 + \dots \right) \right\}, \\ \varphi_0 &= \frac{1 - \cos \theta}{\sin \theta} \left(\frac{\Delta H}{H_1} - \frac{1}{2} \left(\frac{\Delta H}{H_1} \right)^3 + \dots \right), \\ \varphi_0 &= \tau \omega_0 \sqrt{M_x^2 + M_y^2} = \tau \omega_0 M_1 \left(1 + \frac{1}{2} \left(\frac{\Delta H}{H_1} \right)^2 + \dots \right) M_x = M_1 \sin \theta. \end{aligned} \quad (22)$$

Angle φ_0 in these formulas is counted off from axis y' in the direction of precession.

From the above, it follows that during large detunings the radio-frequency field \vec{H}_1 renders on \vec{M} only a rapidly varying effect with an insignificant angular amplitude, which when $\Delta H \ll H_1$ is so small that it cannot cause any observed effects. It is for this reason that we disregarded above the effect of the component (18b) revolving to the opposite side.

b) Processes in the Receiving Coil. Operation of the System in the Mode of a Narrow-Band Narrow-Band Nuclear Resonance Filter

Precession of the vector of nuclear magnetization continues after emergence of the volume element from the phasing field. The magnitude of the longitudinal

¹This phase shift, in general, is undesirable, since it can cause an additional measuring error during operation of the system in a nonuniform field (see § 2, part c). For this reason, and also to decrease demagnetization, an increase in H_1 leading to the reduction of the time of stay in the phasing field, is desirable.

component (M_z) will no longer be of interest to us, since it does not affect the signal induced in receiving coil. Moreover, we leave aside the phenomenon of reaction of circuit (see [5]), inasmuch as in the operation of the NRG based on the described principle it plays a secondary role.

After the interval of time τ_1 after flowing from the phasing field, the considered element of the sample enters the receiving coil and starts to participate in the formation of a useful signal. The time of the stay in this part of the system is great enough so that attenuation of the precessing component M_x will appear:

$$M_x(t) = M_x(\tau_0 + \tau_1 + \tau_2 + \tau_3) e^{-\frac{t - \tau_0 - \tau_1 - \tau_2 - \tau_3}{T_2}} \quad (23)$$

Inasmuch as the frame of time reference accepted thus far; as can be seen from (23), starts leading to awkward expressions, we will subsequently use time \bar{t} , counted off from the moment of exit from the phasing field:

$$\bar{t} = t - (\tau_0 + \tau_1 + \tau_2) \quad (24)$$

after which (23) takes a more simple form:

$$M_x(\bar{t}) = M_x(\tau_3) e^{-\frac{\bar{t}}{T_2}} \quad (25)$$

or

$$M_x(\bar{t}) = M_x(0) e^{-\frac{\bar{t}}{T_2}} \quad (25^1)$$

Continuing the examination of precession with the help of the rotating coordinate system introduced in point "a," § 2, we, as before, will read off the phase angle $\varphi(\bar{t})$ from axis y' . For the case of a uniform field H_0 , having the same magnitude in both the phasing field and the receiving coil,

$$\varphi(\bar{t}) = \varphi_0 + \omega_H \bar{t} \quad (26)$$

where the second component describes the phase, incoming in connection with the

¹The form of notation (25¹) is based on the fact that in the interval $0 < \bar{t} < \tau_3$, M_x decreases with the same characteristic time T_2 as later on (inside the receiving coil). Thereby formula (10), where we disregarded the distinction of T_2 from T_1 , is defined somewhat more accurately. Usually τ_1 is so small that this distinction is immaterial; however, we will return again to the discussion of the construction with a large τ_1 .

difference of angular velocity of free precession of vector \vec{M} from the speed of rotation of the coordinate system (connected, as was already indicated, with the frequency of the phasing signal). If, however, heterogeneity of the field takes place, then H_0 for the moving volume element becomes a function of time, and (26) is replaced by

$$\varphi(\vec{r}) = \varphi_0 + \gamma \int \omega_0(\vec{r}) d\vec{r}. \quad (27)$$

where $\omega_0(\vec{r}) = \omega_0(\vec{r}) - \frac{\omega}{\gamma}$.

Expressions (26) or (27) allow making the following conclusion, which is very significant for a correct understanding of processes in systems with a flowing sample: although the precession of vector \vec{M} in every moving volume element occurs with the natural frequency $\omega_0(\vec{r}) = \gamma H_0(\vec{r})$, the emf induced in receiving coil in steady-state operation of the system has the same frequency ω as the phasing signal.

In order to prove this property, paradoxical at first sight, we will examine a certain motionless volume element located at point A inside the receiving coil. Obviously, it is characterized by the constant interval of time \bar{T}_A , which is required, so that the moving particle of the sample, having come from the phasing field, will reach point A.¹ But this means that the phase shift of precession $\varphi(\vec{r}_A)$ is constant. Thus, at a fixed point (this means not connected with any defined particle of the sample) component \vec{M}_A maintains a constant direction in the system $x'y'z'$, i.e., it revolves together with the system with a frequency ω . Inasmuch as by A we can imply any point inside the receiving coil, the result formulated above can be considered proven.

The conclusion at which we arrived does not contradict the presence of free precession with the frequency ω_1 for each volume element of the flowing sample. The possibility of such a distinction of frequencies is due to the fact that at a given moment of time different elements of the volume precess with unequal initial phases $\varphi(\vec{r})$, since \vec{r} for them is different (an exception is only the case of a uniform field with tuning to resonance, when ω and ω_0 coincide). Inasmuch as the phase relationships in the system with a flowing sample present certain difficulties for understanding, it is worthwhile to turn to the clearest model possessing the

¹During the turbulent flow this affirmation is true only on the average. However, all further conclusions, as it is easy to see, remain in force if the total speed of the flow of sample through the system remains constant.

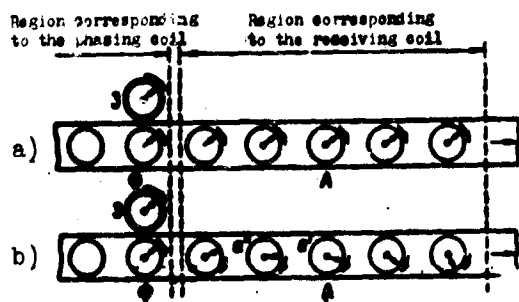


Fig. 8. Phase relationships in a nuclear-resonance generator with flowing water, illustrated on a model. a) speed of clock movement on the conveyer is equal the speed of the movement of the standard clocks (analogy with the case of an exact adjustment to resonance, $\omega = \omega_0$); b) speed of the clock movement on the conveyer is greater than the speed of movement of the standard clocks (analogy with the case $\omega > \omega_0$).

standard clocks ϑ . The clocks on the conveyer are assumed identical, but their rate of movement can be both equal (case a, corresponding to coincidence of ω and ω_0) and unequal (case b, illustrating deviation from exact resonance) to the speed of the rate of the clocks.

In the first case, as it is easy to see, all hands are parallel (since all the clocks show the same exact time). In the second case, the error increases in proportion to the distance from point ϑ . However, at any fixed point (for instance, at the operating place designated A), this error is constant and is determined only by the error of the rate of the clocks on the conveyer and the time of its movement from ϑ to A. Therefore, from the point of view of the operator at A, the clocks have a correct rate of movement, although they show the time with some error. The fact that in reality the clocks are fast is compensated by the replacement of clocks a' by clocks a'', which somewhat lag behind a', etc.

Figure 8 allows the making of one more qualitative conclusions: the maximum magnitude of the signal induced in the receiving coil takes place during exact resonance ($\omega = \omega_0$; Fig. 8a), since in just this case the influences of all volume elements coincide in phase and accumulate. In proportion to the detuning of the frequency of the phasing signal the amplitude of oscillations in the receiving coil should drop (in a limit up to zero), even if the quantity $M_1(\omega)$ by some method is maintained constant. Thus, not only actual phasing (see point "a," § 2), but

same properties. Let us consider a conveyer, on which clocks are assembled (Fig. 8).

For simplicity on every dial only one hand is represented (for instance, the second hand). Essentially the figure for the nuclear-resonance generator would look exactly the same, with the only exception being in this case the length of the hand (i.e., the magnitude of M_1) would gradually decrease in accordance with (25) in proportion to movement from left to right (see Fig. 1).

The influence of the phasing field is simulated here by the fact that at point ϑ every clock on the conveyer is set to the

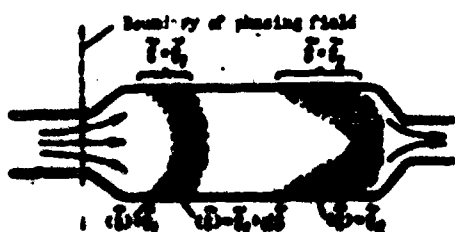


Fig. 9. Schematic representation of the flow of liquid inside the receiving coil. OOO - locus of points for which the mean value of time \bar{t} (i.e., time necessary for a volume element of the sample just coming from the phasing field to attain a given point) is equal to \bar{t} ; the mean value of \bar{t} is designated by $\langle \bar{t} \rangle$. XXX - the same for $\bar{t} = \bar{t}_1$. Turbulence leads to a certain scattering of instantaneous values of \bar{t} , which is conditionally shown by shading.

is located. Therefore, time \bar{t} in a known sense can be considered as the longitudinal coordinate of a point in the receiving coil, although in reality the dependence of the speed of flow on transverse coordinates, and also turbulence, introduce certain complications (Fig. 9).

Thus for we have traced the changes of the vector \vec{M} in a separate volume element of the sample in proportion to its motion through system. However, the signal in the receiving coil is the result of the simultaneous influence of many elements of the volume, which are characterized at the same moment by different values of \bar{t} in the interval from \bar{t}_1 to $\bar{t}_1 + \Delta \bar{t}$. Therefore, it becomes necessary to introduce also the flow time ζ common for the whole system.

Let us consider the totality dV_1 of volume elements for which \bar{t} lies in the interval from \bar{t}_1 to $\bar{t}_1 + d\bar{t}$ (see Fig. 9). Evidently the signal guided by them can be written as

$$dS(\zeta) = A(\bar{t}) M_s(\bar{t}) \cos[\omega(\zeta + \bar{t})] dV_1 \quad (28)$$

where $dV_1 = c d\bar{t}$ (c is the sample flow rate in cm^3/sec), and coefficient $A(\bar{t})$ depends on properties of the receiving coil and also on the position of the examined volume element inside the coil (more accurately only on coordinates of \bar{t} , since it is

also the transmission of the signal into, the receiving coil, has a resonance character, and, at least for the established conditions we are completely justified in saying that the system operates in the mode of a narrow-band nuclear-resonance filter.

In order to obtain amplitude-frequency and phase-frequency characteristics of this filter, it is sufficient to formulate mathematically the above-mentioned qualitative considerations. The volume element, located at a certain point A, is characterized, generally speaking, by a greater value \bar{t}_A the further "downstream" it

assumed that within dV_1 averaging is realized).¹ The form of notation of (28) remains valid in the presence of turbulence, but then $A(\vec{r})$ must be considered, averaged all over the possible scattering of positions of points taking place when $\vec{r} = \vec{r}_1$.

Considering (25) and producing a summation of influences from separate parts of the sample, we obtain the expression for the signal induced in the receiving coil:

$$E(t) = cM_1(t) \int_{V_1} A(\vec{r}) e^{-i\vec{r} \cdot \vec{r}_0} \cos[\omega t + \varphi(\vec{r})] d\vec{r} \quad (29)$$

where $\varphi(\vec{r})$ is expressed from (27). The obtained formulas in principle allow determining the amplitude and phase of the signal by numerical methods; however, calculations will inevitably appear difficult, since finding $A(\vec{r})$ requires detailed information on the distribution of speeds of flow inside the receiving coil (of course it is especially difficult to consider turbulence). Therefore, in the same way that it was repeatedly done above, we turn to a somewhat rougher approximation, although quite sufficient for our purpose, which will allow continuing calculation in the general form. For this we will replace $A(\vec{r})$ by its mean value over the whole volume (i.e., along \vec{r} from \vec{r}_0 to $\vec{r}_0 + \vec{r}_1$); furthermore, we will consider the field H_0 uniform, enabling us to express $\varphi(\vec{r})$ by the simple formula (26). We obtain

$$E(t) = cM_1(t) \overline{A(\vec{r})} \int_{V_1} e^{-i\vec{r} \cdot \vec{r}_0} \cos[\omega t + \vec{r} \cdot \vec{r}_0] d\vec{r} \quad (30)$$

Calculation of integral (30) after a series of transformations gives:

$$E(t) = B(t) \cos[\omega t + \theta(t)]. \quad (31)$$

where

$$B(t) = cM_1(t) \overline{A(\vec{r})} \frac{V_1 e^{-i\vec{r}_0 \cdot \vec{r}_0}}{\sqrt{1 + \gamma^2}} \sqrt{1 - 2\gamma^2 \cos \theta + \gamma^4} \quad (32)$$

¹It is possible to show that $A(\vec{r})$ is proportional to the average (over volume dV_1) field strength, which would create unit current flowing in the receiving coil. We will not need the explicit form of $A(\vec{r})$ since we will not derive formulas for the absolute intensity of the signal.

Strictly speaking, the last factor in (28) should have been written in the form $\cos[\omega t + \varphi(\vec{r}) + \psi]$, where ψ is the phase shift between precession and the induced signal, in turn depending on the coordinates of the volume element. However, for the region inside the receiving coil the indicated dependence is small, and it can be completely disregarded. Then $\psi = \text{const}$, and by the corresponding selection of the reference point of time t it is possible to satisfy condition $\psi = 0$, as a result of which (28) is obtained.

and

$$\Phi(\omega) = \varphi_0 + \Delta\varphi + \arctan \frac{\omega T_2}{1 - \omega^2 T_1 T_2} - \arctan \frac{\omega^2 T_1 T_2}{1 - \omega^2 T_1 T_2} \quad (33)$$

Expression (32) and (33) are the sought characteristics (amplitude-frequency and phase-frequency, respectively) which describe properties of the system during its operation the narrow-band nuclear-resonance filter mode. In general, $M_1(\omega)$ and φ_0 in turn are functions of ω (or $\omega W = \frac{\omega}{\omega_0}$) in accordance with (22). However, in the usual structures of the volume of the sample occurring in a phasing field, many are less than the internal volume of the receiving coil (i.e., $V_s \ll V_c$). This requires comparatively large H_1 , and from (22) it is easy to see that the dependence of $M_1(\omega)$ and φ_0 on ωW becomes immaterial. In limit

$$\begin{aligned} M_1(\omega) &= M_0 \sin^2 \theta_1 \nu_s \\ \varphi_0 &= 0 \end{aligned} \quad (34)$$

We can say, moreover that in virtue of the brevity of the time of stay of the sample in the phasing field, the process of phasing possesses a considerably wider frequency response curve than the subsequent transmission of the signal into the receiving coil.

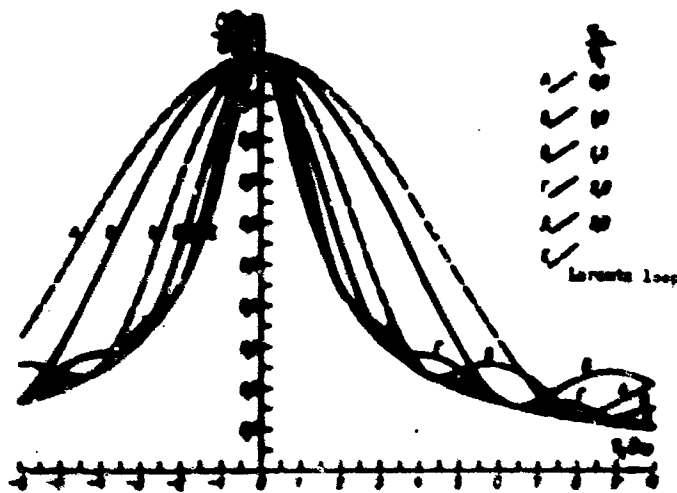


Fig. 10. Amplitude-frequency response curves of the nuclear-resonance filter.

$$M_1(\omega) = \sqrt{\frac{1 - \frac{\omega^2 T_1 T_2}{1 - \omega^2 T_1 T_2}}{1 + \frac{\omega^2 T_1 T_2}{1 - \omega^2 T_1 T_2}}}$$

Response curves (32) and (33) are presented graphically in Figs. 10 and 11 for five different values of $\frac{\omega}{\omega_0}$. They clearly illustrate the broadening of the resonance curve (and, correspondingly, the decrease of the slope of the phase

response) in proportion to the reduction of the time of stay τ_0 of the volume element in the receiving coil. It should be noted that here as usual, the resonance curve for transmission through the system of the external (inducing) signal coincides with the envelope of the spectrum of corresponding free process; the latter in this case is the segment of the damped sinusoid (resonance frequency) included in the interval from $\bar{t} = \bar{t}_0$ to $\bar{t} = \bar{t}_0 + \tau_0$. In particular, when $\frac{\tau_0}{T} \gg 1$ the damping of precession inside the receiving coil is almost complete, and the envelope of the spectrum tends toward the usual Lorentz circuit. This circumstance is easily established also for the resonance curve (32), since the last cofactor (radical) in this expression, becomes unity when $\frac{\tau_0}{T} \rightarrow \infty$. The Lorentz circuit and the phase response corresponding to it are shown, as limiting cases, on Figures 10 and 11. On the other hand, it is possible to show that during immaterial damping ($\frac{\tau_0}{T} \ll 1$) a transition takes place to the spectrum of a square pulse with sinusoidal filling.

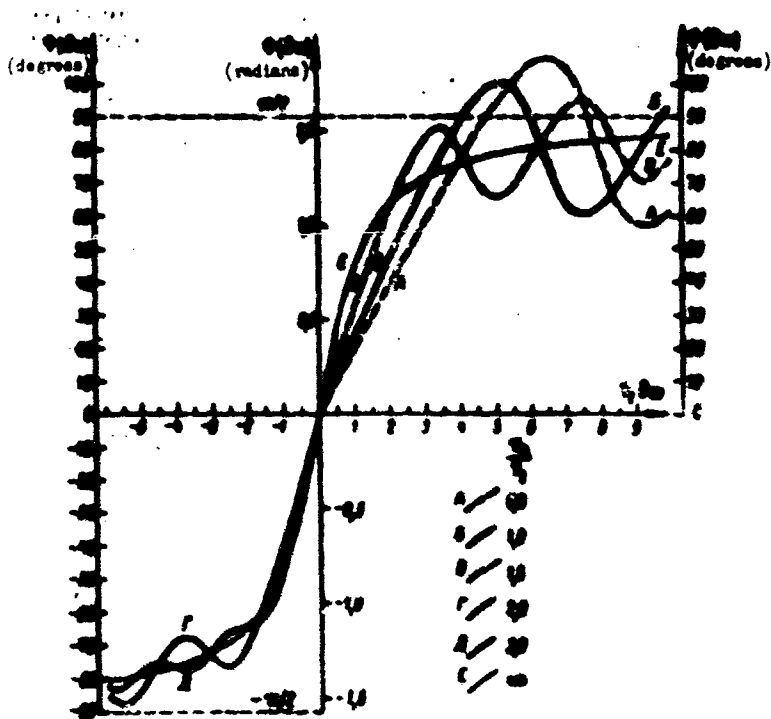


Fig. 11. Phase-frequency response curves of the nuclear-resonance filter with a moving sample. Along the axis of ordinates function (33) is plotted for the case $\tau_0 \rightarrow \infty$ and $\tau_0 \rightarrow 0$.

From (33) it directly follows that $\phi(\omega) = \phi_0$. If, furthermore, condition (34) is fulfilled, $\phi(\omega) = 0$. We can say that the reference point of time t accepted by us is so selected that the phase of the signal is measured from its value in the

absence of detuning.

In conclusion let us discuss the dependence between the amplitudes of signals at the input and at the output of system. If we were to change the amplitude of the phasing action, leaving the remaining parameters of the system constant, then $M_1(0)$ will change in accordance with (22) or (34). On the other hand, the signal in the receiving coil depends linearly on $M_1(0)$. Thus, in the considered case the amplitude characteristic of the filter essentially coincides with (34). With small H_1 it can be considered linear. With an increase in the amplitude of the signal nonlinearity described by the sine law appears at the input

c) Operation in the Nuclear-Resonance Generator Mode

The case of the closing of the feedback circuit by means of supplying to the phasing coils an amplified signal of free nuclear induction represents the greatest practical interest. However, there is no need to discuss it much, since properties of the self-oscillation system are easily derived from characteristics of the nuclear-resonance filter, connected in the feedback circuit, and these characteristics have already been derived by us in the preceding point.

Let us first of all discuss the question of self-excitation of the system. The well-known condition according to which the sum of the phase shifts of the signal during the bypass along the feedback coil should be an integral multiple of 2π

$$\phi(\omega) + \sum_i \varphi_i(\omega) = 0, \pm 2k\pi, \quad (35)$$

can be satisfied by the corresponding fine adjustment of the phase inverter connected included between the amplifier and the phasing coils. For typical designs of the nuclear-resonance filter the transmission factor is of the order of 10^{-3} - 10^{-4} . Thus, for the appearance of natural oscillations it is sufficient to ensure an amplification factor of the order of several thousand. Inasmuch as the amplitude characteristic (34) has the greatest steepness near $H_1 = 0$, we should expect mild conditions of self-excitation. As was already mentioned, just such conditions have been observed in practice. With an increase in feedback the increase in the amplitude of oscillations is limited by nonlinearity, it is interesting to note that in this case the nonlinearity is caused not by properties of tube, but by the condition $M = \text{const}$, $M_1 < M$ in the phasing process. The limiting amplitude is

attained with a feedback at which H_1 becomes equal to $\frac{1}{\pi Q}$. A further increase of the amplification factor in the considered closed circuit, as the experiment shows, leads to unstable conditions reminiscent of pulse generation. No theoretical analysis of this case has thus far been produced.

The very high slope of the phase-frequency response curve of the nuclear-resonance filter leads, in accordance with (35), to the effect of the stabilization of the frequency of the generator by the resonance frequency, i.e., to the automatic tracking of the level of the measured field mentioned in point "b," § 1. This effect is absolutely analogous to the stabilization of the frequency with the help of a quartz, and also to processes in different types of molecular generators. Like all such devices, the nuclear-resonance generator is characterized by which coincidence between the generated and natural frequencies although very good, is still not absolute: equality (35) in general, is satisfied at a ω different from ω_0 .

In view of the paramount importance of this problem for the determination of the real accuracy of measurement of magnetic fields by the method considered it is necessary to dwell on it in greater detail. For this let us separate from the sum in (35) the phase response of the receiving circuit possess a negligible frequency dependence of the phase shift introduced by them:

$$\sum \Delta \varphi_i(\omega) = \arctan T_2(\omega - \omega_0) + \sum \Delta \varphi_{i1} \quad (36)$$

where ω_0 is the resonance frequency of circuit, $T_2 = \frac{1}{Q}$ its time constant, and Q its quality.¹

It is expedient to select the adjustment of the above-mentioned phase inverter in such a way that $\sum \Delta \varphi_i$ will prove to be close to zero (a phase which is a multiple of 2π is of no practical interest, and we subsequently will omit it). At the same time, for the purpose of the preservation of generality of conclusion, the exact equality of this sum to zero will not be assumed. Taking into account, furthermore,

¹Let us note that sufficiently well-known expression used here for the phase response of the oscillation circuit can also be obtained by means of analogy from the above-mentioned results. For this it is necessary in (33) to turn to the Lorentz circuit ($\epsilon_1 = 0$, $\epsilon_2 = 0$, $\omega/T_2 \rightarrow \omega$) and to replace T_2 by T_k .

The expression $\arctan T_2(\omega - \omega_0)$ pertains to the phase shift of the current in the receiving coil with respect to external emf. The signal picked up in parallel to the oscillation circuit, of course, in turn will be out of phase. However, we consider that this circumstance, like other constant shifts, is allowed for in

$\sum \Delta \varphi_i$

(33) and (22), condition (35) can be written in the explicit form

$$\frac{1 - \cos \theta_0}{2} \frac{\sin \theta_0}{\theta_0} + \arctg T_1(\omega_0 - \omega) - \arctg \frac{\sin \theta_0 (\omega_0 - \omega)}{1 - \cos \theta_0} + \arctg T_2(\omega_0 - \omega) = -\sum \Delta \varphi_i \quad (37)$$

This equality can be considered as the equation for determining the generated frequency ω . In the most practically important case of small detuning (i.e., within the linear section of the steepest of the participating phase responses) instead of (37) we have

$$\left[\frac{1 - \cos \theta_0}{2} \frac{\sin \theta_0}{\theta_0} + \arctg T_1 - \frac{\omega - \omega_0}{1 - \cos \theta_0} \right] (\omega_0 - \omega) + T_2(\omega_0 - \omega) = -\sum \Delta \varphi_i \quad (38)$$

whence

$$\omega = \omega_0 + \frac{\sum \Delta \varphi_i + T_2(\omega_0 - \omega)}{\frac{1 - \cos \theta_0}{2} \frac{\sin \theta_0}{\theta_0} + \arctg T_1 - \frac{\omega - \omega_0}{1 - \cos \theta_0} + T_2} \quad (39)$$

Let us note that during the construction of a more complete theory we should consider also the possibility of direct induction from the phasing coils to the receiving coil combined with the useful signal, which, in general, will lead to the appearance of one more cause of the frequency-dependent phase shift. A preliminary consideration of this question showed, however, that with small $\Phi(\omega_0)$ direct induction changes basically the amplitude of the signal, but not its phase. Thus, formula (39) remains valid, although the limits of its applicability will demand, perhaps, a more precise definition.

Summing up, we can say that the condition of generation of the signal exactly with the resonance frequency is

$$\sum \Delta \varphi_i + T_2(\omega_0 - \omega) = 0 \quad (40)$$

In particular, if $\sum \Delta \varphi_i = 0$, the receiving circuit should be exactly tuned to the resonance frequency.

It should be considered, that ω_0 changes continuously together with the measured field, for which (40) cannot be satisfied once and for all. In order to clarify the possible magnitude of the appearing error, it is expedient to consider a typical

numerical example. Let us assume that ω_0 and $\Omega_0 \sim 13.5 \cdot 10^6 \text{ sec}^{-1}$, $T_k = 3 \cdot 10^{-3} \text{ sec}$, $T_2 = 3 \text{ sec}$, $\tau_0 = 5 \text{ sec}$, and that the first, second, and fifth components in the denominator of (39) can be disregarded. We obtain

$$\omega = \omega_0 + 0.544 \sum_i \Delta \omega_i + \frac{\Omega_0 - \omega_0}{613}. \quad (41)$$

For instance, if $\Omega_0 = \omega_0$ and $\sum_i \Delta \omega_i = 0.1 \text{ rad}$, the error in the generated frequency will be 0.0544 sec^{-1} , i.e., about 0.2γ in units of the field. Further, the detuning of the receiving circuit enters into the result with the coefficient $1/613$. Thus, the number 613 in the considered example has the meaning of the stabilization factor of frequency of the generator owing to the inclusion into the feedback circuit of the nuclear-resonance filter.

The above-mentioned figures correspond to $Q = 20$, and from considerations of the preservation of the intensity of the signal it is undesirable to allow detuning $\Omega_0 - \omega_0$ greater than $\pm \frac{\Omega_0}{Q}$, i.e., $\pm 100 \text{ sec}^{-1}$ (it is easy to show that this corresponds to 27% decrease of amplitude of the signal of the generator or greater, depending upon its conditions). With such detuning the error in the measurement of the field will be $\pm 1\%$.

Thus, the error due to the inaccurate adjustment of the receiving circuit is indeed small and cannot serve as an obstacle for the use of the nuclear-resonance generator for magnetometric purposes. At the same time, during the designing of this principle of especially sensitive instruments it is necessary to provide for a certain method allowing the weakening or compensating of the influence of this factor. We can point out at least three such methods:

1) A sufficiently accurate automatic fine adjustment of the receiving circuit. In the example considered the measuring error will not exceed $\pm 0.5\%$, if $\Omega_0 - \omega_0$ is held within $\pm 5 \text{ cps}$. These limits can be expanded by means of lowering the quality Q .

2) Retuning of the circuit by means of selection of one of the discrete values of Ω_0 , each of which corresponds to a separate range of measurements. The error in each range is corrected during calibration of the instrument.

3) The creation, instead of a receiving circuit, of systems with a mildly sloping phase response. The simplest variant is an untuned receiving coil. Such a way is conjugate with deterioration of the signal-to-noise ratio by \sqrt{Q} times. However, the nuclear-resonance generator, apparently, is able to operate normally

during low signal-to-noise ratios, and before supplying the frequency meter this ratio can be improved with the help of an additional narrow-band filter or amplifier, not entering into the feedback ring. Another possibility is in the development of more complex oscillatory circuits (for instance, coupled circuits) with a sloping section of the phase response in a certain interval of frequencies, with the preservation of gain in the amplitude of the signal owing to resonance.

It is very possible that in the process of further development it will prove expedient to use not one of the indicated methods but some combination of them. The interesting but as yet almost untouched problem is the creation of methods of control of the magnitude of error Δ in the process of the instrument's operation. It is not excluded that it will be possible to carry out such a control by means of an artificial supply of direct induction from the phasing coils to the receiving coil and measurement of the appearing frequency drift of the generator.

Almost all the theoretical conclusions pertained to the steady-state operating conditions of the instrument and, besides, in the uniform external field H_0 . A more general theory as yet is absent, in connection with which here we will be limited only a few additional remarks.

A. Operation in a nonuniform field H_0 . With small heterogeneities the instrument measures the average field in the volume of the sample located inside the receiving coil. Moreover, in connection with the natural damping of precession, the volume elements located "downstream" will enter with smaller weight. If the gradient of the field exceeds $\sim 0.2; 0.3/\text{cm}$ along the axis of the instrument (or $\sim 0.5; 0.7/\text{cm}$ in a transverse direction), it will start to show a decrease of amplitude of the signal owing to the dephasing of nuclear precession. Furthermore, the average frequency of precession in the receiving coil will be already noticeably different from the resonance frequency in the region of the phasing field. As a result of this there will appear an additional detuning of the phasing signal, i.e., the phase shift φ , and together with that the generated frequency, to a certain degree will depend on the character of heterogeneity of the field; this effect, obviously, will be lesser the greater the magnitude of the phasing field H_1 . It is necessary, however, to note that for the majority of practical applications (we have in mind geomagnetic measurements) the case of considerable gradients is not of special interest. Indeed, the source of heterogeneity of the field, especially the remote one, almost inevitably will noticeably influence the average quantity H_0 .

RADIATION OF Sb^{125}

N. M. Anton'yeva and G. S. Katykhin

The radiation of Sb^{125} ($T_{1/2} = 2.6 \pm 0.1$ g) [1] has been studied earlier by many researchers [2-5], but as yet the complicated decay scheme $\text{Sb}^{125} \rightarrow \text{Te}^{125}$ has not been established.

In this work the β -spectrum and conversion-electron spectrum of Sb^{125} were studied with the help of a magnetic spectrometer of the Ketron type [6] and also a magnetic spectrograph of the Danish type with a resolving power of 0.15% and with measurement of the magnetic field by the method of proton resonance.

The investigations were carried out with one source, which was obtained by chemical isolation from tin irradiated by neutrons. In view of the small specific activity the preparation was quite thick, and therefore the measurements were conducted practically starting from ~ 70 keV.

β -spectrum of Sb^{125} . The general form of the β -spectrum of Sb^{125} and the conversion-electron spectrum obtained by us is shown in Fig. 1.

The Kurie plot for the continuous β -spectrum of Sb^{125} is shown in Fig. 2. As can be seen from this figure, the β -spectrum is complicated. The boundary of the hard component of the β -spectrum is equal to (628 ± 3) keV. The value $lg ft$ is great for this transition and equal to 9.0. The segment of the Kurie plot characterizing the hard component is small, a total of 450 to 540 keV: on the part of low energies a softer β -spectrum is superimposed with $E_{\text{pp}} = 430$ keV, and on the part of high energies conversion lines of γ -transitions are superimposed with energies of 600, 606, and 635 keV. This hampers the investigation of the

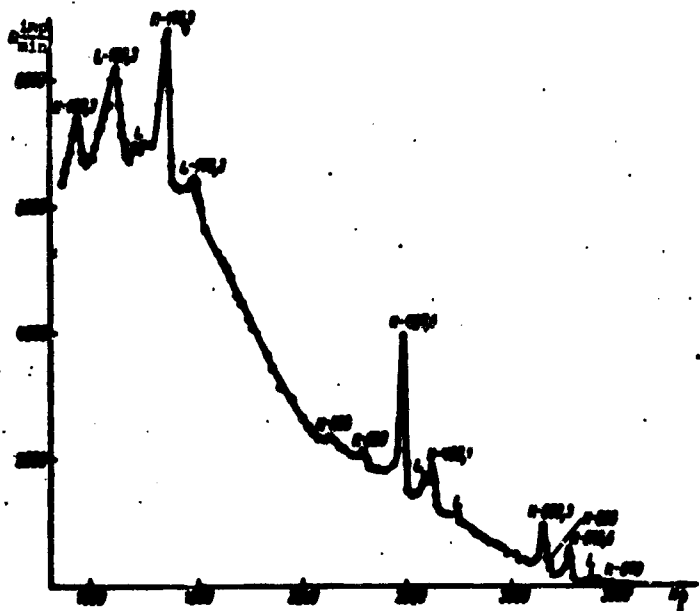


Fig. 1. General form of the β -spectrum and conversion-electron spectrum of Sb^{125} .

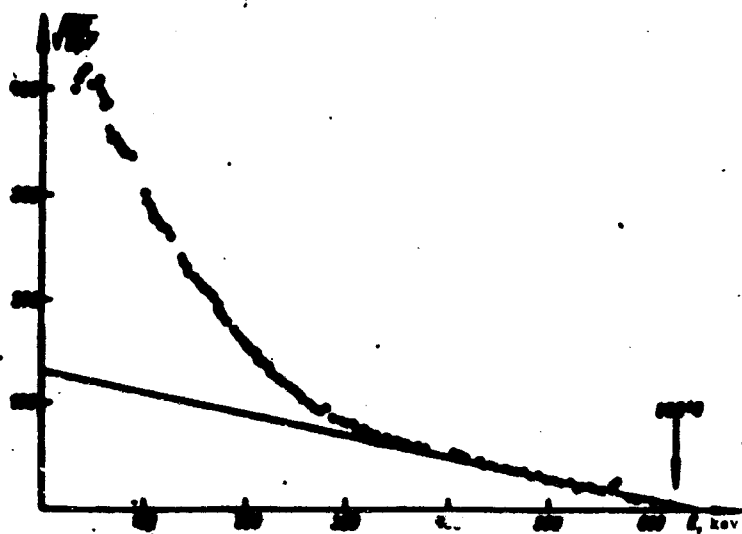


Fig. 2. Kurie β -spectrum plot of Sb^{125} .

β -spectrum form.

For the determination of relative intensities of components of the β -spectrum, it is necessary to obtain a softer spectrum by subtraction from the experimental spectrum of the hard component, etc. In all cases we assumed that the Kurie plot of the hard component is rectilinear.

Data on the measurement of components of the β -spectrum of Sb^{125} are given in

Table 1

| E_{Tp} keV | $J(\%)$ | $\eta/\%$ |
|---------------------|---------|-----------|
| 628 ± 3 | 23 | 8.9 |
| 430 ± 10 | 10 | 8.9 |
| 300 ± 15 | 46 | 7.7 |
| < 300 | 19 | — |

Table 1. It should be noted that the β -spectrum with $E_{\text{Tp}} < 300$ keV is complicated. For an investigation of this region of the β -spectrum a thinner, recently isolated source of Sb^{125} (without Te^{125*}) is necessary.

In the theses of the 12th Annual Conference on Nuclear Spectroscopy [7] we erroneously gave a weak (1.4%) hard component with an end-point energy of 750 keV. The relative intensity of this component as compared to the component of 628 keV was changed in time (~8 months).

Conversion-electron spectrum of Sb^{125} . The spectrum of conversion electrons observed by us consists of 21 lines corresponding to 12 γ -transitions. Data on the energies of the γ -transitions and on relative intensities of the conversion lines are given in Table 2.

Table 2

| E_{γ} keV | Observed line | $K/L+M \times 100$ | $\frac{K}{L+M}$ | $K/L+M$ |
|------------------|----------------------------|--------------------|---------------------|---------|
| 1023 ± 0.1 | K, L, L_{ep}, M_1 | — | $\frac{L+M}{K} = 2$ | — |
| 1733 ± 0.3 | K, L | 20 | 0.3 ± 0.0 | 11.5 |
| 206 ± 3 | K | 20 | — | — |
| 320 ± 3 | K | 20 | — | — |
| $376 \pm 3(7)$ | K | weak (?) | — | — |
| 380 ± 3 | K | 20 | — | — |
| 427.8 ± 0.4 | K, L | 100 | 0.3 ± 0.7 | 0.5 |
| 428.1 ± 0.4 | K, L | 20 | 0.9 ± 1.0 | 0.2 |
| 473.3 ± 0.3 | K, L | 20 | 0.3 ± 0.0 | 7.9 |
| 480 ± 3 | K | 2.5 | — | — |
| 484.6 ± 0.6 | K, L | 14 | 7.8 ± 1.0 | 0.4 |
| 600 ± 3 | K, L | 1.3 | — | — |

Up to now there has been no complete information in literature on the conversion electron spectrum of Sb^{125} . Relative intensities of conversion lines and the ratio $K/(L + M)$ were determined by us for the first time.

Conversion lines of γ -transitions with energies of 206, 320, 376, and 380 keV are on the intense β -spectrum, and therefore their observation is hampered. The conversional line K -376 was observed by us only on the magnetic spectrograph as a very weak line. Its existence requires still an additional check.

Figures 3 and 4 show sections of the β -spectrum with groups of conversion lines. In view of the fact that the difference of energies of conversion lines L and M is relatively small (for Te of 3.9 keV), these lines were not resolved by us and we had to calculate the area of the total line ($L + M$). However, it is known

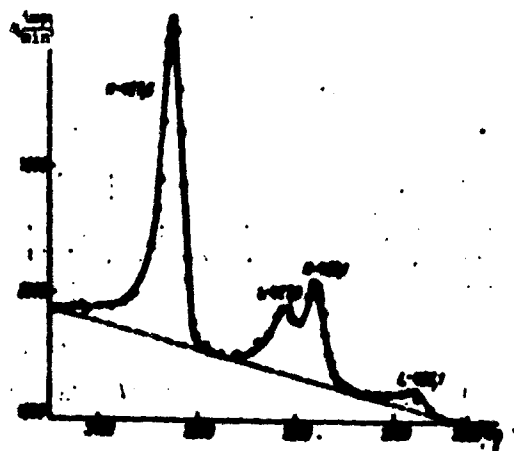


Fig. 3. Section of the β -spectrum with groups of conversion lines K-, L-427.6, and K-, L-463.1 kev.

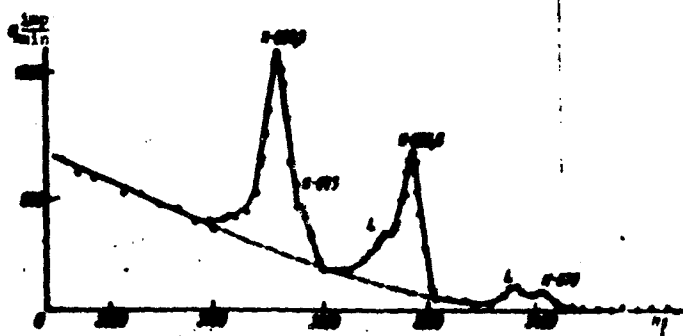


Fig. 4. Section of the β -spectrum with groups of conversion lines K-, L-600.3, K-606, K-, L-635.6 and K-670 kev.

that in many cases $M/L \approx 0.25$ [8]. Therefore, for an appraisal of the K/L ratio, on the basis of the known ratio $K/(L + M)$ we used the following approximate equality:

$$\frac{K}{L} = \frac{K}{L+M} \left(1 + \frac{M}{L}\right) \approx 1.25 \frac{K}{L+M}.$$

The values thus obtained for K/L are given in the last column of Table 2.

Energy of γ -rays of Sb^{125} . Values of energies of γ -rays of Sb^{125} , according to different authors, are given in Table 3.

Table 3

| Energy of γ -radiation of Sb^{125} , kev | | | | |
|---|-------|-------|-------|-------------|
| Data from literature | | | | Our data |
| [9] | [10] | [11] | [12] | |
| 236.1 | 236.1 | 236.1 | 236.1 | 236.1 ± 0.1 |
| 236.2 | 236.2 | 236.2 | 236.2 | 236.2 ± 0.1 |
| 236.3 | 236.3 | 236.3 | 236.3 | 236.3 ± 0.1 |
| 236.4 | 236.4 | 236.4 | 236.4 | 236.4 ± 0.1 |
| 236.5 | 236.5 | 236.5 | 236.5 | 236.5 ± 0.1 |
| 236.6 | 236.6 | 236.6 | 236.6 | 236.6 ± 0.1 |
| 236.7 | 236.7 | 236.7 | 236.7 | 236.7 ± 0.1 |
| 236.8 | 236.8 | 236.8 | 236.8 | 236.8 ± 0.1 |
| 236.9 | 236.9 | 236.9 | 236.9 | 236.9 ± 0.1 |
| 237.0 | 237.0 | 237.0 | 237.0 | 237.0 ± 0.1 |
| 237.1 | 237.1 | 237.1 | 237.1 | 237.1 ± 0.1 |
| 237.2 | 237.2 | 237.2 | 237.2 | 237.2 ± 0.1 |
| 237.3 | 237.3 | 237.3 | 237.3 | 237.3 ± 0.1 |
| 237.4 | 237.4 | 237.4 | 237.4 | 237.4 ± 0.1 |
| 237.5 | 237.5 | 237.5 | 237.5 | 237.5 ± 0.1 |
| 237.6 | 237.6 | 237.6 | 237.6 | 237.6 ± 0.1 |
| 237.7 | 237.7 | 237.7 | 237.7 | 237.7 ± 0.1 |
| 237.8 | 237.8 | 237.8 | 237.8 | 237.8 ± 0.1 |
| 237.9 | 237.9 | 237.9 | 237.9 | 237.9 ± 0.1 |
| 238.0 | 238.0 | 238.0 | 238.0 | 238.0 ± 0.1 |

In works [9, 10] for the determination of the energy of γ -rays data were used both on conversion electrons and also on photoelectrons. But investigations were conducted with thick preparations and on a lens spectrometer with a resolving power of 3.5-5%. In work [11] the energy of γ -rays was measured on a scintillation γ -spectrometer.

The most exact values of energies of γ -rays are given in our work and work [4]. We determined the energy by the method of proton resonance on a magnetic spectrograph with a resolving power of 0.15%. In work [4] energies of transitions were measured by an absolute comparison with standard conversion lines ThB.

The transition of 35.6 keV was not measured, in view of the presence of a thick source. We have no hint of the presence of γ -transitions with energies of 109, 171, 203, and 652 keV. The conversion lines of γ -transitions with energies of 109 and 171 keV could not be noticed on a ketron, since the resolving power on line K-175 was ~1%, instead of the instrument 0.5%. The K lines of these transitions could not be resolved from the intense conversion lines K-109.3 and K-176.3. The conversion line K-203 merges in energy with L-176.3 and also could not be noticed. All these conversion lines had to be resolved on the magnetic spectrograph, but we did not observe them on the plate. Apparently, the exposure time was insufficient. This is confirmed by the fact that conversion lines of γ -transitions with energies of 206 and 320 keV, the intensity of which, apparently, are greater, are not noticed on the plate.

The conversion line K-652 should be between lines K-635.6 and L-635.6. If it is, then its intensity is 0.5 less than the intensity of K-427.

Multipolarity of transitions. The large number of lines in the γ -spectrum of Sb^{125} indicates the complexity of the decay scheme of this isotope. For constructing a decay scheme knowledge of the multipolarity of transitions is important. We tried to determine the multipolarity of certain transitions from an analysis of the conversion spectrum. Given in Table 2 are the ratios of coefficient of conversion on shells K and L for certain transitions. A comparison with theoretical values [12], given in Table 4, for different multiplicities makes it possible to assume the type of transition. As can be seen from the table, single-valued simple ascribing of the type of transition by these data cannot be made.

Table 4

| α keV | Experi- mental value of $\frac{K}{L}$ | Theoretical values of $\frac{K}{L}$ (%) | | | | | | Assumed type of transition |
|-----------------|--|---|-----|-----|-----|-----|-----|-------------------------------|
| | | E1 | E2 | E3 | E4 | E5 | E6 | |
| 652 | 2.06 | 2.06 | 7.0 | 2.0 | 2.0 | 2.0 | 2.0 | E1 + E2, E3, E4, E5, E6 |
| 320 | 2.06 | 2.06 | 7.0 | 2.0 | 2.0 | 2.0 | 2.0 | E1 + E2, E3, E4, E5, E6 |
| 206 | 2.06 | 2.06 | 7.0 | 2.0 | 2.0 | 2.0 | 2.0 | E1 + E2, E3, E4, E5, E6 |

A. A. Zhdanov, for the investigation on the magnetic spectrograph; and also N. Stegalkina, L. Kolmykova, and Yu. Golubev for their help in the measurements.

Summary

The β -spectrum and the spectrum of conversion electrons of Sb^{120} has been studied with the help of the "coctron" type magnetic spectrometer ($\frac{\Delta E}{E} = 0,5\%$), and a magnetic spectrograph with photographic recording ($\frac{\Delta E}{E} = 0,15\%$). more precise data of the Sb^{120} decay being obtained.

Literature

1. E. H. Klehr and A. F. Voigt. J. inorg. nucl. chem., 16, 8, 1961.
2. B. S. Dzhelepov and L. K. Peker. Decay schemes of radioactive nuclei. Leningrad, Publishing House of the Academy of Sciences of the USSR, 342, 1958.
3. D. Strominger, J. M. Hollander, and G. T. Seaborg. Rev. mod. phys., 30, 585, 1958.
4. R. S. Narcisi. N.S.A., 13, 2873, 1959.
5. G. Chandra. Proc. Ind. Acad. Sci., 46, 360, 1957.
6. B. S. Dzhelepov and A. A. Bashilov. News of the Academy of Sciences of the USSR, physics series, 14, 263, 1950.
7. N. M. Anton'yeva and G. S. Katykhin. Program and theses of reports of the 12th Annual Conference on Nuclear Spectroscopy in Leningrad. Moscow-Leningrad Publishing House of the Academy of Sciences of the USSR, 57, 1962.
8. M. A. Listengarten. News of the Academy of Sciences of the USSR, physics series, 22, 1759, 1958.
9. K. Siegbahn and W. Forsling. Ark. fys., 1, 505, 1949.
10. B. D. Kern, A. C. G. Mitchell, and D. J. Zaffarano. Phys. rev., 76, 94, 1949.
11. N. H. Lazar. Phys. rev., 102, 1058, 1956.
12. Gamma rays. Edited by Sliv. Moscow-Leningrad Publishing House of the Academy of Sciences of the USSR, 370, 1961.
13. J. Moreau. Arkiv fys., 7, 391, 1954.
14. L. N. Zyryanova. Unique beta-transitions. Publishing House of the Academy of Sciences of the USSR, properties of atomic nuclei series, Issue 2, 1960.

Submitted
15 Nov 1962

DEPENDENCE OF ANGLES OF ORIENTATION IN DYNAMIC DOUBLE
REFRACTION ON THE VELOCITY GRADIENT

V. P. Budtov

Consideration of Anisotropy of a Hydrodynamic
Interaction

During the study of double refraction in the field of the velocity gradient we usually encounter two problems: the study of the double refraction during small hydrodynamic stresses and, in the whole scale, of stresses obtainable experimentally. The first allows us to make definite conclusions about the form, chemical structure, thermodynamic flexibility, and other properties characterizing the macromolecule in the undisturbed flow state. The second allows to us to judge the behavior of macromolecules in flow, i.e., on the deformation, orientation and kinetic rigidity of the molecules.

The region of small hydrodynamic stresses has been studied well enough both experimentally and also theoretically. However, in the region of large velocity gradients there exists only a qualitative conformity of experimental data with theoretical positions [1-4].

The theory of the dependence of the angle of orientation on the velocity gradient was developed most fully for rigid ellipsoids [5, 6]. Experimental data for solutions of rigid macromolecules indicate that qualitatively the predictions of the theory are justified; however, for the best coincidence it is necessary, to consider the influence of polydispersity of the sample [7, 8].

For ideally flexible macromolecules W. and H. Kuhn obtained, at all velocity gradients, [9]

$$\alpha_2 = \beta.$$

(1)

where $\varphi = \frac{\pi}{4} - \alpha$ (α is the angle between directions of orientation of the macromolecules and the flow rate); $\beta = \frac{M[\eta]}{4RgT} g$ (M is the molecular weight, $[\eta]$ the characteristic viscosity, R the gas constant, T the absolute temperature, g the velocity gradient, η_0 viscosity of the solvent).

In the case of kinetically rigid coils for the effect of intrinsic anisotropy they obtained, at small velocity gradients, [10]

$$\lg \beta = 2\beta(1 - 11.7\beta^2 + \dots) = 2\beta[1 - 1.3(3\beta)^2 + \dots]. \quad (2)$$

It is clear that initial slopes of the dependence of the angle of orientation on β for the kinetically flexible model are three times less than for the kinetically rigid model; however, with an increase in the velocity gradient this difference decreases.

Using the distribution function for a kinetically rigid coil [10] we obtain for the angle of orientation of the effect of form (the model of the equivalent ellipsoid [11] and model Čopič [12] at small velocity gradients coincide):

$$\lg \beta = 2.5\beta(1 - 9.1\beta^2 + \dots) = 2.5\beta[1 - 1.45(2.5\beta)^2 + \dots]. \quad (3)$$

Thus, it is clear that with a decrease in kinetic rigidity of the coil (ratio of the internal viscosity to the viscosity of the solvent) the character of the dependence of the angle of orientation on the velocity gradient changes.

1. Dependence of the Angle of Orientation on the Velocity Gradient and Concentration of the Polymer in Solution

We studied angles of orientation of solutions of polymethyl methacrylate [PMMA] (PMMA) in tetrabromoethane [acetylene tetrabromide] for six fractions and an unfractionated sample in the region of velocity gradients from 4 to 2000 sec^{-1} . The obtaining and fractionation of PMMA and the characteristics of the instrument are given in a previous work [13]. Solvents were selected so that the effect studied was the only effect of form. The viscosity of solvents η_0 varied from 6 to 15.6 cp.

During the study of the gradient dependence of the angle of orientation in the region of medium velocity gradients various authors [7, 8, 14, 15] have cited ratios which are a particular case of the relationship [8]:

$$\frac{\alpha}{\beta} = \tau^{-1} + A_2(\eta - \eta_0), \quad (4)$$

where A_2 is numerical coefficient, η the viscosity of solution, τ the initial slope

of the angle of orientation. On the basis of this empirical dependence [8] a method was proposed for obtaining the "initial slope" τ of the angle of orientation. However, as the author himself stresses this relationship [4] is accurate only in a

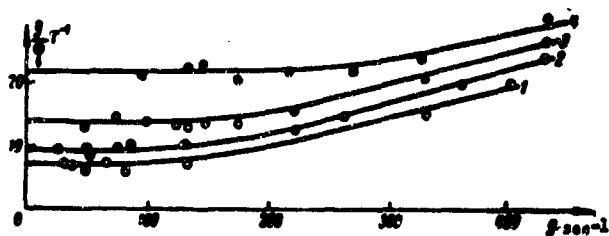


Fig. 1. Dependence of the quantity g^τ on the velocity gradient for solutions of V fraction in solvents with various viscosities. 1 - 15.6; 2 - 11.4; 3 - 9.4; 4 - 6.6 cp.

defined region of velocity gradients.

We showed that in the region of small velocity gradients $\frac{g^\tau}{g}$ is a parabolic function of g (Fig. 1). Thus, in finding the "initial slope" τ of the angle of orientation it is necessary to present $\frac{g^\tau}{g}$ as a function of g^τ ,¹ then on the axis of ordinates the segment equal to τ is cut off.

For all the solutions studied τ were found by this method. However, the enumerated methods are inaccurate, since the extrapolation to $g \rightarrow 0$ is produced basically by measurements obtained at small velocity gradients, where there is a large error of the measurements.

If we express $\lg 2\varphi = f(g^\tau)$, then the experimental points for solutions of the given fraction in the given solvent fall on one curve for all concentrations. As a result we find it possible to find τ on the whole curve which expresses the dependence of the angle of orientation on the velocity gradient. The convenience of this method is that the possibility appears to checking the correctness of the finding of τ by measurements at large g and large concentrations of polymer in the solution.

For small viscosities of the solvent (large kinetic rigidity of the macromolecule) this method coincides with the method of Peterlin [16] when $\lg 2\varphi$ is represented as a function of $g^{\frac{1-\alpha}{\alpha}}$ (τ is proportional to $\frac{1-\alpha}{\alpha}$).

Consequently, we managed to find the generalized parameter $\lg \tau$, which is determining in the kinetics of orientation of macromolecules in flow. The obtained results reflect the fact that the orientation of dynamic double refraction during any velocity gradients depends on the time of relaxation τ , both the relaxation time of orientation (great kinetic rigidity) and the relaxation time of deformation

¹The exponent of g in the original text is illegible; " g^τ " appears below and may be the quantity used here (Tr. Ed. note).

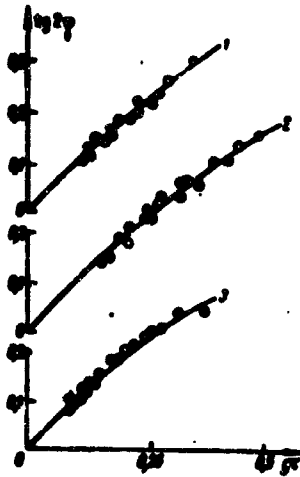


Fig. 2. Dependence of quantity $\text{tg } 2\varphi$ on $g\tau$ for solutions of fraction V in butylacetate (1), in methyl ethyl ketone (2), and in acetone (3). Points for different concentrations in Figs. 2, 3, 4, 5 are designated by various signs.

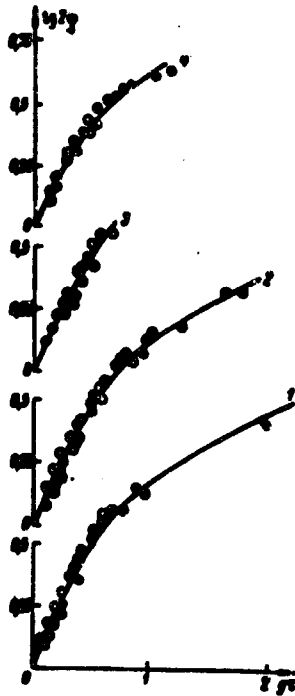


Fig. 3. Dependence of quantity $\text{tg } 2\varphi$ on $g\tau$ for solutions of fraction V in bromoform (1) and in tetrabromoethane at temperatures $t = 21^\circ$ (2), $t = 15^\circ$ (3), $t = 7^\circ$ (4).

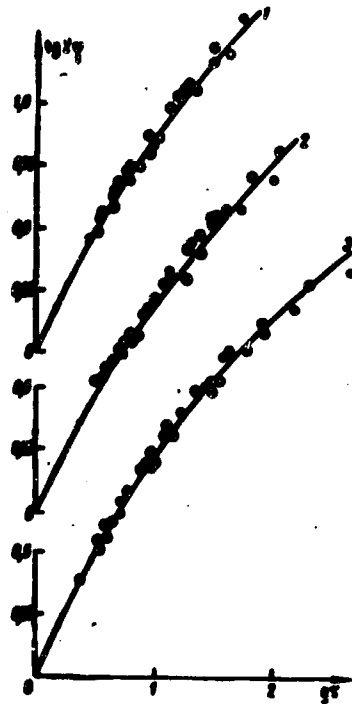


Fig. 4. Dependence of quantity $\text{tg } 2\varphi$ on $g\tau$ for solutions of fraction IV in tetrabromoethane at temperatures of $t = 26^\circ\text{C}$ (1), $t = 21^\circ\text{C}$ (2), $t = 15^\circ\text{C}$ (3).

(great flexibility of macromolecules) (Figs. 2-5). The dependence $\text{tg } 2\varphi = f(g\tau)$ when $g\tau < 1$ has the form

$$\frac{\text{tg } 2\varphi}{g\tau} = 1 - Ag^{2\tau} + \dots \quad (5)$$

It should be noted¹ that in the viscous solvents ($\eta_0 > 5 \cdot 10^{-2}$ poise) $A = 0.23 \pm 0.07$ for all six fractions studied, whereas for solutions of fraction V in low-viscosity solvents ($\eta_0 < 2 \cdot 10^{-2}$ poise) $A > 0.9$. For solutions of fraction V in solvents with an intermediate viscosity ($2 \cdot 10^{-2} < \eta_0 < 3 \cdot 10^{-2}$ poise) $A \approx 0.5$. Thus, with a change in the viscosity of the solvent (change of the kinetic rigidity of the

¹Earlier [13] angles of orientation were studied for solutions of one of the PMMA fractions in 9 solvents, the viscosity of which varied by more than 50 times. Experimental data indicate that when $\eta_0 < 2 \cdot 10^{-2}$ poise the dynamo-optometric effect has an orientational nature, and when $\eta_0 > 3 \cdot 10^{-2}$ poise, it has a deformation nature.

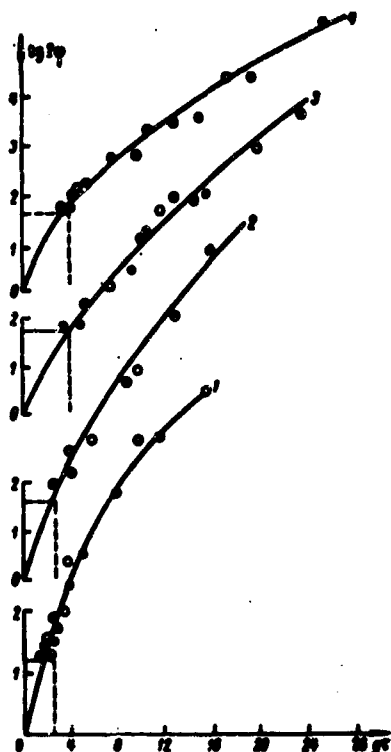


Fig. 5. Dependence of quantity $\text{tg } 2\varphi$ on $g\tau$ for solutions of fractions of PMMA in tetrabromoethane ($t = 15^\circ\text{C}$). 1 - fraction III, 2 - fraction II, 3 - unfractionated sample, 4 - fraction A.

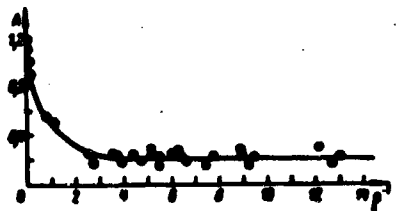


Fig. 6. Dependence of quantity A on ρ^{-1} for solutions of six fractions in various solvents.

macromolecule), the gradient dependence of the angle of orientation changes when $g\tau < 1$. For solutions of unfractionated polymethyl methacrylate $A = 0.05$.

As a characteristic of kinetic rigidity let us introduce the parameter $\rho = k \frac{B}{\Lambda}$, where B and Λ are friction coefficients of the macromolecule, depending on the internal viscosity and viscosity of the solvent, and k is a numerical coefficient. Using data of the works,¹ we can obtain for B/Λ the following ratio

$$\frac{B}{\Lambda} = \frac{A}{k\rho} \quad (6)$$

Since for fraction V in solvents with a viscosity from 2 to 3 cp the influence of orientation and deformation are comparable [13], it is possible to consider for them $\rho = 1$, which gives the value $k \approx 3$. Given in Fig. 6 is the dependence A on ρ^{-1} . From the figure it is clear that during a change of kinetic rigidity A changes from 1.2 for a kinetically rigid coil to 0.2 for an easily deformed coil. When $\rho < 0.1$, ($\eta_0 \approx 15.6 \cdot 10^{-2}$ poise) no longer depends on the viscosity of the solvent within error of the measurements. Thus, the magnitude of the change of A from 1.2 to 0.2 qualitatively agrees with conclusions of the theory of the

deformed dumbbell [9, 10]. The distinction consists in the fact that the experimental quantity $A \neq 0$ for the easily deformed macromolecule, while the

¹The article Yu. A. Gotlib and V. P. Budtov, "On the theory of double refraction in solutions of polymeric chains possessing kinetic rigidity," will be published in 1964 in the journal Herald of Leningrad State University, and the article of V. N. Tsvetkov and V. P. Budtov; "Characteristic angles of orientation of double refraction of PMMA solutions," in the journal High-Molecular Compounds.

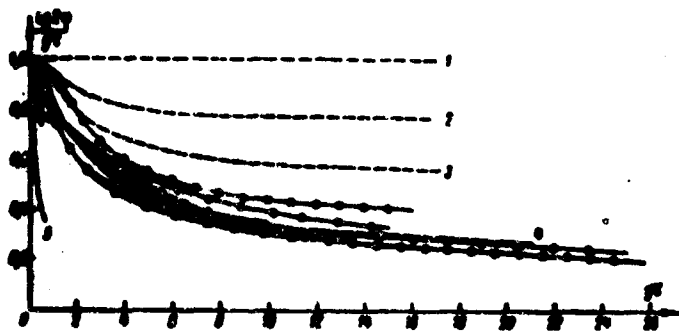


Fig. 7. Dependence of quantity $\frac{\eta_{sp}}{c}$ on $g\tau$. For an ideally flexible coil (1), for a kinetically rigid coil (5), for rigid ellipsoids with $p = 1$ (1), $p = 2$ (2), $p = 3$ (3), $p > 10$ (4). For solutions of PMMA fractions in tetrabromoethane: \bullet - unfractionated sample; \ominus - fraction A; $\omin�$ - fraction II; $\omin�$ - fraction III, $\omin�$ - fraction I - fraction IV; $\omin�$ - fraction V; in low-viscosity solvents: \square - fraction V.

the fractions, which the dependence given in the same place for the unfractionated sample indicates. The dotted lines correspond to the theoretical dependence for rigid ellipsoids [5, 6], ideally flexible dumbbells [9] and kinetically rigid dumbbells [10].

2. Consideration of Anisotropy of Hydrodynamic Interaction

The value $A = 0.2 \neq 0$ for an easily deformed coil can be obtained if we take into consideration the anisotropy of the hydrodynamic interaction of the segments.

As is known [17, 18] a consideration of the anisotropy of hydrodynamic interaction allows obtaining the dependence of the characteristic viscosity on the velocity gradient of the flow without an introduction of the internal viscosity of the coil.

In the case of the isotropic hydrodynamic interaction the deforming and orienting influence of the flow are identical [9], and consequently the magnitude of viscosity of the solution [9, 20] and the quantity $\frac{\eta_{sp}}{c}$ do not depend on the velocity gradient (mod λ of an ideally flexible coil). However, when account is taken of the anisotropy of the hydrodynamic interaction [17, 18], as well as of the internal viscosity (kinetic rigidity ρ) [21, 23], a dependence of $\frac{\eta_{sp}}{c}$ on the velocity gradient appears. The consideration of anisotropy of the hydrodynamic interaction and consideration of the internal viscosity gives a coefficient A of one sign (5), although in the first case the friction coefficient

theory [9] gives $A = 0$.

In Fig. 7 the dependence $\frac{\eta_{sp}}{c}$ is represented as a function of $g\tau$. From the figure it is clear that $tg 2\varphi$ is proportional to $g\tau$ when $g\tau \ll 1$ and when $g\tau > 15$, and the proportionality factor changes from 1 ($g\tau \ll 1$) to 0.2 ($g\tau > 15$). The divergence of the curves for various fractions in the region of large $g\tau$ is probably the result of residual polydispersity of

along the axis of macromolecule is less than the friction coefficient perpendicular to the axis, and in the second case the reverse is true.

For clarification of this contradiction we consider velocity u_{\parallel} of the end of the macromolecule in the direction $\vec{\lambda}$ (see, for instance, [10]):

$$u_{\parallel} = \frac{\lambda_{\parallel}}{\lambda_{\parallel} + B} v_{\parallel} - \frac{a_{\parallel}}{\lambda_{\parallel} + B} \quad (7)$$

where λ_{\parallel} and B are the friction coefficient along the chain and coefficient of internal viscosity, v_{\parallel} is the speed of the liquid in the direction $\vec{\lambda}$, a_{\parallel} is a quantity characterizing the force of the entropy and diffusion character (a_{\parallel} is always of the same sign v_{\parallel} [9, 10]). In the case of deformation of the chain $v_{\parallel} > 0$, $a_{\parallel} > 0$, $\frac{a_{\parallel}}{\lambda_{\parallel}} > 0$.

For isotropic hydrodynamic interaction [18] $\lambda_{\parallel} = \lambda$. For anisotropic hydrodynamic interaction

$$1 - \frac{\lambda_{\parallel}}{\lambda} = \frac{c \lambda_0 \sqrt{N}}{1 + c \lambda_0 \sqrt{N}} = \zeta \quad (8)$$

where N is the number of subchains and λ_0 is a parameter depending on the friction coefficient and length of the segment ($0 < \zeta < 0.14$) [17, 18]:

Let us formulate the difference of velocities of the end of an ideally flexible macromolecule with the isotropic hydrodynamic interaction u_{\parallel} and of a macromolecule with internal viscosity and anisotropic hydrodynamic interaction:

$$\Delta u_{\parallel} = u_{\parallel} - u_{\parallel}^0 = \frac{a_{\parallel}}{\lambda_{\parallel} + B} v_{\parallel} - \frac{a_{\parallel}}{\lambda} \frac{1 - \zeta}{1 + \zeta} v_{\parallel} \quad (9)$$

In case $\rho = 0$ $\Delta u_{\parallel} > 0$, and in the case $\zeta = 0$ $\Delta u_{\parallel} > 0$. Thus, the speed of deformation with account taken of internal viscosity and anisotropic hydrodynamic interaction is less than the speed of deformation for an ideally flexible coil with the same orienting action of the flow.

Let us examine the influence of anisotropy of hydrodynamic interaction on the dependence of the angle of orientation on g during small hydrodynamic stresses.

In formulating equations for the distribution function of particles in the flow we will proceed from the dumbbell model of the macromolecule [17]. Substituting the velocity of macromolecules into the equation of continuity of flow, we can obtain for the distribution function ψ equations taking into account anisotropy of the hydrodynamic friction (plane case)

$$\frac{1}{2} \left(\frac{1}{2} + \frac{3}{2} - \frac{3}{2} \beta \sin 2\theta \right) + \frac{1}{2} + \frac{1}{2} \frac{3}{2} + \frac{3}{2} (1 - \cos 2\theta) \frac{1}{2} = 0, \quad (10)$$

where $\beta = \frac{1}{2} \frac{L^2}{R^2}$, L is the undisturbed mean square of the distance between the ends of the macromolecule, and θ is the angle between directions of the flow and \vec{L} .

Since $\frac{1}{2} = 1 - \zeta$, where ζ is small quantity, a solution will be sought in the form $\theta = \theta_0 + \zeta \theta_1 + \dots$. We can obtain relationship for moments:

$$\begin{cases} \beta \langle L^2 \sin 2\theta \rangle - \langle L^2 \rangle + 1 = 0, \\ \langle L^2 \sin 2\theta \rangle + \beta \langle L^2 \cos 2\theta \rangle - \beta \langle L^2 \rangle = -\langle \cos 2\theta \rangle, \\ \langle L^2 \cos 2\theta \rangle - \beta \langle L^2 \sin 2\theta \rangle = \zeta \langle \sin 2\theta \rangle. \end{cases} \quad (11)$$

If the right sides of the equations are averaged with the distribution function ψ_0 then we will obtain linear members in expansion with respect to ζ . For the angle of orientation

$$\langle \theta \rangle = \frac{\langle L^2 \cos 2\theta \rangle}{\langle L^2 \sin 2\theta \rangle} = \beta \left(1 + \frac{\zeta}{\beta} \right) \left[1 - \frac{3}{2} \zeta^2 + \dots \right] = \beta \left[1 - \frac{3}{2} \zeta^2 + \dots \right]. \quad (12)$$

The corresponding calculations for the characteristic viscosity give

$$[\eta] = [\eta]_0 \left(1 - \frac{7}{2} \zeta^2 + \dots \right), \quad (13)$$

which with an accuracy of numerical coefficients coincides with results of works [17, 18].

For the quantity of double refraction (effect of untrinsic anisotropy) we can obtain

$$\left(\frac{\Delta n}{\sigma} \right)_{\infty} = k \left[1 + \frac{1}{2} \beta^2 \left(1 - \frac{7}{2} \zeta \right) + \dots \right], \quad (14)$$

where $k = \beta \left(1 + \frac{1}{2} \beta \right)$, and k is a constant.

Thus, in the case of an ideally flexible coil, but taking into account the anisotropy of the hydrodynamic interaction, we obtained $A = \frac{3}{2} \zeta \neq 0$. In view of the roughness of the model these calculations pretend only to a qualitative coincidence with the experiment. It is possible to give a maximum appraisal $\frac{A}{k} < \frac{7}{2}$, considering that calculations are made for the effect of intrinsic anisotropy [cf (2), (3)].

It is interesting to compare the theoretical curves of the dependence of the angle of orientation on the velocity gradient for coils [8, 9] and rigid

ellipsoids [5, 6]. It is evident (see Fig. 7) that the curve for the rigid ellipsoids lies between the curves for the ideally flexible coil (isotropic hydrodynamic interaction), and for the kinetically rigid coil, where the dependence for the rigid ellipsoids with $p = 1$ coincides with the dependence for an ideally flexible coil.

Using the equations for coefficients of forward friction [19] we can obtain the magnitude of the anisotropy of coefficient of hydrodynamic friction of rigid ellipsoids:

$$1 - \frac{A}{A_0} = \begin{cases} 0,1 \frac{p-1}{p} & \text{where } p \approx 1, \\ \frac{1}{p} & \text{where } p > 10. \end{cases} \quad (15)$$

Consequently, the difference of the gradient dependence of the angle of orientation for rigid ellipsoids with different p 's is connected with the anisotropy of the coefficient of hydrodynamic friction. An analogous result is obtained for ideally flexible coils with anisotropy of hydrodynamic interaction.

In conclusion the author expresses gratitude to Prof. V. N. Tsvetkov for his valuable advice and help in the work.

Conclusions

1. The dependence is studied of the angle of orientation of double refraction (effect of form) on the velocity gradient in a wide region of hydrodynamic stresses for solutions of 6 fractions of polymethyl methacrylate during a change of viscosity of the solvent for fraction V from 0.3 to 15.6 cp, and for the remaining fractions from 5 to 15.6 cp.
2. A method is proposed for finding the initial slope of the dependence of the angle of orientation on the velocity gradient, taking into account the measurements taken during large velocity gradients and for solutions of high concentrations of polymer.
3. The influence of the anisotropy of hydrodynamic interaction on the gradient dependence of the angle of orientation is considered.
4. A comparison is made of experimental data with the theory for ideally flexible and kinetically rigid macromolecules and also with the theory for rigid ellipsoids. Taking into account the anisotropy of hydrodynamic interaction, it is possible to coordinate well experimental data with conclusions of the theories.

Summary

The hydrodynamic stress dependence of the extinction angle is studied in a broad interval of rates of shear in solution of 6 fractions of PMAA, the viscosity of solvents being changed in a wide range.

The influence of the hydrodynamic anisotropy interaction is taken into account, and a new method of extrapolation of the extinction angle, when $g \rightarrow 0$, is proposed.

Literature

1. V. N. Tsvetkov and E. V. Frisman. Reports of the Academy of Sciences of the USSR, 106, 42, 1956.
2. V. N. Tsvetkov and I. N. Shtenninkova. High-molecular compounds, 2, 646, 1960.
3. Hsu Mao. Author's abstract of candidate's dissertation. Publishing House of Leningrad State University, 1962.
4. V. N. Tsvetkov, E. V. Frisman, O. B. Ptitsyn, and S. Ya. Kotlyar. ZhTF, 28, 1428, 1958.
A. A. Peterlin, M. Szwarc. *Angew. Chem. Phys.* 21, 21, 1949
G. H. A. Edsall, J. Scheraga, G. Gee. *J. chem. phys.* 19, 1169, 1951
J. J. Veej. *J. Amer. chem. soc.* 83, 2428, 1961
A. J. Leroy. *J. chem. phys.* 31, 303, 1959
S. W. Koba, M. Koba. *Makromol. chem. arch.* 22, 122, 1958
S. W. Koba, M. Koba. *Makromol. chem. arch.* 22, 122, 1958
11. V. N. Tsvetkov and E. V. Frisman. Reports of the Academy of Sciences of the USSR, 74, 647, 1954.
12. M. Čopić. *J. Polym. sci.*, 20, 593, 1956.
13. V. N. Tsvetkov and V. P. Budtov. High-molecular compounds, 4, 83, 1964.
M. A. Wissler. *Angewandte Chemie*, Bern, 1958
M. A. Wissler. *Angewandte Chemie*, Bern, 1958
M. A. Peterlin. *J. Polym. sci.* 13, 44, 1954
M. A. Peterlin, M. Čopić. *J. appl. phys.* 37, 424, 1964
M. V. Voda. *J. phys. colloid chem.* 52, 302, 1948
M. V. Koba, M. Koba, P. Becker. *Exptl. cant. Molecular* 22, 67, 1961
M. Szwarc. *J. chem. phys.* 24, 229, 1956
M. Szwarc. *J. phys. colloid chem.* 52, 122, 1948

Submitted
24 April 1965

DETERMINATION OF HYDROGEN IN ALUMINUM ALLOYS BY THE
METHOD OF ISOTOPIC BALANCING

N. M. Orlova and A. A. Petrov

The difficulty in the determination of hydrogen in aluminum and its alloys lies in the relatively small content of hydrogen in them (of the order of $5 \cdot 10^{-5}\%$) and the formation of a surface hygroscopic film of aluminum oxide, actively absorbing water vapor from the atmosphere.¹ The quantity of hydrogen in this film comprises a magnitude of the same order as the quantity of hydrogen dissolved in the metal itself. Moreover, the ratio between the quantity of "surface" and "volumetric" hydrogen depends both on the form of the sample and the nature of treatment of its surface.

The method used at present for the determination of hydrogen in aluminum, the method of hot extraction proposed as early as 1937 by Yu. A. Klyachko [3] and developed then in a number of works [4, 5, 6], appears to us to be inadequate for two reasons. First, a sharp decrease of gas generation at a given temperature cannot serve as the criterion of complete degassing of the sample [7], owing to which the results of determining the content of hydrogen in a metal can appear understated. Secondly, in conditions of this method the full desorption of "surface" hydrogen cannot occur also because of the interaction of the surface film Al_2O_3 and water adsorbed on it, resulting in the formation of stable aluminum hydroxide. According to data of work [8] hydroxyl groups are partially

¹It is possible that during the adsorption of large quantities of water vapor aluminum hydroxide is formed [1]. The adsorption of hydrogen in the oxidized film is insignificant, and it, apparently, can be disregarded [2].

retained in films of aluminum oxide even at 800-900°C. Therefore, we are inclined to consider that, although the scheme of the separate determination of "surface" and "volumetric" hydrogen, presented, for instance, in work [4] is theoretically true, the quantitative data obtained in this work are somewhat understated.

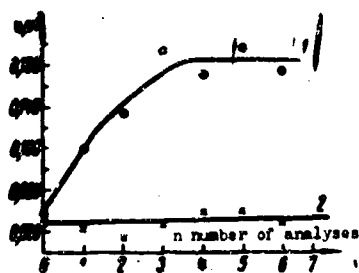
For proof of this we conducted the degassing of aluminum at 600°C and found by applying the method given below, that after two hours of pumping there remains in the metal up to 50%, after six hours, about 30%, and even after 15-20 hours, about 10% of the initial total content of hydrogen, which comprises in different samples 1.0-2.0 cm³/100 g. Proceeding from the above, we should make a conclusion concerning the possibility of systematic errors leading to understated appraisals of the quantity of both "volumetric," and "surface" hydrogen produced in the method of vacuum extraction.

Truer appraisals, in our opinion, can be given by the method of isotopic balancing, inasmuch as it does not require the full liberation of gas from the metal and, furthermore, it is known [8] that equilibrium is established sufficiently fast in the deuterioexchange of films of aluminum hydroxide at 500°C.

The installations on which we developed the spectral-isotopic method of the determination of hydrogen in aluminum and its alloys are analogous to those used earlier [9]. The investigation is carried out on samples of aluminum and its alloys of various compositions, both cast and pressure-worked.

Isotopic balancing was carried out on cylindrical samples with a diameter of 5-6 mm and a weight of 10-20 g at a temperature of 500°C, i.e., comparatively far from the melting point of aluminum, inasmuch as the vapor pressure of certain components of alloys, for instance Mg, is sufficiently high, and on the walls of the exchanger a metallic sublimate can be formed which is able of actively absorbing water vapor and hydrogen from the atmosphere. Moreover, the correction of the reference [?] experiment increases from experiment to experiment (see figure), attaining a considerable magnitude (0.2 ± 0.02) cm³. Such a magnitude of correction and its scattering essentially lower the sensitivity and reproducibility of the method, which is impermissible during the analysis of those small concentrations of hydrogen which occur in aluminum and its alloys.

Therefore, we used the removal of the sublimate by calcination of the exchanger under pumping for 15-20 minutes at a temperature of 1000-1100°C after each analysis. Here the correction of the reference experiment decreased to (0.025 ± 0.005) cm³



Dependence of correction of reference experiment on the number of analyses. 1 - without calcination, 2 - with calcination of the exchanger.

and remained constant in time (see figure). In those cases when alloys were analyzed which practically did not give sublimates at 500°C, and the correction was $(0.05 \pm 0.01) \text{ cm}^3$, the exchanger was not calcined after every experiment, but control experiments were periodically produced.

As was noted above, results of experiments (in particular, the magnitude of the "surface correction") depend on the specific surface of the samples.

Therefore, we strove in all experiments to conduct the machining of samples as identically as possible. However, undoubtedly, complete uniformity of machining in all cases is impossible to attain, and apparently the scattering of the "surface correction" (Table 1) to a considerable degree is determined by this circumstance. In all experiments the samples were washed in ether directly before packing in the exchanger.

| Characteristics of the sample | "Surface correction," ml/cm ² ¹ |
|-------------------------------|---|
| Cost | $(5.0 \pm 0.8) \cdot 10^{-3}$ |
| Cost | $(5.0 \pm 0.8) \cdot 10^{-3}$ |
| Cost | $(5.5 \pm 0.4) \cdot 10^{-3}$ |
| Cost | $(4.0 \pm 1.0) \cdot 10^{-3}$ |
| Treated by pressure | $(3.5 \pm 0.5) \cdot 10^{-3}$ |
| Treated by pressure | $(3.3 \pm 0.4) \cdot 10^{-3}$ |
| Treated by pressure | $(3.2 \pm 0.2) \cdot 10^{-3}$ |

¹The correction variance is represented by the mean arithmetic deviation of the unit measurement.

The first stage of the development of the method was the determination of the time of isotopic balancing under the conditions indicated above. It consists of 25-30 minutes outside the dependence on the presence in samples of Mg, Mn, Cu, and certain other impurities in a quantity of several per cent.

We noted no influence of the treatment of the sample ("cost" or "treated by pressure") on the speed of the isotope exchange.

For the separation of the "volume" and "surface" content of hydrogen we used the process proposed in work [4], introducing certain changes into it. The samples were degased in a vacuum ($p = 10^{-5}$ mm Hg) at a temperature of 500°C for 15-20 hours. The method of isotopic balancing was used to determine the residual content of hydrogen in them; it proved to be equal, for different samples, to $0.1-0.2 \text{ cm}^3/100 \text{ g}$. From thus degased samples the surface developed during prolonged heating was removed by machining, after which they were held in air a different time, upon the expiration of which the quantity of adsorbed hydrogen was determined by the spectral isotope method. Magnitudes of "surface correction" for certain alloys are given in Table 1, and its dependence on the hold time of the sample in air is shown in Table 2.

Table 2.

| Characteristics of the sample | "Surface correction" (ml/cm^2) during holding | | | | |
|-------------------------------|---|---------------------|---------------------|---------------------|---------------------|
| Cast | - | $4.5 \cdot 10^{-3}$ | $5.5 \cdot 10^{-3}$ | $5.0 \cdot 10^{-3}$ | $5.0 \cdot 10^{-3}$ |
| Cast | - | $6.0 \cdot 10^{-3}$ | $5.5 \cdot 10^{-3}$ | $5.5 \cdot 10^{-3}$ | $5.0 \cdot 10^{-3}$ |
| Treated by pressure | $3.5 \cdot 10^{-3}$ | $3.3 \cdot 10^{-3}$ | $3.1 \cdot 10^{-3}$ | $3.2 \cdot 10^{-3}$ | - |
| Treated by pressure | $3.4 \cdot 10^{-3}$ | $3.2 \cdot 10^{-3}$ | $2.9 \cdot 10^{-3}$ | $3.3 \cdot 10^{-3}$ | - |

From Table 1 it follows that the magnitude of the "surface correction" is somewhat higher for the cast samples as compared to those treated by pressure. Apparently, the specific surface during the machining of the samples turns out to be somewhat larger in the first case than in the second.

From an examination of Table 2 it follows that the formation of a hygroscopic film on aluminum and the adsorption on it of water vapor occur immediately after grinding of the sample, which is in accordance with the data of other authors [10, 11]. It is possible to confirm that, at least, during the week after grinding the magnitude of the "surface correction" remains constant. This undoubtedly facilitates the procedure of carrying out the analyses. Apparently the "surface correction" for alloys treated by pressure remains constant during a significantly long time, which, as it seems to us, is impossible to say about certain cast alloys. Probably, in cast alloys there is a slow penetration of water vapor into the thickness of the metal through the microcapillary defects existing in it. Proceeding from this assumption, we should conclude that the determination of truly dissolved hydrogen in cast samples after their prolonged holding in air

is possible only with a considerable systematic error, caused by the presence of microcapillaries. The magnitude of this error will depend, apparently, both on the quality of the casting and on the hold time of the samples and the moisture of the medium. For this reason we must especially investigate the possibility of using cast samples as hydrogen standards for the spectral method of the determination of hydrogen in aluminum alloys; this will possibly be created in the future.

Regarding the "surface correction," we attempted to reduce it to a negligible quantity by means of preliminary treatment of the sample in the process of the analysis itself, since it is obvious that the elimination of a source of systematic error leads to more reliable determinations. With this goal we tried to carry out desorption of surface hydrogen by evacuation for 10-40 minutes at a temperature of 300-400°C, i.e., under conditions during which the extraction of gas from the metal itself can still be disregarded [12, 13]. However, as one can see from Table 3, with such treatment of the sample less than 50% of the surface hydrogen can be liberated. Apparently, in these conditions there occurs intense formation of aluminum hydroxide, accompanied by only partial extraction of hydrogen. Processes of desorption of hydrogen have been studied in great detail by a number of authors [14-17], and the result obtained by us fully agrees with their data.

Table 3

| Temperature of desorption, °C | 300 | | | | 400 |
|--|-----|-----|-----|-----|-----|
| | 10 | 20 | 30 | 40 | 10 |
| Time of desorption, minutes | | | | | |
| Surface correction ¹ ·10 ⁻³ , ml/cm ² | 2.0 | 2.5 | 1.9 | 2.1 | 2.4 |

¹Prior to desorption the "surface correction" was equal to $3.3 \cdot 10^{-3}$ ml/cm².

Inasmuch as we did not manage essentially to decrease the quantity of "surface" hydrogen during desorption, we gave up this method, and we determined the content of hydrogen in metal (V_{MET}) taking into account the "surface correction" by the formula

$$V_{MET} = V_{GM} - V_{SM} \cdot S.$$

where S is the surface area of the sample.

The total amount of hydrogen (V_{00M}) was determined for each sample under the above-indicated conditions of isotopic balancing; the magnitude of the "surface correction" (V_{NOB}) was found in those same conditions beforehand from a series of parallel experiments with preliminarily degased samples of the given alloy.

From Table 4, in which results of such determinations are given it is clear that the hydrogen content in the metal itself is comparable to, and for certain samples even less than, the quantity of surface gas.

Table 4

| Sample | V_{adm} | $\frac{1}{\Delta V_{adm}}$ | V_{adm-S} | $\Delta(V_{adm-S})^2$ | $\frac{V_{adm} - V_{adm-S}}{V_{adm} - V_{adm-S}}$ | $\frac{1}{\frac{\Delta V_{adm}}{V_{adm}}}$ |
|--------|-----------|----------------------------|-------------|-----------------------|---|--|
| 1 | 2.5 | 0.4 | 0.6 | 0.15 | 0.7 | 20 |
| 2 | 2.5 | 0.4 | 0.6 | 0.15 | 1.5 | 10 |
| 3 | 3.1 | 0.3 | 0.6 | 0.15 | 2.2 | 20 |
| 4 | 2.5 | 0.4 | 0.6 | 0.15 | 1.5 | 15 |
| 5 | 2.5 | 0.4 | 1.0 | 0.1 | 1.5 | 10 |
| 6 | 2.5 | 0.4 | 0.6 | 0.15 | 1.4 | 15 |
| 7 | 1.5 | 0.7 | 0.6 | 0.1 | 1.0 | 10 |
| 8 | 1.5 | 0.7 | 0.6 | 0.05 | 0.6 | 10 |
| 9 | 1.5 | 0.7 | 0.6 | 0.07 | 0.7 | 10 |

¹Mean arithmetic scattering of unit measurement.

The essential difference in the quantity "volumetric" hydrogen in the investigated alloys can be a random effect of the prehistory of the samples; however, as it seems to us, we should pay attention to a number of circumstances. Samples which went through treatment by pressure contain, as a rule, a smaller quantity of gas as compared to cast samples. Possibly this is connected with the decrease of microcapillary defects during treatment of the metal under pressure. It is also possible that the comparatively high content of hydrogen in a number of alloys is connected with the great concentration of magnesium in them, since it is known [10] that the addition to aluminum of magnesium in quantities of more than 5-6% considerably increases the capability of such an alloy to dissolve hydrogen in the solid state.

From Table 4 it follows further that the random error of the analysis is a magnitude of the order of 10-20%; which in such a complicated case as the analysis of aluminum alloys we can consider to be a completely satisfactory result.¹

¹The reproducibility of results is determined mainly by scattering of the surface correction. However, during an appraisal of the reproducibility of the method only ΔV_{00M} , is considered since the magnitude of the surface correction was determined beforehand from a sufficiently great series of parallel measurements.

Regarding the accuracy of the determinations, as was noted above, it is necessary to give preference to the spectral-isotope method over the method of vacuum extraction.

We especially did not clarify the magnitude of the systematic error connected with the difference of solubility of hydrogen isotopes in aluminum in conditions of our experiments. However, the fact that results of determinations at the temperatures 500°C and 800°C are identical indicates the proximity of the solubility of hydrogen and deuterium. In any case, this difference does not exceed the random error of the method.

The authors thank Prof. A. N. Zaydel' for his valuable advice.

Summary

A spectral-isotopic method of the determination of hydrogen in aluminum and in some of its alloys was developed. The method enables for a separate determination of gas content in the surface layer as well as in the bulk.

Some aspects of the sorption and desorption of hydrogen in the surface oxide layer have been studied.

Literature

1. M. S. Beletskiy. Reports of the Academy of Sciences of the USSR, 75, 4, 1950.
2. K. F. Topchiyeva and I. F. Moskovskaya. Herald of Moscow State University, No. 2, 22, 1960.
3. Yu. A. Klyachko. Journal of applied chemistry, 10, 1329, 1937.
4. V. A. Danilkin, K. M. Konstantinov, and G. I. Bulatova. Industrial laboratory, 27, 259, 1961.
5. C. Griffith and M. Mallet. Anal. chem., 25, 10851, 1953.
6. D. Carney, J. Chipman, and N. Grant. Trans. AIME, 188, 397, 1950.
7. M. Willachon and G. Chadron. C. R. Acad. sci., 2, 324, 1929.
8. J. B. Peri and R. B. Hannan. J. phys. chem., 64, 1526, 1960.
9. A. N. Zaydel', A. A. Petrov, and G. V. Veynberg. Spectral-isotope method of determination of hydrogen in metals. Publishing House of the Leningrad State University, 1957.
10. M. P. Slavinskiy. Physico-chemical properties of elements. Moscow Metallurgy Publishing House, 1952.
11. N. A. Shishakov, V. V. Andreyeva, and N. K. Andrushenko. Structure and mechanism of the formation of surface films on metals. Moscow Publishing House of the Academy of Sciences of the USSR, 1959.
12. K. Smithells and H. Ransley. Proc. Roy. soc., 152, 706, 1935.
13. K. Smithells. Gases and metals. Moscow, Metallurgy Publishing House, 1940.

14. A. I. Litvintsev and E. P. Belova. Collection: "Heat-durable material from baked aluminum powder." Moscow, Oborongiz, 77, 1961.
15. A. I. Litvintsev and V. M. Polyanskiy. Collection: "Heat-resistant material from sintered aluminum powder," Oborongiz, 100, 1961.
16. V. M. Polyanskiy, M. G. Bogolepov, A. I. Litvintsev, and A. V. Panov. News of school of higher education. Nonferrous metallurgy. Ordzhonikidze, 1, 112, 1961.
17. V. G. Korotkov. Questions of the theory and practice of foundry production. Moscow, Metallurgy Publishing House, 1956.

Submitted
20 March 1963

ON THE "MEAN TIME OF THE FREE PATH" OF O_2 MOLECULES

A. K. Suslov

If we assume that the expansion of telluric lines of O_2 is connected with damping due to collisions [1], then it is possible to construct a theoretical path of the line. However, with such assumption is there a noticeable divergence between the theoretical and observed paths of the first line of the P-branch, which is difficult to explain by random errors [2]. For the determination of time of the free path T_0 this formula was used:

$$i = 1 - \frac{(2\pi T_0)^{-1}}{(\nu - \nu_0) + (2\pi T_0)^{-1}} \quad (1)$$

it was derived under the condition that the intensity in the center of the line $i_0 = 0$ [3]; for the line used in the preceding work [2] $i = 0$ not only in the center, but on a certain section with an extension of 0.3 \AA . During the investigation of the path the intensity at each point is usually divided by the value of the intensity of the continuous spectrum. With a line width of several angstroms it is possible to consider that the many errors connected with atmospheric extinction are reduced, if they are proportional to the initial flux. In the interval of the wavelength where $i = 0$ the solar energy does not reach the lower layers of the atmosphere and, consequently, some of the O_2 molecules are not involved in absorption. Therefore, it is difficult to separate the change in transparency from the change in the number of molecules, and the lines obtained at a different times will correspond to different growth curves. In order to avoid this, it is necessary among lines of band A to select a line for which in the center the

blackening is so close to zero that the ratio (1) is fulfilled. This condition is satisfied most frequently by the 18th line of branch P_Q . With a further growth in the reference number the blackening in the center starts to differ noticeably from zero.

For an appraisal of the time of the free path line P_{18} was selected in band A with a wavelength of 7659.37 \AA in the spectrum of the center of the solar disk, obtained at AOKGU¹, 5 March 1959, at 11^h11^m Moscow time. The spectrum measured photometrically on an MF-2 every 0.01 mm, which allows constructing the dependence between $x = 2 \lg M$ and $y = \lg \left(\frac{1}{T} - 1 \right)$ (Fig. 1). With this $\Delta l = l - l_0$, and l_0 is the scale reading of the [MF-2] (MB-2) corresponding to the center of the line. This dependence turns out to be linear, with sufficient accuracy, for the greater part of the path with the angle of dip of the straight line at 45° :

$$x + y = D. \quad (2)$$

Since

$$D = -2 \lg(2\pi T_0). \quad (3)$$

then with the obtained mean value $\bar{D} = 8.9755$ will be $-\lg(2\pi T) = 9.4878$ or $1/2\pi T_0 = 0.307$. On the other hand

$$\Delta \nu = \nu_0 - \nu = -\frac{\Delta l}{\lambda^2} \cdot 10^8. \quad (4)$$

We finally obtain $T_0 = 7659^2 / 0.307 \cdot 2.998 \cdot 10^8 \cdot 1.225 \cdot 10^{10} \cdot 2\pi = 8.4 \cdot 10^{-12}$ sec.

This confirms the value of T_0 calculated earlier [2]. For checking we substitute the calculated value T_0 into formula (2), construct the theoretical line (dotted line), and compare it with the observed line (solid line - Fig. 2).

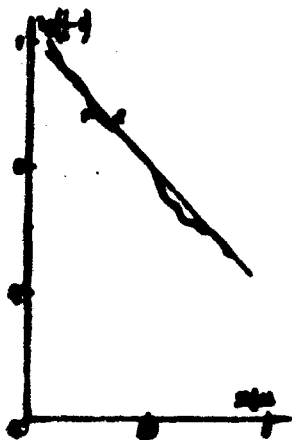


Fig. 1.

For an approximate determination of the parameter T_0 we can use a simple method. Let us transform (1) and integrate over the whole path:

$$\int_0^1 (1 - \Delta l) dx = \frac{1}{2\pi T_0} \int_0^1 \frac{dx}{x^2 + (2\pi T_0)^{-2}}. \quad (5)$$

Consequently,

$$W_\lambda = \frac{1}{2\pi T_0}. \quad (6)$$

In our case $W_\lambda = 0.915 \text{ \AA}$. Expressing equivalent width W in units of frequency, we obtain $T_0 = 11 \cdot 10^{-12}$ sec. This

¹The Astronomical Observatory of the Kazan, Kiev, or Kirgiz State University [Tr. Ed. note].

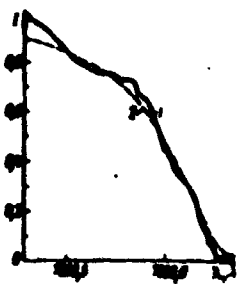


Fig. 2.

makes it possible to determine T_0 from the intensity of lines for all spectra, where there are lines, with zero intensity in the center, if it is known that damping is caused by collisions. Here the lifetime of the upper level for absorption lines should considerably exceed the mean time of the free path. For C_2 molecules this condition is observed, since the upper level $^1\Sigma_g^+$ is metastable and has a

mean lifetime of the order of 10 sec [5].

According to the kinetic theory of gases the number of collisions between molecules per unit time is expressed by the following formula [4]:

$$\nu = 2\sqrt{\frac{2\pi}{m_0}} (n_1\sigma_1 + n_2\sigma_{12}) \sqrt{\frac{2\pi}{m_0}} \quad (7)$$

where n_1, n_2 are the number of molecules O_2 and N_2 per unit volume; σ_1, σ_{12} are the effective cross sections during collision; m_1, m_2 are the corresponding values of molecular weight, where $m_0 = m_1 + m_2$; T is the absolute temperature; and k is the Boltzmann constant. We produce calculations with the following assumptions. Air consists of a mixture of 2 gases. The total number of particles per unit volume is $N = 2.688 \cdot 10^{19}$; $\sigma_1 = 3.2 \text{ \AA}^2$; $\sigma_2 = 3.5 \text{ \AA}^2$; $m_1 = 32.00$; $m_2 = 28.02$. Having substituted the indicated values into formula (7), we obtain for $T = 273^\circ\text{K}$
 $\nu = 2 \cdot 10^9 \text{ sec}^{-1}$.

Thus, there is a considerable disagreement between the result of the theoretical calculation and data of spectrophotometric investigations. First, the expansion of the path is connected not only with collisions but also with the Doppler effect. In this case the path can be represented by equation

$$s = s_0 \int \frac{v_0}{v_0 + v} dv \quad (8)$$

where

$$s = \frac{c}{\nu}, \quad s_0 = \frac{c}{\nu_0}, \quad v = \frac{c}{\nu}, \quad v_0 = \frac{c}{\nu_0} \quad (9)$$

One of the subsequent problems is investigating the influence of Doppler expansion on the line contour. Secondly, oxygen is distributed in the atmosphere nonuniformly, and different layers have different pressures and temperatures.

The observed path appears as a result of certain averaging over all layers. An important practical problem is the interpretation of observed circuits on the

basis of different models of the standard atmosphere. For checking the mentioned assumptions the spectrum of the center of the solar disk was photographed from the observatory of Moscow State University GAISH¹ (in the mountains of Zailiyskiy Ala-tau; H = 3060 m above sea level) [6] by means of a [DFS-3] (ДФС-3) spectrograph with a reverse dispersion of 3.995 Å/mm. Spectrographing was carried out at 10^h53^m Alma-Ata time. For determining parameter T₀ line P₈ with $\lambda = 7632.17 \text{ \AA}$ is selected it possesses maximum intensity and a central density of blackening close to zero. Equivalent width turned out to be $W = 1.0269 \text{ \AA} = 0.528 \cdot 10^{11} \text{ sec}^{-1}$. Hence the approximate value $T = 0.948 \cdot 10^{-11} \text{ sec}$ is obtained. With the help of photometry of the contour the above-described method gives an exact value $T_0 = 8.21 \cdot 10^{-12} \text{ sec}$. From the conducted investigations the following conclusions can be made.

1. The path of atmospheric lines of O₂ can be represented by the formula of Lorentz expansion due to collisions.
2. The parameter of the Lorentz path T₀ does not coincide with the value of the mean time of the free path for the lower layer of air.
3. For an appraisal of the mean time of the free path it is sometimes possible to use the equivalent line width of absorption.

Summary

The formula for the determination of the time of the free path T₀ is derived by means of the photometry of the absorption line O₂. Only such lines, which have intensity equal 0 only in the very center, are used. The difference between the theoretical and observed value T₀ is found. It is possible to use this method for making model of the standard atmosphere more precisely. The value T₀ = 8 · 10⁻¹² sec is received.

Literature

1. C. W. Allen. Line contours of the atmospheric oxygen bands. Ap. J., 85, No. 3, 156, 1937.
2. A. K. Suslov. On the profile of the telluric line of O₂. Astronomical circular, No. 212, 5, 1960.
3. L. Kh. Aller [L. H. Haller]. Astrophysics, 1, 275, Moscow, Foreign Literature Publishing House, 1955.
4. S. Chapman. Kinetic theory of gases. Viscosity, thermal conduction, and diffusion. (Collection: "Basic formulae of physics," edited by D. Menzel, 1951, 1957, Moscow, Foreign Literature Publishing House).

¹GAISH - P. K. Shternberg State Astronomical Institute [Tr. Ed. note].

5. W. H. J. Childs. Absorption measurements and transition probabilities for the A(0.0) and B(0.1). London, Edinburgh and Dublin phil. mag., 14, No. 95, 1049, 1932.

6. A. K. Suslov. Change in telluric lines of O_2 with the rise above sea level, Astronomic circular, No. 213, 8, 1960.

Submitted
20 March 1963

APPROXIMATION OF ISOLATED LINE DURING TRANSFER OF RADIATIVE
ENERGY IN THE UPPER ATMOSPHERE

G. M. Shved

The use of the approximation of the isolated line during modeling of infrared absorption spectra in the mesosphere and upper stratosphere proves to be possible due to the decrease in line width with a drop in of pressure. In this article we discuss the limits of validity of this approximation, for a calculation of fluxes and of radiant energy. The former require the assignment $\frac{\partial A_p(z, z')}{\partial z}$, and the latter $\frac{\partial A_p(z, z')}{\partial z}$, where $A_p(z, z')$ is the function of absorption for a radiant flux between atmosphere levels z and z' . In the case of a separate line with the Lorentz-Doppler contour and the intensity of the line constant along optical path and concentration of the absorbing substance [1]

$$\frac{\partial A_p(z, z')}{\partial z} = C_1(z) \int_0^\infty d\alpha H(\alpha, \alpha) E_1(\alpha, \alpha'; \alpha); \quad (1)$$

$$\frac{\partial A_p(z, z')}{\partial z} = C_2(z, z') \int_0^\infty d\alpha H(\alpha, \alpha) H(\alpha', \alpha) E_1(\alpha, \alpha'; \alpha); \quad (2)$$

$$E_1 = \int_0^\infty dx x^{-2} e^{-\alpha x} \int_0^\infty H(\alpha', \alpha) dx$$

$$\gamma = \frac{2\alpha x}{2\alpha + \alpha_D}; \quad H(\alpha, \alpha) = \frac{S}{\alpha} \int_0^\infty dx \frac{e^{-x}}{\alpha + (\alpha - x)^2};$$

$$\alpha = \sqrt{\ln 2} \frac{\alpha_D(\alpha)}{\alpha_D}; \quad \alpha' = \sqrt{\ln 2} \frac{\alpha_D(\alpha')}{\alpha_D}.$$

where S is the intensity of the line; α_D and α_L are the Doppler and Lorentz halfwidths of the line, respectively; c is the volumetric concentration of the absorbing gas; p_0 , ρ_0 and α_{0L} are correspondingly pressure, density, and the Lorentz

halfwidth under normal conditions; ν_0 corresponding to the center of the line; $C_1(z)$ and $C_2(z, z')$ are certain coefficients [1].

Curves of Fig. 1 give the approximate dependence on the parameter of the line γ of the lower boundary of layers of the atmosphere (by parameter a), for which outside the intervals $(-12, 12)$ and $(-120, 120)$ there is not more than 1 and 10% of the full value of $\frac{\partial A_p}{\partial z}$. For lines 15-micron band of CO_2 , of the considered in detail, on the assumption that $\alpha_D = 5.6 \cdot 10^{-4} \text{ cm}^{-1}$, $\alpha_{OL} = 7.2 \cdot 10^{-2} \text{ cm}^{-1}$ and $c = 3 \cdot 10^{-4}$, heights of the lower boundary of the indicated layers are converted to km (model of the atmosphere ARDC-1959 [2]).

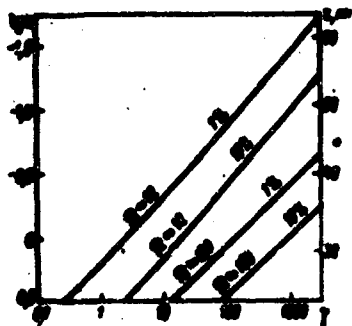


Fig. 1.

The 15-micron band of CO_2 consists [1] of small frequency intervals with a great concentration of lines and more rarely occupied regions of overlapping P and R branches of different vibration-rotational bands, which belong to the same several most widespread isotopic varieties of CO_2 .

In the P and R branches the distance between adjacent lines which belong to any vibrational transition is close to 1.6 cm^{-1} . Assuming random imposition of different P and R branches, the use of the approximation of the isolated line will depend on the arrival in this interval of lines which are essential in the transfer of radiation and on their distribution by intensities. In the interval 1.6 cm^{-1} in the region of frequencies $615-700 \text{ cm}^{-1}$ 5-10 lines are necessary, where including not more than two with a value of $\gamma \gtrsim 100$. It should also be noted that the intervals $(-12, 12)$ and $(-120, 120)$ correspond to frequency intervals $1.6 \cdot 10^{-2}$ and $1.6 \cdot 10^{-1} \text{ cm}^{-1}$. Then, according to Fig. 1, it is possible to assume that the calculation of $\frac{\partial A_p}{\partial z}$ during the transfer of radiation between levels lying higher than 25 km in the approximation of the isolated line does not yield an error of more than several percent.

Q-branches of different vibrational transitions creating a 15- μ band occupy frequency intervals from several tenths of a cm^{-1} to several cm^{-1} . Distances between adjacent lines in the majority of the Q-branches vary in a wide interval, $10^{-3} - 10^{-1} \text{ cm}^{-1}$, with values of the order of 10^{-2} cm^{-1} being most characteristic. For overlapping Q-branches, lying in the interval $667-672 \text{ cm}^{-1}$ and belonging to the most intense vibrational transitions, the calculation of $\frac{\partial A_p}{\partial z}$ in the

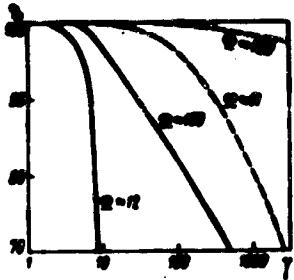


Fig. 2.

approximation of the isolated line, correct to several per cent, can be carried out above 50 km, and for the remaining Q-branches, above 30-35 km.

Curves of Fig. 2 give the approximate dependence on γ of fraction $\frac{\partial A_F}{\partial \nu}$, lying in a certain interval $(-\Omega, \Omega)$ for two cases: 1) during the transfer of radiation from the upper boundary of the mesosphere to a level characterized by the value $a = 1.27$ (30 km for the 15μ band of CO_2); 2) during the transfer of radiation from the level $a = 2.6 \cdot 10^{-2}$ (60 km) to level $a = 3.6 \cdot 10^{-2}$ (58 km). In the first case this is the solid curve in Fig. 2, and in the second case, dotted curve. The curves are given for the transfer of radiation downward; however, they can also be used in the appraisal of the approximation of the isolated line during the transfer of radiation upward.

From Figs. 1 and 2 it follows that the region of application of the considered approximation starts from somewhat greater heights with a calculation of $\frac{\partial A_F}{\partial \nu}$ as compared to $\frac{\partial A_F}{\partial \nu}$, and the greater the difference in heights the more intense the lines in the frequency interval. This occurs because the "mass" of integral (2) is more concentrated near ν_0 as compared to that of integral (1). The region of application of the approximation should especially be reduced in the interval $667-672 \text{ cm}^{-1}$.

The form of the distant wings of the line is described by the statistical theory of expansion. A theoretical discussion of the influence of wings of statistical form on the transfer of radiation in the atmosphere is carried out in works [3, 4]. Experimental investigations of the form of distant wings of infrared lines of certain molecules, namely, HCl, CO, H_2O , and CO_2 (4.3μ band), were made by Benedict and his colleagues [5, 6, 7]. From the theoretical appraisals and experimental data it may be concluded that under atmospheric pressures the Lorentz form of lines in infrared spectra of molecules becomes a statistical form at distances from the center of the line of the order of 1 cm^{-1} and more. But the use of the approximation of the isolated line in the atmosphere, for instance in the 15μ band of CO_2 , usually requires that the transfer of radiation be concentrated in much narrower intervals. Thus, in this approximation the Lorentz-Doppler approximation of the form of the line is valid.

Summary

Values of the frequency interval, in which radiative transfer through a single line in the mesosphere and upper stratosphere proceeds, are considered. The regions of validity for the non-overlapping lines model are estimated in the case of the 15μ CO₂ band.

Literature

1. G. M. Shved and I. V. Tsaritsyna. On functions of absorption of infrared radiation in the mesosphere and upper stratosphere. Collection 1: "Problems of physics of the atmosphere," Publishing House of the Leningrad State University, 1963.

2. Handbook of geophysics. Chap. 1. Middle atmosphere. N. Y., 1959.

3. G. H. Plass & Warner. J. meteorol., 9, 289, 1952.

4. A. E. Curtis & M. Goody. Quart. J. Roy. meteorol. soc., 80, 139, 1954.

5. W. S. Benedict, R. Herman, G. E. Moore, & Silverman. J. chem. phys., 24, 229, 1956.

6. W. S. Benedict, R. Herman, G. E. Moore, & Silverman. Astrophys. J., 134, 277, 1952.

7. K. Ya. Kondrat'yev. Symposium on radiation. Achievements in the physical Sciences, 76, 174, 1962.

Submitted
3 May 1963

C H E M I S T R Y

ON POLYANIONS IN SOLUTIONS¹

L. G. Sillen

Considering the ever increasing interest in multinuclear complexes forming in solution and, especially, in multinuclear anionic complexes, we consider it useful to make a short survey of the results attained in this region of investigation.

Polyborates. Figure 1 shows a group of curves [1], which are connected with the reaction $B(OH)_3 + OH^-$.

On the axis of abscissas $\log h = \log [H^+]$, on the axis of ordinates, Z , i.e., the average of hydroxyl ions which interacted with a molecule of boric acid. In this case Z is the average charge at a boron atom.

In the most acid solutions $Z = 0$; boron wholly enters in composition of boric acid. In strongly alkaline solutions $Z = -1$; boron comes forward in the form of an ion formed by connection of one OH^- group to $B(OH)_3$. Between them is an area where an equilibrium is obviously established between the various forms of boron compounds. All these data were obtained by us several years ago by potentiometric titrating. By measuring the emf we established $[H^+]$ and by analysis we determined the quantity of reagent added to the solution. Consequently, it is simple to calculate how much OH^- is combined with boron, and thus to obtain Z .

¹After arriving in Leningrad in 1961 the known Swedish researcher in the region of polymerisation of ions in solutions, L. G. Sillen, read a lecture to the chemical department of the Leningrad State University about the latest successes in the chemistry of complex compounds.

This article is a short account of this lecture, amiably given by L. G. Sillen to the editor.

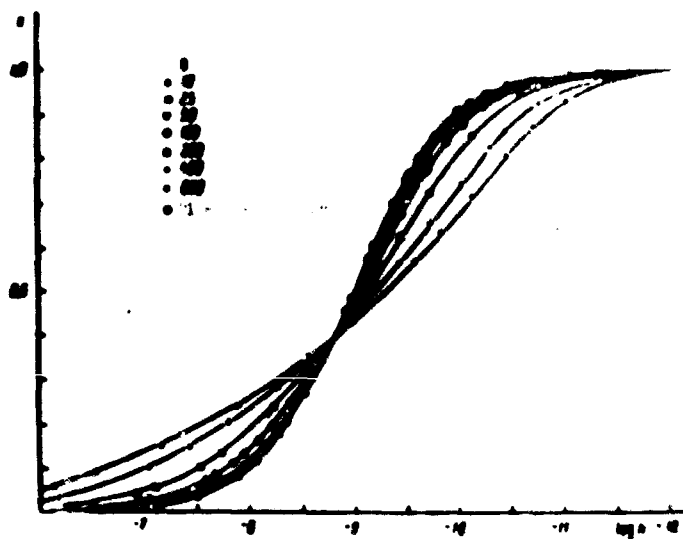


Fig. 1. Experimental data of $\log K$ vs $\log m_B$ for equilibria borate.

The various curves pertain to different concentrations of boron. At low concentrations the curves approach a "limiting curve," which has the form characteristic for the curve of simple dissociation of an acid. Subtracting the logarithm of the equilibrium constant, e.g., in the case of the point where $m_B = 0.5$, we obtain $\log K = -9.00$. What reaction does this equilibrium constant refer to? Ordinarily the reaction is written thusly:



However, this is doubtful. During all measurements the activity of water was almost constant; therefore, it is impossible to answer the question of how many molecules of H_2O enters into the complex. From our data about equilibrium at low concentrations of boron we know only that there are two complexes, one without charge and one with a charge of -1. The uncharged complex can be B(OH)_3 , or $\text{B(OH)}_2\text{OH}_2$, or $\text{B(OH)}_2\text{OH}_2$, etc. The anion can be BO_2^- , or H_2BO_2^- , or H_2BO_2^- , etc. In order to determine which of the above-named formulas are correct it is necessary to carry out a detailed investigation.

X-ray diffraction investigations [1, 2] indicated the presence of complexes B(OH)_3 and B(OH)_2^- in the crystals, i.e., trihydroxyboric acid and tetrahydroxyborate. It was possible to determine the structure of the boron tetrahydroxyborate complexes in solutions with infrared spectra of the crystals when the structure of the complexes is known. Eke [3] and others [4] have established that the

concluded that aqueous solution contains these two complexes: $B(OH)_3$ and $B(OH)_4^-$. Consequently, the most probable reaction will be



Let us return to the curves in Fig. 1. At the highest concentrations of boron the curves differ from the "limiting curve." It is obvious that other complexes (polyborate anions) are also formed.

Chemical literature contains many assumptions about formulas of polyborates. Certain authors consider that there are two separate questions; what is the form of the complexes and what is their durability. However, in our opinion these two questions are indivisible and they must be solved together.

If we have a transparent aqueous solution, then it is interesting to know what complexes are in it? To solve this problem we tried many methods, both the most contemporary and also old ones. For instance, for borates the lines of the Raman spectra are too weak. We obtained good lines for $B(OH)_3$ and $B(OH)_4^-$; but the lines of the new complexes are not distinctive. The application of nuclear-magnetic resonance turned out to be useless.

For system of borates, just as for most systems, the most reliable method turned out to be the method of equilibrium analysis with the help of emf. With such investigations, in our opinion, it is necessary to consider the following: one must make no prerequisites about formulas of products; one must keep the ionic medium as constant as possible (this ensures a constancy of coefficients of activity, without which it is very difficult to obtain reliable conclusions about formulas of products); one must conduct the measurements and analyses as accurately as possible; one must attain as wide as possible a range of concentrations of central group and H^+ .

Tungstenates. Figure 2 shows the corresponding curves during acidation of tungstate-ion [5]. Along the axis of abscissas $\log h$, is placed; along the axis of ordinates Z , i.e., the number of H^+ which on the average reacted with every anion WO_4^{z-} . $z = Z - 2$ is the average charge at every W atom. In alkali solutions W exists only in the form of WO_4^{2-} , so that $Z = 0$, $z = -2$. The different curves pertain to different general concentrations of tungsten. By mathematical analysis of the data it may be concluded that in these conditions only one complex with six atoms W and charge of -5 will be formed. The curves in Fig. 2 are calculated assuming that only this reaction occurred



The experimental points, obtained by Sasaki from measurements of the emf and the theoretical curves well coincide. It is necessary to note that such data are three-dimensional. Two coordinates are Z and $\log h$. Imagine that the third coordinate is $\log B$, where B is the general concentration of the central group, i.e., $[\text{W}]_{0.06M}$. In this case these data present part of a three-dimensional surface. The problem consists of finding such a theory, i.e., such reactions and such equilibrium constants, that the surface calculated proceeding from this theory coincides with the experimental data. From Fig. 2 it is clear that we managed

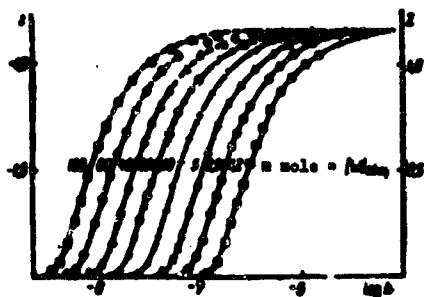


Fig. 2. Experimental data of $Z(\log h)_B$ for oxidation of tungstenates. Curves are calculated proceeding from assumed reaction (2) with $\log K = 60.67$ [5].

to solve this problem.

Experiments show that if the segment of the surface is sufficiently wide the solution of the problem is almost simple. With other complexes or other constants the theoretical surface does not coincide with the experimental data, i.e., in a projection such as in Figs. 1 and 2 either the form of curves or the distance between curves differ from the experimental data.

It is possible to compare the "three-dimensional data" with the "two-dimensional."

If there are measurements only at one concentration, the data are "two-dimensional." With their help it is also possible to exclude certain theoretical assumptions.

There are also "one-dimensional data." Thus, e.g., if we change the composition of the solution and simultaneously measure some other magnitude (electrical conductivity, viscosity, specific density, etc.), we will obtain a curve on which sometimes there is a clear break; in certain cases we can assume a break. But only result of such measurements is an approximate determination of the position of this break. This is why I called such curves one-dimensional. If there is only one complex and if this complex is mononuclear, then from the "one-dimensional data" it is possible to make a definite conclusion. But if there are many complexes and if there are multinuclear complexes among them, then "one-dimensional and two-dimensional data" are insufficient for such a conclusion.

In the chemical literature contains a series of formulas of complexes, which



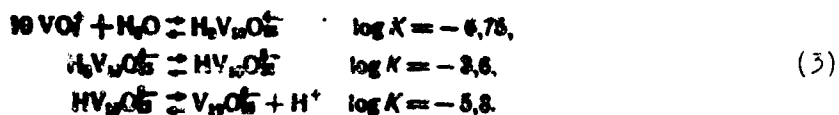
Fig. 3. Experimental data of $Z(\log h)_E$ for the reaction $VO_2^+ + OH^-$. Curves are calculated proceeding from the assumption about the formation of decavanadates with equilibrium constants given in the text [6].

appeared on the basis of "one-dimensional" or "two-dimensional data," but which lose their value when "three-dimensional data" are used. This also occurs in the case of tungstenates.

Regarding tungsten, it is possible to add that reaction (2) is only the first of the acidation reactions; equilibrium in it is rapidly attained. Upon adding a surplus of acid and heating other complexes are also formed. In the future we hope to investigate them at a higher temperature.

Vanadates. In strongly acid solution pentavalent vanadium is in the form of a VO_2^+ cation; upon adding OH^- an interaction occurs. Figure 3 shows the data F. Rossotti and H. Rossotti [6]. As in the preceding cases, on the axis of abscissas is $\log h$, and on the axis of ordinates, Z , i.e., the average number of OH^- , combined with each VO_2^+ ion. At high concentrations of acid $Z = 0$, i.e., there is only VO_2^+ . We can imagine that VO_2^+ and OH^- form a neutral complex such as, e.g., VO_2OH or HVO_3 . This would correspond to $Z = 1$. But with such concentrations this is not observed. The curves attain $Z = 1.4$, i.e., $1.4 OH^-/VO_2^+$ without an interruption; anions of approximately $(V_x \dots)^{-0.4x}$ are immediately formed. Solutions containing these anions are orange.

Until F. Rossotti and H. Rossotti made this investigation, all textbooks indicated that orange solutions contained hexavanadates, i.e., complexes with 6 V atoms. But mathematical analysis of the data showed that conformity with experiment is obtained only if we consider that there are decavanadates with 10 V atoms:



Brito and Ingri continued the investigation of vanadates in more alkaline solutions [7]. Their data are represented in Fig. 4. On the axis of abscissas is $\log [\text{OH}^-]$, on the axis of ordinates is Z . Z is the average number of $\text{A} = \text{H}^+$, which reacted with each $\text{B} = \text{HVO}_4^{2-}$. At $Z = 0$ we have "pyrovanadates" with charge of $-2/V$; at $Z = 1$ we have "metavanadates" with charge of $-1/V$.

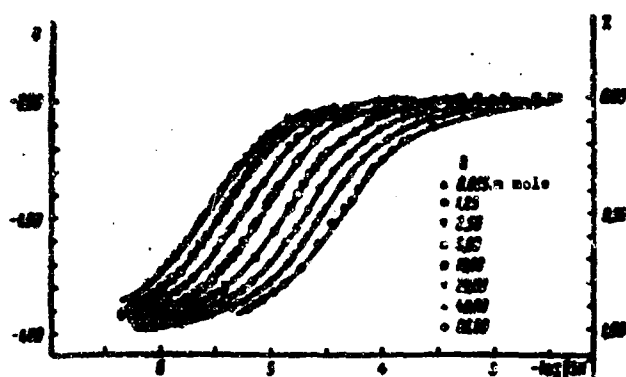
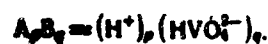


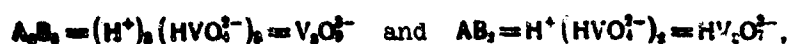
Fig. 4. Experimental data of $Z(-\log \text{OH}^-)_p$ for acidation of HVO_4^{2-} . Curves are calculated proceeding from assumed reactions and constants, given in text [7].

The general formula of the complex can be written

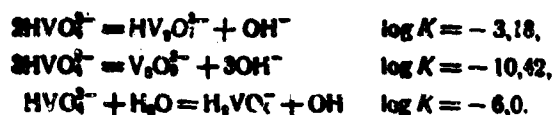


From the data of $Z(\log h)_B$ we can calculate the average composition of complexes (\bar{p} and \bar{q}) without any prerequisites; the mathematical calculation is simple [8]. Figure 5 shows \bar{p} and \bar{q} calculated thusly. The small crosses correspond to possible

complexes. Based on this calculated \bar{p} , \bar{q} it may be concluded that at the highest concentrations of vanadium the predominant complexes are



in which a minimum quantity of water is assumed. All these conclusions are made without any assumptions about the compositions of complexes. The presence of the shown complexes was confirmed by more exact calculation and the following final constants of equilibrium were obtained:



The question arises: why are just $\text{V}_3\text{O}_9^{3-}$ and $\text{HV}_2\text{O}_7^{3-}$ formed and not, for instance, $\text{HV}_3\text{O}_9^{2-}$ and $\text{V}_2\text{O}_7^{4-}$? This formulation of the problem shows that we reason by an analogy with the chemistry of phosphorus. Phosphorus has a coordination number of

4, so that PO_4^{3-} , $P_2O_7^{4-}$, $P_3O_9^{3-}$, etc., are formed. But for vanadium the coordination number most frequently is 5. Consequently, the HVO_4^{2-} ion, in our opinion, is more likely $VO_2(OH)_3^-$; from measurements of equilibrium in aqueous solutions it is possible to conclude the number of V atoms and the charge, but it is impossible to conclude the number of water molecules, so that the formulas HVO_4^{2-} and $VO_2(OH)_3^{2-}$ cannot be distinguished. Thus, it is possible to explain the two complexes $HV_2O_7^{3-}$ and $V_3O_9^{3-}$, i.e., $(VO_2)_2(OH)_5^{3-}$ and $(VO_2)_3(OH)_6^{3-}$; in the first complex there is a OH bridge between the two VO_2 groups; the second is a ring with three OH bridges. However, these structures are hypothetical; their confirmation would

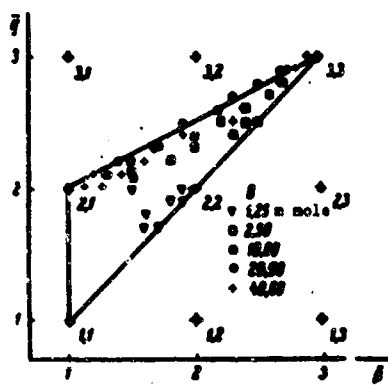


Fig. 5. Average composition (\bar{p} and \bar{q}) of complexes $(H^+)_p(HVO_4^{2-})_q$.

be of interest.

Figure 6 shows the total the data of F. Rossotti and H. Rossotti and Ingri and Brito. There are two regions: " VO_2^+ + deca" and "meta-pyro." If we mix a solution corresponding to the region " VO_2^+ + deca" with acid or another solution from the same region, then equilibrium is established very rapidly. If we mix a solution from the "pyro-meta" region with an alkali or another "pyro-meta" solution, equilibrium is also instantly obtained.

Between them is a region characterized by very slow reactions; we called it the region of instability. If a solution is in this region briefly, then equilibrium is not attained; it may be that in this case a colloid will be formed. Thus occurs, e.g., if a "pyro-meta" solution is mixed with a solution containing " VO_2^+ + deca" with an acid. We think that exactly this is the cause of the difficulties of many previous investigations.

Molybdates. Figure 7 depicts different curves obtained by Sasaki [9] from measurements of emr and analyses. On the axis of ordinates Z is the average number of H^+ combined with each MoO_4^{2-} ion. The average charge at each Mo, $z = Z - 2$. At $pH > 8$, $Z = 0$ and there is only MoO_4^{2-} . As before, the curves are calculated theoretically, and the points are obtained experimentally. An analysis of the curves (Fig. 8) shows that at the highest concentrations of molybdenum basically ions with 7 Mo atoms are formed and that the $(H^+)_8(MoO_4^{2-})_7$ complex, i.e., $Mo_7O_{24}^{6-}$, is especially stable. It is very probably that this is the same

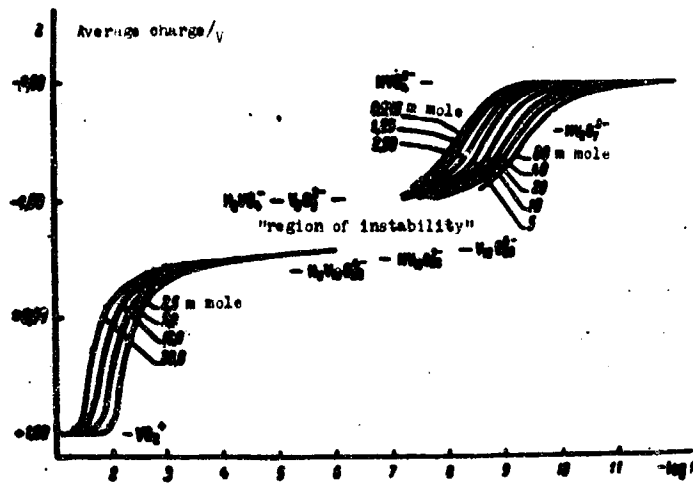


Fig. 6. Survey of the totality of experimental data on vanadium. Between the regions " VO_2^+ + deca" and "meta + pyro" is a region of instability [6, 7].

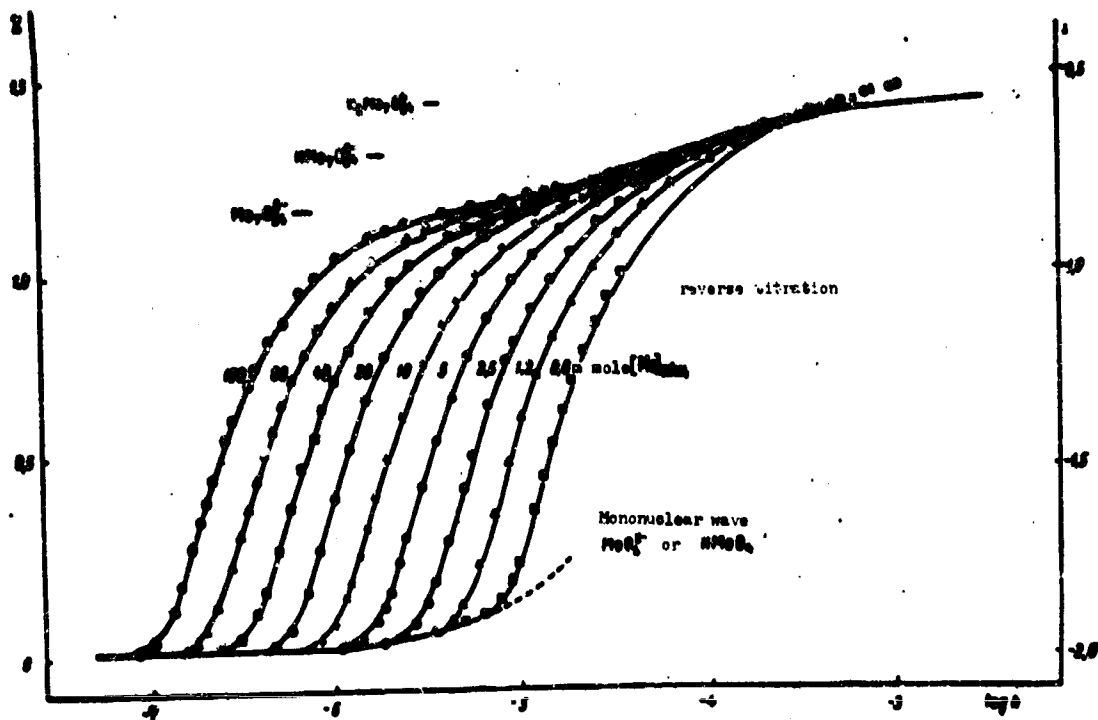


Fig. 7. Experimental data of $Z(\log h)$ for acidation of molybdate.

para-molybdate, which Lindkvist found in structures of crystals [10].

Table 1 gives those reactions which we concluded on the basis of our data. Here we give the constants of equilibrium from article [9] and those constants which we obtained during treatment of wider material with help of an electronic

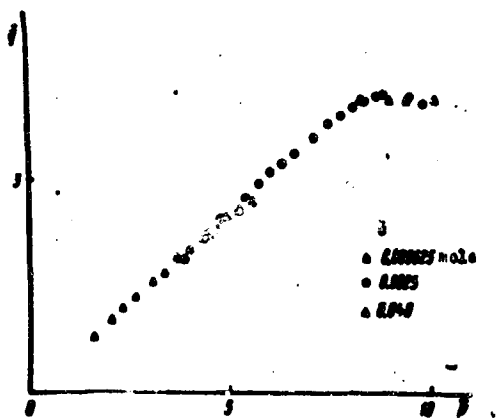


Fig. 8. Average composition \bar{p} , \bar{q} of complexes $(H^+)_p(MoCO_4^{2-})_q$. Calculated directly from experimental data [10] according to method [8].

computer [11]. Our data can be explained by assuming that there are basically complexes with one or seven Mo atoms. In our opinion, only in strongly acid solutions are there cations with charge of +1; however, by this we still cannot determine how many Mo atoms are in it. At high concentrations of molybdenum there is a more complicated complex, perhaps, $Mo_{18}O_{56}^{4-}$.

In the chemical literature various assume the following complexes: MoO_4^{2-} ,

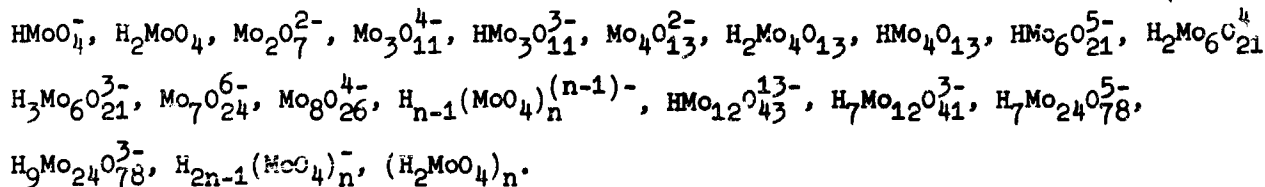


Table 1. Equilibrium of Molybdates According to [9] and [11]

| Reactions | log K [9] | log K [11] |
|---|-----------|------------|
| $MoO_4^{2-} + H^+ = HMoO_4^-$ | 4.06 | 3.9 |
| $HMoO_4^- + H^+ = H_2MoO_4$ | - | 3.8 |
| $7MoO_4^{2-} + 8H^+ = Mo_7O_{24}^{6-} + 4H_2O$ | 87.7 | 87.76 |
| $Mo_2O_7^{2-} + H^+ = HMo_2O_7^-$ | 4.38 | 4.41 |
| $HMo_2O_7^- + H^+ = H_2Mo_2O_7$ | 3.7 | 3.6 |
| $H_2Mo_2O_7 + H^+ = H_3Mo_2O_7^-$, also possible and $(MoO_4)_n H^+$ ($n=1,2\dots$) cations and $Mo_nO_{3n}^-$ complex | - | 2.6 |

Four of these formulas coincide with ours; the presence of other complexes is not confirmed by our measurements; however from the investigations of the Stockholm authors there are still new formulas: $HMo_7O_{24}^{5-}$, $H_2Mo_7O_{29}^{4-}$, and $H_3Mo_7O_{24}^{3-}$.

The method offered by us allows conducting a certain simplification and sampling of data in chemistry of polyanions.

Chromates. Sasaki [12] thoroughly investigated solutions of chromates by the spectrophotometric method and the emf method. Figure 1C shows his results (designated by points) obtained by the method of measuring emf (Z is the average number of H^+ with reacted with each CrO_4^{2-} group). From an analysis of these data

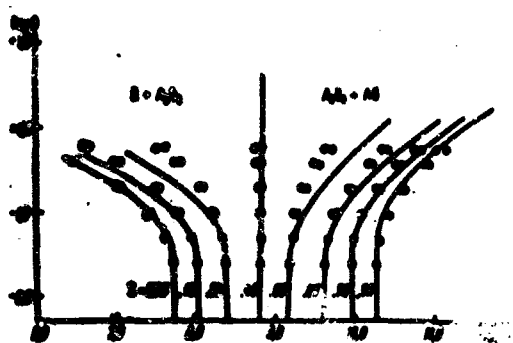


Fig. 9. Experimental data for acidation of the CrO_4^{2-} ion. Curves are calculated proceeding from assumption that only HCrO_4^{2-} and $\text{Cr}_2\text{O}_7^{2-}$ exist with equilibrium constants given in text [17].

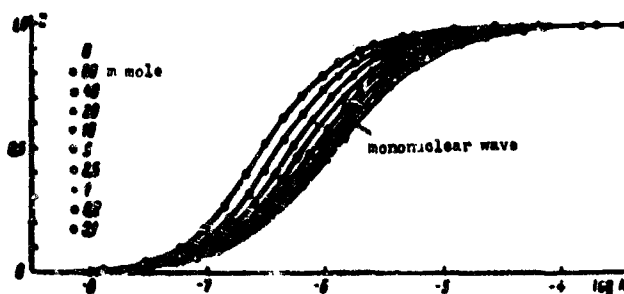


Fig. 10. Connection of the surface by $\log B(\log h)_Z$ at constant Z . Curves are theoretically calculated proceeding from the assumption that there are only complexes B (boric acid), AB (monoborate-ion) and A_2B_5 (pentaborate-ion with charge of -5) [1]. Points designate experimental data of Fig. 1.

Saski concluded the possibility of two reactions occurring and obtained equilibrium constants for them; the curves in Fig. 9 were calculated theoretically, proceeding from these assumptions. Almost the very same constants were obtained from the spectrophotometric data:

| Reaction | log K | |
|---|-----------------|--------------------|
| | emf | spectrophotometric |
| $\text{H}^+ + \text{CrO}_4^{2-} \rightleftharpoons \text{HCrO}_4^-$ | 5.89 ± 0.02 | 5.91 ± 0.01 |
| $2\text{HCrO}_4^- \rightleftharpoons \text{Cr}_2\text{O}_7^{2-} + \text{H}_2\text{O}$ | 2.20 ± 0.03 | 2.18 ± 0.03 |

Thus, in a system of chromates we find namely those complexes, CrO_4^{2-} , $\text{Cr}_2\text{O}_7^{2-}$, and HCrO_4^- , whose existence was assumed by all authors.

In order to reveal the essence of some of our methods we will return to boron.

The French researcher, Carpeni [13], noted that curves such as are depicted in Fig. 1 approximately correspond to $Z = 0.4$. It follows from this, according to his assumption, that there are mainly polyanions of this composition, i.e., with five B atoms and charge of -2. It is not difficult to check the correctness of such an assumption. The data in Fig. 1 present a three-dimensional surface; each curve of $Z(\log h)$ is a cross section at a constant general concentration B .

Figure 10 shows cross sections of the same surface $B(\log h)_Z$ at constant Z . It is easy to prove that if there are only three complexes, schematically B_1^0 , B_1^{-1} , and B_5^{2-} , that the totality of cross sections has to have the same form (curves in Fig. 10). In the same case it would have been possible to displace theoretical curves

in such a way, so that they coincided with the experimental points. It is obvious that this is impossible, and, therefore, the hypothesis of Carpeni can be excluded.

From a mathematical analysis of our data it follows that is a B_3^- complex and also complex with charge of -2. But the range of concentration for boron was too narrow to finally solve the question about the number of boron atoms; 3 or 4; i.e., B_3^{2-} or B_4^{2-} . Since the basic difficulty of solving this problem is connected with the narrow range of concentrations, this question naturally appeared: why not work at very high concentration of borate and use the actual borate instead of perchlorate as the ionic medium? This is the method we called self-medium (self-medium method).

At first we will mention the fact that when a medium created by a neutral, e.g., sodium perchlorate, is used the activity of $\{H_2O\}$ and ions creating the medium, e.g., $\{Na^+\}$ and $\{ClO_4^-\}$, is almost constant, as a result of which it is impossible to establish from measurements of equilibrium how many molecules of water or ions creating the medium and in the composition of the complex. For instance, the triborate ion with charge of -1 could have the general formula of $\{(OH^-)[B(OH)_3]_3 \cdot Na_x(ClO_4)_y H_2O\}^{x-y-1}$. However, Na^+ and ClO_4^- are not an essential part of this complex. This can be concluded from the fact that the same complex and almost the very same equilibrium constant is also obtained in medium of NaBr or KBr [14]. The quantity of H_2O can be judged by the structures of crystals, where there is a $B_3O_3(OH)_4^-$ complex which corresponds to $Z = -3$. If we now use sodium monoborate, $Na^+B(OH)_4^-$ as a medium, the general formula of complexes will be $(H^+)_p[B(OH)_4^-]_q(Na^+)_x(H_2O)_y$. From measurements of equilibrium in a self-medium one can determine only p , i.e., the number of H^+ in the complex; the other magnitudes (q, x, y) are not determined.

It is important to note that now we have possibility separate ions into groups on the basis of the magnitude p . A group where $p = 1$, i.e., a group with one H^+ ion and an unknown quantity of $B(OH)_4^-$ correspond to: boric acid, diborate with charge of -1, triborate with charge of -2, etc., (B^0, B_2^-, B_3^{2-} , etc.). In a group where $p = 2$, we find $B^+, B_2^0, B_3^-, B_4^{2-}$, etc. Now it is possible to answer which point of view is more correct: assuming B_3^{2-} or B_4^{2-} . Our measurements in a self-medium indicate that protons, possibly, come forward by pairs:



This means that tetraborate (2-) ($p = 2$) is more probable than triborate (2-) ($p = 1$).
The magnitude of the constant of the assumed reaction:



well coincides with that we obtained in a neutral medium $\log K = 7.10$ (3M NaClO₄) (it is difficult to expect then to be fully identical).

An analysis of data shows that in acid solutions and at high concentrations of boric acid there is one more complex: either B_4^- or B_5^- . We checked this assumption by the LETAGROP method (this is program for an electronic computer, developed by us in Stockholm). LETAGROP can be presented as a generalized method of least squares applied when the functions are not linear and not even.

Table 2 gives the "best magnitudes" of constants and their average error, and also the average error for Z obtained from the results of processing 180 experimental points (90 in a medium of 3M NaClO₄ and 90 in a medium of 0.1M NaClO₄). It is evident that the average error is less assuming B_5^- , and it seems to us that this complex is the most probable [13].

Table 2. Equilibrium Constants Calculated by the LETAGROP Method from Data for Borates, According to Two Different Assumptions

| Reactions | $\log K$ in 3M NaClO ₄ | $\log K$ in 0.1M NaClO ₄ |
|---|--------------------------------------|--|
| $\text{H}_2\text{O} + \text{B}(\text{OH})_3 = \text{H}^+ + \text{B}(\text{OH})_4^-$ | -8.804 ± 0.008 | -8.976 ± 0.003 |
| $2\text{B}(\text{OH})_3 = \text{H}^+ + \text{B}_2\text{O}_2(\text{OH})_4^- + 2\text{H}_2\text{O}$ | -6.904 ± 0.017 | -7.283 ± 0.014 |
| $3\text{B}(\text{OH})_3 = \text{H}^+ + \text{B}_3\text{O}_3(\text{OH})_6^- + 3\text{H}_2\text{O}$ | -6.95 ± 0.009 | -7.137 ± 0.008 |
| Z | 0.0001 | 0.0016 |
| $\text{H}_2\text{O} + \text{B}(\text{OH})_3 = \text{H}^+ + \text{B}(\text{OH})_4^-$ | -8.807 ± 0.008 | -8.978 ± 0.003 |
| $2\text{B}(\text{OH})_3 = \text{H}^+ + \text{B}_2\text{O}_2(\text{OH})_4^- + 2\text{H}_2\text{O}$ | -6.888 ± 0.008 | -7.288 ± 0.008 |
| $3\text{B}(\text{OH})_3 = \text{H}^+ + \text{B}_3\text{O}_3(\text{OH})_6^- + 3\text{H}_2\text{O}$ | -6.848 ± 0.017 | -6.772 ± 0.004 |
| Z | 0.0001 | 0.0011 |

Thus, from our data we concluded that in solutions of borates there are mainly polyanions: B_3^- , B_4^{2-} , and B_5^- . It is interesting these complexes which we concluded on the basis of our data were independently found in structures of crystals: $\text{B}_4\text{O}_5(\text{OH})_4^{2-}$ [15] and $\text{B}_5\text{O}_6(\text{OH})_4^-$ [16]; however the third $\text{B}_3\text{O}_3(\text{OH})_4^-$ is not revealed in crystals while only $\text{B}_2\text{O}_3(\text{OH})_5^{2-}$ [17].

Summary

In this paper is given a critical survey on the polymerization of anion-complexes in aqueous solutions. The author draws his attention to the systems of polyborates, wolframate, vanadates, molybdates and chromates. A new theoretical method using computer technique has been proposed. This method has given good results based on experimental measurements. The question on the structure of polymers is studied as well. [English summary]

Literature

1. N. Ingrí, G. Lagerström, M. Frydman, L. G. Sillén. *Acta chem. Scand.*, **11**, 1954, 1957.
2. W. H. Zachariasen. *Zs. Krist.*, **68**, 189, 1904.
3. M. Ferrasseri. *Periodico mineral. Roma*, **10**, 102, 1942; **12**, 137, 1952.
4. J. O. Edwards, G. C. Morrison, V. F. Rosa, J. W. Schultz. *J. Amer. chem. soc.*, **77**, 264, 1955.
5. Y. Sasaki. *Acta chem. Scand.*, **15**, 173, 1961.
6. P. J. C. Rossotti, M. S. Rossotti. *J. Inorg. nuclear chem.*, **2**, 284, 1952; *Acta chem. Scand.*, **10**, 957, 1954.
7. N. Ingrí, P. Brito. *Acta chem. Scand.*, **12**, 1971, 1959; P. Brito, N. Ingrí. *Annuaire chim. Sué.*, **145**, 1959.
8. L. G. Sillén. *Acta chem. Scand.*, **10**, 1421, 1951.
9. Y. Sasaki, I. Lindqvist, L. G. Sillén. *J. Inorg. nuclear chem.*, **9**, 63, 1959.
10. I. Lindqvist. *Arkiv Kemi*, **2**, 226, 1952.
11. N. Ingrí, L. G. Sillén. *Acta chem. Scand.*, **10**, 173, 1952.
12. Y. Sasaki. *Acta chem. Scand.*, **10**, 719, 1952.
13. G. Carpent. *Bull. soc. chim. France*, **60**, 244, 1949.
14. N. Ingrí. *Proc. 7 ICCC*, **102**, 1952.
15. H. Morimoto. *Minerology*, **1**, **2**, 1, 1956.
16. W. H. Zachariasen. *Zs. Krist.*, **68**, 289, 1907.
17. C. L. Christ, J. R. Clark. *Acta crystal.*, **9**, 639, 1956.

QUESTION ABOUT PHASE TRANSITIONS IN SOLID BODIES

R. B. Dobrotin, A. V. Suvorov, and Yu. V. Kondrat'yev

The problem of phase transitions is one of the most interesting problems of solid state physical chemistry. Besides the basic thermodynamic parameters of phase transition (temperature, heat, entropy), the anomalous increase of heat capacity near the phase transition and the observed in connection with this interval of temperatures of transition has great value.

About the nature of the mentioned temperature interval there are several points of view. Certain authors explain it by the influence of impurities [1] and others by the appearance near the transition of different type fluctuations or a large number of defects and so forth. In the last case the interval of phase transition should be intimately connected to the nature of a given solid body [2, 3]. The spread of phase transition can be greatly affected by the actual method of measuring heat capacity. In the literature comparatively little attention is paid to this factor.

This work has the goal of obtaining data about thermal effect and magnitudes of temperature interval of transition with the help of the calorimetric method. As objects we chose halides of tungsten and tantalum, rather well studied from the thermodynamic side and having temperatures of fusion and phase transitions in the region of average temperatures.

The instrument on which we conducted measurements is the usual type of calorimeter of pulse heating with internal heater without adiabatic shell. The thermal impulse (4.5 to 5.5 cal) lasted 30 sec. To decrease the heat radiation the

internal part of calorimeter was evacuated to 10^{-5} mm Hg. The temperature of the thermostat was supported with accuracy of 0.01° ; the rise of temperature in the main period of the experiment was measured by a thermocouple with accuracy of 0.005° and did not exceed 1.5° . The result of every experiment corresponding to a definite initial temperature of the thermostat was the usual calorimetric curve: temperature - time.

The investigated substance was placed in a soldered glass ampule with an internal pocket for a heater. The application of glass ampule is explained by the specific character of the behavior of the investigated heat capacities of solid bodies. Nevertheless, the more significant endothermic effects accompanying phase transitions in our instrument could be measured sufficiently reliably.

The preparation of WCl_6 investigated by us was prepared by a known method [4] and contained not more than 0.2% impurities. A preparation of $TaCl_5$, containing not more than 0.03% impurities, was kindly given to us by A. R. Kurbanov. The ampules were filled in a vacuum, without contact with air. The suspension of the investigated substance weighed 5-10 g. "Chemically pure" KNO_3 was used for calibration. It was subjected to special purification and was heated for a long time in a vacuum to remove traces of moisture.

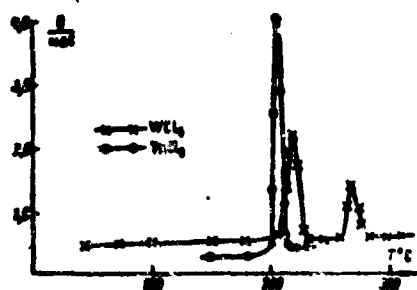


Fig. 1.

The results of experiments on WCl_6 and $TaCl_5$ are represented in Fig. 1. The ordinate shows a conditional magnitude proportional to heat capacity and including thermal values of calorimeter in calories/degree. On the figure one can distinctly see the anomalous heat capacity in the α - β region of transition of WCl_6 and during fusion of WCl_6 and $TaCl_5$. It is obvious that the areas limited from one side by the line of anomalous heat capacity and from other by the continuation of smooth movement of curve have to give an absolute value of the heat of phase transitions in calories. Inasmuch as the error of experimental magnitudes in the region corresponding to a peak is sufficiently large, to obtain more exact data it is necessary to introduce a correction according to the melting heat of the calibration substance (the curve for KNO_3 is not given on the graph).

The heats of transition obtained by the above-described method are given in

| Investigated substance | Character of transition | Heat of transitions | |
|-----------------------------|----------------------------|---------------------|---------------|
| | | Our data | Literary data |
| WCl ₆ | $\alpha \rightarrow \beta$ | 5.5 | 5.6 [4] |
| WCl ₆ | fusion | 4.2 | 2.8 [4] |
| TaCl ₅ | fusion | 8.6 | 8.4 [5] |

the table. The table also contains a comparison with magnitudes known from the literature.

As already noted, the question about the interval of temperatures in which an anomalous heat capacity is observed during phase transition is of great interest.

A consideration of the process of heating a substance in an instrument indicates the presence in the volume of the sample of noticeable gradients of temperature. At the moment of supply of thermal impulse the heater brings the layers of substance nearest to it to higher temperatures compared with the external layers. Consequently, the initial temperature of the mentioned interval should correspond to the state when the temperature of layer of substance near the heater becomes equal to the temperature of transition. The fixed temperature of the external surface of ampule can be much lower. With such a situation a small portion of thermal impulse will be absorbed as a result of transformation of part of the substance in the sample. With subsequent increase of experimental temperature a larger and larger share of the substance will experience transformation, which will cause an even more significant absorption of heat and corresponding lowering of temperature in main period of the experiment. Such a position and will seem like a growth of anomalous heat capacity. The summit of the peak in Fig. 1 corresponds to maximum absorption of energy of thermal impulse, and the extreme high-temperature end of the "region of transition" corresponds to the moment of almost full transformation of all the investigated sample.

It is necessary to note that in the short time of the main transition (30-40 sec) in spite of the unbalanced conditions, the portion of the substance subjected to transformation could not return to the initial state. Therefore, the process of reverse transition (in particular, crystallization) accompanied by liberation of heat occurred in the final period. This circumstance can be confirmed by the difference in the rate of cooling of calorimeter in the region of anomalous heat capacity and outside of it. Figure 2 gives the cooling constant of

the calorimeter in arbitrary units depending upon the experimental temperature. We see that in the region of phase transition the cooling constant sharply drops, which corresponds to an anomalous rate of cooling of the calorimeter in the final period due to a delay in the process of heat liberation.

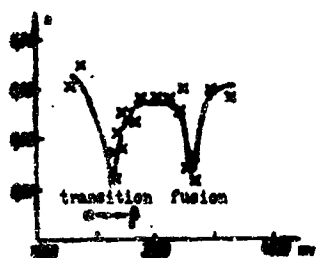


Fig. 2.

The above-stated considerations indicate that anomaly of heat capacity near the phase transition may be basically attributed to the peculiarities of thermal balance of the instrument.

It seems to us that this circumstance affecting the interval of phase transition pertains not only to the method chosen by us. The same pertains to the method of measuring true heat capacity in a calorimeter of continuous heating with an adiabatic shell spreading from 15 to 100°. In certain cases a shift of temperatures of the interval of phase transition occurs during heating and cooling [7]. Here the appearance of the interval of transition can also be partially explained by the peculiarities of thermal balance of the calorimeter. Actually, with a continuous supply of heat the appearance of temperature gradients, especially for the presence of two phases, is inevitable. Nonetheless, it is necessary to indicate that in spite of this the heat of phase transitions measured in such a way turns out to be correct. The fact is that the energy content leading to full transformation of the substance obviously, will not depend on the thermal balance of the calorimeter. The difference will be only in the time needed for transformation of all the investigated sample.

A qualitative appraisal of the temperature gradient in the calorimeter during transition from a single-phase to a two-phase region can be gotten from the magnitude of temperature transfer a . As is known, $a = \gamma/d \cdot C$, where γ is the thermal conduction of the substance, C is the specific heat capacity and d the specific gravity.

Let us assume that 10% of a certain substance passed into a high-temperature form and the heat of transition is equal to 20 kal/g. We can assume that γ and d change not very strongly. However, in the case of formation of a new phase the magnitude a , besides heat capacity, will also include ΔH , the enthalpy of the transformed part of substance. As it is simply calculated, the magnitude C will be increased with the accepted assumptions by more than 10 times. This will

correspond to a decrease of temperature transfer a also by 10 times.

The method of measuring heat capacity by periodic heating with an adiabatic shell should give a minimum drop of temperatures. Actually, sometimes the heat capacities measured by this method in region of fusion in general do give no anomaly or "region of transition" [8]. In other a cases sharp rise of heat capacity in the region of fusion is nevertheless observed [9].

An analysis of the thermal balance in a calorimeter of pulse heating with adiabatic shell showed that, as the boundary of phase transformation moves further from the heater and the thermometer, a temperature gradient can appear in the investigated sample. When there are two phases in the calorimeter the final period of the calorimetric experiment turns out to be distorted, which naturally leads to increased data on heat capacity. In our opinion, this circumstance can also be one of the possible causes of anomalies of heat capacities.

In conclusion it is necessary to note that it is impossible to doubt the objectiveness of the existence of an interval of transition and an anomalous increase of heat capacity. However it is necessary to consider that along with influence of fluctuation, defects or impurities, a large role can be played by factors connected with the method of measuring heat capacity, especially when phase transition is accompanied by a comparatively large energy effect.

The authors express deep gratitude to Prof. S. A. Shchukarev and Associate Professor G. I. Novikov for their attention and valuable indications.

Summary

The heat absorption in the temperature region of phase transformation of WCl_6 and $TaCl_5$ has been measured. Some considerations concerning the influence of the character of heat transfer in the calorimetric cell on the temperature interval of specific heat anomaly have been expressed. [English summary]

Literature

1. A. A. Remizova and A. A. Tamarin. Izv. vyssh. uch. zaved. fizika, No. 6, 1960.
2. G. M. Bartenev. ZhFKh, 22, 587-590, 1948.
3. A. B. Ubbelohde. Trans. Faraday soc., 34, 292, 1938.
4. S. A. Shchukarev and A. V. Suvorov. ZhNKh, 6, 1488, 1961.
5. K. M. Alexander and F. Fairbrother. J. chem. soc., 2472, 1949.
6. M. M. Popov and G. A. Gal'chenoko. ZhOKh, No. 12, 2220, 1951.
7. A. Mustajoki. Ann. Acad. sci. Fennicae., VI, 5, 1957.

8. V. A. Sokolov and N. Ye. Shmidt. Izv. SFKhA, 26, 123, 1955.
9. V. A. Sokolov and N. Ye. Shmidt. Izv. SFKhA, 27, 217, 1956.

Submitted
29 June 1962

ELECTROKINETIC PROPERTIES OF DEPOSITS OF COPPER FERROCYANIDE
OBTAINED IN DIFFERENT CONDITIONS

I. F. Karpova, V. N. Smirnova, and L. A. Fridrikhsberg

An investigation of the colloidal-chemical properties of ferrocyanides [FTs] (Φ) of copper and other metals is of interest in connection with the solution of a number of problems, e.g., the separation of heavy metals by the method of froth flotation of FTs [1], the quantitative determination of metals through FTs complexes [2], obtaining osmotic semipermeable membranes and others.

It is known that the composition and properties of copper FTs considerably depend on the conditions of obtaining it [3], in particular on the composition of reacting salts and the ratio their concentrations. An investigation of the structurally-mechanical properties [4] showed that the anionic composition of the initial solution strongly affects the magnitude of resistance to shift by copper FTs ashes.

The physical properties of the obtained ashes and deposits, e.g., their color and dimensions of particles, also change depending upon the conditions of production, which is combined not only with structural parameters, but also with change in the composition of the obtained FTs. The composition of the solid phase obtained in a surplus of copper ions is close to pure copper FTs, whereas in a surplus of potassium ions mixed FTs of potassium and copper are obtained [5]. Between them can be a whole series of transition complex compounds, in many cases unstable and transient from one state to another. Process of formation of the solid phase is complicated by absorption of ions and molecules, which are in the solution.

All these circumstances, even at strict constancy of production conditions, lead to our not always attaining good reproducibility of properties of obtained deposits, inasmuch as it is impossible completely to control the ratio of reagents at the moment of formation of the solid phase.

There are also indications that the solid phase is not always uniform in composition and, possibly, consists of particles with different charge signs. Thus, negatively charged copper FTs adsorbs not only cations, but also anions [6] and coagulates under the effect of both cations and anions [7].

In spite of the complexity of composition and insufficient reproducibility, nevertheless we can trace the influence of production conditions on the properties of FTs. This work is undertaken to further investigate this connection, and namely, to study the electrokinetic properties of copper FTs. In works on measuring the ζ -potential of copper FTs by the method of electroosmosis [8] the production conditions were not considered. In a work [9] studying FTs membranes on a collodion basis it is established that the anionic composition of solution renders a considerable influence on the electrochemical activity of a diaphragm, characterized by a change in the ion migrations number.

In this work we investigate the magnitude of ζ -potential and surface conductivity of dried deposits of copper FTs depending upon production conditions.

The influence of composition and concentration of initial reagents on properties of an FTs deposit can be subdivided into:

1) the influence of a surplus of one of the two ions forming the solid phase, i.e., the potential-determining ions Cu^{2+} and $[\text{Fe}(\text{CN})_6]^{4-}$;

2) the influence of the copper salt anion, not entering into the regular¹ composition of the solid phase.

To study the influence of a surplus the deposits were prepared by different methods. A surplus of $[\text{Fe}(\text{CN})_6]^{4-}$ was attained by pouring a solution of copper salt into a solution of $\text{K}_4[\text{Fe}(\text{CN})_6]$ of equivalent (type A) or higher concentration (type AA). Deposition in surplus of Cu^{2+} was attained by changing the order of pouring (type B) and also by increasing the concentration of Cu^{2+} (type BB).

¹We did not exclude the possibility of it entering the solid phase in the form of some other inclusion.

To study the anion influence the following copper salts were selected: CuSO_4 , CuCl_2 , $\text{Cu}(\text{CH}_3\text{COO})_2$, and $\text{Cu}(\text{NO}_3)_2$. Deposits were obtained by pouring equal volumes of the solutions in the shown order with continuous mixing. After ripening of deposit for 10 hours, it was filtered on a Buchner funnel and washed to the absence of the surplus ions in the filtrate, after which it was dried at 70°C to a constant weight.

In a surplus of $[\text{Fe}(\text{CN})_6]^{4-}$ we frequently obtained highly dispersed suspensions, in such cases the dispersed phase was separated on a sharpless supercentrifuge.

The ζ -potential on dried deposits (powders) was measured in solutions of KCl , HCl , and CuCl_2 . In the first case we studied powders preliminarily treated by a 0.2 n solution of KCl (i.e., in K^+ form), and also untreated powders; the obtained data almost did not differ, inasmuch as deposition occurred in a medium rich in potassium ions. Measurements in HCl solutions were connected on powders preliminarily treated with a 0.05 n solution of HCl .

The ζ -potential was determined by the method of flux potential with correction for surface conductivity [10, 11] in a 0.001 n solutions, and also by the method of electrophoresis in 0.01 n solutions in the Chaykovskiy instrument.

The data obtained for different samples of one type differ from each other significantly more than for separate portions of one sample. An examples of

Table 1. Data of Parallel Measurements of ζ -Potential (Millivolt) in 0.01 n HCl (Electrophoresis)

| Type | Sample | Portion | | |
|------|--------|---------|-----|-----|
| | | 1 | 2 | 3 |
| A | I | -88 | -78 | -78 |
| | II | -88 | -82 | -88 |

reproducibility of data is given in Table 1.

The average (per sample) values of ζ -potential are given in Table 2 (electrophoresis) and Table 3 (flux potential). The pointer designates the order of

pouring. The title shows the initial copper salt.

A comparison of data in Tables 2 and 3, in spite of the difference in methods of measuring and insufficient reproducibility of samples, allows us to make the following conclusions:

1. The magnitude of ζ -potential increases with decrease of concentration of electrolyte from 0.01 n (Table 2) to 0.001 n (Table 3), i.e., the dependence of ζ on c has a normal character.

Table 2. Magnitude of ζ -Potential According to the Method of Electrophoresis in 0.01 N Solutions of KCl and HCl

| Type | Sample | Initial concentration eq/liter | | CuSO ₄ | | CuCl ₂ | |
|------|--------|--------------------------------|----------------|-------------------|------|-------------------|-------|
| | | Cl ⁻ | H ⁺ | KCl | HCl | KCl | HCl |
| AA | I | 0.2 | 0.2 | -4.0 | -7.2 | -0.4 | -0.5 |
| | II | 0.2 | 0.1 | -4.8 | -8.0 | -0.8 | -0.6 |
| A | I | 0.4 | 0.4 | -6.1 | -7.8 | - | - |
| | II | 0.4 | 0.4 | -7.5 | -6.8 | - | - |
| B | I | 0.4 | 0.4 | -0.7 | +0.4 | -11.8 | -11.5 |
| | II | 0.4 | 0.4 | -0.3 | -0.5 | -11.3 | -12.7 |
| BB | I | 0.4 | 0.2 | +3.0 | +1.0 | -0.3 | -0.3 |
| | II | 0.4 | 0.2 | +3.6 | +2.1 | - | - |

Table 3. Magnitude of ζ -Potential According to the Method of Flux Potential in 0.001 N Solutions of KCl and HCl (Concentration, the Same as in Table 2)

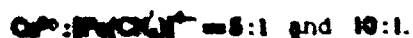
| Type | CuSO ₄ | | CuCl ₂ | | Cu(CH ₃ COO) ₂ | | Cu(NO ₃) ₂ | |
|------|-------------------|-------|-------------------|-------|--------------------------------------|------|-----------------------------------|-------|
| | KCl | HCl | KCl | HCl | KCl | HCl | KCl | HCl |
| AA | -0.4 | - | - | - | -3.7 | -7.8 | -14.9 | -10.2 |
| A | -0.8 | -7.0 | -4.8 | -3.0 | - | - | - | - |
| B | +0.8 | +0.5 | - | - | -0.5 | -0.3 | -10.8 | -10.5 |
| BB | +0.8 | +11.1 | +0.8 | +10.5 | -0.5 | -7.8 | -11.3 | -13.5 |

2. The values of ζ -potential in solutions of KCl and HCl differ little from each other. Thus, the durability of the bond of anions H⁺ and K⁺ with negatively charged surface is of one order, which is characteristic for ionites of the strong-acid type.

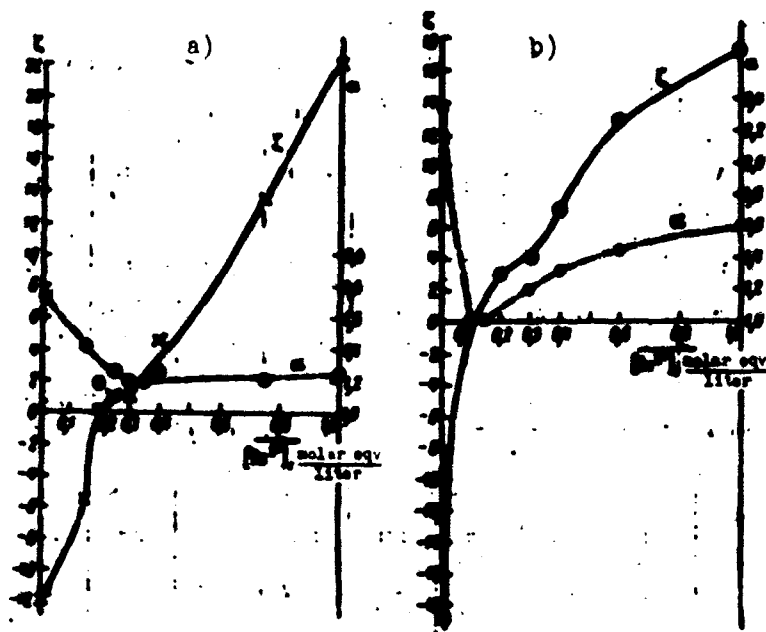
3. In a surplus of CuSO₄ and CuCl₂ positively charged powders are obtained. Till now we did not encounter indications of the existence of copper FTs with positive charge in the literature.

4. The influence of the copper salt anion is expressed so strongly that it suppresses the influence of a surplus of the potential-determining ion, Cu²⁺.

In accordance with point 4 the investigated powders can be divided into 2 groups. Deposits obtained from copper sulfate and chloride reveal a change in the sign of charge, in accordance with the Paneth-Fajans rule, whereas copper acetate and nitrate form negatively charged deposits with a stable magnitude of ζ -potential, almost independent of the ratio of concentrations of reacting ions. For a check we obtained deposits at a ratio



the ζ -potential of these powders remained negative and close to the values given in Table 3 for type BB.



Dependence of magnitudes ζ and α on concentration of Cu^{2+} for a powder obtained from CuSO_4 (a) and $\text{Cu}(\text{NO}_3)_2$ (b).

Thus, excess Cu^{2+} ions either are not adsorbed on these powders in general, or after adsorption they depart from the surface in process of washing, drying (the effect of $\text{O}_2 + \text{CO}_2$) or the influence of the electrolyte. To analyze these assumptions we conducted experiments on measuring ζ -potential in solutions of CuCl_2 .

For this different portions of one sample were processed (for several days) by solutions of $\text{CuCl}_2 + \text{KCl}$ taken in various ratios, but at identical total concentration (1 molar eqv/liter). The data on ζ -potential (flux potential) and surface conductivity in these solutions are shown in the figure for powders of the AA type obtained from sulfate (a) and nitrate of copper (b).¹

An analysis of curves ζ -c shows that a change of charge sign, and consequently also of Cu^{2+} ions adsorption occurs for the powder obtained from nitrate, just as for the sulfate. Thus, the difference of properties noted above is apparently caused by the smaller stability of the Cu^{2+} ion on surface of deposits obtained from nitrate and acetate.

¹Analogous curves were also obtained for copper acetate.

The character of ζ -c curves is like curves obtained for typical ionic crystals, e.g., BaSO_4 and AgI [10].

On curves of the dependence of coefficient of effectiveness [11] on c is observed minimum in region of the isoelectrical point. For powders obtained from $\text{Cu}(\text{NO}_3)_2$ the surface conductivity $\kappa_s = (\alpha - 1)\kappa_v$ disappears completely at this point ($\alpha = 1, \kappa_s = 0$) analogous to that revealed in experiments with adsorption of organic ions [12]. However, for powders obtained from CuSO_4 the surface conductivity does not disappear ($\alpha > 1$). Apparently, this testifies to heterogeneity of the powder; in other words, at the isoelectrical point part of the particles (or sections of the surface) possesses negative ζ -potential and part positive, and only the total effect gives $\zeta = 0$. Thus, the data on surface conductivity are also revealed influence of production conditions on the properties of FTs.

The conducted investigation shows that the influence of an anion of the initial copper salt is not limited by the degree of dispersiveness or structure of the deposit, but changes the nature of surface layer, since powders obtained in a Cu^{2+} surplus (types B and BB) are distinguished not only in magnitude, but also in sign of ζ -potential.

Conclusions

1. Copper ferrocyanide powders obtained in $\text{K}_4[\text{Fe}(\text{CN})_6]$ surplus are negatively charged in solutions of KCl and HCl .
2. The charge of powders obtained in a Cu^{2+} surplus depends on the anion of the initial copper salt. From CuSO_4 and CuCl_2 positively, and from $\text{Cu}(\text{NO}_3)_2$ and $\text{Cu}(\text{CH}_3\text{COO})_2$ negatively charged powders are obtained.
3. In solutions of CuCl_2 all the powders studied are charged positively.
4. Surface conductivity attains a minimum at the isoelectrical point.

Summary

The charge of precipitates measured in KCl and HCl solutions depends on the anionic nature of copper salt employed for precipitation. The precipitates formed under the conditions of the excess of copper ions are positively charged in the case of copper sulphate and copper chloride. In other investigated cases the charge is negative.

In CuCl_2 solutions all precipitates acquire positive charge. Surface conductance has a minimum and in some cases reaches zero at the isoelectrical point. (English summary)

Literature

1. L. D. Skrylev and S. G. Mokrushin. Koll. zh., 22, No. 3, 134, 1960; V. I. Borisikhina, L. D. Skrylev and S. G. Mokrushin. Koll. zh., 23, No. 6, 669, 1961.

2. N. A. Tananayev, T. A. Glushkova, and G. B. Seyfer. *ZhNKh*, 1, No. 1, 66, 1956.
3. I. Duclaux. *Colloids et gels*. Paris, 1953; H. A. Tananayev and M. M. Levina. *ZhAKh*, 1, No. 4, 224, 1946.
4. I. F. Karpova and T. P. Spasibenko. *Herald of LGU*, No. 16, 126, 1958.
5. V. Freise. *Zs. Elektrochem.*, 55, No. 1, 511, 1951; *Zs. phys. Chem. Neue Folge*, 15, 48, 1958; K. F. Bonhöffer. *Parkas Memor. Vol. Jerusalem*, 219, 1952.
6. A. T. Austin, E. I. Hartung, and G. M. Willis. *Trans. Faraday soc.*, 40, 520, 1944; I. D. Tolliday, E. F. Woods, and E. I. Hartung. *Trans. Faraday soc.*, 45, 149, 1949.
7. K. C. Sen. *J. Phys. chem.*, 29, 517, 1925; M. Frankert and J. Wilkinson. *J. phys. chem.*, 28, 651, 1924.
8. N. Hayash. *Koll. Zs.*, 39, 208, 1926.
9. I. F. Karpova and A. N. Dolzhenkov. *Herald of LGU*, No. 16, 1957.
10. G. R. Kroyt. *Science about colloids*. Moscow, IL., 1, 1955.
11. O. N. Grigorov, Z. P. Koz'mina, A. V. Markovich and D. A. Fridrikhsberg. *Electrokinetic properties of capillary systems (monograph collection)*, Press of Academy of Sciences of USSR, 169, 1956.
12. D. A. Fridrikhsberg, N. G. Gerasimova, and L. P. Popkova. *Koll. zh.*, 22, No. 4, 489, 1960.

Submitted
10 December 1962

SEPARATING AND IDENTIFYING REACTION PRODUCTS OF DEEP SPLITTING
OF GERMANIUM BY FAST PROTONS¹

A. N. Murin, S. B. Tomilov, and I. A. Yutlandov

One of the basic peculiarities of the reaction of deep splitting is wide distribution of products in A and Z. Therefore, in an investigation of similar processes one encounters very complicated mixed radio elements. As a rule, several radioactive isotopes will be formed for each element, which substantially hampers their identification and control of radiochemical cleanness.

In most published works to separate the reaction products of deep splitting the method of isotopic carriers was used; its only condition of applicability is the presence of full and sufficiently fast exchange of the isotopic carrier between radioactive atoms and stable atoms. A deficiency of this method is the duration and presence of great quantities of carriers.

To separate the reaction products of deep splitting of germanium we applied the method of ion-exchange chromatography. This method is sufficiently fast and allows us to obtain carrier-free radioactive preparations, which in a number of cases is very significant. We separate radioactive isotopes of following elements: As, Ga, Zn, Cu, Ni, Co, Fe, Mn, Cr, V, Ti, Sc, and K.

Ion-exchange separation of certain combinations of groups of elements of interest to us is described in works [1-10]. The chromatographic columns and technology of separation we used do not differ from those offered by B. K. Preobrazhenskiy to separate carrier-free radioactive elements [8].

¹Work was accomplished in 1959.

Experimental Part

A target $8 \times 8 \times 1 \text{ mm}^3$ was prepared from metallic germanium of brand ["GD"] ("ГД"). Irradiation was produced on an internal bundle of a [OIVaI] (OIVaI) Joint Institute for Nuclear Research synchrocyclotron by protons with energy of 660 Mev for 15-30 minutes. Separation of the products of splitting germanium was executed on Dowex-1 x 10-12 anionite (or [AV-17] (AB-17)) and Dowex-50 x 8 cationite (or [KU-2] (KV-2)). The dimensions of resin grains is $\sim 10 \mu$. The columns had a cross section of 0.04 cm^2 and height of resin pole of 6-9 cm. The free volume of the column was 3-4 drops. The eluant was distilled hydrochloric acid of different concentration, passed through the column with a speed of approximately one drop per minute. The drops gathered on the polyethylene bases and were dried, after which their activity was measured.

Separation was conducted in the following way. The irradiated target was dissolved in aqua regia. Quadruple distillation by boiling the solution with concentrated hydrochloric acid ensured full distillation of germanium tetrachloride [11-15]. The fullness of distillation was controlled by a colored reaction with phenyl fluorone [16]. The germanium tetrachloride was gathered in ice water. The acidity of the obtained solution was brought to 6 N on H_2SO_4 , after which germanium was precipitated in the form of a sulfide by hydrogen sulfide.

In experiments, which yielded arsenic during distillation of germanium tetrachloride a small concentration of HNO_3 was supported in the solution to hold the arsenic in a pentavalent state. Presence of nitric acid in the solution does not affect the quality of separation. After distilling the germanium tetrachloride the solution was steamed to minimum volume, cooled, saturated by gaseous hydrogen chloride and applied on column with anionite in the Cl^{-2} form. The walls of the column were washed several times with concentrated HCl, after which elutriation with hydrochloric acid, whose concentration was changed in process of separation as shown on diagram 1, started. As can be seen from the diagram, during the first transmission of initial mixture through anionite fractions of Ti, Co, Cu, and Zn quantitatively separate.

For good separation of Cu and Co it is necessary to apply column not less than 9 cm long. The groups of elements, Cr, Ni, V, and K and Mn, Sc, and As emerge from the column at 12 N HCl in pairs, not quite clearly divided, with peaks. The activity of intermediate drops is caused by isotopes of vanadium. Therefore it is

Diagram 1

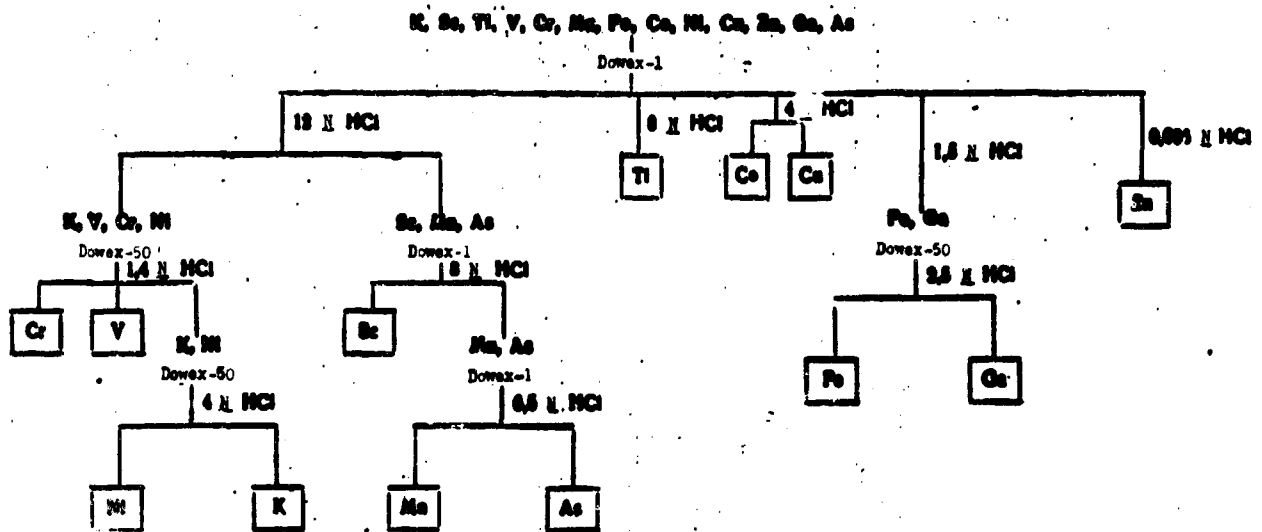
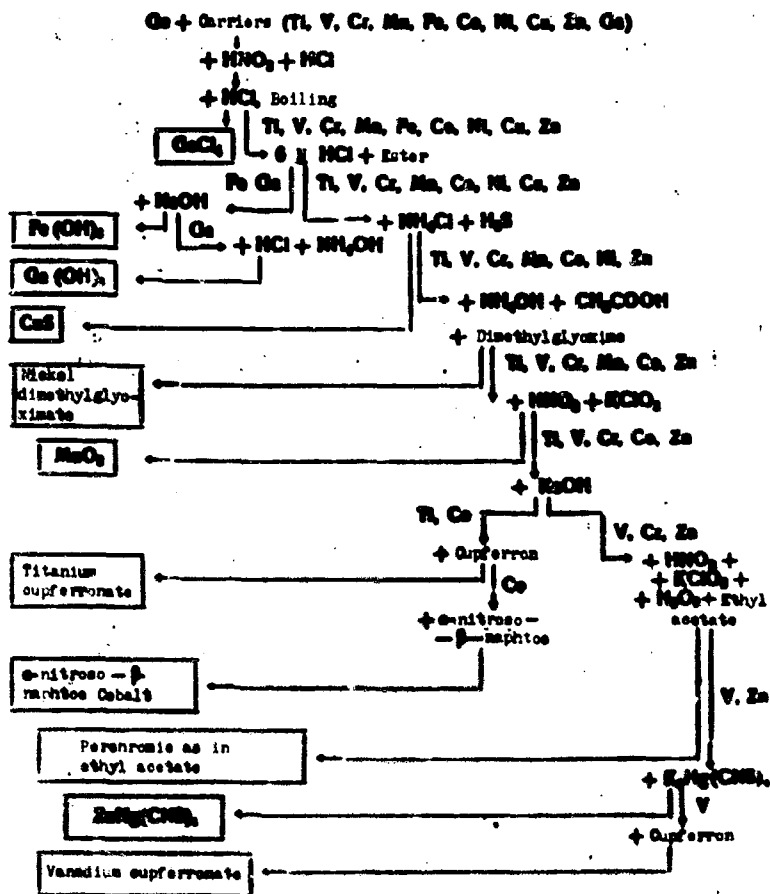


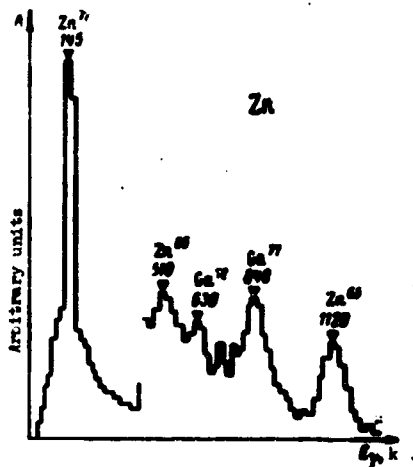
Diagram 2



necessary to purify the group of elements Mn, Sc and As from impurities of V by repeated transmission through anionite in the same conditions. Separation of Cr, Ni, V, and K was produced on cationite. For this the gathered drops were steamed, dissolved in two drops of 1 N HCl and applied on column with Dowex-50. Further there are two possible variants of separation: a) during transmission through the column of 1 N HCl chromium emerges already in the first free volume. After transmission of 10 free volumes of 1 N HCl the concentration of the acid was increased to 1.5 N. With this V and K quantitatively were separated from Ni not separated from each other; b) if elutriation is started with 1.5 N HCl, Cr and V manage to quantitatively divide. The separation of Ni and K, although not fully quantitative, can be carried out on cationite with the help of 4 N HCl. The activity of the intermediate drops in this case is caused by isotopes of Ni.

| Element | Mass number of isotope | Tabular values [32] | | Experimental values | |
|---------|------------------------|---------------------|--------------------------------------|---------------------|--------------------------------------|
| | | Period of half-life | Energy of the most intense lines kev | Period of half-life | Energy of the most intense lines kev |
| V | 51 | 12.5 hr | 1870 | — | 1500 |
| | 52 | 22.4 hr | 371, 614 | 22 hr | 370, 615 |
| Cr | 52 | 2.5 days | 270 | 2.5 days | 273 |
| | 53 | 2.0 hr | 1200 | — | 810, 1145 |
| Ni | 60 | 6.0 days | 820, 1100 | — | 820, 1120 |
| | 63 | 2.0 days | 100 | 2.5 days | 100 |
| Zn | 65 | 4.0 hr | 920, 1000, 1200 | 4.0 hr | 1000, 1300 |
| | 66 | 2.1 hr | 300 | 2.2 hr | 310 |
| Mn | 54 | 15 days | 920, 1214 | 15.4 days | 810, 920, 1315 |
| | 55 | 26 hr | 110, 240 | 22 hr | 110, 310 |
| Fe | 59 | 27.3 days | 320 | — | 320 |
| | 57 | 4.7 days | 720, 940, 1400 | 6 hr | 510, 720, 940, 1400 |
| Co | 60 | 5.3 hr | 167 | 5.2 days | 510, 1000 |
| | 60 | 5.3 days | 100, 1000, 1200 | — | 100, 1100, 1700 |
| Cu | 64 | 12.8 hr | 477, 910 | 12.7 hr | 510, 900 |
| | 65 | 77.3 days | 840, 1200 | — | 840, 1200 |
| Zn | 68 | 29.1 days | 120 | — | 120 |
| | 70 | 71.3 days | 300 | — | 300, 315 |
| Ga | 71 | 130 min | 72 | 25 min | 72 |
| | 72 | 17.2 days | 170, 200 | 7 days | 100, 200 |
| Ge | 73 | 12.5 hr | 120, 1370 | 37 hr | 240, 120, 1300 |
| | 74 | hr | None | 30 hr | None |
| As | 75 | hr | 70, 200, 300 | 2.5 hr | 510, 70, 200, 300 |
| | 76 | hr | None | 12.5 hr | None |
| Se | 78 | hr | 20, 100 | 20 hr | 20, 100 |
| | 79 | hr | 40, 70, 200 | 10 hr | 40 |
| Br | 80 | 15.1 days | 120 | — | 120 |
| | 81 | 115 hr | 40 | 14.2 hr | 40 |
| Kr | 81 | hr | None | 40 hr | 100 |
| | 82 | 100 hr | 100 | 10 hr | 210, 1000 |
| Rb | 85 | 47.3 days | 92, 100, 200, 300 | 40 hr | 90, 100, 200, 300 |
| | 87 | 48.8 hr | 120 | 14 hr | 120, 170 |
| Sr | 89 | 50.5 hr | 120 | 21 hr | 120, 170 |
| | 90 | 28.1 hr | 120 | 21 hr | 120, 170 |

Fe and Ga, outgoing from anionite in one peak, can be quantitatively separated into cationite with the help of 2.5 N HCl. Mn, Sc and As are divided into anionite.



γ -spectrum of zinc fraction.

During elutriation with 8 N HCl not fully quantitative separation of Sc from Mn and As occurs. Mn and As are quantitatively separated with the help of 6.5 N HCl.

To identify the separated isotopes and check their radiochemical cleanness their half-life was measured on a [B-2] (B-2) instrument supplied with an end-window counter of the [MST-17] (MCT-17) type and their γ -spectra were measured on a scintillation γ -spectrometer with a NaI (Tl) crystal and [AMA-3a] (AMA-3c) multichannel analyzer. The half-life was determined in this case by the decrease in intensity of characteristic γ -lines. However, the complexity of isotope composition of separated fractions frequently made deciphering the γ -spectra very difficult. To avoid possible errors, on the basis [12, 13, 14, 17-31] a diagram of separating the products of splitting germanium by the method of isotopic carriers (see diagram 2¹) was developed. The coincidence of γ -spectra of fractions of one and the same element separated by two different methods and simultaneous coincidence of the obtained data with tabular are convincing proof of the radiochemical cleanness of preparations. The table gives the isotopes identified by us. All preparations, except for chromatographically separated Fe containing an unidentified impurity, were radiochemically pure. In the γ -spectrum of Zn fractions (separated by both the method of isotopic carriers and also chromatographically) a previously unknown γ -line was revealed with energy of 145 keV (figure) disintegrating with half-life of ~49 hours, which was ascribed by us to the Zn⁷² isotope.

In conclusion authors express their deep gratitude to V. N. Pokrovskiy and I. Yu. Levenberg, with whose direct participation the γ -spectrometric part of the work was accomplished.

Conclusions

1. From a germanium target irradiated by protons with energy of 660 MeV

¹Fractions of As, Sc and K did not separate and were not investigated by this method.

we separated 13 fractions of elements, in which 34 radioactive isotopes were identified (see table).

2. A diagram of separation of these elements by the method of ion-exchange chromatography was developed.

3. In the γ -spectrum of Zn^{72} a new γ -line was revealed with energy of 145 kev (see table and figure).

Summary

A gallium target was irradiated with 600 Mev protons. The spallation products were separated by ion-exchange chromatographic methods. Identification of isotopes and check of radiochemical purity of separated fractions was carried out by means of a gamma-spectrometer. A 145 keV γ -line found out in the zinc fraction was ascribed to Zn^{72} . [English summary]

Literature

1. S. Sweet and W. Rieman. J. Benken Kamp. anal. chem., 24, 952, 1952.
2. G. M. Kolosova and M. M. Senyavin. Abstract of reports at First All-Union Conference on Organic Reagents. Moscow, Press of Academy of Sciences, USSR, 27, 1956.
3. M. M. Senyavin, G. M. Kolesova, and V. A. Nikashina. ZhNKh, 3 No. 104, 1958.
4. K. Kraus and G. Moore. J. Amer. chem. soc., 75, 1460, 1953.
5. K. Kraus, F. Nelson, and G. Smith. J. Phys. chem., 58, 11, 1954.
6. A. K. Lavrukhina, L. D. Krasavina, and A. A. Pozdiyakov. DAN SSSR, 119, No. 1, 56, 1958.
7. G. Moore and K. Kraus. J. Amer. chem. soc., 74, 843, 1952.
8. B. K. Preobrazhenskiy. ZhNKh, 3, No. 1, 119, 1958.
9. B. K. Preobrazhenskiy, V. P. Tsvelekhovskiy, and V. N. Mel'hikov. Radiochemistry, 2, 73, 1960.
10. K. Kraus, D. Michelson, and F. Nelson. J. Amer. chem. soc., 81, 3204, 1958.
11. S. G. Rudstam. Phil. mag., 46, 344, 1955.
12. Radiochemical studies: Fission products, 3. N.Y., 1951.
13. R. E. Batzel, D. K. Miller, and G. T. Seaborg. Phys. rev., 84, 671, 1951.
14. I. P. Alimarin, Yu. V. Yakovlev, and A. I. Zhabin. Collection: "Application of labeled atoms in analytic chemistry," Moscow, Press of Academy of Sciences of USSR, 58, 1955.
15. A. N. Murin, V. D. Nefedov, and I. A. Yutlandov. Successes of chemistry, XXIV No. 5, 159, 1955.
16. A. I. Busev and N. G. Polyanskiy. Collection: "Application of organic reagents in inorganic analysis," Moscow, Press of Academy of Sciences of USSR, 51, 1958.
17. S. G. Rudstam. Spallation of medium weight elements. Uppsala, 1956.

18. L. Marquez. Phys. rev., 92, 1511, 1953.
19. I. W. Meadows. Phys. rev., 91, 885, 1954.
20. F. P. Bartell, A. C. Helmholtz, S. D. Softky, and D. B. Stewart. Phys. rev., 80, 1006, 1950.
21. N. A. Perfilov and V. A. Ostroumov. DAN SSSR, 103, No. 2, 1955.
22. B. V. Kurchatov, V. N. Mekhedov, N. I. Borisova, M. Ya. Kuznetsova, L. N. Kurchatova, and A. V. Chistyakov. Transactions of Session of Academy of Sciences of USSR, 1-5 July, 1955, p. 178.
23. A. N. Murin and I. A. Yutlandov. Press of Academy of Sciences, USSR, OKhN, No. 4, 408, 1957.
24. A. Turkevich and N. Sugarman. Phys. rev., 94, 728, 1954.
25. R. I. Dels, J. T. Eisinger, A. W. Faishall, I. Halpern, and H. G. Richer. Phys. rev., 97, 1325, 1955.
26. A. K. Babko and F. G. Zharkovskiy. Zav. lab. No. 1, XXV, 42, 1959.
27. P. Reasheck and I. E. Warren. J. Inov. nucl. chem., 7, 343, 1958.
28. G. Wagner and E. O. Wiig. J. Amer. chem. soc., 74, 1101, 1952.
29. L. Marquez. Phys. rev., 88, 225, 1952.
30. S. G. Rudstam, P. C. Stevenson, and R. L. Folger. Phys. rev., 87, 358, 1952.
31. R. E. Botzel and G. T. Seahorg. Phys. rev., 82, 607, 1951.
32. D. Ströminger, J. M. Hollander, and G. T. Seahorg. Rev. mod. phys., 30, No. 2, IV, 1958.

Submitted
5 March 1960

THERMODYNAMIC INVESTIGATION OF SOLID SOLUTIONS IN A
NaCl - KCl - CdCl₂ SYSTEM AT TEMPERATURES
OF 540, 580, 623°C

M. M. Shul'ts and I. M. Bushueva

III. Thermodynamic Properties of Solid Solutions¹

In the system we investigated as shown in [1], three-component solid solutions, NaCl - KCl - CdCl₂ are formed; at a temperature ~600°C they endure stratification, forming two fields of crystallization of solid solutions: α and β (see Fig. 1 of

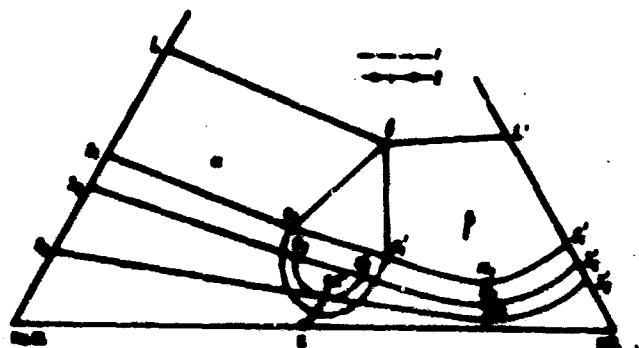


Fig. 1. Diagram of soliduses and fields of crystallization of solid solutions. LBL' is the length of liquidus curve at 540°C; K' is the critical temperature of stratification of triple solid solutions (~600°C); K is the critical temperature of binary solid solutions (502°C); 1 are binodals of two-phase equilibrium of solid solutions; 2 is the critical curve.

equilibrium analysis: melt - solid solution. On the basis of experimentally

this article).

The aim of this work is to obtain the thermodynamic characteristics of these solid solutions in the temperature interval of 540-623°C (i.e., lower and higher than the critical temperature of stratification). To solve this problem we used the method of the third component [2], proposing not a direct study of solid solutions, but an isothermal

¹I and II were published in the Herald of LGU, No. 22, 1963.

obtained compositions of equilibrium phases and activity of one of the components in the melt (third component, in given system, CdCl_2) we calculated the activity of components of solid solutions. All experimental results necessary for calculation by this methods are given in our preceding works [1, 3]. Because of the specific character of the applied method we could obtain data only for solid solutions whose composition corresponds to isotherms of the surface of solidus line. Isotherms of solidus line are represented in Fig. 1; curves $S_1 - S_1'$ (540°), $S_2 - S_2'$ (580°), $S_3 - S_3'$ (623°). Before discussing the thermodynamic properties of solid solutions it is expedient to describe certain peculiarities of the slope of curves of solidus line. As can be noted, all investigated solid solutions contain comparatively little cadmium chloride (≤ 5 molar %); therefore the solidus lines incline to the $\text{NaCl} - \text{KCl}$ side. The maximum content of cadmium chloride was apportioned to $\text{NaCl} - \text{CdCl}_2$ solid solutions, i.e., the ends of the curves of solidus line rise toward $\text{NaCl} - \text{CdCl}_2$ (points S_1 , S_2 and S_3 correspond to 3.2; 2.6; 2.3 molar % of CdCl_2 respectively). All curves are curved towards $\text{NaCl} - \text{KCl}$; i.e., the molar share of CdCl_2 on them passes through a minimum (points m_1 , m_2 , and m_3). At 540 and 580° a break in miscibility of components of solid solutions is observed (sections $a_1 - a_1'$, $a_2 - a_2'$ on curves $S_1 - S_1'$, $S_2 - S_2'$ respectively). It is necessary to indicate that the break in miscibility of components of triple solid solutions, in spite of the minute content of CdCl_2 in these solutions, is observed considerably higher than for binary solid solutions of $\text{NaCl} - \text{KCl}$. For triple solid solutions the critical temperature is $\sim 600^\circ\text{C}$; for binary it is 502°C [9].

Thus, upon introduction of comparatively small additions of CdCl_2 in solid solutions of $\text{NaCl} - \text{KCl}$ the temperature of the start of disintegration of solid solutions is increased by approximately 100°C , which can testify to a considerable change in the thermodynamic properties during formation of three-component solutions. This is confirmed by the thermodynamic data given below.

The activities of components of solid solutions were calculated according to the following formulas:

$$\begin{aligned}
 & \left[\frac{a_1}{a_1'} \right] = \frac{a_1}{a_1'} \quad (1) \\
 & \left[\frac{a_2}{a_2'} \right] = \frac{a_2}{a_2'} \quad (2)
 \end{aligned}$$

where $x_1^{(k)}$ are molar shares; $a_1^{(k)}$ is activity of components (sub 1 designates: 1 - NaCl; 2 - KCl; 3 - CdCl₂; super (k) marks the phase; 1 - solid solution; 2 - melt).

In calculating the activities of components of solid solutions, and also other thermodynamic functions (ΔG_{sup} , ΔS_{sup} , ΔH_{sup}) as standard (or initial) states pure solid substances of NaCl, KCl and CdCl₂ were accepted at temperatures of 540, 580 and 623°C. Equations (1) and (2) were integrated from values of variables for binary systems of NaCl - CdCl₂ (during calculation of $a_1^{(1)}$) or KCl - CdCl₂ (for calculation of $a_2^{(1)}$) to values of variables corresponding to a three-component system. In equations (1) and (2) on the left in the denominator the asterisks designate activity of NaCl ($a_1^{(1)*}$) and KCl ($a_2^{(1)*}$) relative to the solid phases, which are in equilibrium with binary melt NaCl - CdCl₂ and KCl - CdCl₂. However, from binary saturated melts NaCl - CdCl₂ and KCl - CdCl₂ not their pure components NaCl and KCl, but their solid solutions with CdCl₂ including comparatively small quantities of the latter, crystallize. Therefore in calculating the activities $a_1^{(1)*}$ and $a_2^{(1)*}$ could not be equated to unity as in other cases of application of the method of the third component [4, 5], but with sufficient accuracy could be accepted by equal to molar shares of NaCl and KCl in the appropriate binary solid solutions, being in equilibrium with binary melts ($a_1^{(1)*} = x_1^{(1)*}$ and $a_2^{(1)*} = x_2^{(1)*}$). With the above-indicated selection of the standard state, pure solid substances, further thermodynamic calculation for components NaCl and KCl did not cause difficulties, since at the shown test temperatures these substances are solids. Calculating the activities of CdCl₂ with analogous selection of standard state was rather difficult, since at the test temperatures of 580 and 623°C this component is liquid ($t_{melt} \text{ CdCl}_2 = 568^\circ\text{C}$). At a temperature of 540°C, lying lower than temperature of fusion of cadmium chloride cadmium, it is possible to directly take as the standard state for CdCl₂ pure solid CdCl₂ for both the liquid and also the solid solution. In this case according to the obtained values of emf of the element



the activity of CdCl₂ in liquid and solid phases can be calculated by the equation

$$\ln a_3^{(1)} - \ln a_3^{(2)} = \frac{E - E_0}{RT} \quad (3)$$

where E_0 is the emf of the element containing a melt as electrolyte in equilibrium with pure solid cadmium chloride; E pertains to any melt including the melt in

equilibrium with the solid solution [3]. At temperatures of 580 and 623°C E_0 in equation (3) pertains to pure liquid CdCl_2 ; therefore at these temperatures a correction was introduced in values of CdCl_2 activity to obtain data pertaining to the selected standard state, solid CdCl_2 at 580° and 623° (hypothetical state). This correction, which was considered as the difference of chemical potentials of solid and liquid CdCl_2 at the appropriate temperatures, was calculated by the equation

$$\Delta \ln a^0 = \frac{\Delta \mu^0}{RT} = \frac{\mu_{\text{liq}}^0 - \mu_{\text{sol}}^0}{RT} = -\frac{1}{RT} \int_{T_m}^T \Delta S^0 dT. \quad (4)$$

where ΔS^0 is the difference of entropy of CdCl_2 in liquid and solid states, which does not very sharply change with temperature, therefore we took its constant and equal value, corresponding to the temperature of fusion [6]

$$\Delta S_{\text{m}}^0 = \frac{3000 \text{ cal}}{T_{\text{m}}}.$$

With this approximation the correction $\Delta \mu_3^0$ at temperatures of 580 and 623°C is -76 and -347 cal respectively.

The values of activities calculated by formulas (1)-(4) and corresponding coefficients of activities $\left(\gamma_i^0 = \frac{a_i^0}{x_i^0}\right)$ for different temperatures are represented in Tables 1 (540°C); 2 (580°C); 3 (623°C) and the activities of all three components as a function of the composition of the solid solution $\frac{x_i^0}{x_1^0 + x_2^0}$ are shown in Fig. 2. The components NaCl and KCl, as can be seen on the figure, reveal positive deflections from the ideal at all temperatures. On the activity curves at 540 and 580° regions of break in miscibility of components of solid solutions (dotted lines) are visible. At 623°C the activity curves of all components have a continuous slope, but reveal an evident tendency to form a horizontal site, corresponding to an approach to the critical state. In general, for a three-component system the appearance of horizontal tangent to the activity curve of a given component at approach to the critical point is observed in the section corresponding to a constant ratio of molar fractions of the other two components

$$\left(\frac{\partial a_i^0}{\partial x_j^0}\right)_{x_k} \rightarrow 0 \quad \text{and} \quad \left(\frac{\partial a_j^0}{\partial x_i^0}\right)_{x_k} \rightarrow 0 \quad (5)$$

Table 1

| $a_1^{(1)}$ | $a_2^{(1)}$ | $a_3^{(1)}$ | $a_4^{(1)}$ | $A_1^{(1)}$ | $a_2^{(2)}$ | $A_2^{(1)}$ | $a_3^{(2)}$ | $A_3^{(1)}$ | $-a_{cap}$ | a_{cap} |
|-------------|-------------|-------------|-------------|-------------|-------------|-------------|-------------|-------------|------------|-----------|
| 0.952 | 0.000 | 0.032 | 0.968 | 1.00 | 0.000 | — | 0.12470 | 3.897 | 187 | 70 |
| 0.970 | — | 0.030 | 0.978 | — | — | — | 0.00860 | 2.87 | 148 | 67 |
| 0.968 | 0.002 | 0.030 | 0.987 | 1.02 | 0.034 | 19.0 | 0.00595 | 1.98 | 168 | 73 |
| 0.950 | 0.023 | 0.030 | 0.991 | 1.044 | 0.101 | 4.38 | 0.03554 | 1.32 | 244 | 133 |
| 0.944 | 0.050 | 0.030 | 0.986 | 1.045 | 0.170 | 5.66 | 0.02317 | 0.89 | 265 | 146 |
| 0.936 | 0.038 | 0.034 | 0.984 | 1.05 | 0.184 | 4.85 | 0.02127 | 0.80 | 277 | 167 |
| 0.916 | 0.065 | 0.032 | 0.975 | 1.065 | 0.252 | 4.00 | 0.01468 | 0.70 | 320 | 222 |
| 0.905 | 0.076 | 0.019 | 0.979 | 1.08 | 0.343 | 4.52 | 0.00930 | 0.44 | 338 | 248 |
| 0.887 | 0.097 | 0.016 | 0.955 | 1.08 | 0.355 | 3.66 | 0.00879 | 0.55 | 350 | 296 |
| 0.813 | 0.179 | 0.008 | 0.945 | 1.15 | 0.415 | 2.32 | 0.00661 | 0.82 | 400 | 423 |
| 0.704 | 0.288 | 0.004 | 0.882 | 1.35 | 0.505 | 1.75 | 0.00443 | 0.55 | 530 | 505 |
| 0.615 | 0.378 | 0.002 | 0.820 | 1.35 | 0.572 | 1.51 | 0.00343 | 0.57 | 582 | 544 |
| 0.273 | 0.725 | 0.002 | 0.820 | 3.04 | 0.572 | 0.79 | 0.00343 | 1.71 | 754 | 318 |
| 0.237 | 0.772 | 0.001 | 0.822 | 2.12 | 0.690 | 0.80 | 0.00384 | 3.84 | 738 | 132 |
| 0.178 | 0.840 | 0.002 | 0.847 | 1.39 | 0.834 | 1.02 | 0.00413 | 2.21 | 658 | 123 |
| 0.120 | 0.876 | 0.001 | 0.151 | 1.26 | 0.926 | 1.05 | 0.00497 | 1.24 | 594 | 128 |
| 0.062 | 0.934 | 0.001 | 0.082 | 1.34 | 0.982 | 1.08 | 0.00573 | 1.43 | 300 | 119 |
| 0.017 | 0.977 | 0.000 | 0.017 | 4.57 | 0.990 | 1.01 | 0.00582 | 0.98 | 136 | 55 |
| 0.000 | 0.993 | 0.007 | — | — | 0.993 | 1.00 | 0.00624 | 0.80 | 68 | — |

Table 2

| $a_1^{(1)}$ | $a_2^{(1)}$ | $a_3^{(1)}$ | $a_4^{(1)}$ | $A_1^{(1)}$ | $a_2^{(2)}$ | $A_2^{(1)}$ | $a_3^{(2)}$ | $A_3^{(1)}$ | $-a_{cap}$ | a_{cap} |
|-------------|-------------|-------------|-------------|-------------|-------------|-------------|-------------|-------------|------------|-----------|
| 0.974 | 0.000 | 0.025 | 0.974 | 1.00 | — | — | 0.14620 | 5.62 | 128 | 76 |
| 0.974 | — | 0.025 | 0.980 | 1.01 | — | — | 0.10250 | 3.94 | 133 | 80 |
| 0.976 | — | 0.024 | 0.994 | 1.02 | — | — | 0.07860 | 3.17 | 114 | 77 |
| 0.954 | 0.013 | 0.025 | 1.005 | 1.04 | 0.115 | 8.85 | 0.04420 | 1.91 | 161 | 141 |
| 0.955 | 0.025 | 0.020 | 1.000 | 1.06 | 0.195 | 7.72 | 0.02430 | 1.21 | 180 | 182 |
| 0.944 | 0.055 | 0.013 | 1.008 | 1.07 | 0.257 | 6.77 | 0.01580 | 0.88 | 200 | 224 |
| 0.917 | 0.070 | 0.013 | 1.004 | 1.09 | 0.293 | 4.19 | 0.01270 | 0.90 | 235 | 310 |
| 0.843 | 0.149 | 0.008 | 0.983 | 1.17 | 0.353 | 2.41 | 0.00850 | 1.07 | 352 | 442 |
| 0.735 | 0.258 | 0.007 | 0.920 | 1.26 | 0.459 | 1.78 | 0.00810 | 1.16 | 488 | 545 |
| 0.691 | 0.303 | 0.007 | 0.909 | 1.32 | 0.487 | 1.61 | 0.00430 | 0.72 | 535 | 562 |
| 0.614 | 0.380 | 0.006 | 0.850 | 1.38 | 0.627 | 1.55 | 0.00230 | 0.39 | 530 | 650 |
| 0.506 | 0.691 | 0.002 | 0.850 | 2.78 | 0.627 | 0.91 | 0.00240 | 1.20 | 650 | 429 |
| 0.286 | 0.712 | 0.001 | 0.850 | 2.43 | 0.82 | 0.96 | 0.00240 | 1.20 | 657 | 382 |
| 0.240 | 0.759 | 0.001 | 0.847 | 2.03 | 0.775 | 1.02 | 0.00305 | 3.06 | 629 | 315 |
| 0.202 | 0.798 | 0.000 | 0.807 | 1.52 | 0.883 | 1.12 | 0.00000 | — | 572 | 296 |
| 0.160 | 0.845 | 0.001 | 0.807 | 1.42 | 0.943 | 1.12 | 0.00390 | 3.93 | 494 | 258 |
| 0.133 | 0.866 | 0.002 | 0.809 | 1.47 | 0.958 | 1.10 | 0.00380 | 1.90 | 448 | 229 |
| 0.044 | 0.972 | 0.000 | 0.133 | 3.48 | 0.960 | 1.03 | 0.00400 | 1.01 | 206 | 140 |
| 0.020 | 0.988 | 0.000 | 0.138 | 0.90 | 0.986 | 1.01 | 0.00400 | 1.01 | 127 | 82 |
| — | 0.998 | 0.000 | — | — | 0.988 | 0.99 | 0.00430 | 0.87 | 66 | 16 |
| 0.000 | 0.995 | 0.005 | — | — | 0.995 | 1.00 | 0.00599 | 1.20 | 82 | — |

Table 3

| $a_1^{(1)}$ | $a_2^{(1)}$ | $a_3^{(1)}$ | $a_4^{(1)}$ | $A_1^{(1)}$ | $a_2^{(2)}$ | $A_2^{(1)}$ | $a_3^{(2)}$ | $A_3^{(1)}$ | $-a_{cap}$ | a_{cap} |
|-------------|-------------|-------------|-------------|-------------|-------------|-------------|-------------|-------------|------------|-----------|
| 0.977 | 0.000 | 0.003 | 0.977 | 1.00 | — | — | 0.09370 | 4.07 | 137 | 57 |
| 0.977 | — | 0.003 | 0.985 | 1.01 | — | — | 0.0630 | 2.75 | 159 | 56 |
| 0.975 | 0.002 | 0.022 | 0.993 | 1.02 | 0.068 | 34 | 0.04080 | 1.77 | 153 | 68 |
| 0.973 | 0.006 | 0.022 | 1.001 | 1.03 | 0.110 | 24.0 | 0.02740 | 1.25 | 158 | 86 |
| 0.970 | 0.010 | 0.020 | 1.013 | 1.04 | 0.250 | 25.0 | 0.01240 | 0.62 | 150 | 148 |
| 0.958 | 0.025 | 0.017 | 1.016 | 1.06 | 0.273 | 10.9 | 0.01330 | 0.78 | 168 | 117 |
| 0.901 | 0.040 | 0.009 | 0.976 | 1.08 | 0.608 | 6.8 | 0.00180 | 0.20 | 219 | 454 |
| 0.775 | 0.020 | 0.006 | 0.978 | 1.25 | 0.623 | 2.83 | 0.00160 | 0.32 | 267 | 724 |
| 0.673 | 0.324 | 0.003 | 0.940 | 1.37 | 0.723 | 2.23 | 0.00110 | 0.37 | 314 | 843 |
| 0.572 | 0.445 | 0.003 | 0.880 | 1.55 | 0.770 | 1.81 | 0.00097 | 0.32 | 357 | 890 |
| 0.444 | 0.554 | 0.002 | 0.872 | 1.96 | 0.780 | 1.41 | 0.00093 | 0.46 | 378 | 873 |
| 0.413 | 0.585 | 0.002 | 0.865 | 2.09 | 0.795 | 1.36 | 0.00093 | 0.46 | 370 | 865 |
| 0.339 | 0.659 | 0.002 | 0.860 | 2.54 | 0.838 | 1.27 | 0.00093 | 0.46 | 323 | 846 |
| 0.291 | 0.705 | 0.001 | 0.810 | 2.76 | 0.862 | 1.22 | 0.00104 | 1.04 | 308 | 780 |
| 0.215 | 0.785 | 0.000 | 0.714 | 3.27 | 0.906 | 1.16 | 0.00060 | — | 272 | 661 |
| 0.172 | 0.827 | 0.001 | 0.95 | 3.16 | 0.942 | 1.14 | 0.00161 | 1.63 | 267 | 572 |
| 0.114 | 0.884 | 0.002 | 0.512 | 4.67 | 0.902 | 1.08 | 0.00183 | 0.91 | 216 | 441 |
| 0.077 | 0.920 | 0.003 | 0.430 | 5.59 | 0.980 | 1.07 | 0.00226 | 0.75 | 182 | 347 |
| 0.020 | 0.968 | 0.002 | 0.369 | 12.73 | 0.988 | 1.02 | 0.00262 | 0.87 | 181 | 167 |
| — | 0.996 | 0.004 | — | — | 0.995 | 0.998 | 0.00318 | 0.77 | 50 | 17 |
| 0.000 | 0.996 | 0.004 | — | — | 0.996 | 1.000 | 0.00345 | 0.86 | 47 | — |

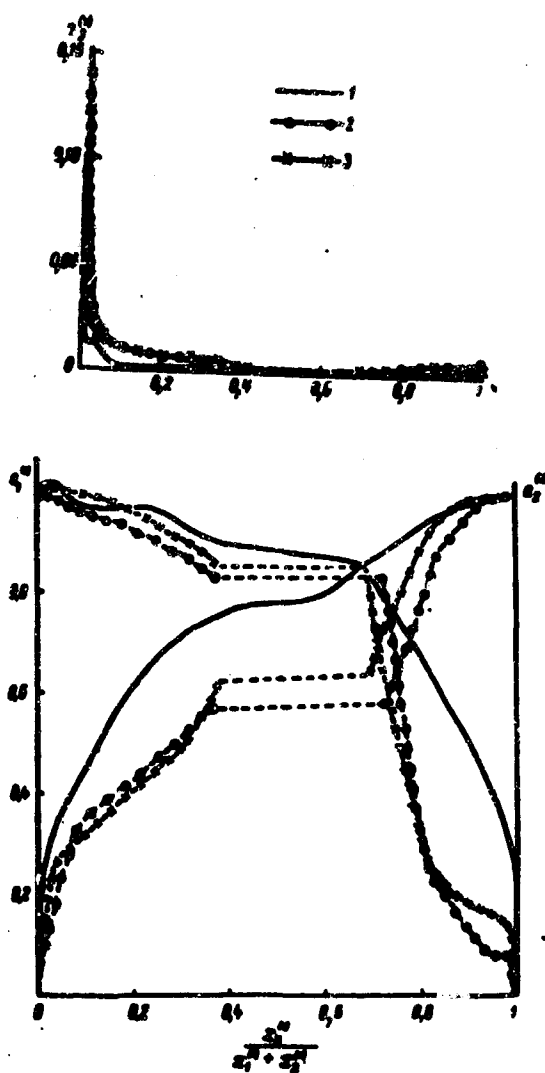


Fig. 2. Dependence of activities of NaCl ($a_1^{(1)}$), KCl ($a_2^{(1)}$), and CdCl₂ ($a_3^{(1)}$) on composition of solid solutions and temperature. 1 - 540, 2 - 580, 3 - 623°C.

concentration), as can be seen from the slope of the solidus in the corresponding region of the composition (see Fig. 1). We can assume that in structure of solid solution first of all K⁺ ions replace Cd²⁺ ions; with this the concentration of defects in cation lattice points should decrease. This probably leads to certain weakening of the bond of Na⁺ ions in the structure and to a corresponding increase of NaCl activity. Actually, with decrease of concentration of defects the shielding of charge of Na⁺ ions by cation encirclement will be increased. When a considerable part of the Cd²⁺ ions are replaced by K⁺ ions further increase of their content in the solid phase is accompanied by a corresponding decrease of activity

for NaCl and KCl respectively. We considered the slope of activity curves according to isotherms of solidus line. However, they do not deviate very strongly from the corresponding secant.

It is interesting to note the certain peculiarities of the dependence of activity of NaCl on composition. On the activity curves of sodium chloride at all temperatures an extremum (swing) is

observed when $\frac{x_1^{(2)}}{x_2^{(2)}} = \frac{x_1^{(1)}}{x_2^{(1)}}$, i.e., the

composition of the solid phase corresponds to a node which coincides with the secant outgoing from summit of NaCl [2]. On activity curves of CdCl₂ at 623°C there is an extremum corresponding to a minimum

of CdCl₂ activity, when $\frac{x_1^{(2)}}{x_2^{(2)}} = \frac{x_1^{(1)}}{x_2^{(1)}}$. The

insignificant increase of NaCl activity observed in the region of small additions of KCl can be explained by the following. With increase of KCl concentration in the solid solutions the CdCl₂ decreases (at comparatively small change of NaCl

concentration and a decrease of its activity. As can be seen from Fig. 2, on the activity curves of KCl at 540 and 580°C there are sections which, one would think, have to correspond to negative deflections from the ideal for this component, which could signify a strengthening of the interaction between components in the solid phase. However, this has to affect the behavior of the other component, NaCl, i.e., and for it there should be a region of negative deflection, which in reality is not observed. Such "anomalous behavior of potassium chloride most probably is combined not with an increase in the strength of the KCl bond, but is determined by a very short increase of NaCl activity, which according to the correlation of activity by the Gibbs-Duhem equation should lead to a sharp drop of activity for KCl (activity of the third component, CdCl₂, changes little in this region).

For many systems an increase of temperature leads to a decrease of deflections from the ideal. In the solutions we studied we observed the reverse regularities; an increase of temperature leads to a considerable increase in the coefficients of activity, and also in the activities. Analogous regularities are observed for a whole series of systems; methyl alcohol - water, ethyl alcohol - water, triethylamine - water, diethylamine - water and others [7]. Such uniqueness of behavior of systems also affects other thermodynamic magnitudes: $\Delta H < 0$, $T\Delta S^{\text{ex}} < 0$, $\Delta H > T\Delta S^{\text{ex}}$, therefore $\Delta\phi^{\text{ex}} > 0$. We will not discuss these thermodynamic functions for our investigated system.

According to the data for activities of components we calculated the change of isobaric potential ($\Delta\phi_{\text{is}}$) and excess values of this function by the equations

$$\Delta\phi_{\text{is}} = RT \sum_i x_i \ln a_i \quad (6)$$

$$\Delta\phi_{\text{ex}} = RT \sum_i x_i \ln f_i \quad (7)$$

The calculated magnitudes of $\Delta\phi_{\text{is}}$ and $\Delta\phi_{\text{ex}}$ are represented in Tables 1, 2, and 3 and the values of $\Delta\phi_{\text{is}}$ at 601.5°C are given in Fig. 3. As can be seen from Fig. 3

the curve of $\Delta\phi_{\text{ex}}$ built as a function of composition of solid phase $\frac{x_1^{(1)}}{x_1^{(1)} + x_2^{(1)}}$

has an assymetrical form. Actually, $\Delta\phi_{\text{ex}}$ grows faster with substitution of K⁺ ions for Na⁺ ions in the NaCl grid and slower with substitution of Na⁺ ions for K⁺ ions in the KCl grid, which can probably be combined with larger difficulties when substituting larger K⁺ ions (1.33 Å) into the grid of smaller Na⁺ ions (0.98 Å) than when substituting smaller ions for larger. Calculating the entropy (ΔS) and

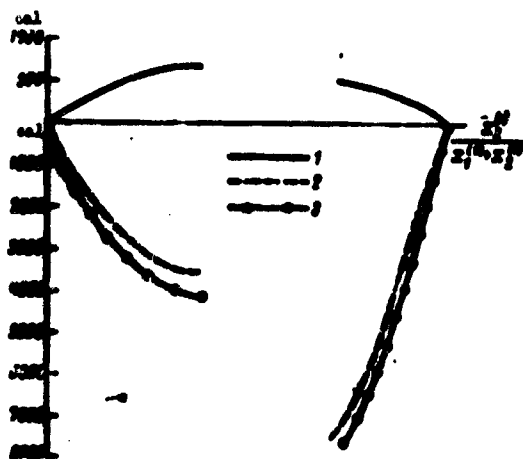


Fig. 3. Dependence of $\Delta S_{\text{sol}}, \Delta H_{\text{sol}}$ on composition of solid solutions ($t^{\circ} = 601.5^{\circ}\text{C}$). 1 - ΔS_{sol} ; 2 - ΔH_{sol} ; 3 - ΔG_{sol} .

enthalpy (ΔH) in the formed solid solutions was rather difficult in our case, since we could not carry the values of $\Delta\Phi$ at various temperatures to the same compositions of solid solutions. Therefore we found approximate values for ΔS based on calculation of entropy of formation according to the following equation;

$$\Delta S = - \left(\frac{\partial \Phi}{\partial T} \right)_{P, T, x_1, x_2} = - \left[\left(\frac{\partial \Phi}{\partial T} \right)_{P, T, x_1^0} - \left[\left(\frac{\partial \Phi}{\partial x_1^0} \right)_{P, T, x_2^0} \times \left(\frac{dx_1^0}{dT} \right)_{P, T, x_1^0} + \left(\frac{\partial \Phi}{\partial x_2^0} \right)_{P, T, x_1^0} \left(\frac{dx_2^0}{dT} \right)_{P, T, x_1^0} \right] \right] \quad (8)$$

where

$$\left(\frac{\partial \Phi}{\partial x_1^0} \right)_{P, T, x_2^0} = (\Delta p_1^0 - \Delta p_2^0) = R \ln \frac{a_1^0}{a_2^0};$$

$$\left(\frac{\partial \Phi}{\partial x_2^0} \right)_{P, T, x_1^0} = (\Delta p_2^0 - \Delta p_1^0) = RT \ln \frac{a_2^0}{a_1^0};$$

and calculation of magnitudes ΔH_{sol} by the equation

$$\Delta H = \Delta\Phi + T\Delta S \quad (9)$$

The calculated values of ΔS_{sol} , ΔH_{sol} and ΔG_{sol} at 601.5°C (mean value of the temperature interval, $580-623^{\circ}\text{C}$) are given in Table 4 and Fig. 3.

Table 4

| $\frac{x_1^0}{x_1^0 + x_2^0}$ | $-\Delta G_{\text{sol}}$ | $-\Delta H_{\text{sol}}$ | $-\Delta S_{\text{sol}}$ | $\frac{\Delta H_{\text{sol}}}{RT}$ | $\frac{\Delta H_{\text{sol}}}{RT}$ | $\frac{\Delta H_{\text{sol}}}{RT}$ |
|-------------------------------|--------------------------|--------------------------|--------------------------|------------------------------------|------------------------------------|------------------------------------|
| 0.10 | 1.70 | 2.26 | 1730 | 0.63 | 682 | 677 |
| 0.20 | 2.26 | 3.00 | 26.20 | — | — | — |
| 0.30 | 2.82 | 4.00 | 34.00 | 1.45 | 808 | 1185 |
| 0.40 | 3.38 | 4.80 | 32.00 | — | — | — |
| 0.50 | 4.00 | 5.15 | 7800 | 1.67 | 877 | 1364 |
| 0.60 | 4.60 | 7.20 | 60.00 | — | — | — |
| 0.70 | 5.17 | 7.81 | 2230 | 0.70 | 664 | 620 |
| 0.80 | 5.70 | 1.57 | 1410 | — | — | — |

It is necessary to note the very complicated character of the dependence of thermodynamic functions on composition, which significantly distinguishes the

investigation three-component solutions of NaCl - KCl - CdCl₂ from the studied earlier binary solid solutions of NaCl - KCl (in spite of the comparatively small concentrations of CdCl₂, up to 5 molar %). To compare the properties three-component solid solutions with binary solutions of NaCl - KCl Fig. 4 gives the ΔH_{sep} of binary solid solutions. It is possible to note a small scattering in the magnitudes of ΔH_{sep} for NaCl - KCl binary solid solutions for the same compositions of solid solutions determined calorimetrically by different authors [8, 9, 10]. This scattering is probably explained by incomplete homogeneity of the investigated samples. A deficiency of all works is also the following; in the shown works all samples were prepared by homogenization and annealing of solid solutions at high temperatures 500-600°C with their subsequent hardening by cooling to room temperature. Thus, when the vibration component of the energy of formation of solid solutions is 25°C, the configurational component of the energy is the frozen equilibrium at a temperature of annealing. This fact should affect the magnitude of ΔH_{sep} of solid solutions. The most reliable the represented data, as it seems to us, are the data of Barret and Wallace, Lister and Meyers [9, 10]. The works of these authors have great thoroughness during preparation of samples and fulfillment of the whole experiment. The results obtained by authors [9, 10] pertain to binary solid solutions of NaCl - KCl which are formed at 630°C with an endothermic effect. Our data pertain to the formation of triple solid solutions of NaCl - KCl - CdCl₂ at 601°C, but with an exothermic effect.

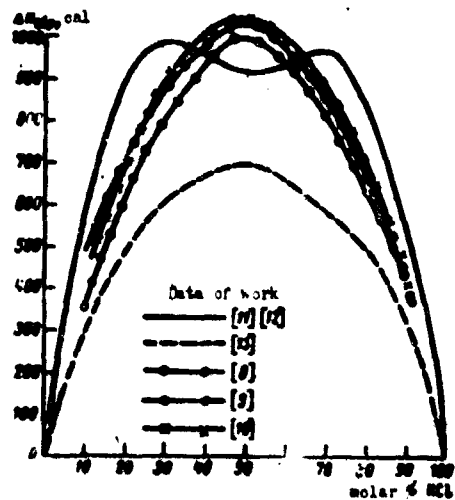


Fig. 4. Dependence of ΔH_{sep} of binary solid solutions of NaCl - KCl on composition.

Besides the experimental data on heats of formation of solid solutions, above considered, Fig. 4 also represents the results of theoretical calculation of heats of formation of binary solid solutions obtained in examining a definite model of the formation of solid solution of halides of alkaline metals [11-13]. There are calculated data of Wasastjerna and Hovi, obtained assuming free distribution of ions in solution, and corresponding magnitudes for solutions in which local order in distribution of ions is assumed. It is possible to note that the data Barret and Wallace are nearer to the

magnitudes of heats of formation obtained assuming the existence of a partially ordered solution ("local order"). However, the calculated values are higher than entropy of an ideal solution, whereas for existence of local order in solution there have to be negative deflections from the ideal (according to the theory of Wasastjerna). Such high values of entropy of formation of NaCl - KCl solid solutions can be a result either of the existence of a large number of defects, disturbances in crystal lattice of solid solutions in comparison with clean salts, or can be combined with a change in the vibration component of entropy during formation of the solid solution. Comparing the data of pycnometric and X-ray densities for these solid solutions showed that in the studied solid solutions the number of Schottky defects is very great (up to 1%). In theoretical calculations of entropy of formation of solid solution with a grid having Schottky defects, Barret and Wallace confirmed the assumption of these authors about the presence in investigated solid solutions of a large number of Schottky defects.

It is useful to discuss our results being based on certain general assumptions. As follows from the diagram of the state of the investigated system and with even greater definitiveness from the data [1] and above mentioned dependencies of activities on composition of solutions, the third component evokes stratification of solid solutions and increases the critical temperature of stratification.

Still M. S. Vrevskiy [14] showed on a series of examples that this effect of the third component can be connected with the specific interaction of the introduced component with one or both components of the binary solution. This position was also discussed on the basis of thermodynamic consideration of the problem. In particular, Prigogin and Defay, [15] on the basis of general positions of thermodynamics and the theory of regular solutions showed that the third component increases the critical temperature of stratification if it is much better dissolved in one of the components of the system than in the other. In this case $\left(\frac{\partial T}{\partial x_3}\right) > 0$, at comparable solubility $\left(\frac{\partial T}{\partial x_3}\right) < 0$. They affirmed and illustrated a series of examples of the generality of this position. In our investigated system the above-indicated regularities are confirmed, CdCl₂ will dissolve better NaCl ($x_3^{(1)} = 0.030$) than in KCl ($x_3^{(1)} = 0.007$); an increase in the temperature of stratification of solid solutions is observed. In the recently carried out work of A. I. Rusanov [16] for a phenol - water system it is shown that upon introduction of a third component,

isopropyl alcohol, more strongly interacting with water than with phenol, an increase of the critical temperature is also observed with growth of x_3 . An essential result of this work is the following; it showed that with movement along the critical curve from lower temperature (for the binary system) to higher temperature (in the tertiary system) the excess free energy of the critical phase increases and the derivative $(\frac{\partial G}{\partial T}) > 0$, as in case of our system too.

In accordance with the general assumptions of the effect of the third component on stability of binary solutions it is possible to consider that introducing CdCl_2 into a $\text{NaCl} - \text{KCl}$ structure leads to the establishment of "local" order, since due to predominant interactions of $\text{CdCl}_2 - \text{NaCl}$ and $\text{CdCl}_2 - \text{KCl}$ the appropriate quasicomplexes are formed in the structure. (In this connection one should note that analogous compounds are formed in binary systems $\text{Cd}:\text{Na}$, 1:2; $\text{Cd}:\text{K}$, 1:4, 1:1.) The establishment of local order should lead to a decrease of entropy, as was observed. However, apparently, here not only the configurational component of entropy, but the oscillatory component play a significant role. The essential role of change in the energy of interaction during formation of triple solutions is obviously indicated by the great exothermic effect of the formation of solid solutions, which, furthermore, can be connected with the formation of complexes. Among the components of ΔH_{sol} are both the component of ΔH_{sol} corresponding to complexes and the ΔH of disintegration of binary solid solutions.

Thus, our obtained data, characterizing the thermodynamic properties of three-component solid solutions in comparison with data for binary solid solutions, graphically testify to the considerable influence of introducing even small additions of a third component (CdCl_2) has on the properties of solid solution.

Summary

The activities of the components of the solid solutions $\text{NaCl} - \text{KCl} - \text{CdCl}_2$ at 540, 580, 623°C have been determined by the method of the third component. ΔG , ΔH , ΔS of the formation of these solid solutions have been calculated. [English summary]

Literature

1. M. M. Shul'ts and I. M. Bushuyeva. Herald of Leningrad State University, No. 22, 1963.
2. A. V. Storonkin and M. M. Shul'ts. Herald of Leningrad State University, No. 11, 154, 1964.

3. I. M. Bushuyeva and M. M. Shul'ts. Herald of Leningrad State University, No. 22, 1963.
4. M. M. Shul'ts, A. V. Storonkin, and T. P. Markova. Journal of Physical Chemistry, XXXII, No. 11, 2518, 1958.
5. A. P. Patner and L. L. Makarov. Journal of Physical Chemistry, XXXII, No. 8, 1809, 1958.
6. Reference book of chemistry. 1, 793, 1951.
7. M. I. Shakhporonov. Introduction to molecular theory of solutions. Goskhozdat, 290, 1956.
8. M. S. Ivankina. Herald of Higher Educational Institutions, Physics series, No. 3, 165, 1958.
9. W. F. Barrett and W. E. Wallace. J. Amer. chem. soc., 76, No. 2, 1954.
10. M. W. Lister and N. F. Mayers. J. Phys. chem., 62, No. 2, 145, 1958.
11. I. A. Wasastjerna. Soc. scient. Fennica-comment. Phys.-math., XV, No. 3, 1949.
12. V. Hovi. Ann. Acad. scient. Fennica comment. Phys-math., XV, No. 12, 1950.
13. G. S. Durham and J. A. Hawkins. J. Chem. phys., 19, 149, 1951.
14. M. S. Vrevskiy. Works on the theory of solutions. Press of the Academy of Sciences of USSR, 60-61, 1953.
15. I. Prigogin und Defay. Chem. Thermodyn. Leipzig, 5, 280, 1962.
16. A. I. Rusanov. Herald of Leningrad State University, No. 16, 99, 1958.

Submitted
28 June 1963

AMPEROMETRIC TITRATING CERTAIN CATIONS BY TRILON B WITH
REVOLVING MICROPLATINUM ELECTRODES

L. S. Reyshakhrit, M. P. Pustoshkina, and
Z. I. Tikhonova

In polarography and amperometric titrating in recent years a new class of complex formers, known under the name of complexones, has found application [1]. Applying complexones, in particular trilon B, in amperometric titrating uses a revolving microelectrode [1, 2, 3].

This work attempts, using trilon B as a reagent, to conduct amperometric titrations with revolving microplatinum electrode of Sr^{2+} , Ca^{2+} , Mg^{2+} , Cu^{2+} , and Ni^{2+} salts and also molybdates, tungstenates and chromates.

Method. Measurements were conducted on the usual polarographic installation with revolving microplatinum anode at given values of electrode potential and temperature. All readings of current and electrode potential were conducted visually. Current was fixed by a galvanometer with accuracy of ± 0.01 microamperes; potential difference was fixed by a voltmeter with accuracy of ± 2 millivolts, the speed of rotation of electrode was measured by a tachometer. All values of potentials relate to a calomel electrode with saturated solution of KCl at 20°C . The electrolytic cell was open with capacity of 150 ml. Electrodes were of two forms: a) a platinum wire 4 mm long soldered in a glass tube; b) a platinum disk with area of 0.15 cm^2 soldered in a glass tube.

Results of experiments and their discussion. In using trilon B as a reagent it was necessary to preliminarily remove polarization curves of anodic oxidation of trilon B on a revolving disk and microplatinum anodes in surplus of inert

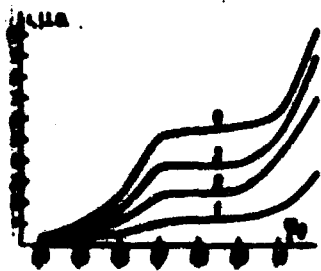


Fig. 1. Polarization curves of oxidation of trilon B on a revolving electrode. Background, 1.0 N KNO_3 ; $t = 25^\circ\text{C}$; $\omega = 880$ rpm. 1 - $5 \cdot 10^{-5}$; 2 - $1 \cdot 10^{-4}$; 3 - $1.5 \cdot 10^{-4}$; 4 - $2 \cdot 10^{-4}$ g-mole/liter of trilon B.

electrolytes (a) 0.1 N $\text{NH}_4\text{NO}_3 + \text{NH}_4\text{OH}$ pH of the solution 8.2-10; b) 1 N KNO_3 , pH of the solution ~5.7; c) 1 N $\text{KNO}_3 + \text{HCl}$, pH of the solution 4-5) at different speeds of electrode rotation and different concentrations of trilon B. On the basis of the obtained experimental data it was established that trilon B, oxidizing on the platinum electrode, gives polarization curves with a clearly expressed region of limiting current, which starts at potential of 0.7 v in a solution of 1 N KNO_3 and at 0.85 v in an ammonium background (Fig. 1). Obtaining of well reproducible polarization curves with clear site of

limiting current is attained only upon heat treatment of the electrode in flame of a burner before every experiment. V. L. Knouzeyev and F. F. Kvashina [3], measuring polarization curves of trilon B in approximately the same conditions, did not obtain clear limiting currents on polarization curves. Apparently, before carrying out the experiment they insufficiently thoroughly purified the electrode surface.

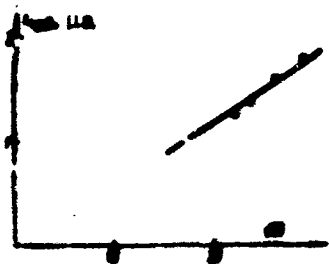


Fig. 2. Dependence of limiting current on $\sqrt{\omega}$. $\omega = 880$ rpm; $t = 25^\circ\text{C}$, background - 1.0 N KNO_3 .

From Fig. 2 it follows that the magnitude of limiting current is directly proportional to the square root of the speed of rotation of the disk electrode. This allows us to consider that for a rate of the process of anodic oxidation of trilon B it is possible to apply V. G. Levich's equation of convection diffusion for a revolving disk electrode [4]. The obtained experimental data (Figs. 1 and 2) allow us to make the conclusion that the rate of anodic oxidation of

trilon B is limited by its diffusion to the electrode at potentials larger than +0.7 v. The observed linear dependence between trilon B concentration in the solution and limiting current in the interval of potentials from +0.7 to +0.95 v (Fig. 3) allows us to apply trilon B as a reagent in amperometric titrating.

The titrating of certain ions by trilon B in three inert electrolytes was accomplished:

- a) on a background of 0.1 N NH_4NO_3 (pH of the solution, 8.2-10) at electrode

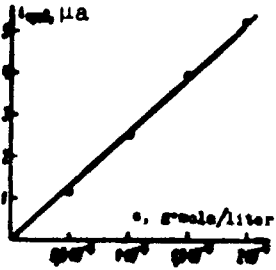


Fig. 3. Dependence of limiting current on trilon B concentration. Background - 1 N KNO₃; t = 25°C; m = 880 rpm; E_{pot} = +0.85 v.

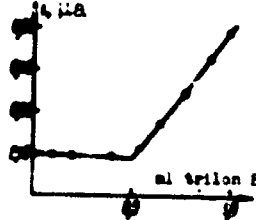


Fig. 4. Curve of amperometric titrating of a solution by trilon B. Background - 0.2 N KNO₃; E_{pot} = +0.85 v; 1 ml 0.01 N NiSO₄; trilon B 0.01 m; t = 20°C.

potential of +0.84 v; the speed of its rotation was equal to 700 rpm and t was 20°C; the cations were Sr²⁺, Ca²⁺, and Mg²⁺;

b) on a background of 0.2 N KNO₃ (pH of the solution ~5.7) at electrode potential of +0.85 v; the speed of its rotation was 880 rpm and t was 20°C, the cations were Cu²⁺, Ni²⁺, WO₄²⁻, and CrO₄²⁻.

c) a solution of H₇[P(Mo₂O₇)₆] on a background of 0.2 N KNO₃ + HCl (pH of the solution, 4-5) at electrode potential of +0.85 v and temperature of 35-40°C.

Table 1. Amperometric Titrating of a Sr(NO₃)₂ Solution by Trilon B

| m, mg | | Relative error in % | pH of the medium | m, mg | | Relative error in % | pH of the medium |
|-------|-------|---------------------|------------------|-------|-------|---------------------|------------------|
| taken | found | | | taken | found | | |
| 0.6 | 0.5 | 4 | 10 | 0.3 | 0.3 | 0 | 0.6 |
| 1.2 | 1.2 | 4 | 10 | 7.0 | 6.9 | 0 | 0.6 |
| 2.4 | 2.4 | 2 | 10 | 8.8 | 8.4 | 4 | 0.6 |
| 3.6 | 3.6 | 1 | 10 | 17.8 | 17.3 | 2 | 0.6 |
| 4.8 | 4.8 | 4 | 9.5 | 26.5 | 24.8 | 1 | 0.6 |
| 6.0 | 5.8 | 2 | 9.5 | 35.2 | 32.8 | 1 | 0.6 |
| 7.2 | 7.2 | 2 | 9.5 | 44.0 | 42.4 | 4 | 0.6 |
| 8.4 | 8.4 | 1 | 9.5 | 52.8 | 52.0 | 2 | 0.6 |
| 9.6 | 9.6 | 0 | 9.5 | 61.6 | 61.6 | 0 | 0.6 |
| 10.8 | 10.8 | 11 | 9.5 | 70.4 | 70.4 | 0 | 0.6 |

Table 2. Amperometric Titrating of CuSO₄ and NiSO₄ Solutions by Trilon B

| m, mg | | Relative error in % | m, mg | | Relative error in % |
|-------|-------|---------------------|-------|-------|---------------------|
| taken | found | | taken | found | |
| 0.6 | 0.6 | 17 | 0.6 | 0.6 | 17 |
| 1.2 | 1.2 | 10 | 1.2 | 1.2 | 17 |
| 1.8 | 1.8 | 11 | 1.8 | 1.8 | 11 |
| 2.4 | 2.4 | 8 | 2.4 | 2.4 | 8 |
| 3.0 | 3.0 | 7 | 3.0 | 3.0 | 6 |
| 3.6 | 3.6 | 6 | 3.6 | 3.6 | 6 |
| 4.2 | 4.2 | 4 | 4.2 | 4.2 | 4 |
| 4.8 | 4.8 | 3 | 4.8 | 4.8 | 3 |

Table 3. Amperometric Titrating of Trilon B by a Solution of H₇[P(Mo₂O₇)₆]

| m, mg | | Relative error in % | m, mg | | Relative error in % |
|-------|-------|---------------------|-------|-------|---------------------|
| taken | found | | taken | found | |
| 0.6 | 0.6 | 10 | 0.6 | 0.6 | 10 |
| 1.2 | 1.2 | 10 | 1.2 | 1.2 | 10 |
| 1.8 | 1.8 | 14 | 1.8 | 1.8 | 10 |

The form of curves of amperometric titrating is depicted in Fig. 4.

Satisfactory results were obtained during amperometric titrating of Sr^{2+} , Cu^{2+} , Ni^{2+} , and Mo^{6+} salts. The results of experiments are given in Tables 1, 2, and 3 where the mean values from 3-5 determinations are given. Amperometric determination does not yield in accuracy to the data of A. I. Busev and Chzhan Fan' [5], developed for amperometric titrating of Mo^{6+} with a mercury drop electrode. As can be seen from the tabular data the error in the determination is from 1% to 17%.

The data on amperometric titrating of Mg^{2+} , Ca^{2+} , WO_4^{2-} , and CrO_4^{2-} salts did not give satisfactory results and require an additional thorough check.

Conclusions

1. It was determined that oxidation of trilon B on a revolving smooth platinum anode in solutions of 0.1 N $\text{NH}_4\text{NO}_3 + \text{NH}_4\text{OH}$ (pH 8.3-10) and 1 N KNO_3 (pH ~5.7) is limited by diffusion at electrode potentials more positive than +0.7 v and +0.85 v respectively.

2. Is shown the possibility of carrying out amperometric titrating with a microplatinum anode of $\text{Sr}(\text{NO}_3)_2$ solutions on a background of 0.1 N $\text{NH}_4\text{NO}_3 + \text{NH}_4\text{OH}$ and CuSO_4 , NiSO_4 , $\text{H}_7[\text{P}(\text{Mo}_2\text{O}_7)_6]$ on a background of 0.2 N KNO_3 with application of trilon B as the reagent.

In conclusion we express gratitude to Ya. V. Durdin for valuable council and indications.

Summary

An investigation of the oxidation process of trilon B has been carried out on rotating platinum anode in solutions of 0.1 n $\text{NH}_4\text{NO}_3 + \text{NH}_4\text{OH}$ (pH = 8.3-10.0) and 1 n KNO_3 (pH = 5.7) at 20° C. The oxidation rate is determined by diffusion at potentials more positive, than +0.7 v and +0.85 v respectively.

Demonstrated is the possibility of amperometric titration with a microplatinum rotating electrode of $\text{Sr}(\text{NO}_3)_2$ solutions against 0.1 n $\text{NH}_4\text{NO}_3 + \text{NH}_4\text{OH}$ and those of CuSO_4 , NiSO_4 , $\text{H}_7[\text{P}(\text{Mo}_2\text{O}_7)_6]$ - against 0.2 n KNO_3 with the contents of Sr, Cu, Ni and Mo from 0.25 to 70 mg using trilon B. [English summary]

Literature

1. S. I. Sinyakova. ZhAKh, 10, 139, 1955.
2. Yu. I. Usatenko and M. A. Vitkina. Scientific reports of high school (chemistry and chemical technology), No. 3, p. 502, 1958.
3. V. A. Khodeyev and F. F. Kvashina. Herald of higher educational institutions, (chemistry and chemical technology), 3, 251, 1960.
4. V. G. Levich. Physical chemistry of hydrodynamics, Moscow, Press of Academy of Sciences of USSR, 1952.

5. A. I. Busev and Chzhen Wan'. Herald of Moscow State University, No. 2,
203, 1959.

Submitted
18 June 1963

OXIDATION RATE OF COPPER DURING BRIEF HEATING TO HIGH TEMPERATURES

V. I. Tikhomirov and E. I. Korytkova

In studying the oxidation rate of metals and alloys one usually conducts experiments in isothermal conditions, controlling the weight gain of samples or growth of thickness of oxide layers. On the basis of the obtained data one can determine the character of the time dependence and magnitude of the oxidation rate constant. By conducting a series of experiments at different temperatures, one can determine the dependence of the constant of the reaction rate on temperature. The duration of heating in isothermal conditions is selected sufficiently great, so that the period of temperature rise and cooling does not essentially affect the experimental results. However, such a method does make it possible to study the initial period of oxidation, occurring in conditions of increased temperature. Furthermore, this method is also not suitable for the study of oxidation kinetics during brief heating to high temperatures. Placing before ourselves the goal of investigating the oxidation rate of metals during brief heating to high temperatures, we developed a method of determining the basic kinetic parameters according to experiments on oxidation in conditions of variable temperature.

It is known that oxidation of metals and alloys usually follows either a logarithmic law, observed mainly during oxidation at comparatively low temperatures, or a linear or parabolic law. Significantly less often a more complicated dependence of oxidation rate on duration of oxidation is observed.

The linear or parabolic law of oxidation can be presented in the form of following equation:

$$\frac{d(q^n)}{d\tau} = k, \quad (1)$$

where q is the quantity of oxygen, reacting with metal calculated on 1 cm^2 of sample surface; τ is the time; n is the exponent, equal to one for a linear dependence and two for a parabolic dependence; k is the rate constant depending on the temperature of oxidation,

$$k = A \exp(-E/RT), \quad (2)$$

where A is a constant, not depending on temperature; E is the activation energy, T is the temperature; R is the gas constant. Putting in equation (1) instead of k its value from equation (2), we will obtain

$$d(q^n) = A e^{-E/RT} d\tau. \quad (3)$$

Parameters n , A and E can be determined on the basis of carrying out nonisothermal experiments. Let us assume that three experiments differing in conditions are performed; for these tests it is possible to compose the following equations;

$$\begin{aligned} d(q_1^n) &= A e^{-E/RT} d\tau, & (4) \\ d(q_2^n) &= A e^{-E/RT} d\tau, & (5) \\ d(q_3^n) &= A e^{-E/RT} d\tau, & (6) \end{aligned}$$

with $T = f(\tau)$.

In equations (4)-(6) q_1 , q_2 , and q_3 are determined experimentally. For all three experiments also the dependence of T on τ is also determined experimentally throughout the process.

Integrating these equations within limits of change of q from 0 to q_x and τ from 0 to τ_x , we will obtain

$$q_1^n = A \int_0^{\tau_x} e^{-E/RT} d\tau, \quad (7)$$

$$q_2^n = A \int_0^{\tau_x} e^{-E/RT} d\tau, \quad (8)$$

$$q_3^n = A \int_0^{\tau_x} e^{-E/RT} d\tau. \quad (9)$$

Designating the integrals in equations (7), (8) and (9) respectively by Φ_1 , Φ_2 , and Φ_3 , dividing term by term equation (7) by equation (8) and equation (7) by equation (9), and finally, by logarithmizing the two obtained equations, we will have

$$\ln \frac{q_1^n}{q_2^n} = \ln \frac{\Phi_1}{\Phi_2}, \quad (10)$$

$$n \lg \frac{\Phi}{\Phi_0} = \lg \frac{\Phi_1}{\Phi_0}. \quad (11)$$

One can determine the values of integrals Φ_1 , Φ_2 , and Φ_3 graphically with the help of the curves of the dependence of $e^{-E/RT}$ on τ , which, in turn, are constructed on the basis of graphs of the dependence of T on τ .

However, the magnitudes of Φ_1 , Φ_2 , and Φ_3 will depend on the values of E selected during calculation. It is possible to show that in sufficiently narrow limits of change of E the dependence of $\lg \Phi$ on E can be approximately presented in the form of a linear equation

$$\lg \Phi = a + bE. \quad (12)$$

Thus, by determining the values of integrals Φ_1 , Φ_2 , and Φ_3 for the two given extreme values of E it is possible for each of these magnitude of Φ to determine the dependence of $\lg \Phi$ on E in the form of equation (12). Putting in equations (10) and (11) instead of $\lg \Phi_1$, $\lg \Phi_2$, and $\lg \Phi_3$ the expressions in the form of equation (12), we will obtain

$$n \lg \frac{\Phi_1}{\Phi_0} = a_1 - a_2 + (b_1 - b_2)E, \quad (13)$$

$$n \lg \frac{\Phi_2}{\Phi_0} = a_1 - a_3 + (b_1 - b_3)E. \quad (14)$$

In system of equations (13) and (14) the unknowns are only the magnitudes n and E , which are easily found by solving this system of equations.

The value of magnitudes n and E can be found without resorting to the approximate equation (12). For this the magnitudes of Φ_1 , Φ_2 , and Φ_3 must be determined not only for extreme values of E of the selected interval, but also for a series of intermediate values, and the whole solution must be produced by graphic means.

Certainly, strict application of the described method of determining the parameters of the equation of oxidation rate is possible only if the oxidation follows one regularity (linear or parabolic) in the set experiments. Otherwise we will obtain fractional values for the exponent n . However, even in this case this method can give valuable information about the oxidation process.

To study the oxidation rate during brief heating to high temperature we applied the following method (Fig. 1). The test sample 1 in the form of a wire or tape was pressed between contacts 2. Heating the sample was produced by electrical current, passed to the sample through a step-down transformer 3 fed from a network of alternating current. The rate of heating was regulated by

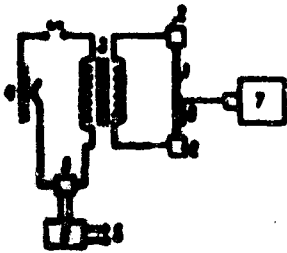


Fig. 1. Diagram of an installation for studying the oxidation rate of metals during brief heating to high temperature.

rheostat 4. The duration of heating was regulated by an electrical time relay 6, which closed and opened the circuit by means of a mercury contact 5. Heating of samples was usually produced for several seconds.

Temperature of samples was measured during heating by the cinematographic method. The principle of this method consists of the following.

At a distance of 65 cm from the heated sample "Kiev" 7 movie camera operating on 16 millimeter film was set up.

The image of the heated sample was focused on the film by means of an "Industar"-50 telephoto lens. Directly in front of the heated sample light filter 8 was established, absorbing part of the radiation. The light filter was established so that it shielded only part of the image of the sample during photographing. At previously selected aperture and shutter speed (number of frames per second and exposure) the sample was photographed during its heating. The conditions of photography (distance from chamber to object, objective, aperture, shutter speed, light filter, and characteristics of film) always remained constants, both during construction of calibration curves, and also during photographing of heated objects.

After photographing the film was developed in standard conditions (composition of developer and fixing bath, temperature and duration of development). Later the density of blackening of images of heated sample in parts of the image obtained during photographing with and without the light filter was determined; these measurements of blackening density were produced as close as possible to the edge of the light filter. A [MF-2] (MF-2) microphotometer was used to determine blackening density. According to the measurements of blackening density with help of a previously constructed calibration curve in coordinates of the blackening density determined the temperature of the sample, corresponding to each separate frame. From the obtained data further we constructed a graph of the dependence of T on τ .

The calibration curve was constructed in this way. The temperature of the heated object was determined by a thermocouple or an optical pyrometer, and heating object was determined by a thermocouple or an optical pyrometer, and heating or cooling was produced by steps, i.e., after every rise or lowering of the temperature

was kept constant for some time, and during this time the temperature of the object was measured exactly and the sample was photographed. In all calculations of temperature the difference in radiation of real bodies and an ideal black body was considered. Since the photographic width of the film did not allow to construct one calibration graph embracing a wide range of temperatures, a light filter was applied and two calibration graphs (with light filter and without light filter) were constructed. Photographing of tested samples, as already indicated, was also produced with and without a light filter.

In our experiments we used a copper wire as the test object. According to spectral analysis the copper contained Pb ~ 0.01%, Fe and Mg ~ 0.001% and traces of Si. The presence of other elements was not revealed by spectral analysis.

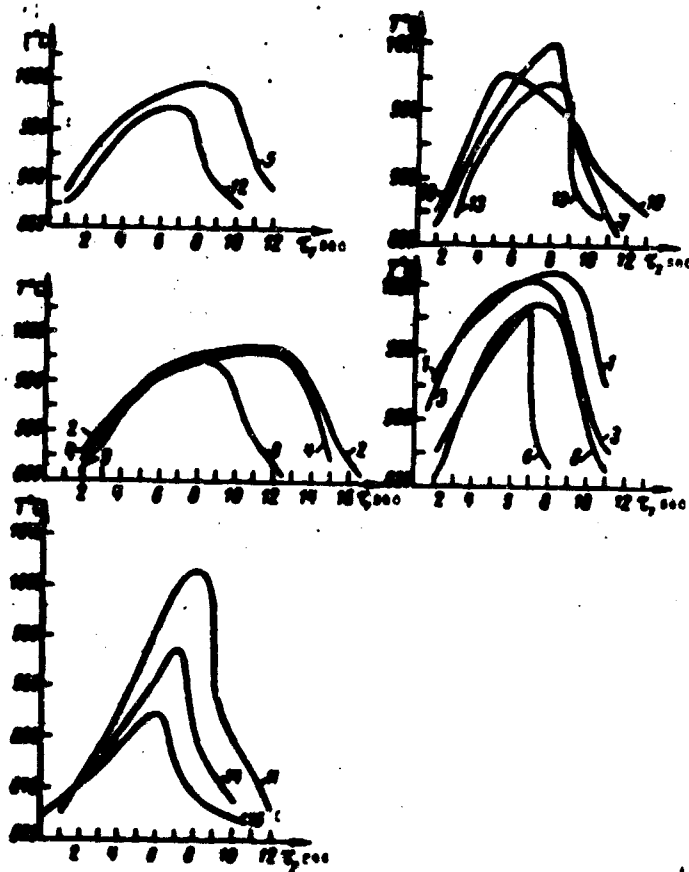


Fig. 2. Curves of change of temperature during brief heating of copper samples. Numeration of the curves coincides with numeration of experiments in the table.

Figure 2 shows graphs of the change of temperature of heated copper wires for all experiments on brief heating. After termination of each experiment from the wire subjected to heating we cut a segment about 4-5 cm long; the cut section

was selected so that its center corresponded to the edge of the light filter at the moment of photographing. The taken segments of wire were weighed on analytic scales, processed with diluted hydrochloric acid to dissolve the layer of cinder, washed in water and alcohol, dried and weighed again. The cinder determined by difference in weight was recalculated for oxygen, considering that it basically consisted of cuprous oxide. The found weight gain of oxygen was calculated per unit of sample surface. The experimental results are presented in the table.

| No of experiment | Duration of heating at a temperature higher than 800°C, sec | Maximum temperature, °C | -lg φ for | | Weight gain of oxygen 10 ³ , g/cm ² | | % of divergence |
|------------------|---|-------------------------|-----------------|-----------------|---|------------|-----------------|
| | | | g-2000 cal/mole | g-2000 cal/mole | Experimental | Calculated | |
| 1 | 14 | 1000 | 2.0000 | 2.0004 | 0.501 | 1.100 | 12.0 |
| 2 | 17 | 1000 | 2.0004 | 2.0008 | 0.977 | 1.112 | 12.2 |
| 3 | 19 | 1000 | 2.1276 | 2.1287 | 0.931 | 1.048 | 8.5 |
| 4 | 23 | 1000 | 2.2042 | 2.2053 | 0.888 | 1.000 | 10.0 |
| 5 | 19 | 1000 | 2.1181 | 2.1193 | 0.888 | 1.000 | 12.5 |
| 6 | 6 | 1000 | 2.0000 | 2.0000 | 0.731 | 0.712 | -2.6 |
| 7 | 11 | 1000 | 2.0000 | 2.0002 | 0.731 | 0.714 | 11.4 |
| 8 | 19 | 1000 | 2.0000 | 2.0002 | 0.682 | 0.701 | 12.5 |
| 9 | 23 | 1000 | 2.0000 | 2.0002 | 0.682 | 0.704 | 10.2 |
| 10 | 15 | 1000 | 2.0000 | 2.0002 | 0.682 | 0.701 | 10.2 |
| 11 | 11 | 1000 | 2.0000 | 2.0002 | 0.682 | 0.701 | 10.2 |
| 12 | 11 | 1000 | 2.0000 | 2.0002 | 0.682 | 0.701 | 10.2 |
| 13 | 9 | 800 | 2.4105 | 2.4105 | 0.515 | 0.777 | 49.7 |
| 14 | 9 | 800 | 2.4105 | 2.4105 | 0.435 | 0.688 | 32.9 |
| 15 | 9 | 800 | 2.7124 | 2.7124 | 0.379 | 0.488 | 22.9 |
| 16 | 9 | 800 | 2.7450 | 2.7450 | 0.385 | 0.488 | 20.8 |

Figure 3 shows the results of experiments in the form of graph in coordinates of $\lg q - \lg \phi$. The scales on the coordinate axes are selected so that a 45° slope of curves was executed at $n = 2$.

If we take for solution of the system of equation (13) and (14) the data of experiments 1 and 12 (see table), on the basis of which are the curves in Fig. 3 are conducted, and as the third point select the median point on curves correspond to $\lg q = -3.11$, as a result of solving this system of equations we will obtain $n = 1.97$. This indicates that in experiments from 1 to 12 inclusive the oxidation process of copper during brief heating to high temperature is stabilized as parabolic, in spite of the short period of oxidation on the order of 10-20 sec. In the right part the slope of curves in Fig. 3 changes, which corresponds to a decrease of exponent n . For the right side of curves exponent n is on the order of 1.3-1.6. This indicates that in experiments 13, 14, and 15 the parabolic law of oxidation is not predominant and a considerable part of the time process apparently follows the linear law of oxidation. It is necessary to note that in experiments 13, 14, and 15, in contrast to all others, oxidation occurs at somewhat

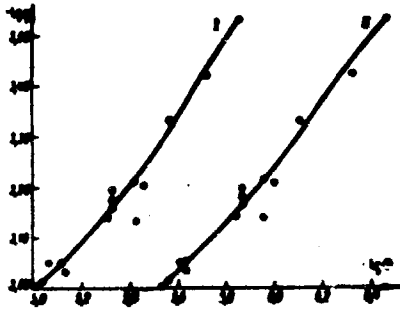


Fig. 3. Graph of the dependence of $\lg q$ on $\lg \phi$. Curve I is built for $E = 36,000$, curve II for $E = 39,000$ cal/mole.

within limits of $1020-1070^{\circ}\text{C}$. To determine E by equations (13) and (14) it is necessary to take a wider range to temperature. The comparatively low fusion temperature of copper (1083°) did not allow us to expand the region of investigated temperatures.

To compare our data with the literary data with the help of equation (7) and equations of the type of (12) we calculated q for each experiment. According to [1], we took $n + 2$, $A = 0.266 \text{ g}^2 \cdot \text{cm}^{-4} \cdot \text{sec}^{-1}$ and $F = 37,700 \text{ cal/mole}$. In the next to the last column of the table results of similar calculations are given, but the last column of the table shows the percent of divergence of calculated and experimentally found magnitudes of q . As follows from the table, the magnitudes of q calculated from the literary data and the directly found magnitudes are close to each other. For experiments 1-12, as was shown, a parabolic law is observed, and this divergence on the average composes 11.5%. A certain exceeding of the calculated magnitudes above the experimentally found is apparently explained by the fact that, nevertheless, in the beginning the process follows a linear law of oxidation. In experiments 13, 14, and 15 this effect is even greater, since here the period of linear oxidation is much longer.

Conclusions

1. A method of studying the oxidation rate of metals and alloys during brief heating (on the order of seconds) to high temperatures has been developed.
2. It is shown that oxidation of copper during brief heating (10-20 sec) to temperature on the order of $1020-1070^{\circ}\text{C}$ follows a parabolic law. With decrease of maximum temperature of heating to $900-1010^{\circ}\text{C}$ a linear dependence noticeably starts to predominate.

lower temperature and the maximum temperature of oxidation is 1010 , 950 and 900°C respectively.

It is impossible to calculate E from the data represented in the table with sufficient accuracy. To determine the activation energy it is necessary to produce experiments in wide range of temperature change. However, all experiments represented in the table are very close to each other in temperature regime. The maximum temperature of experiments 1-12 lies

Summary

The methods of investigation of the oxidation rate of metals and alloys during heatings of short duration (about some seconds) up to the high temperature have been developed.

It has been shown that copper oxidation during heatings of short duration (10-20 seconds) up to 1020-1070° C follows the parabolic law. When the temperature decreases as low as 900-1000° C, the linear law begins to predominate. (English summary)

Literature

1. O. Kubashevskiy and B. Gopkin*. Oxidation of metals and alloys, Moscow, IL, 230, 1955.

Submitted
13 January 1963

SPECTROPHOTOMETRIC INVESTIGATION OF ASCORBINATE COMPLEXES

K. P. Stolyarov and I. A. Amantova

1. Investigation of Complexes of Elements of Groups II and III of the Periodic Table

As is known [1-8] in analytic practice ascorbic acid is widely used as a reducer and in separate cases as complex former.

The goal of this work is the systematic spectrophotometric investigation of the possibility of using ascorbic acid as a complex former. L-ascorbic acid ($C_6H_8O_6$) has a structure of 2,3-endiol-L-gulono-1,4-lactone (Kherst, 1933).



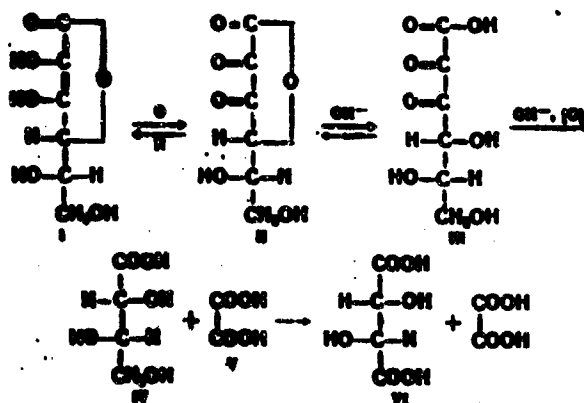
The acid properties are caused by hydroxyl group being in position 3 and only partially in position 2 ($pK_1 = 4.17$; $pK_2 = 11.57$ [9] and $pK_1 = 9.20$ [10]).

The complex forming functions of ascorbic acids are caused by presence of endiol grouping $-C(OH) = C(OH)-$.

The reducing properties of ascorbic acids are connected with the presence grouping with two conjugate double bonds $-C(OH) = C(OH) - C = O$ [9].

During oxidation of ascorbic acid (I) at first dehydroascorbic acid (II) is obtained, then 2,3-diketogulonic acid (III), and in definite oxidizing conditions

splitting of the molecule with formation of *l*-threonic (IV) and oxalic (V) acids, occurs and then even *l*-tartaric at pH \approx 9 [9]. There is an indication about the formation of oxalic acid in aqueous solutions of ascorbic acid in air at pH = 8 [11].

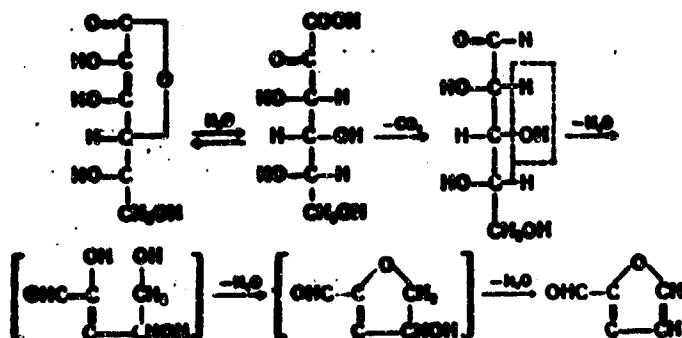


The oxidation of ascorbic acid to dehydroascorbic acid is reversible. The oxidizing-reducing potential at equal molecular ratios of these acids at pH = 2.04, $E_0 = 0.281$ v; at pH = 5.75, $E_0 = 0.106$ v; and at pH = 7, $E_0 = 0.185$ v [12].

The oxidation of aqueous solutions of ascorbic acid is accelerated in the presence of heavy metal ions [13], with increase of temperature [14], increase of solution alkalinity [15] and under the influence of ultraviolet light [4].

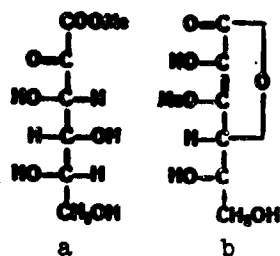
To increase the stability of ascorbic acid solutions it is recommended to add formic and oxalic acids [4, 18], ammonium thiocyanate [19], trilon B [3, 4, 16, 17] and to store the solutions in an atmosphere of CO_2 , N_2 [16, 17]. In our work we used freshly prepared solutions of ascorbic acid of high concentration, 1.25 M.

Besides oxidizing splitting ascorbic acid is inclined to hydrolytic splitting, the rate of which is increased with increase of alkalinity [9].



Under the effect of strong alkalis the unsaturated γ -lactone ring will be

released; a salt of ketonic acid (a) and not a salt of unsaturated hydroxy acid will be formed.



With weak alkalis ascorbic acid will easily form neutral monoalkali enolate without release of the lactone ring (b).

Considering the complicated character of behavior of ascorbic acid in an alkaline solution, oxidizing and hydrolytic decomposition [4, 9] as a rule, we investigated in solutions with pH < 7.

In strongly acid solutions the formation of ascorbate complexes has low probability, since ascorbic acid is weak and its dissociation is suppressed at low pH. Therefore, an investigation at pH < 2 had no meaning.

Light absorption of ascorbic acid solutions depends on pH; a curve of the type of a parabola reflects the process of development of yellow color during increase of alkalinity [20].

It is necessary to indicate the peculiarities of spectrophotometric investigations, connected with the optical characteristics of ascorbic acid. The absorption band of ascorbic acid is in the ultraviolet region, which is explained by the $\begin{array}{c} | \\ -C - C - OH \\ | \end{array}$ group. The absorption maximum is 270 m μ , which corresponds to the presence of a five-member ring [21]. The absorption maximum is mobile; from 245 m μ in acid solutions to 265 m μ in neutral alkaline, which is connected with the presence of conjugate double bonds [9]. $\epsilon_{245} = 695$ (pH = 2, hydrochloric acid solution), $\epsilon_{265} = 940$ (pH = 6.4, phosphate buffer). Values of ϵ are obtained for $0.5 \cdot 10^{-4}$ M solutions in the presence of d-sorbitol as a stabilizer [22]. True, d-sorbitol increases the absorption ascorbic acid [23]. The absorption spectra of an ascorbic acid solution depending upon pH and concentration, obtained by us, are represented in Fig. 1.

In the investigation of ascorbate complexes it is necessary to apply a great surplus of ascorbic acid (for full formation of complexes) and perform spectrophotometry, consequently, a relatively free sample, containing a complex

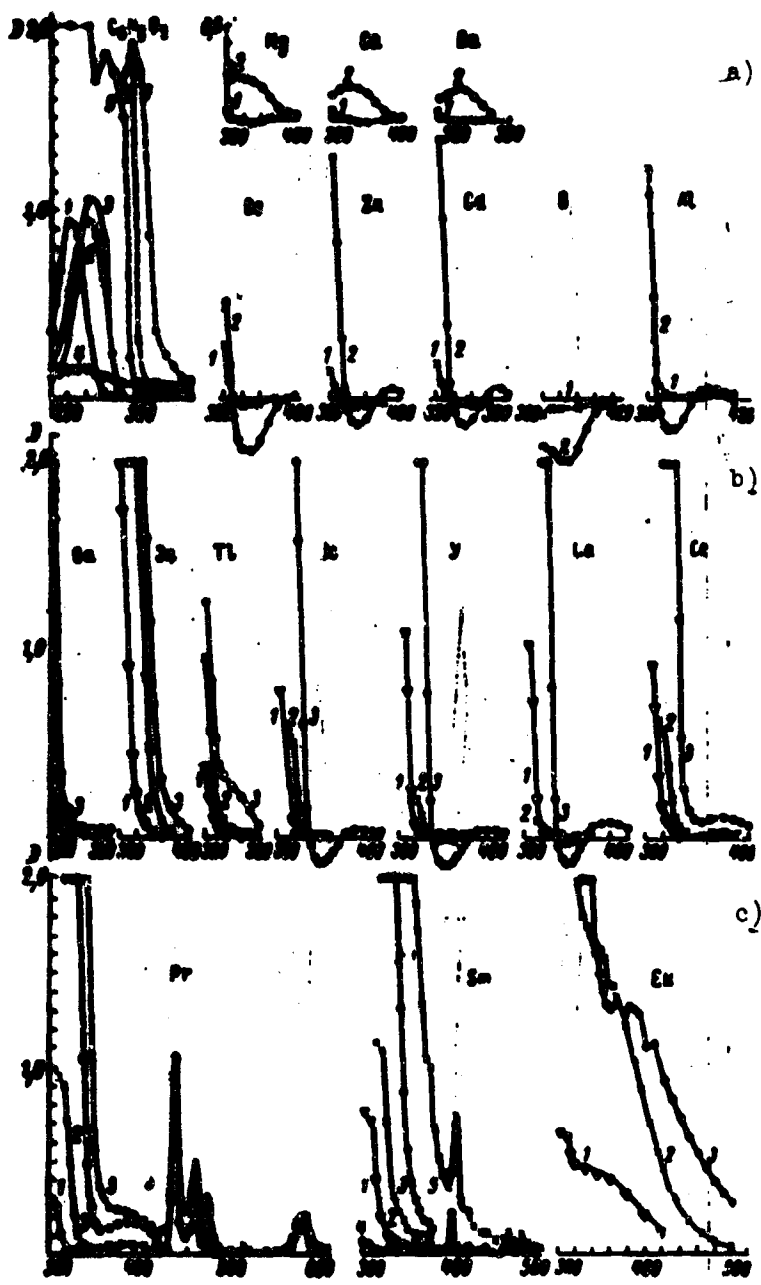


Fig. 1.

former in the same quantity and at the same pH of solution. The absorption of the free sample is compensated by slot of spectrophotometer, starting only with $\lambda = 300-320 \text{ m}\mu$.

Spectrophotometry was produced on [SF-4] (CΦ-4) and SF-5 spectrophotometers in quartz cuvettes 1 cm thick.

"Chemically pure" and "pure for analysis" were used, chiefly chlorides of metals (in case of deviation from this rule the appropriate indications are made), and medical ascorbic acid.

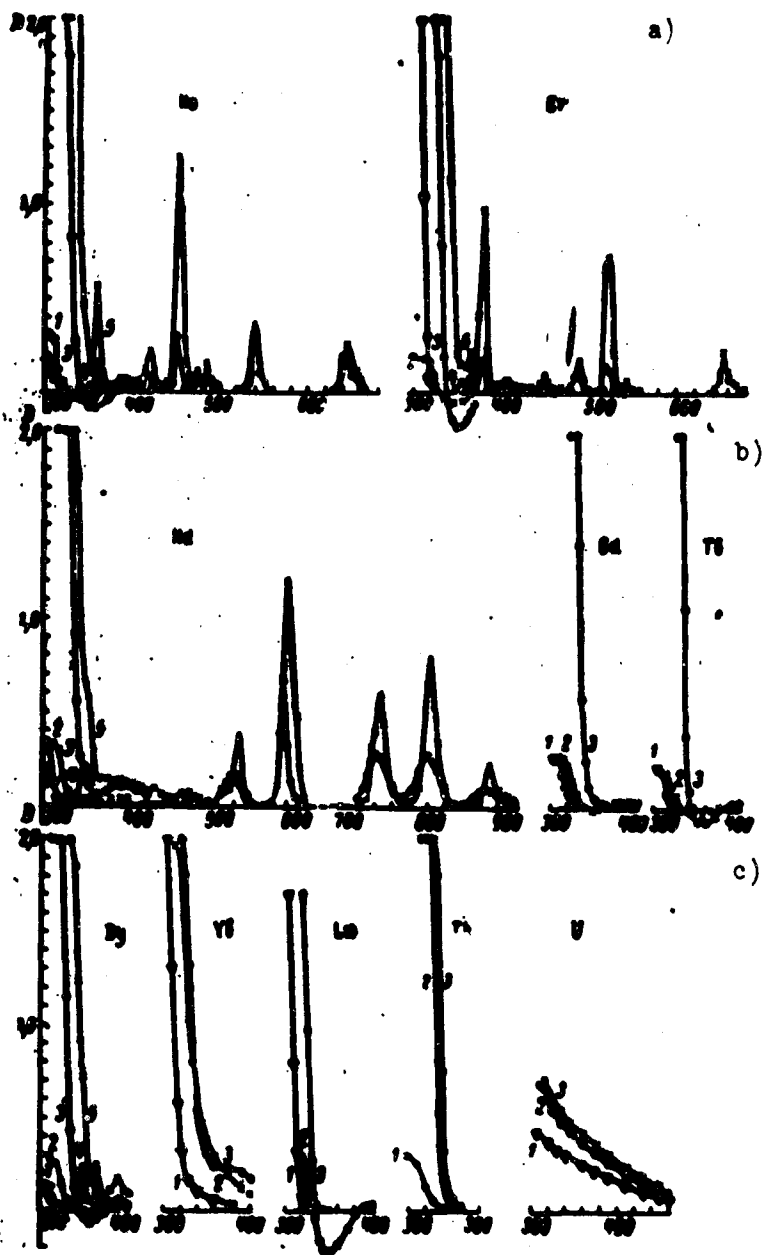


Fig. 2.

The pH of solutions was measured by a pH meter with a glass electrode.

The given value of pH was attained by adding solutions of hydrochloric acid and caustic soda or ammonium. In diluted solutions of ascorbic acid a 0.25 M solution of sodium acetate was introduced as a buffer.

In this report considers the interaction of ascorbic acid with elements of groups II and III of the periodic table.¹

¹Alkali metals were not investigated, since in this case it is possible to speak only about the formation of simple salts, and not complexes. For sodium ascorbate $K_{\text{дисс}} = 1.47 \cdot 10^{-2}$ [24]. The elements of an additional subgroup of group I: copper [25, 26], silver [27, 29] and gold [30-32] are reduced by ascorbic acid to metal and also were not investigated.

Table 1

| No of figure | Element | Molecular concentration of the element | Molecular concentration of ascorbate complexes | pH | No of curve according to pI |
|--------------|---------|--|--|---------------------|-----------------------------|
| 1 | Be | 10 ⁻⁴ | 10 ⁻⁴ | 4.5; 4.7; 4.7; 10.0 | 1, 2, 3, 4 |
| 2 | Mg | 10 ⁻⁴ | 10 ⁻⁴ | 4.5; 4.7; 4.7; 10.0 | 1, 2, 3, 4 |
| 3 | Ca | 10 ⁻⁴ | 10 ⁻⁴ | 4.5; 4.7; 4.7; 10.0 | 1, 2, 3, 4 |
| 4 | Ba | 10 ⁻⁴ | 10 ⁻⁴ | 4.5; 4.7; 4.7; 10.0 | 1, 2, 3, 4 |
| 5 | Zn | 10 ⁻⁴ | 10 ⁻⁴ | 4.5; 4.7; 4.7; 10.0 | 1, 2, 3, 4 |
| 6 | Cd | 10 ⁻⁴ | 10 ⁻⁴ | 4.5; 4.7; 4.7; 10.0 | 1, 2, 3, 4 |

The basic data on the investigated solutions are given in Table 1 and the obtained results are represented in Figs. 1 and 2.

Elements of Group II

In the literature there are data on about $K_{\text{ДМСС}} = 2.8 \cdot 10^{-3}$ for magnesium ascorbate [24]; the formation of an ascorbate complex of zinc [33] and also the reduction of mercury solutions to metal [33, 34] are described.

We investigated the interaction of solutions of beryllium, magnesium, calcium, strontium, barium, zinc and cadmium with ascorbic acid at pH = 4.5 and 5.5. The formation of colorless complexes occurs at pH > 4.5 (at pH = 4.5 only for beryllium, zinc and cadmium). On curves of light absorption maxima (see Fig. 1) are observed: for the magnesium complex at 320-350 mμ; calcium and barium, 345 mμ; zinc and cadmium, 390 mμ. Salts of strontium do not form an ascorbate complex.

The presence of negative values of optical density on curves of light

absorption of ascorbate complexes of beryllium, zinc and cadmium testify to a decrease in absorption by these complexes as compared to free ascorbic acid in the given wavelength interval. This can be explained by a change of the steepness of the absorption band, the long-wave boundary is steeper for complexes than for the acid.

Elements of Group III

Main subgroup

The interaction of boron, aluminum, gallium, indium, and monovalent thallium with ascorbic acid (Fig. 1a, b) has been investigated.

For solutions containing boron a considerable decrease of light absorption is observed in the region of 320-340 μ and pH = 5.5 as a result of the formation of boric-ascorbic acid (by analogy with the formation boric-tartaric acid [35]).

For solutions containing aluminum a decrease in absorption in the region of 330-370 μ is connected with the sharp growth of optical density at $\lambda \approx 330 \mu$.

For ascorbate complexes of gallium, indium and monovalent thallium there are absorption curves with sharp slopes, without maxima. For thallium the formation of a complex starts at pH > 2.5, since the absorption curves of solutions of thallium nitrate and ascorbate at pH = 2.5 coincide, and an increase in optical density is observed at pH > 2.5.

For ascorbate complex of indium the absorption band is wider.

With growth of pH the absorption bands shift into the long-wave region; solutions are colored pale yellow.

We investigated 0.004 M solutions of gallium and indium and a 0.04 M solution of thallium (pH = 5.5) at ascorbic acid concentrations of 0.04, 0.1 and 0.5 M. At an ascorbic acid concentration less than 0.1 M the complex of gallium hydrolyzes. With increase of ascorbic acid concentration up to 0.5 M an accumulation of ascorbate complexes of gallium and thallium occurs (for thallium the concentration is 10 times larger than for gallium and indium). For indium a 0.1 M concentration of ascorbic acid is sufficient for full formation of the complex, i.e., a 25 fold surplus in the molar ratio.

Of the last three complexes the most durable and interesting in an optical sense is the complex of indium. Spectrophotometric determination of indium in the form of an ascorbate complex can be conducted at indium concentration $n \cdot 10^{-4}$ M (0.1 M solution of ascorbic acid; pH = 5.5; cuvette, 1 cm).

Additional subgroup

From the source material we know about the formation of an ascorbate complex of thorium and about the wide use in colorimetric analysis of an ascorbate complex of uranium. About thorium we know that at $\text{pH} = 4-4.5$ a negatively charged complex will be formed, but at $\text{pH} = 0-1$, a positively charged one. The first is adsorbed by anionites in the ascorbate form, along with Ti, Zr, U, V, Mo and W [36, 37]; the second is adsorbed by cationite in the H^+ form (Dowex-5) together with elements of the additional subgroup of group IV [38].

Works [36, 37] indicate that rare earth elements do not form negatively charged ascorbate complexes.

We know that uranium will form a yellow-brown ascorbate complex at $\text{pH} = 4-4.2$; its solutions obey the Beer law at $410 \text{ m}\mu$ [20, 39]. The composition of the complex is 1:1 [40]; $K_{\text{H}} = 1.3 \cdot 10^{-3}$; $\epsilon_{465} = 3.92 \cdot 10^{-2}$ [41]. The behavior of the complex on anionite amberlite, IRA = 400, is investigated in work [36]; it was established that the maximum adsorption occurs at $\text{pH} = 4-4.5$; desorption is carried out by a 0.1 N solution of hydrochloric acid, the complex is weaker than acetate. In the area of $\text{pH} = 5-7$ the complex will have the structure $\text{NH}_4[\text{UO}_2(\text{OH})_2(\text{C}_6\text{H}_7\text{O}_6)]$ added to it; at $\text{pH} < 3$ during a positive or neutral complex will be formed [42].

We investigated the interaction of ascorbic acid with solutions of scandium, yttrium, lanthanum, trivalent cerium, praseodymium, neodymium, samarium, gadolinium, dysprosium, erbium, ytterbium, europium, terbium, holmium, lutetium, thorium and uranium.

The initial solutions of salts were hydrochloric acid; titer of solutions was calculated by suspensions of oxides and carbonates (in the last case it was checked). To prepare solutions of cerium, gadolinium and thorium we used nitrates, uranium - acetate.

The obtained results are represented in Fig. 1b, c and Fig. 2.

For all the above-mentioned elements the formation ascorbate complexes is connected with a sharp growth of optical density in the region of $\lambda \approx 330-340 \text{ m}\mu$. With increase of solution pH the absorption bands are displaced into the long-wave region; this appears especially for europium. The absorption maxima of solutions of simple salts increase, especially at $\text{pH} = 4.5$; in certain cases they are displaced somewhat into the long-wave region. Maxima of light absorption

undergoing the strongest changes are represented in Table 2.

For scandium, yttrium, lanthanum, terbium, dysprosium, holmium, erbium and lutetium in the region of $\lambda = 340-380 \text{ m}\mu$ the absorption of ascorbate complexes is less than the absorption of ascorbic acid, negative values of optical density; the minima of optical density with increase of pH are deepened and shift into the long-wave region.

The color of solutions of ascorbinates of rare earth elements is yellow or pale yellow for scandium, yttrium, lanthanum, cerium, samarium, dysprosium, europium (intensely yellow, orange at great concentration), ytterbium and uranium (intensely yellow). The complexes for gadolinium, terbium, lutetium and thorium are colorless. For praseodymium the complex is yellow-green, for neodymium - blue, for holmium - yellow-pink, for erbium - pink.

Table 2

| Element | Maximum in solution of simple salt | | Maximum in solution of ascorbate | |
|---------|------------------------------------|-----------|----------------------------------|-----------|
| | $\lambda, \text{m}\mu$ | $D_{0.1}$ | $\lambda, \text{m}\mu$ | $D_{0.1}$ |
| Sc | 340 | 0.115 | 340 | 0.115 |
| Y | 340 | 0.175 | 340 | 0.175 |
| La | 340 | 0.235 | 340 | 0.235 |
| Ce | 340 | 0.295 | 340 | 0.295 |
| Pr | 340 | 0.355 | 340 | 0.355 |
| Nd | 340 | 0.415 | 340 | 0.415 |
| Pm | 340 | 0.475 | 340 | 0.475 |
| Sm | 340 | 0.535 | 340 | 0.535 |
| Eu | 340 | 0.595 | 340 | 0.595 |
| Gd | 340 | 0.655 | 340 | 0.655 |
| Tb | 340 | 0.715 | 340 | 0.715 |
| Dy | 340 | 0.775 | 340 | 0.775 |
| Ho | 340 | 0.835 | 340 | 0.835 |
| Er | 340 | 0.895 | 340 | 0.895 |
| Lu | 340 | 0.955 | 340 | 0.955 |

*In these cases the rise in maximum is caused by a general increase of light absorption in the shortwave region.

It is necessary to note that elements of the cerium group (0.1 M solutions of elements in 0.5 M solutions of ascorbic acid) at pH = 5.5 probably deposit in the form of basic ascorbinates; elements of the yttrium group stay in solution even at large values of pH.

For spectrophotometric analysis of greatest interest are ascorbinates of europium and samarium (not counting uranium). It has been shown that these elements can have a valence of +2. It is possible that the formation of ascorbate complexes of europium and samarium is connected with their initial reduction.

Conclusions

The formation of ascorbate complexes for elements of groups II and III of the periodic table (excluding strontium and mercury) evokes a change in absorption spectra of solutions of simple salts; maxima of light absorption are increased and sometimes are displaced into the long-wave region (Pr, Nd, Ho, Er); absorption strongly increases in the region of 320-340 m μ , combined with a shift absorption band of ascorbic acid into the long-wave region (Zn, Cd and elements of group III, excluding B); for certain elements negative values of optical density are obtained in the region of $\lambda = 320-370$ m μ , i.e., light absorption decreases (Be, Zn, Cd, B, Al, Sc, Y, La, Tb, Dy, Ho, Er, Lu); new maxima appear (Mg 320-340 m μ ; Cu and Ba, 345 m μ ; Zn and Cd, 390 m μ).

Summary

The formation of ascorbic complexes of the elements of the second and third groups of the periodic system (excluding strontium and mercury) causes variations in the absorption spectra of simple salt solutions: the maxima of light absorption increase and sometimes shift into long wave region (Pr, Nd, Ho, Er); there increases absorption in the 320-340 m μ region associated with the displacement of the absorption band of ascorbic acid into long wave region (Zn, Cd and elements of the third group, excluding B); obtained for some elements are negative values of optical density in the $\lambda = 320-370$ m μ region, i.e. light absorption decreases (Be, Zn, Cd, B, Al, Sc, Y, La, Tb, Dy, Ho, Er, Lu); there appear new maxima (Mg 320-340 m μ ; Cu and Ba 345 m μ ; Zn and Cd 390 m μ). (English summary)

Literature

1. Ye. M. Brunberg, I. A. Pavel, and K. P. Stolyarov. ZhAKh, 5, 195, 1950.
2. L. Erdey and E. Bodor. Magyar. Kém. Folyoirat, 56, 277-287, 1950.
3. L. Erdey. ZhAKh, 8, 356, 1953.
4. G. Gopala Rao, V. Narayana Rao. Zn and Chem., 147, 4, 388-347.
5. A. H. Donald. Ind. chem. abstr. 32, 545-547, 1932.
6. N. Kuznetsovsky. Vnd. zool., 12, 1, 1-7, 1934.
7. A. Kh. Batalin. Transaction of the Orenburgsk Institute of Agriculture, 10, 339, 1960.
8. Singh Balwant. res. bull. Panjab univ., 11, No. 3-4, 221-226, 1960, 1961.
9. V. M. Perezovskiy. Chemistry of vitamins. Vitamin C, Moscow, Pishchepromizdat, 40-80, 1959.
10. I. I. Gal. Bull. Inst. chim. ind. "Bark Khimich", 4, 71-77, 1932.
11. M. S. Sergeev, E. Becker. Ann. ent. biophys. chim. phys., 75-81, 1934.
12. L. Erdey, E. Bodor. Ann. chem., 51, 412, 1932.
13. E. S. West. J. Ind. Chem., 147, 102, 1932.
14. L. Erdey, A. Bodor. Zn and Chem., 134, 472, 1937.
15. B. V. Ptitsyn and V. A. Kozlov. ZhAKh. 4, 1, 135, 1949.
16. L. Erdey, A. Bodor. Zn and Chem., 132, 102, 1937.
17. S. Brown. J. Pharm. Soc., 51, 422-424, 1932.
18. W. Fiedler. Pharmaz., 14, 13-15, 1934.
19. M. Pleschka, N. Zavayeva. Zn and Chem., 132, 170, 1934.

17. G. H. Khadobesh, E. Medvedeva, and E. Palash. *Acta chim. acad. sci. Hung.*
7, 47-417, 1961.

21. G. A. Anstey. *J. appl. physics*, 33, 41, 1962.
22. J. S. Lawendel. *Nature*, 183, 1428, 1957.
23. J. S. Lawendel. *Nature*, 178, 672, 1955.

24. P. S. Romanchuk. *DAN SSSR*, 117, 663, 1957.

25. L. Erdey, G. Sipos. *Zs. anal. Chem.*, 107, 105, 1957.
26. J. Kerkisch, A. Farag. *Mikrochim. acta*, 20 & 645, 1958.
27. E. Stathis, H. Gates. *Anal. chem.*, 30, 271, 1958.
28. O. Horn-Rosenblatt. *Acta Med.*, 55, 215, 1954.
29. L. Erdor, L. Buzas. *Acta chim. Acad. sci. Hung.*, 4, 105, 1954.
30. E. Stathis, H. Gates. *Ind. eng. chem. anal. ed.*, 31, 501, 1954.

31. I. K. Fshenitsyn and S. N. Ginzburg. *News of sector of platinum, IONKh*,
No. 30, 171, 1955.

32. L. Erdey, G. Raay. *Tokyo*, 1, 133-143, 1955.
33. M. v. Šušic. *Bull. Inst. nuclear sci. "Boris Kidrich"*, 5, 66-68, 1955.
34. G. Rao. *Zs. Anal. Chem.*, 108, 28, 1955.
35. D. Sriwatsava. *Rev. anal. chem.*, 34, No 2, 289-290, 1955.
36. J. Kerkisch, A. Farag, P. Hecht. *Mikrochim. acta*, 414, 1955.
37. J. Kerkisch, A. Farag. *Zs. anal. chem.*, 105, 161, 1955.
38. J. Kerkisch, P. Antal. *Zs. anal. Chem.*, 170, 129-130, 1957.
39. A. Emmerle. *Acta brev. serri. physiol. pharmcol. microbiol.*, 4, 141, 1954.
40. Z. Gregorzyk. *Acta Polon. Pharmaceutica*, 15, 2, 123, 1958.
41. Z. Gregorzyk. *Acta Polon. Pharmaceutica*, 15, 4, 233, 1958.
42. I. J. Gal. *Bull. Inst. nuclear sci. "Boris Kidrich"*, 6, No 119, 173, 1955.

Submitted
28 January 1963

REDUCING PROPERTIES OF IONITES

N. A. Nechay, M. N. Zvereva, and T. M. Grekovich

The reducing properties of ionites have been investigated comparatively little, in spite of the fact that a large number of works are devoted to the study of exchange of ions on hard sorbents. For analytic chemistry the knowledge of reducing properties of ion exchangers has practical value.

A number of investigators [1-7] observed the reducing ability of cationites.

V. N. Lenskaya [8] considered the influence of pH, temperature, concentration of solutions of oxidizers and other factors on the oxidation processes of resins of brands [NSK] (HCH), [RSK] (PCK), [PFSK] (ΠФСК), [SPG] (СНГ), [SBS] (СБС), [MSF] (МСФ), [GKh] (ГХ), [TN] (ТН), [NO] (НО), also others. Her work allows us to make the following conclusion: under the effect on ionites of buffered solutions of oxidizers containing oxygen in their molecule is a dependence of the oxidation rate and quantity of reduced oxidizer on concentration of hydrogen ions, is observed; there is a certain selectivity of the action of different oxidizers on ionites; an increase in oxidizer concentration evokes an increase of the rate of the oxidizing-reducing process; the oxidation reaction of ionite is not reversible and the reducing ability of ionite is gradually lowered.

V. N. Lenskaya with colleagues [9, 10] showed the possibility of using ionites as specific reducers, valuable for analytic chemistry by the fact that they do not introduce outside inorganic ions into the investigated solution.

In a number of works [11-15] it is noted that ionic exchange and reduction of ions in the solution occur simultaneously and independent of each other; that the

source of reducing properties of resins is not ionogen groups or elementary nuclei of resins (sulphophenolic and sulphostyrene).

The goal of this work is the investigation of the reducing ability of certain ionites of Soviet brands with respect to different oxidizers. For the first time we investigated the reducing properties of cations of [KU-2] (KV-2), KU-2-4, KU-2-12, KU-2-16, [SBSR] (CECP), [KB-4P-2] (KB-4П-2), and anionites [AN-1] (AH-1), [EDE-10-P] (ЭДВ-10П), [AV-16] (AB-16), and AV-17. As oxidizers we applied solutions of KMnO_4 , $\text{K}_2\text{Cr}_2\text{O}_7$, NH_4VO_3 , and $\text{Fe}_2(\text{SO}_4)_3$, whose normal oxidizing potentials are 1.51, 1.36, 1.01 and 0.77 v respectively.

Experiments were conducted by the static method by means of agitating a suspension of resin (0.5 g) with 50 ml of a solution having a definite concentration of oxidizer and hydrogen ions. Time of agitation (2-10 hours) necessary to establish equilibrium between the resin and the solution was determined by preliminary experiments.

The influence of acidity of the medium on the oxidizing-reducing process may be seen in Fig. 1. The minimum, existing on the reduction curve of potassium permanganate, is in region with pH = 5-6; in an acid medium full reduction of Mn^{+7} to Mn^{+2} occurs; in an alkaline medium full reduction of Mn^{+7} to Mn^{+4} . The least reduction of manganese occurs in the region close to neutral. During reduction of Cr^{+6} and V^{+5} the reducing ability of resins drops as the acidity of the solution decreases.

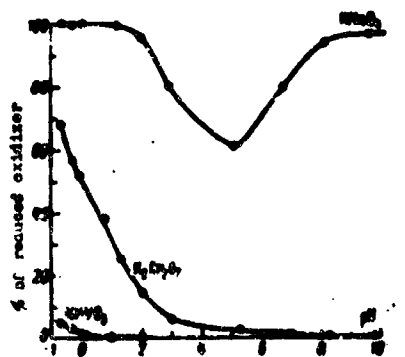


Fig. 1. Oxidization of cationite SBSR by different oxidizers (concentration of oxidizers in initial solutions was 0.05 N).

To investigate the influence of different content of divinylbenzene [DVB] (ДВВ) on the reducing properties of resin we took three brands of cationite KU-2; KU-2-4, KU-2-12, and KU-2-16. In experiments with solution of potassium permanganate full reduction of Mn^{+7} to Mn^{+4} and Mn^{+2} by all brands of KU-2 resin occurred.

Experiments with potassium bichromate showed (Table 1) that an increase in the percentage of DVB in resins of brand KU-2 increases their resistance to oxidizers in an insignificant degree. This is possibly explained by the fact that the easily oxidizing groups of resin are located at the ends of macromolecules and the packing of the structure essentially does not affect the oxidizing-reducing

Table 1. Effect of Potassium Bichromate on Cationite KU-2 with Different Content of DVB (Concentration of $K_2Cr_2O_7$ solution, 0.04 N)

| Acidity of solution | Quantity of reduced chromium, in % | | | Acidity of solution | Quantity of reduced chromium, in % | | |
|---------------------|------------------------------------|---------|---------|---------------------|------------------------------------|---------|---------|
| | KV-4-4 | KV-4-12 | KV-4-25 | | KV-4-4 | KV-4-12 | KV-4-25 |
| 4.00 N | 20.6 | 20.7 | 20.3 | 3.9 | 3.1 | 2.6 | 2.4 |
| 2.00 | 20.3 | 20.0 | 24.3 | 8.3 | 1.2 | 0.4 | 0.3 |
| 1.17 | 21.7 | 21.0 | 18.5 | 0.9 | 0 | 0 | 0 |
| pH=0.8 | 18.1 | 13.4 | 9.5 | 0.4 | 0 | 0 | 0 |
| 1.3 | 14.3 | 3.7 | 4.3 | 0.8 | 0 | 0 | 0 |
| 2.0 | 3.3 | 2.8 | 3.0 | | | | |

process.

From the obtained data on reduction of potassium by different ionites depending upon medium acidity (Table 2) it is clear that the stablest are from cationites KB-4P-2 and from anionites AV-17. During reduction of potassium bichromate (Table 3) the stablest also turned out to be KB-4P-2 and AV-17. The biggest reducing ability with respect to Cr^{+6} belongs to AV-16, EDE-10-P and SBSR, which reduce chromium in a wide interval of acidity up to pH 7, which agrees with the data of V. N. Lenskaya on oxidation of other brands of ionites.

Table 2. Oxidation of Ionites by Potassium Permanganate (Concentration of $KMnO_4$ Solution, 0.02 N)

| Acidity of solution | Quantity of reduced manganese in % | | | | | | |
|---------------------|------------------------------------|------|---------|------|----------|-------|-------|
| | KV-4 | CSCP | KB-4P-2 | AN-1 | EDE-10-P | AS-16 | AS-17 |
| 4.00 N | 100 | 100 | 100 | 100 | 100 | 100 | 100 |
| 2.00 | 100 | 100 | 100 | 100 | 100 | 100 | 100 |
| 1.17 | 100 | 100 | 100 | 100 | 100 | 100 | 100 |
| 1.3 | 100 | 100 | 87.4 | 100 | 100 | 100 | 100 |
| 2.0 | 100 | 81.7 | 81.1 | 100 | 100 | 100 | 100 |
| 3.1 | 100 | 81.7 | 81.3 | 81.3 | 100 | 100 | 100 |
| 4.5 | 98.4 | 81.6 | 28.0 | 81.3 | 98.6 | 99.7 | 87.5 |
| 6.0 | 98.6 | 81.9 | 72.8 | 100 | 100 | 100 | 87.9 |
| 8.4 | 100 | 81.7 | 84.8 | 100 | 100 | 100 | 100 |
| 9.8 | 100 | 80 | 85.8 | 100 | 100 | 100 | 100 |

Table 3. Oxidation of Ionites by Potassium Bichromate (Concentration of $K_2Cr_2O_7$ Solution, 0.02 N)

| Acidity of solution | Quantity of reduced chromium in % | | | | | | |
|---------------------|-----------------------------------|------|---------|------|----------|-------|-------|
| | KV-4 | CSCP | KB-4P-2 | AN-1 | EDE-10-P | AS-16 | AS-17 |
| 4.00 N | 20.6 | 20.3 | 21.1 | 20.0 | 100 | 100 | 100 |
| 2.00 | 20.7 | 20.4 | 0 | 20.4 | 100 | 100 | 100 |
| 1.17 | 21.3 | 21.4 | 0 | 21.1 | 100 | 100 | 100 |
| 1.3 | 17.3 | 20.3 | 0 | 4.6 | 100 | 100 | 100 |
| 2.0 | 13.4 | 14.1 | 0 | 4.0 | 100 | 100 | 100 |
| 3.1 | 4.6 | 6.0 | 0 | 2.0 | 100 | 100 | 100 |
| 4.5 | 3.7 | 3.0 | 0 | 0.4 | 100 | 100 | 100 |
| 6.0 | 0 | 0 | 0 | 0 | 100 | 100 | 100 |
| 8.4 | 0 | 0 | 0 | 0 | 100 | 100 | 100 |
| 9.8 | 0 | 0 | 0 | 0 | 100 | 100 | 100 |

Table 4 gives data on reduction of pentavalent vanadium by ionites.

Table 4. Oxidation of Ionites by Ammonium Vanadate
(Concentration of NH_4VO_3 Solution, 0.02 N)

| Acidity of solution | Quantity of reduced vanadium in % | | | | | | |
|---------------------|-----------------------------------|------|---------|-------|-------|------|----------|
| | KU-2 | CSCP | KB-4P-2 | AV-16 | AV-17 | AN-1 | SBS-10-P |
| 0.02 N | 0.8 | 4.4 | 0 | 2.5 | 0 | 0.5 | 2.3 |
| 0.05 N | 0.8 | 1.7 | 0 | 2.1 | 0 | 0.5 | 1.9 |
| 0.1 N | 0.8 | 0.5 | 0 | 1.9 | 0 | 0.1 | 1.5 |
| 0.2 N | 0.8 | 0 | 0 | 1.5 | 0 | 0 | 1.2 |
| 0.5 N | 0.8 | 0 | 0 | 0.8 | 0 | 0 | 0.5 |
| 1 N | 0.8 | 0 | 0 | 0.5 | 0 | 0 | 0.1 |
| 2 N | 0.8 | 0 | 0 | 0 | 0 | 0 | 0 |

From Table 4 it is clear that vanadium oxidizes AV-16 and EDE-10-P; in very acid solutions KU-2, AN-1 and SBS. KB-4P-2 and AV-17 resist the action of vanadium.

With all the above-mentioned brands of resins we made experiments to study their interaction with $\text{Fe}_2(\text{SO}_4)_3$ solutions. It was found that of all the studied ionites iron oxidizes only AV-16 to an insignificant degree (~1.5%); as one should expect for iron, oxidation does not depend on pH.

According to magnitude of reducing ability the investigated ionites can be placed in a series: AV-16 > EDE-10-P > SBSR > KU-2 > AN-1 > AV-17 > KB-4P-2.

For the quantitative characteristics of the reducing properties of ionites with respect to KMnO_4 and $\text{K}_2\text{Cr}_2\text{O}_7$ we calculated the percent of reduced manganese and chromium for 1 g of resin depending upon the number of sorption - desorption cycles. Experiments were produced by means of agitating a suspension of resin (0.5 g) with 50 ml of a solution, having a 0.05 N concentration of oxidizer and acidity of 1 N by H_2SO_4 , until equilibrium is established. We filtered the ionite and extracted from it the absorbed ions, shifting simultaneously the cationite to the H^+ form and anionite to the OH^- form. In united filtrates we determined the content of reduced oxidizer. The regenerated resin was again agitated with a solution of oxidizer, etc.

It turned out that the reducing ability of ionites with respect to potassium permanganate is kept practically completely for 5 cycles, except for anionites AN-1, EDE-10-P and AV-16 which on the 3-5th cycle are destroyed. In Fig. 2 one may see the gradual extinction of reducing properties of ionite with respect to potassium bichromate.

Anionites AV-16 and EDE-10-P were completely dissolved on the fourth cycle. Since the solubility of resin is increased with decrease of transverse bonds in

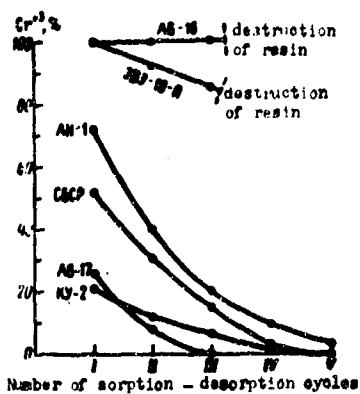


Fig. 2. Reducing properties of ionites with respect to $K_2Cr_2O_7$ depending upon the number of sorption - desorption cycles.

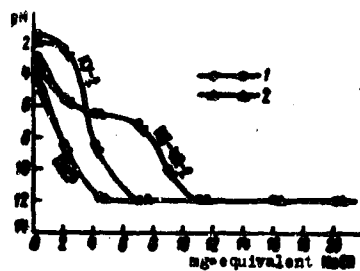


Fig. 3. Curves of potentiometric titrating of cationites by a NaOH solution. 1 - before the effect of oxidizer; 2 - after the effect of oxidizer.

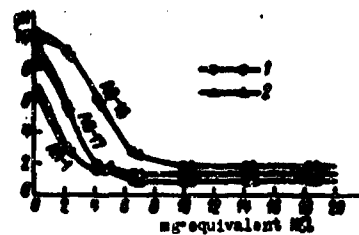


Fig. 4. Curves of potentiometric titrating of anionites by a HCl solution. 1 - before the effect of oxidizer; 2 - after the effect of oxidizer.

the polymer, we can assume that during oxidation of ionites transverse bonds i.e., methylene bridges, are destroyed.

I. P. Losev and A. S. Tevlina [12] assume that the source of the reducing properties of ionites are not the ionogen groups, but aldehyde and quinoid groups. Consequently, the oxidizers do not have to affect the exchange capacity of ionite. To check this assumption we investigated the exchange capacity of ionite by the method of potentiometric titrating of a resin by solutions of HCl (anionite) or NaOH (cationite) before and after the effect of an oxidizer. As oxidizer we took a 0.02 N solution of potassium bichromate having acidity of 1.17 N by H_2SO_4 . As can be seen from Figs. 3 and 4 partial oxidation of ionite practically does not affect the slope of titrating curves of the investigated ionite, and, consequently, during oxidation ionogen groups do not participate.

Summary

It has been demonstrated by the present investigation that ion-exchange resins КУ-2, КВ-4П-2, СБСР, ЭДЭ-10-П, АН-1, АН-17 are not oxidized by 0.02 n solutions $Fe_2(SO_4)_3$ at $[H^+] = 10^{-10} - 5 \frac{g-ion}{l}$; the resins АН-17 and КВ-4П-2 are not oxidized by 0.02 n solutions NH_4VO_3 at $[H^+] = 10^{-7} - 5 \frac{g-ion}{l}$ and КУ-2 - at $[H^+] = 10^{-7} - 2.6 \frac{g-ion}{l}$; КВ-4П-2 is not oxidized by 0.02 n solutions $K_2Cr_2O_7$ at $[H^+] = 10^{-10} - 2.6 \frac{g-ion}{l}$, and АН-17 - at $[H^+] = 10^{-10} - 10^{-3} \frac{g-ion}{l}$; all investigated ion-exchange resins are oxidized by 0.02 n solutions $KMnO_4$ at $[H^+] = 10^{-10} - 5 \frac{g-ion}{l}$.

According to their stability towards oxidants ion-exchange resins can be arranged in a row as follows: КВ-4 П-2 > АН-17 > КУ-2 > АН-1 > СБСР > ЭДЭ-10-П > АН-16.

The partial oxidation of the ion-exchange resins by 0.02 n solution $K_2Cr_2O_7$ has been stated to have practically no effect on the exchange capacity value. [English summary]

Literature

1. F. G. Prokhorov and K. A. Yankovskiy. *Zav. lab.*, 13, 6, 656, 1947.
2. Yu. I. Usatenko and O. V. Datsenko. *Zav. lab.*, 15, 7, 7791, 1949.
3. I. E. Apel'tsin, V. A. Klyachko, Yu. Yu. Lur'e, and A. S. Smirnov. *Ionites and their application*, Moscow, Standartgiz, 55, 1949.
4. L. I. Ryabchikov and Ye. . Terent'yev. *Successes of chemistry*, 19, 2, 220, 1950.
5. G. Ye. Boyd, I. S. Shubert, and A. V. Adamson. *Collection: Chromatographic method of separating ions*, Moscow, IL., 257, 1949.
6. H. T. Mills, E. K. Stadtman, and W. W. Killey. *J. Amer. chem. soc.*, 76, 15, 4041, 1954.
7. N. Hartler and O. Samuelson. *Anal. chem. acta*, 8, 2, 130, 1953.
8. V. N. Lenskaya. *Transactions of the commission for analytic chemistry*, 6, Issue 9, 333, 1955.
9. V. N. Lenskaya and L. N. Kul'berg. *Scientific annual of Saratov University for 1954*, 519.
10. V. N. Lenskaya, M. T. Chernysh, Ye. P. Zayonts, and L. V. Aleksandrova. *Uch. zap Saratov University*, 71, 211-215, 1958.
11. Ye. V. Trostyanskaya. *Transaction of commission on analytic chemistry*, 6, Issue 9, 215, 1955.
12. I. P. Losev and A. S. Tevlina. *Transactions of commission for analytic chemistry*, 6, Issue 9, 326, 1955.
13. Ye. B. Trostyanskaya, I. P. Losev and A. S. Tevlina. *Successes of chemistry*, 24, 1, 79, 1955.
14. Ye. B. Trostyanskaya, I. P. Losev, and A. S. Tevlina. *ZhAKh*, 11, 6, 578, 1956.
15. A. G. Davydov and G. M. Lisovskaya. *Koll. zh.*, 23, 2, 145, 1961.

Submitted
14 November 1962

INFRARED ABSORPTION SPECTRA OF ANHYDROUS SULFURIC AND
ORTHOPHOSPHORIC ACIDS

S. A. Shchukarev, T. G. Balicheva, K. Ya. Borchka, and
M. A. Kukhareva

The wide application of anhydrous mineral acids in a whole series of organic productions requires the thorough study of their behavior in pure form.

We attempted to study the state of isostructural molecules of acids of the third period of periodic table and, in particular, the influence of the tied hydrogen bond on the proton donar function of these acids, by using the high sensitivity of infrared vibration spectra to change of structure of molecules. Informations about oscillatory frequencies of sulfuric and orthophosphoric acids, obtained basically from spectra of combination diffusion, are rather contradictory [1-6]. Region of valent O - H vibrations due to the large experimental difficulties is studied very little.

Table 1 gives the presently available information about frequencies of valent O - H vibrations for anhydrous sulfuric acid.

Table 1

| Substance | Method of investigation | Maximum of absorption band, cm^{-1} |
|-------------------------------------|-------------------------|--|
| H_2SO_4 liquid 100% | Raman [1] | 2985 |
| H_2SO_4 liquid 100% | Raman [2] | 3025 |
| H_2SO_4 liquid 100% | Raman [3] | 2850, 3000 |
| H_2SO_4 liquid 100% | IKS [4] | 2970 ± 50 |
| H_2SO_4 solid 100% | IKS [4] | 2980 |

If frequency of valent O - H vibrations for H_2SO_4 is needed only in a more precise definition, then the matter is worse with these frequencies for orthophosphoric acid. Médard [2] found in region of valent O - H vibrations a wide band, spreading from 3700 to 2700 cm^{-1} with maximum near 3300 cm^{-1} . Simon [6-7]; not finding in this region even a weak absorption band in the Raman-spectrum of orthophosphoric acid, considers that the system investigated by Médard did not correspond to a composition of orthophosphoric acid.

Therefore, the goal of our investigation was a more precise definition of the results in the region of valent O - H vibrations and also the investigation of the influence of lowered temperature on position of the maximum and bandwidth of absorption of the O - H . . . O complex.

The results, obtained by Giguère [4] for solid 100% sulfuric acid, evokes surprise both in the small magnitude of displacement $\Delta\tilde{\nu} = 10^{-1}$ cm and also in the direction of displacement, indicating a weakening of hydrogen bonds in the O - H . . . O complex with lowering of temperature. Crystalline orthophosphoric acid, roentgenographically studied by Furberg [7], is characterized by three identical P - O bonds 1.57 Å long. The fourth P - O bond, assumed "keto," with shorter length of 1.52 Å P - O - H . . . O = P; the very short distance $R(O \cdot \cdot \cdot O) = 2.53$ Å should correspond to a very durable hydrogen bond of the associating molecule of phosphorous acid. The distance between hydroxyls (P - O - H . . . O - H), equal to $R(O \cdot \cdot \cdot O) = 2.84$ Å, should correspond to a weaker hydrogen bond. On the basis of given X-ray structural data one should have expected the appearance in vibration spectrum of absorption of H_3PO_4 in the region of valent O - H vibrations of two bands, from which one should be strongly widened and considerably displaced in the low frequency region, corresponding to a strong hydrogen bond with distance O . . . O = 2.53 Å.

According to X-ray diffraction analysis of Pascard [8], in the grid of sulfuric acid there are also 2 types of hydrogen bonds, O - H . . . O - H and O - H . . . O = S with corresponding distances of 2.84 Å and 2.64 Å. We have no information about the distance O . . . O in anhydrous chloric acid, but the proximity and number of observed frequencies of vibrations $\nu = O$ and $\nu = O$ in orthophosphoric, sulfuric and chloric acids testify to a tetrahedral configuration of their anions and an analogy in the structure of acids.

We obtained 100% orthophosphoric acid by two methods:

1. From crystalline 96% H_3PO_4 ; to melt at $t = 50^\circ C$ we added a calculated quantity of "chemically pure" P_2O_5 .

2. Prolonged dehydration of 8.5% H_3PO_4 in a vacuum with subsequent double recrystallization according to method of Simon [7]. In the H_3PO_4 crystals obtained by this method, a $H_4P_2O_7$ impurity was completely absent, its content by the first method was 2-12% depending upon modification of the applied P_2O_5 . The composition of the obtained acid was controlled by titrating 0.1 N KOH and qualitative reactions with $AgNO_3$ in the absence of pyrophosphoric and metaphosphoric acids.

100% H_2SO_4 was obtained by adding to a suspension of oleum a calculated quantity of concentrated "chemically pure" H_2SO_4 , $d = 1.832 \text{ g/cm}^3$. The composition was also controlled by titrating. Vibration spectra of substances were taken on a recording double-beam [IKS-14] (MHC-14) infrared spectrometer on LiF and NaCl prisms; the light source was a globar.

Calibration was produced on an vibration rotary spectra NH_3 , C_6H_6 , HCl , CO and CO_2 . The stability of calibration was constantly checked by a standard spectrum of polystyrene. The optical windows of the convette were plane-parallel thin

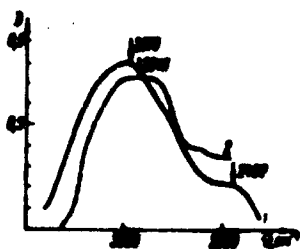


Fig. 1. Infrared absorption spectrum of anhydrous sulfuric acid, thickness of film $\sim 2.6 \mu$. a - $t = 20^\circ C$; b - $t = -40^\circ C$.

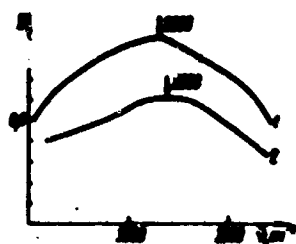


Fig. 2. Infrared absorption spectrum of anhydrous orthophosphoric acid, thickness of film, $\sim 6 \mu$. a - $t = 20^\circ C$; b - $t = -40^\circ C$.

windows of quartz, fluorite and optical AgCl.

The obtained absorption spectra in the frequency range of $3500-2350 \text{ cm}^{-1}$ are shown in Figs. 1 and 2.

Indeed, the very wide absorption band of orthophosphoric acid is displaced by 120 cm^{-1} as compared to the absorption

band of H_2SO_4 and by 540 cm^{-1} as compared to anhydrous $HClO_4$ [9] in the low-frequency region, testifying to the large durability of hydrogen bonds associating the molecule of phosphoric acid. Due to this the force constant of the O - H bond decreases, and the length of O - H is increased. This may be seen from our tentatively calculated values of force constant and interatomic distance, given in Table 2.

The force constant of the O - H bond was calculated by the formula of vibrations of a harmonic oscillator [10]

$$f = 8,889 \cdot 10^{-1} \frac{\nu^2}{r_0 + r_0^3}$$

Table 2

| Substance | $\tilde{\nu}$, cm^{-1} | $f \cdot 10^5$, $\text{dyne} \cdot \text{cm}^{-1}$ | $r_{\text{O-H}}$ Å |
|-------------------------------------|----------------------------------|---|--------------------|
| HClO_4 liquid 100% | 3390 | 6.4 | 0.997 |
| H_2SO_4 liquid 100% | 2970 | 4.9 | 1.06 |
| H_3PO_4 liquid 100% | 2850 | 4.5 | 1.08 |

and the interatomic $r_{\text{O-H}}$ distance, by the approximation formula of Badger [11]

$$r = \sqrt[3]{\frac{f}{c_{1j}}} + D_{1j}$$

The values of constants c_{1j} and D_{1j} are accepted by us in reference to atoms H and O equal to $\sqrt[3]{c_{1j}} = 87.1$, $D_{1j} = 0.335$.

Figure 3 built on these data shows the explicit functional dependence between the weakening of durability of the O - H bond and increase of length, i.e., interatomic C - H distance, with increase of electronegativity of the anion.



Fig. 3.
Dependence between the force constant of O - H bond and interatomic O - H distance in HClO_4 , H_2SO_4 , H_3PO_4 .

In connection with the fact that the acids we studied possess strong corroding properties and sufficiently large absorption, to study the spectra with controlled thickness of layer we applied the weight method of determining layer thickness, checked for water.

The molar indices found on maxima of absorption bands (the average of 6 close values) are given in Table 3.

Figure 4 illustrates on example of sulfuric acid the good convergence of our results. All operations of filling the convette were conducted in a drying chamber with P_2O_5 .

To study the influence of lowered temperature on spectrum of acids we prepared a vacuum absorbing chamber from molybdenum glass with windows of fluorite; its construction differs little from those described in literature [13, 14].

Table 3

| Substance | $\tilde{\nu}$, cm^{-1} | n , $\text{cm}^{-1} \cdot \text{cm}^{-1} = \frac{f}{c_{1j}}$ |
|-------------------------|----------------------------------|--|
| HClO_4 | 3390 | 6.4 |
| H_2SO_4 | 2970 | 4.9 |
| H_3PO_4 | 2850 | 4.5 |

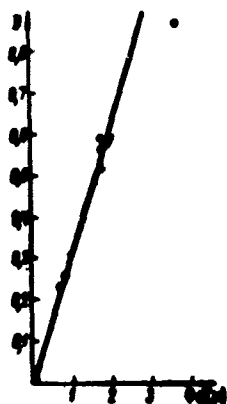


Fig. 4. Dependence between optical density of a substance (D) and thickness of film for anhydrous sulfuric acid.

Due to the low temperatures of fusion of the studied substances ($T_{\text{пл}} \text{H}_2\text{SO}_4 = +10^\circ\text{C}$; $T_{\text{пл}} \text{H}_3\text{PO}_4 = +42.3^\circ\text{C}$) cooling a mixture of acetone with solid carbon dioxide to -40°C was sufficient to have a stable fine crystalline preparation throughout the survey of spectrum. Control of temperature was carried out potentiometrically with a preliminarily calibrated, copper-constantan thermocouple. We took measures to prevent freezing of the convette windows

ditches. The obtained absorption spectra (Figs. 1b and 2b) show a certain decrease of width of absorption bands both for phosphoric, so also for sulfuric acid and, secondly, a displacement of absorption bands in low-frequency region by $\Delta\tilde{\nu} = 30 \text{ cm}^{-1}$, testifying to increased durability of the hydrogen bonds between molecules with decrease of temperature in the $\text{O} - \text{H} \cdots \text{O}$ complex.

Conclusions

1. The infrared absorption spectra were studied in region of $3700\text{-}2350 \text{ cm}^{-1}$ of sulfuric and orthophosphoric acids at room temperature.
2. The displacement of absorption band of valent $\text{O} - \text{H}$ vibrations of molecules of orthophosphoric acid by 120 cm^{-1} as compared to absorption band of anhydrous sulfuric acid and by 540 cm^{-1} as compared to anhydrous chloric acid testifies to a considerable increase in durability of the hydrogen bonds between molecules in the sequence of $\text{HClO}_4 < \text{H}_2\text{SO}_4 < \text{H}_3\text{PO}_4$ and a strong loosening of the $\text{O} - \text{H}$ bonds in molecules, as a result of which the force constant of $\text{O} - \text{H}$ bonds decreases and its length increases.
3. It was shown that lowering of temperature to -40°C increases the durability of hydrogen bonds for crystalline sulfuric and phosphoric acids.
4. The values of molar indices of absorption of the above-mentioned acids were determined.

Summary

The infra-red absorption spectra from 3700 to 2350 cm^{-1} of concentrated anhydrous sulphuric and orthophosphoric acids at 25°C and in the region of valent $\text{O}-\text{H}$ vibrations at -40°C have been studied.

The roughly estimated values of the force constant and those of the interatomic $\text{O}-\text{H}$ bond length in these acids point to the considerable increase of the strength of hydrogen bonds among molecules in the series $\text{HClO}_4 < \text{H}_2\text{SO}_4 < \text{H}_3\text{PO}_4$, as the length of the $\text{O}-\text{H}$ bond increases.

Molar absorption coefficients of sulphuric and orthophosphoric acids have been determined. (continued on next page)

Literature

1. C. S. Venkateswara, Proc. Indian Acad. sci., 7, 12, 1933.
2. L. Négaré, Comptes rendus, 129, 1437, 1907.
3. E. Fendat, Mem. services chim. Etat, 24, 1437, 1909.
4. P. A. Oiguère, R. Savoie, Canad. J. Chem., 28, 2037, 1950.
5. A. Simon, P. Feber, Z. anorg. allgem. Chem., 233, 1, 233, 1937.
6. A. Simon, M. Weist, Z. anorg. allgem. Chem., 233, 301, 1937.
7. S. Farberg, Acta chem. Scand., 9, 1937, 1955.
8. E. Pascard, C. R., 262, 2022, 1923.
9. S. A. Shchukarev, S. N. Andreyev, and T. G. Balichev. DAN SSSR, 4, 606, 1962.
10. K. Kol'raush. Spectra of combinational diffusion, Moscow, IL, 1952.
11. R. M. Bader, J. Chem. Phys., 2, 123, 1934; 2, 710, 1935.
12. R. M. Adams, V. P. Katz, J. Opt. Soc. America, 42, 555, 1952.
13. M. P. Lisitsa and Yu. P. Tsyashchenko. Optics and spectroscopy, 60, Issue 4, 438, 1960.
14. R. L. Wagner, D. F. Horsting, J. Chem. Soc., 92, 293, 1930.

Submitted
10 June 1962

SHORT SCIENTIFIC REPORTS

DEPENDENCE OF ORIENTATION ANGLE OF DOUBLE REFRACTION
IN FLOW ON CONCENTRATION OF SOLUTION

V. P. Budtov

In the preceding work [1] on the example of one function of [PMMA] (ПММА) solutions it was shown that at low viscosity of the solvent double refraction in flow can be considered as an effect of orientation of molecules, but double refraction in flow at high viscosity as an effect of deformation of molecules. In obtaining extrapolated values of the angle of orientation $\left[\frac{\alpha}{\tau}\right]_{c \rightarrow 0}$ a deflections [1] from the rules of Peterlin [2] were noticed in viscous solvents, i.e., in viscous solvents a different concentration dependence of the angle of orientation was observed than in low viscous solvents [3-8].

The semi-empirical theory of Peterlin [2] gives the following expression for the angle of orientation $\alpha = \frac{g}{\tau} - \tau$

$$\left[\frac{\alpha}{\tau}\right]_{c \rightarrow 0} = \tau = \frac{AM}{\eta_0} \frac{g}{c} = [g](1 + 2\tau[\eta] + \dots) \quad (1)$$

where g is the gradient of speed, M is the molecular weight of the polymer, A is a constant, η_0 is the viscosity of the solvent, $[\tau]$ is the characteristic relaxation time, extrapolated for $c \rightarrow 0$, c is the concentration of polymer in the solution, k is the Huggins constant, η_{sp} , $[\eta]$ are the specific and characteristic viscosity of the solution.

Another method of extrapolating the time of relaxation τ on "zero" concentration ($c \rightarrow 0$) was offered by Cerf [9], who showed that there is such a region where the angle of orientation does not depend on concentration. It was established [10] that

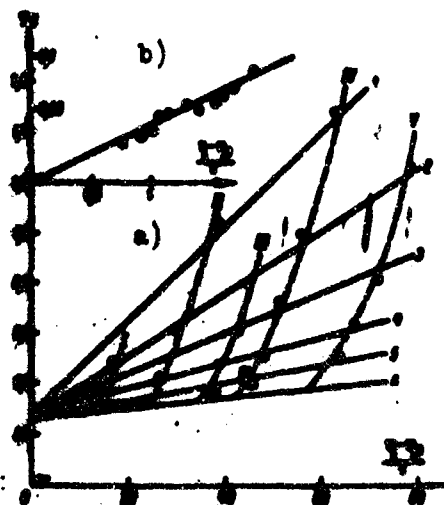


Fig. 1. Dependence of magnitude T_r on $\frac{1-\eta}{c}$ and concentration for solutions of PMMA fraction in tetrabromoethane: a) 1 - $c = 0.36$; 2 - 0.18; 3 - 0.12; 4 - 0.08; 5 - 0.04; 6 - 0.02; I - $\eta_0 = 3.0$; II - 6.4; III - 9.4; IV - 11.4; V - 15.6 centipoises. b) in acetone (○); methylethyl ketone (●); butylacetate (●).

the deformation member in the expression for τ also does not depend on concentration.

In this work we measured the angles of orientation for solutions of six PMMA fractions in tetrabromoethane (viscosity changed from 5 to 15.6 centipoises). The characteristics of samples is given in work [1].

As was shown earlier [11] correct selection of τ is controlled by measurements conducted in the region of large g and large concentrations.

Having obtained relaxation times τ [11], graphs of τ as a function of $\frac{1-\eta}{c}$ were constructed (Fig. 1a). The solid curves express the dependence of τ on viscosity of the solvent, the dotted, on the given specific viscosity of solution η_{sp}/c . One may see, especially in the region of small concentrations,

that the given dependences are expressed by straight lines intersecting on the ordinate axis a segment proportional to the coefficient of internal viscosity [9]. Within limits of experimental error (7-10%) this segment is the same for all concentrations. Thus, for every concentration the dependence of τ on $\frac{1-\eta}{c}$ is expressed by a straight line (at large concentrations $\frac{1-\eta}{c}$ shows an upwards bend); the slopes of these straight lines increase with increase of concentration.

The value of relaxation times τ extrapolated for $c \rightarrow 0$ can be obtained by two methods. It is possible to construct a concentration dependence of τ at identical $\frac{1-\eta}{c}$ and obtain a straight line expressing the dependence of $[\tau]$ on $\eta_0[\eta]$. The convenience of this is that the corresponding dependences of τ on c at the selected $\frac{1-\eta}{c}$ are expressed by straight lines, which facilitates extrapolation (Fig. 2a). However, during this it is necessary to have measurements conducted in solvents with different viscosities.

The other method is that the slopes of straight lines in Fig. 1a are expressed as a function of concentration (Fig. 2b). The obtained straight line representing this dependence intersects on the coordinate axis a segment which coincides with the magnitude of the slope of the straight line $[\tau] = f(\eta_0[\eta])$.

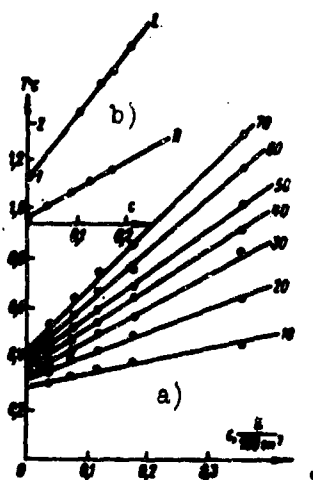


Fig. 2. Dependence of magnitude T_r at a definite $\frac{1-\eta}{c}$ on concentration for solutions V of PMMA fraction. Number on the straight lines give the magnitudes of $\frac{1-\eta}{c}$ (a); the dependence of magnitude $\frac{1-\eta}{c}$ on concentration for solutions II of fraction (I) and V of fraction (II) (b).

concentration for solutions II of fraction (I) and V of fraction (II) (b).

acetone, butylacetate, ethyl acetate, methylethyl ketone) for solutions V of the fraction. The dependence of τ on concentration is expressed by Ceterlin's formula (1).

The graphically expressed dependence of τ on $\frac{1-\eta}{c}$ (Fig. 1a) and concentration (Fig. 2a) can also be analytically presented:

$$\tau = S + \frac{b}{T} \frac{1-\eta}{c} + \frac{d}{T} (1-\eta) = S + \frac{b}{T} \frac{1-\eta}{c} (1 + \frac{d}{b}). \quad (2)$$

The values of b and d are given in the table. The characteristic viscosity of solutions in tetrabromoethane extrapolated for $g \rightarrow 0$ are given in the second column of the table. It is clear that b and d increase with increase of molecular weight. Basically the dependence of τ on concentration is determined by the third member of formula (2). Actually, the dependence of τ on $\eta_r - 1$ is expressed by a straight line (Fig. 3) (along the axis of ordinates we take $\frac{\tau - \tau_0}{\eta_r}$ in order to combine the curves for solutions of the given fraction in various solvents).

The angles of orientation of double refraction were also studied in low-viscosity solvents (in

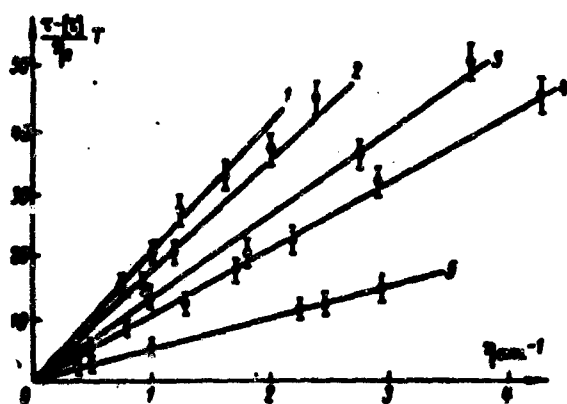


Fig. 3. Dependence of $\frac{\tau - \tau_0}{\eta_r} T$ on specific viscosity $\eta_r - 1$ for solutions of fractions. The numbers on the lines are the numbers of fraction.

| No of fractions | η_{sp}/c | τ | d | No of fractions | η_{sp}/c | τ | d |
|-----------------|---------------|--------|-----|-----------------|---------------|--------|-----|
| I | 0.01 | 1.25 | 20 | IV | 0.01 | 0.04 | 0.7 |
| II | 0.02 | 1.30 | 15 | V | 0.02 | 0.32 | 4.6 |
| III | 0.03 | 1.5 | 9 | | | | |

Thus, if in low viscosity solvents (kinetic rigid ball) the dependence of τ on η_{sp}/c is expressed by a straight line (Fig. 1b) passing through the origin of coordinates, then for viscous solvents (deformed ball) the dependence has a completely different character (Figs. 1a and 2a). Therefore, from the dependence of τ on η_{sp}/c it is possible to judge about the deformation of the macromolecule, which is a very convenient method of qualitative appraisal of macromolecule deformation.

In conclusion the author expresses his gratitude to Prof. V. N. Tsvetkov for valuable council and help in work.

Conclusions

1. The dependence of limiting slope of the angle of orientation of durable refraction (time of relaxation τ) as function of gradient of speed in a wide interval of solvent viscosities (from 0.3 to 15 centipoises) and concentration of polymer (from 0.01 to 0.3 g/100 cm³) was studied.
2. In low-viscosity solvents τ is proportional to η_{sp}/c , which corresponds to the Peterlin rule.
3. In viscous solvents the dependence of τ on η_{sp}/c has a different character. An empirical formula was found and methods of extrapolating τ for $c \rightarrow 0$ are offered.
4. From studying the dependence of τ on η_{sp}/c definite conclusions can be made about the nature of dynamoptical effect and kinetic rigidity of macromolecules.

Summary

The concentration dependence of the extinction angle in polymer solutions has been investigated for 6 fractions of PMMA in solvents of high ($0.3 < \eta_{sp} < 15.5$ sp) and low ($\eta_{sp} < 1$ sp) viscosities. Some methods of extrapolation of $\left(\frac{\Delta n}{\delta}\right)_{c \rightarrow 0}$ have been offered for solvents of high viscosity. It is shown that the study of dependence $\left(\frac{\Delta n}{\delta}\right)_{c \rightarrow 0} = f\left(\frac{\eta_{sp}}{c}\right)$ makes it possible to draw certain conclusions concerning the internal viscosity of macromolecules.

[English summary]

Literature

1. V. N. Tsvetkov and V. P. Budtov. High molecular compounds, 4, 83, 1964.
2. A. Peterlin. J. Pol. sci., 12, 45, 1954.
3. V. N. Tsvetkov and E. V. Frisman. ZhETF, 15, 276, 351, 1945.
4. S. Ya. Magarik and V. Baranov. High molecular compounds, 5, 1072, 1963.
5. R. Signer and A. Peterlin. Helv. chim. acta, 36, 1375, 1953.
6. I. T. Yang. J. Amer. chem. soc., 80, 5139, 1958.
7. V. N. Tsvetkov, N. N. Boytsova and A. Ye. Grishchenko. Herald of Leningrad State University, No. 4, 59, 1962.
8. I. N. Shtennikova. Avtoref, kand. diss. Leningrad Press of Academy of Sciences of USSR, 1963.
9. R. Cerf. J. Chim. phys., 48, 59, 85, 1951.
10. J. Leray. J. Chim. phys., 57, 323, 1960.
11. V. P. Budtov. Herald of Leningrad State University, No. 4, 60, 1964.

Submitted
24 April 1963

ABOUT INFRARED SPECTRUM OF TWILIGHT SKY

Ye. V. Gnilovskoy

One of the most effective indirect methods of studying the structure of atmosphere is the twilight method. Many works are devoted to photometric analysis of twilight. Some of them are not free from essential deficiencies of a methodical character. Photoelectric observations of twilight in separate sections of the spectrum with application of light filters do not give a presentation about the spectrum of twilight sky [1, 2]. In photographing the spectra of twilight sky usually prolonged exposures were applied, which is equivalent to averaging across a large interval of zenith distance of the sun [3].

The goal of this work is to obtain spectra of twilight sky in the near infrared region of the spectrum with the help of scanning over wavelengths of an electrophotometer at various setting angles of the sun on the horizon in zenith and western horizon. As spectral system a monochromator was used with a diffraction grating operating according to the Fasti diagram. The diagram of the installation is shown in Fig. 1. Light of the twilight sky is focused by cond. r_1 on the slot of monochromator 2; collimator mirror 4 transforms divergent bundle proceeding from the slot; it is reflected from a plane rotating mirror 3 in parallel and directs it on grid 5. Light located in the spectrum is focused by spherical mirror 6 in the plane of the exit slit 7. The solid angle of the installation is $4 \cdot 10^{-3}$ steradians.

The candle-power of the monochromator is 1/9. The dimensions of the shaded part of the grid are $70 \times 80 \text{ mm}^2$. The grid has 600 lines per mm. Scanning of

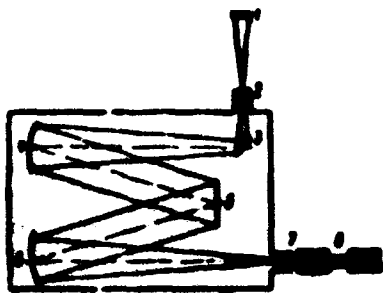


Fig. 1.

spectrum was produced by rotating the grid. During work in the infrared region of the spectrum (0.7-1.1 μ) the grid worked on the first order, to cut the spectrum of the second order a red glass [KS-1] (KC-1) was set up in front of the slot. The dispersion of the monochromator was 22 $\text{\AA}/\text{mm}$.

After exit slit the light strikes the screen of image converter [EOP] (ЭОП) with an oxygen-cesium cathode. The glow of the EOP screen in the blue region of spectrum was perceived by the photoelectronic multiplier [PM] (ФЭУ) of brand EMI with an antimony cesium cathode.

Between the PM cathode and the EOP screen an optical contact was ensured with help of a special light conductor 8. The EOP was placed in a refrigerator. The dark current of the EOP was cold-treated by carbon dioxide.

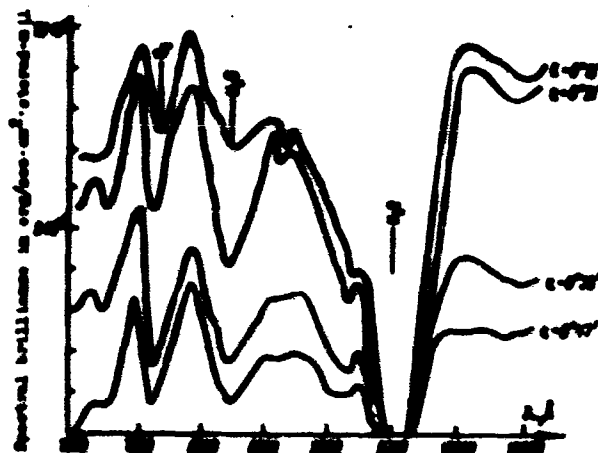


Fig. 2.

The output signal from the enlarger after amplification was recorded by the recorder. The installation was calibrated in absolute units with the help of a standard lamp.

The spectra of twilight sky were recorded at the Pulkovsk astronomical observatory in the summer of 1963 setting angles of the sun on the horizon up to 10° . The obtained spectrograms were corrected for spectral sensitivity of the receiver and change of twilight illuminance during the time of recording, and were recalculated in absolute units.

Figure 2 gives the typical spectra of twilight sky in absolute units for a small interval of angles of setting (angle ϵ), obtained by us in June 1963 in the zenith. On the spectra absorption bands of oxygen and water vapor are clearly visible. The structure of the bands is not solved possibly because of the great optical thickness, passed by the rays.

An interesting peculiarity of the spectra is presence of peak intensity twilight sky in the region of 1μ , comparable in magnitude to the maximum in the region of 0.7μ . It is possible that the first maximum is caused by the "flash" of intrinsic radiation of atmosphere near 1μ discovered by Ye. D. Sholokhova and M. S. Frish in 1955[4]. The obtained infrared spectra in western horizon essentially do not differ from the spectra of zenith.

One should consider the described investigations as preliminary.

This work was carried out in the laboratory of Prof. S. P. Rodionov, to whom the author expresses sincere gratitude for his constant interest and leadership of the work.

Summary

The data on the observation of the twilight sky in the near- and part of the spectrum of about 1μ are given. Apparatus are described, typical spectrum of the twilight sky with the different setting angle of the sun behind the horizon is regarded.
[English summary]

Literature

1. T. G. Megrelisvili. Press of Academy of Sciences, USSR, Geophysics, Series, No. 8, 976, 1956.
2. E. V. Ashburn. J. Geophys. res., 57 (1), 85, 1952.
3. J. Difay et Gauzilt. Ann. d'astrophys., 9, 135, 1946.
4. Ye. D. Sholokhova and M. S. Frish. DAN SSSR, 105, No. 6, 1213, 1956.

Submitted
26 July 1963

PHASE METHOD OF MEASURING MAGNETIC FIELD OF EARTH
WITH A NUCLEAR-RESONANCE FILTER

P. M. Borodin

At present there are several methods of continuous measurement of the magnetic field of earth with the help of different nuclear-resonance generators, for instance [1, 2], which have definite advantages over the others.

In these the methods magnetic field H_0 is measured by the frequency of generation f_0 according to the relationship known in nuclear magnetic resonance

$$f_0 = \frac{\gamma}{2\pi} H_0 \quad (1)$$

where γ is the gyromagnetic ratio of nuclei of sample (usually protons). However, when this measuring small changes the earth's magnetic field ($\approx 1\gamma$) and especially if these changes have a short period, considerable difficulties appear, connected with the necessity of thorough treatment of oscillograms and continuity of the method is lost, since to increase the accuracy it is necessary to increase the time of measurement,¹ due to which only one averaged value of H_0 is obtained.

These deficiencies can be avoided preserving all the merits nuclear-resonance methods if we apply the phase method of measuring earth's magnetic field with the help of a nuclear resonance filter [YaFF] (ЯРФ); for this any device can be used

¹Change of field, $\Delta H_0 = 1\gamma$, as is evident from (1); correspondingly $\Delta f_0 = 0.043$ cps; inasmuch as $\Delta f = \frac{1}{2\pi} \frac{\Delta\varphi}{\Delta t}$, for time of measurement $\Delta t = 0.3$ sec the phase advance will be $\Delta\varphi = 5^\circ$, and for $\Delta t = 3$ sec, $\Delta\varphi = 50^\circ$.

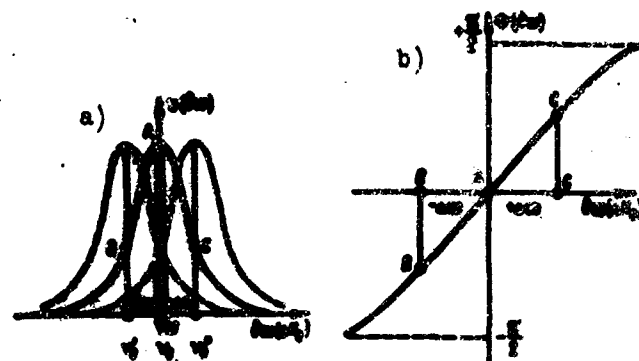


Fig. 1. Change of amplitude ν and phase ϕ of signal of precession of nuclei at the output of a nuclear-resonance filter. a) is amplitude-frequency; b) is phase-frequency characteristics of nuclear-resonance filter; ν_{KB} is the frequency of the external crystal oscillator, $\Delta\omega$ is the frequency difference caused by the modified magnetic field of earth ΔH_0 , B and C are magnitudes of amplitude and phase on the output of the nuclear-resonance filter, corresponding to frequency difference of $-\Delta\omega$ and $+\Delta\omega$.

which has nuclear-resonance characteristics (Fig. 1) with f_0 proportional to H_0 in accordance with (1). If at the input of such a filter we apply voltage u_{KB} from an external stabilized generator, the frequency of which ν_{KB} is equal the resonance frequency of YaRF, then during changes of the earth's magnetic field ΔH_0 , i.e., during appearance of frequency difference $\delta\omega_0(\Delta H_0)$, the amplitude and phase of u_{KB} on the output of the filter will be changed proportional to ΔH_0 in accordance with Fig. 1. Using the phase shift of u_{KB} on the output of YaRF in comparison with the phase of u_{KB} on its input, it is possible to more exactly and more operationally measure the relative changes of the earth's magnetic field (with respect to $H_0 \sim \nu_{KB}$). If, however, we consider that H_0 can always be determined by ν_{KB} , then this method in principle allows us to produce an exact measurement of the absolute value of the terrestrial field.

As a nuclear-resonance filter during an experimental check of the method we used a Skripov generator [1] with broken feedback, the input of which are phasing coils, and the output, a receiving coil (regime of narrow-band filter [3]). The phase shift obtained during change of the earth's field was measured by the diagram of Fig. 2, i.e., by Lissajous figures (roughly), or with the help of a phase detector¹ with subsequent recording on an automatic recording instrument. Exact

¹Before phase detection the amplitude was limited.

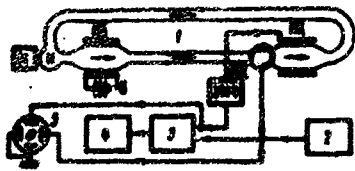


Fig. 2. Block diagram of magnetometric device. 1 - nuclear-resonance filter (HK, magnetizing coil; PK, receiving coil; ΦK , phasing coil; H, pump; M, motor; E, battery 24 v, 10 amp); 2 - oscillator crystal ($f_{KB} = 2500$ cps); 3 - phase detector; 4 - self-recording instrument; 5 - oscillograph.

trimming of H_0 under frequency of crystal oscillator ν_{KB} (installation of system on zero) was carried out with the help of Helmholtz coils or a sheet of light sheet iron, transferred at a distance of 1.5-3 m from the receiving coil.

A prolonged check in field conditions of such a model of the instrument showed that its sensitivity is equal to 0.1-0.3 γ . Undistorted registration of signals of magnetic disturbances is ensured when they are $\tau \geq 2$ sec long.

The simple methods of recording phase shifts applied in these experiments does not ensure linearity during recording of magnetic disturbances exceeding several gammas (due to nonlinearity of the phase characteristics of YaRF and the phase detector). Limits of applicability of such a variant of the instrument can be expanded if decrease the steepness of phase response of YaRF due to decreasing the time of relaxation T_2 (it is of course, necessary to apply a special phase detector or frequency divider); however, this will lead to lowering the sensitivity of the method.

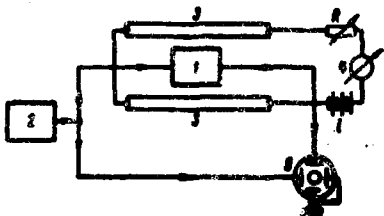


Fig. 3. Block diagram of a simple magnetometric device for measurement of slow changes of the earth's magnetic field of Earth. 1 - nuclear-resonance filter; 2 - oscillator crystal; 3 - Helmholtz coil; 4 - milliammeter with zero intermediary; 5 - oscillograph.

A more coordinated solution of this problem is using the YaRF as a zero-indicator. With such a method of recording magnetic disturbances the instrument will always work on the most linear portion of phase responses of the YaRF and the phase detector. The simplest variant of an instrument using this principle can be built according to the diagram depicted in Fig. 3. In this instrument, which is only useful for measuring slow changes of the earth's magnetic field, the phase shift on the YaRF output recorded, e.g., according to

Lissajous figure on oscillograph, before every measurement is manually established at zero with the help of rheostat R, which varies current i in compensational coils (3). The magnitude of current Δi will be proportional to ΔH_0 and can be calibrated in units of the field. The limits of measurement of such an instrument can be expanded any amount and will be determined only by the construction of the

system of compensating coils.

If, however, the phase shift YaRF output will be established on zero automatically, as this was suggested by A. V. Mel'nikov, then the instrument (4) will continuously examine the changes of the earth's magnetic field i.e., in this case it is possible to record both slow change of H_0 and also its brief variations at any magnitude of ΔH_0 .

In designing magnetometers by the described here method it is desirable to apply more perfect nuclear-resonance filters than YaRF according to the diagram of the Skripov generator, for instance those in which dynamic polarization of nuclei is used. Taking into account all the above-indicated recommendations the instrument can have good sensitivity ($\approx 0.1 \gamma$), high noise immunity, good stability of zero, will not require exact orientation of transducer in the direction \vec{H}_0 and will allow both continuous measurement of short-period variations of total vector of the earth's magnetic field and also recording of its slow changes.

A. V. Mel'nikov and A. A. Morozov took part in an experimental check of the method; to them I express my sincere gratitude.

Summary

The phase method of measurement of the earth magnetic field vector by means of the nuclear-resonance filter is described. It allows to measure simultaneously short-period variations of the field as well as its slow changes. [English summary]

Literature

1. F. I. Skripov. DAN, Academy of Sciences of USSR, 121, 998, 1958.
2. A. Abragam, J. Combrission, and I. Solomon. Comp. rend., 245, 157, 1957.
3. F. I. Skripov. Herald of Leningrad State University, No. 4, 26, 1964.

Submitted
November 1963

SURFACE STRUCTURE, ELECTRICAL AND PHOTOELECTRIC PROPERTIES
OF THIN LAYERS OF SULFUROUS LEAD OBTAINED
BY CATHODE SPUTTERING

R. Ya. Berlaga and M. I. Rudenok

Photoconducting and photovoltaic layers of PbS are usually obtained by chemical method or sublimation in a vacuum on solid bases.

In this work we give the results of investigating the electrical and photoelectric properties and structure of PbS layers obtained by cathode sputtering.

The lead sulfide subjected to sputtering was prepared by heating to 1100°C a mixture of shavings of chemically pure lead and monoclinic sulfur, taken in a stoichiometrical ratio. The mixture of sulfur and lead was placed in a quartz test tube, which was evacuated to $5 \cdot 10^{-4}$ mm Hg and soldered. The massive ingot of sulfurous lead obtained after heating had the form of a cylinder, limited on the one hand by a hemisphere and capable of being cracked along edges of crystals.

Cathode sputtering of PbS was produced under a glass bell at pressures from 10^{-1} mm Hg to $5 \cdot 10^{-2}$ mm Hg on bases of glass and rock salts, heated to $250\text{-}270^{\circ}\text{C}$. The rate of vaporization averaged 0.2μ per hour. The bases were placed approximately 3.5-4 cm from the cathode.

Structure of PbS layers obtained by this method turned out to be very close to the structure of layers obtained by evaporation in a vacuum. A large part of the layers obtained by cathode sputtering did not have noticeable photoconductivity; the greatest photosensitivity was 16% at illuminance of 1200 lux. The photoelectromotive force at the same illuminance attained 25 mv; the sign of the photo emf did not depend on the direction of light.

GRAPHS NOT
REPRODUCIBLE



Fig. 1. Temperature dependence of conductivity of thin polycrystalline PbS layers obtained. 1 - cathode sputtering; 2 - evaporation in a vacuum.



Fig. 2. Absorption spectrum of thin polycrystalline PbS layers obtained by cathode sputtering.



Fig. 3. Electron-microscopic photograph of a profile of a PbS layer obtained by: a) cathode sputtering; b) evaporation in a vacuum.

Conductivity of layers in the process of high-temperature treatment changes just as the conductivity of layers obtained by evaporation in a vacuum; with a temperature rise conductivity decreases attaining a minimum (Fig. 1).

Before oxidation the layers have n-type conductivity, whose character after oxidation changes, it becomes p-type.

The activation energies calculated from the temperature dependence of conductivity for layers obtained by cathode sputtering and vacuum evaporation almost coincided and are 0.39 and 0.37 eV respectively.

The absorption spectra of layers obtained by these methods were also similar (Fig. 2). Externally these layers almost did not differ.

Depending upon the rate of cathode sputtering the layers had a somewhat different form, light-gray mirror, sometimes with a bluish nuance or dark-gray or even dull-black.

As electron-microscopic examination with the help of the method of profile photographs showed, on the surface of dull, dark-gray and black layers there are protrusions different in form. Figure 3 gives profile photographs of layers obtained by cathode sputtering and evaporation, and Fig. 4 is photographs of the surface.

The electron diffraction patterns obtained during reflection of electron beam from the surface of layer sputtered on a hot base had a form typical for polycrystalline layers.

By sputtering PbS on a chip of rock salt we obtained a single crystalline film that one could see from electron diffraction patterns obtained during passage of an electron beam through a thin PbS layer (Fig. 5).

GRAPHIC NOT
REPRODUCIBLE

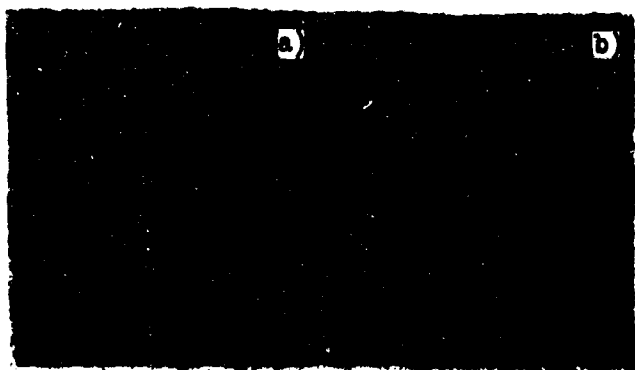


Fig. 4. Electron-microscopic photography of the surface of PbS layers obtained by: a) cathode sputtering; b) vacuum evaporation.



Fig. 5. Electron diffraction patterns of PbS films obtained by cathode sputtering: a) on a glass base; b) on a chip of rock salt.

From the performed investigations one can note that cathode sputtering produces polycrystalline layers, very similarly in their properties and structure to layers obtained by vacuum evaporation. For an oriented effect of the base, sputtering on a chip of rock salt, we obtained single crystalline films.

From electron-microscopic examinations it is clear that the grain of the layer do not have a sufficiently clear, well faceted form, as this is observed during vacuum evaporation. The photoelectric properties, photoconductivity and photo emf, for layers obtained by cathode sputtering are either absent or, if present, then they are lower than for layers coated in a vacuum.

Diploma candidate L. I. Meshcherskaya participated in the work.

Summary

Thin PbS layers were produced by cathode-sputtering method. The activation energy was calculated from temperature dependence of conductivity and the absorption spectrum was measured. Electron microscopic and electron diffraction studies were carried out. Thin PbS layers produced by cathode-sputtering method exhibit the same properties as the layers obtained by the vacuum evaporation method. The ability to produce polycrystalline and monocrystalline PbS films by the cathode-sputtering method was shown.

[English summary]

Submitted
2 July 1965

AVEPAGE HEAT CAPACITY OF SOLID $Fe_2O_3 - Al_2O_3$ SOLUTIONS
AT HEIGHTENED TEMPERATURES

Yu. G. Popov

For certain compounds of variable composition (titanium oxide [1], vanadium oxide [2] and nickel telluride [3]) it has been shown that the average heat capacity is a linear function of the index for the nonmetallic element in the formula of the compound (within limits of the region of homogeneity). In a number of cases the average heat capacity of substances being within limits of region of homogeneity is additively composed of the heat capacities of the corresponding stoichiometrical compounds (titanium oxide, nickel telluride), in case of vanadium oxide a considerable deflection from values corresponding to additive composition occurs.

For solid solutions of oxides of the type of isomorphic substitution data about average heat capacity are apparently absent. At the same time, they are of considerable interest in connection with importance of evaluating the value of the nonconfigurational components of change of thermodynamic potential during formation of solid solutions and in connection with the fact that heat capacity is a structurally sensitive property. This work is dedicated to an investigation of the dependence of average heat capacity on composition in a $Fe_2O_3 - Al_2O_3$ system at heightened temperatures.

Solid solutions, containing 0, 3, 6, 10, 50, 65, 78, 82, 86, 90, 94, 97 and 100 molar % of Fe_2O_3 , were prepared from nitrates of trivalent iron and aluminum (qualification pure for analysis). Solutions of these salts (concentration of 0.1 mole/liter) was established by the volume method [4 p. 633] of the $Al_2H_2O_4$

solution by the weight method [4 p. 338]) were mixed in appropriate ratios. After coprecipitation of hydroxides by the effect of NH_4OH the filtered and dried deposits were heated 8-10 hours at $600-700^\circ\text{C}$ in air, and then at 1100°C in a current of oxygen. As a result of 120 hour heat treatment at this temperature preparations containing 0, 3, 6, 78, 82, 86, 90, 94, 97 and 100 molecular % of Fe_2O_3 according to roentgenographic investigation turned out to be single-phase with a grid of the $\alpha\text{-Al}_2\text{O}_3$ type.

Preparations containing 10, 50 and 65 molecular % of Fe_2O_3 turned out to be two-phase. The positions of boundaries of two-phase regions were estimated as 9 ± 1 and 77 ± 1 molecular % Fe_2O_3 , which agrees with the results of work [5].

The average heat capacity in the $1056-298^\circ\text{K}$ interval was determined on the installation described earlier [1]. The thermal value of calorimeter was established by the electrical method.

| Composition (in molecular % Fe_2O_3) | $H_{1056-298}^{\text{cal}}/g\text{-mole}$ | Composition (in molecular % Fe_2O_3) | $H_{1056-298}^{\text{cal}}/g\text{-mole}$ |
|---|---|---|---|
| 0 | 1056 | 100 | 1056 |
| 3 | 1056 | 94 | 1056 |
| 6 | 1056 | 86 | 1056 |
| 78 | 1056 | 78 | 1056 |
| 82 | 1056 | 78 | 1056 |
| 86 | 1056 | 78 | 1056 |
| 90 | 1056 | 78 | 1056 |
| 94 | 1056 | 78 | 1056 |
| 97 | 1056 | 78 | 1056 |
| 100 | 1056 | 78 | 1056 |

In calculation one calorie was taken as equal to 4.1840 abs joules. The divergence between separate experiments did not exceed 0.3% and when using different weighed samples, 50% and, as a rule, it was smaller.

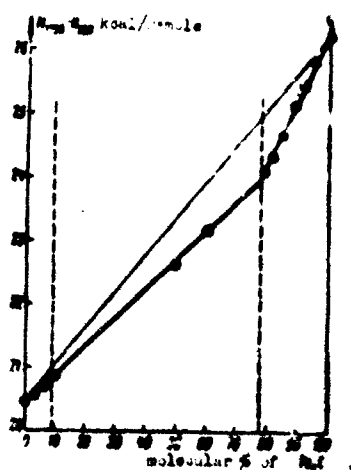
Results of determinations of enthalpy of preparations are given in the table (for different weighed samples of preparations of identical composition the results are averaged).

The magnitude of enthalpy of pure α -corundum is in satisfactory conformity with the magnitude obtained in work [6] (divergence is 0.2%). For $\alpha\text{-Fe}_2\text{O}_3$ the data obtained in this work differ by 1.2% from the data offered in work [7].

The figure depicts the dependence of enthalpy of solid $\text{Fe}_2\text{O}_3 - \text{Al}_2\text{O}_3$ solutions on composition.

In the single-phase regions enthalpy (average heat capacity) is a linear function of composition. The maximum deflection from the averaged straight lines does not exceed 0.5%.

The positions of boundaries of the two-phase region, ensuing from the form of



Dependence of enthalpy of solid $\text{Fe}_2\text{O}_3 - \text{Al}_2\text{O}_3$ solutions on composition. Dotted lines show the boundaries of the two-phase region.

dependence of enthalpy on composition, agree with the positions of boundaries determined from the roentgenographic data.

The deflection of magnitudes of the average heat capacity of solid solutions from values obtained by means of additive composition of the average heat capacity of $\alpha\text{-Al}_2\text{O}_3$ and $\alpha\text{-Fe}_2\text{O}_3$ is rather considerable, attaining at 9 molecular % of Fe_2O_3 1% and at 77 molecular % of Fe_2O_3 3.5%, which correspond to deflections in magnitudes of enthalpy by 200 and 860 cal respectively.

Thus, the contribution of nonconfigurational components to the magnitude of thermodynamic potential of the formation of solid solutions of oxides of

isomorphic substitution can be sufficiently noticeable.

Heat capacity, especially c_p , even at heightened temperatures is a structurally sensitive property; this especially follows from data obtained in this work (see figure).

Correspondingly, the linear dependence of \bar{c}_p on composition within limits of the region of homogeneity, i.e., equality of the average heat capacity of solid solutions to the average heat capacity of a mechanical mixture (the same gross-composition) of extreme compositions (corresponding to pure component and a solid solution, corresponding to the boundary of solubility), gives a definite base for assuming that solid $\text{Fe}_2\text{O}_3 - \text{Al}_2\text{O}_3$ solutions have a submicro-nonuniform structure, i.e., that there is a known segregation of aluminum and iron atoms in them.

Conclusions

1. The average heat capacity of preparations of a $\text{Fe}_2\text{O}_3 - \text{Al}_2\text{O}_3$ system was determined in the temperatures interval of 1056-298°K.
2. It was shown that in single-phase regions the average heat capacity is a linear function of composition.
3. The assumption is made that solid $\text{Fe}_2\text{O}_3 - \text{Al}_2\text{O}_3$ solutions have a submicro-nonuniform structure.

In conclusion the author takes this opportunity to thank S. M. Ariya for direction of this work and colleague of laboratory of roentgenography, I. I. Koshin,

for help in the roentgenographic part of the work.

Summary

The mass heat capacities of solid solutions of the $\text{Fe}_2\text{O}_3\text{--Al}_2\text{O}_3$ system have been found to be a linear function of the composition. This is in good agreement with the assumption of the segregation of aluminum and iron atoms. [English summary]

Literature

1. P. S. Yerofeyeva, N. L. Lukinykh, and S. M. Ariya. ZhFKh, XXXV, No. 4, 772, 1961.
2. M. S. Yakovleva and Z. L. Krasilova. Herald of Leningrad State University, No. 16, 136, 1961.
3. E. F. Westrum. J. chem. phys., 28, 3, 497, 1958.
4. I. M. Kol'tgof and Ye. B. Sendel. Quantitative analysis. Moscow-Leningrad, State Chemistry Press, 1948.
5. Ya. V. Vasil'yev and G. A. Shcherbakova. FTT, 5, 4, 1090, 1963.
6. K. Z. Gomel'skiy. ZhFKh, XXXII, No. 8, 1859, 1958.
7. E. V. Britske and A. F. Kapustinskiy. Thermodynamic constants of inorganic substances. Moscow-Leningrad, Press of Academy of Sciences, USSR, 1949.

Submitted
2 August 1963

ON CHLORONIOBATES OF ALKALI METALS WITH COMPOSITION
OF $\text{Me}_2^{\text{I}}\text{NbOCl}_5$

Ye. K. Smirnova and I. V. Vasil'kova

In 1907 an article [1] was published about the production of anhydrous chloroniobates, Rb_2NbCl_5 and $\text{Cs}_2\text{NbOCl}_5$, by pouring hydrochloric acid solutions of niobium oxychloride and chlorides of alkali metals and subsequent saturation of the solution by hydrogen chloride at 0°C .

Investigation of systems NbOCl_3 chlorides of alkali metals with the help of thermographic analysis [2, 3] showed that K_2NbOCl_5 melts incongruently at 486°C and $\text{Rb}_2\text{NbOCl}_5$ and $\text{Cs}_2\text{NbOCl}_5$ melt congruently at 616 and 642°C respectively.

We first obtained the given compounds from a melt by means of alloying stoichiometrical quantities of niobium oxychloride and chlorides of alkali metals under conditions fixed by thermal analysis [2, 3]. Incongruently melted K_2NbOCl_5 was obtained by heating a mixture of the initial chlorides in a soldered evacuated ampule of [P-15] (Π -15) glass at a temperature somewhat lower than the temperature of peritectic reaction of transformation for 25-30 hours and subsequent slow cooling. Congruently melted $\text{Rb}_2\text{NbOCl}_5$ and $\text{Cs}_2\text{NbOCl}_5$ were obtained by alloying the initial chlorides in soldered under vacuum (evacuated) quartz ampules at a temperature somewhat higher than the temperature of fusion of the salt for 20-25 hours.

The obtained samples of all salts are colored a lilac color. They are stable in an atmosphere of dry air; on humid air they are subjected to hydrolysis with hydrogen chloride given off; they are decomposed by water; in this niobic acid is

deposited:



From the literature it is known that $(\text{NH}_4)_2\text{NbOCl}_5$ is isomorphic with $(\text{NH}_4)_2\text{TiCl}_6$ and is crystallized in a cubic system of the K_2PtCl_6 type. We suggest that oxynidates of potassium, rubidium and cesium also have a similar structure. Powdergrams¹ taken from these products confirm this.

The dimensions of a cubic cell for K_2NbOCl_5 , $\text{Rb}_2\text{NbOCl}_5$ and $\text{Cs}_2\text{NbOCl}_5$ are $9.815 \pm 0.001 \text{ \AA}$, $10.00 \pm 0.01 \text{ \AA}$ and $10.29 \pm 0.01 \text{ \AA}$ respectively.

Thus, the structure of the investigated compounds consists of octahedrons, NbOCl_5^{-2} , and ions of alkaline metals. The first are located in nodes of face-centered cubic grids, the second on physical diagonals of the cube.

Summary

K_2NbOCl_5 , $\text{Rb}_2\text{NbOCl}_5$, $\text{Cs}_2\text{NbOCl}_5$ have been synthesized, and the reactions of their hydrolysis have been investigated. The analyzed compounds have been shown to crystallize into the cubic system according to the K_2PtCl_6 type:

| | | |
|-----------------------------------|----------------------------------|----------------------------------|
| K_2NbOCl_5 | $\text{Rb}_2\text{NbOCl}_5$ | $\text{Cs}_2\text{NbOCl}_5$ |
| $a = 9.815 \pm 0.001 \text{ \AA}$ | $a = 10.00 \pm 0.01 \text{ \AA}$ | $a = 10.29 \pm 0.01 \text{ \AA}$ |

[English summary]

Literature

1. R. F. Weinland and L. Storz. Zs. anorg. Chem., 54, 223, 1907.
2. S. A. Shchukarev, Ye. K. Smirnova, and T. S. Shemyakina. ZhNKh, VII, Issue 9, 2217, 1962.
3. S. A. Shchukarev, Ye. K. Smirnova, and I. V. Vasil'kova. Herald of Leningrad State University, No. 16, 1963.
4. J. Wernet. Zs. anorg. allg. Chem., 272, 279, 1953.

Submitted
19 June 1963

¹The powdergrams were taken on a [URS-50-I] (VPC-50-II) diffractometer on $\text{Cu}_{K\alpha}$ radiation. Samples were pulverized in a dry chamber and were flooded with oil, which gave protection from the influence of atmospheric moisture during the survey.

APPLICATION OF ULTRASONICS TO ACCELERATE QUANTITATIVE
DEPOSITION OF CALCIUM, MAGNESIUM
AND BARIUM

V. V. Vasil'yev and I. L. Sit'ko

To solve different analytic problems we frequently resort to deposition of ions in the form of poorly soluble substances. The basic deficiency of this operation is its duration.

It is natural to assume that ultrasonics, acting through the bottom of retort on the unstable system of the deposit a supersaturated solution, will promote the fastest achievement of equilibrium between liquid and solid phases.

Ultrasonics has huge number of applications of the most various character [1]. Its influence is not only mechanical (splitting, mixing, dispersion, coagulation, purification, washing and so forth), but it also stimulates the chemical processes (oxidation - restoration, hydrolysis, depolymerization, synthesis of certain substances and so forth). Its application in defectoscopy, measuring layer thickness and reservoir depth and so forth are widely known.

For a long time ultrasonics was used to analyze solutions and gas mixtures; the concentration of one or another component is judge by the change in the speed of ultrasonics or its damping [1, 2]. However, these apparently by far do not exhaust the possibility of applying ultrasonics in analytic chemistry. We have used ultrasonics in phase chemical analysis of ores [3, 4]. It was established that under the influence of ultrasonics the time necessary for full extraction of a number of lead and copper minerals by selective solvents is decreased many times.

To clarify the expediency of using ultrasonics in weight chemical analysis¹ to accelerate full settling in the deposit of a poorly soluble substance, we selected the widely known and long ago applied reactions of deposition of barium in the form of a sulfate, calcium in the form of an oxalate and magnesium in the form of a double phosphate of magnesium and ammonium. In just these cases, as in many other, for ripening of deposit and full deposition of the determined ion prolonged standing of the deposit with the mother liquor and heating or leaving it over night before filtration is necessary.

Deposition of ions of barium, calcium and magnesium in the form of the shown poorly soluble substances was produced by the usual means, where deposit before filtration was sustained with the mother liquor for the recommended period of time or was left to the following day [5, 5]. Deposition of the same ions was conducted so that upon adding a solution of reagent of the precipitator the deposit with mother liquor was subjected to the influence of ultrasonics for five minutes with all other conditions of this method of deposition being equal. Filtration followed immediately after the influence ultrasonics, i.e., endurance with mother liquor was not produced.

For this work we applied a piezocrystal vibrator operating with frequency of 540 kilocycles. An electric generator with power of 0.75 kilowatts was hooked up to a [GU-80] (FY-80) lamps. The anode voltage was 2 kv and plate current was 0.32 amp (with the exception of experiments with barium sulfate where the plate current was 0.10-0.12 amp). Ultrasonic vibrations from piezocrystal vibrator were transmitted to the transformer oil surrounding it; a 300 ml conical retort containing the reaction mixture was dipped 1 cm into the oil. The hole of the retort was closed by a funnel.

Deposition of Calcium in the Form of an Oxalate

The initial substance for all experiments in depositing calcium oxalate was a big crystal of synthetic calcite; its calcium carbonate content was close to 100%. A weighed sample of CaCO_3 was put into solution with a minimum quantity of dilute hydrochloric acid.

Potentiometric determination of calcium. To determine calcium without the

¹Here we are actually speaking about deposition of a poorly soluble substance; the final determination does not have to be by weight (e.g., volume or complexometric determination of calcium after its deposition in the form of CaC_2O_4).

influence of ultrasonics we applied the usual method [5, 6], according to which, after adding the reagent, the deposit (CaC_2O_4) was sustained with the mother liquor at $85-90^\circ\text{C}$ for 1.5 hours¹ or was left till the following day.

Under the influence of ultrasonics deposition was conducted by the usual means, except that after pouring the solution of ammonium oxalate the deposit of CaC_2O_4 with the mother liquor was subjected to the influence of ultrasonics for 5 minutes, after which followed filtration. The calcium content in separate tests varied from 210 to 41 mg.

The following results were obtained:

Upon heating the deposit with the mother liquor at $85-90^\circ\text{C}$ for 1.5 hours six parallel determinations of calcium gave an average of $99.7\% \pm 0.03$.

Upon leaving the deposit with the mother liquor till the following day six parallel determinations of calcium gave on average of $99.7\% \pm 0.06$.

Finally, after a five-minute effect of ultrasonics twenty parallel determinations of calcium gave an average of $99.8\% \pm 0.02$.

Weight determination of calcium. After deposition of CaC_2O_4 by the usual means with a half-hour endurance of the deposit $85-90^\circ\text{C}$ before filtration on the one hand, and deposition of it after a five-minute effect of ultrasonics on the other, calcium was determined by weight (form of weighing, CaO). The calcium content in separate tests varied from 50 to 100 mg.

The following results were obtained:

Six parallel determinations of calcium without ultrasonics gave an average of $99.9\% \pm 0.01$.

Six parallel determinations of calcium under the influence of ultrasonics gave an average of $99.9\% \pm 0.02$.

Tribonometric determination of calcium. Finally, calcium was precipitated in the form of an oxalate with final tribonometric titrating. The calcium content in separate tests varied from 50 to 80 mg.

After deposition of CaC_2O_4 without ultrasonics (1.5 hour endurance at $85-90^\circ\text{C}$) six parallel determinations of calcium gave an average of $100.0\% \pm 0.01$.

¹With a half-hour heating of the deposit 6 determinations of calcium gave an average of $98.2\% \pm 0.1$. Thus, far from full deposition is observed here.

Six parallel determinations of calcium under the effect of ultrasonics also gave an average of $100.0\% \pm 0.02$.

Deposition of Magnesium in the Form of a Double Phosphate of Magnesium and Ammonium

Magnesium was precipitated in the form of $MgNH_4PO_4$ by the usual means, i.e., with leaving the deposit for 5 hours, after which followed overdeposition and again leaving it for 16 hours. Finally, the deposit was heated and weighed in the form of a pyrophosphate. Parallel deposition was conducted with a five-minute effect of ultrasonics, after which followed filtration, then overdeposition with a five-minute effect of ultrasonics and then the deposit was immediately filtered. The magnesium content in separate tests varied from 5 to 12 mg.

The following results were obtained:

Without ultrasonics twelve parallel determinations of analytically pure preparation of magnesium sulfate (standard from set for trilonometry) gave an average of $99.9\% \pm 0.04$.

With the effect of ultrasonics twelve parallel determinations gave an average of $99.8\% \pm 0.03$.

Determining Barium in the Form of a Sulfate

For this work we took a weighed sample of $BaCl_2 \cdot 2H_2O$. Barium sulfate was precipitated, as usual, with subsequent endurance of deposit with the mother liquor for 3 hours at $85-90^\circ C$, after which followed filtration, etc., [6]. In the other series of experiments, after adding H_2SO_4 to the hydrochloric acid solution of barium chloride, the deposit of barium sulfate with the mother liquor was subjected to a five-minute effect of ultrasonics, after which filtration followed immediately. The content of barium in separate tests varied from 70 to 160 mg.

The following results were obtained:

Nine determinations of barium without application of ultrasonics gave an average content of dihydrate of barium chloride of $99.5\% \pm 0.02$.

After the effect of ultrasonics twelve parallel determinations gave an average content of pure substance in the preparation of $99.6\% \pm 0.03$.

Conclusions

It was determined that with quantitative determinations of barium, calcium

and magnesium, anticipating their preliminary deposition in the form of barium sulfate, calcium oxalate and double phosphate of magnesium and ammonium, for practically full settling of these ions in the deposit a five-minute effect of ultrasonics on the deposit with the mother liquor is sufficient, instead of prolonged endurance of the deposit with the mother liquor during heating, or leaving them till the following day before filtration.

The observed facts can apparently be a new useful application of ultrasonics in analytical chemistry.

Summary

The data on the new application of ultrasonic in analytical chemistry are given in this paper. In using ultrasonic quantitative precipitation of barium sulphate, magnesium and ammonium diphosphate and calcium oxalate may be achieved for five minutes instead of lengthy exposure of the precipitate with mother liquor to heating or leaving them overnight before filtering. [English summary]

Literature

1. L. Bergman. Ultrasonics. Moscow, IL, 1956.
2. Yu. A. Zolotov. About the use of ultrasonics in analytical chemistry. ZhAKh, XIII, Issue 4, 408, 1958.
3. V. V. Vasil'yev, V. I. Gedeonova, and N. Ye. Muratova. Application of ultrasonics in phase-shift analysis of lead ores. Herald of Leningrad State University, No. 22, 146, 1959.
4. V. V. Vasil'yev, T. D. Kan, and N. Ye. Muratova. Acceleration of selective extraction of copper minerals under the influence of ultrasonics. Collection: "Phase chemical analysis of ores and minerals." Press of Leningrad State University, 50, 1962.
5. I. M. Kol'tgof and Ye. B. Sendel. Quantitative analysis, Moscow-Leningrad, State Chemistry Press, 368, 388, 1948.
6. V. N. Alekseyev. Quantitative analysis. Moscow, State Chemistry Press, 124, 139, 149, 1954.

Submitted
26 October 1962